ORNL/TM-2022/2778
CRADA/NFE-13-04646

Technologist in Residence for Advanced Manufacturing and Materials in Unconventional Oil and Gas Equipment and Infrastructure

Yarom Polsky

November 2022

OAK RIDGE NATIONAL LABORATORY
MANAGED BY UT-BATTELLE FOR THE US DEPARTMENT OF ENERGY

ORNL/TM-2022/2778
CRADA/NFE-13-04646

Advanced Manufacturing Program

Technologist in Residence for Advanced Manufacturing and Materials in Unconventional Oil and Gas Equipment and Infrastructure

Yarom Polsky

Date Published: November 2022

Prepared by
OAK RIDGE NATIONAL LABORATORY
Oak Ridge, Tennessee 37831-6283
managed by
UT-BATTELLE, LLC
for the
US DEPARTMENT OF ENERGY
under contract DE-AC05-00OR22725

1. ABSTRACT

The DOE Technologist in Residence (TIR) program pairs a senior technical staff member from a National Laboratory (Lab Technologist), and a senior technical staff member(s) from a clean energy manufacturing company or consortium of companies (Industry Technologist). Each technologist may represent single or multiple national laboratories, or single or multiple companies. These pairs of Lab and industry technologists work together for a period of 18 to 24 months to accomplish several goals:

1) Identify the participating company's (or companies') technical priorities and challenges, and the resources and capabilities in DOE's National Laboratories that may be highly suitable to address them;
2) Propose collaborative R&D efforts to develop science-based solutions to the company's (or companies') most strategic scientific, technological, and business issues; and
3) Develop a general framework agreement and begin developing specific scopes of work for the proposed collaborative R&D efforts. The proposed R&D will then take place outside of the program and will not use TIR program funds.

Oak Ridge National Laboratory (ORNL) and Pioneer Natural Resources were awarded a TIR project by DOE in late 2016 and the CRADA component of the project was initiated in 2017. This report describes work performed under the CRADA agreement between 2017 and 2020.

2. STATEMENT OF OBJECTIVES

The TIR program endeavors to build deeper relationships between industry and DOE's National Laboratories that result in high-impact collaborative research and development (R&D). ORNL and Pioneer pursued the following goals as part of their TIR project:

- Develop a long-term strategic partnership between ORNL and Pioneer in R&D areas including, but not limited to, advanced materials and coatings for unconventional oil and gas (O&G) applications, smart parts and sensors, efficient manufacturing processes for equipment operating in harsh environments, and advanced material design and additive manufacturing for subsurface equipment.
- Establish a network of researchers and capabilities at ORNL and other National Laboratories to address and roadmap Pioneer's technical priorities in unconventional O&G shale plays.
- Identify challenges and gaps where the National Labs R&D capabilities can advance unconventional O&G shale plays and collaboratively develop R&D priorities.
- Develop streamlined methods for Pioneer and other O&G independents to collaboratively develop technologies and methods to reduce their environmental footprint and promote a deeper understanding of the subsurface through R&D and tech transfer in advanced manufacturing, additive, and computational science, and modeling tools.
- Identify new opportunities and subsequently launch new programs based on common priorities in joint efforts with DOE and other National Laboratory partners.
- Identify transferrable lessons learned for other National Laboratory industry partners.

3. BENEFITS TO THE FUNDING DOE OFFICE'S MISSION

The DOE Office of Energy Efficiency and Renewable Energy Technologist in Residence (TIR) initiative was launched in 2015 to facilitate the building of deeper relationships between industry and DOE's National Laboratories to catalyze high-impact collaborative research and development (R&D). The program endeavored to develop a transparent and streamlined process for companies to establish such relationships with National Laboratories beyond the program period.

4. TECHNICAL DISCUSSION OF WORK PERFORMED BY ALL PARTIES

The primary objective of this project was to foster awareness of Department of Energy R&D activities and capabilities to enhance DOE engagement with Pioneer Natural Resources, a large independent Oil & Gas producer, and to foster collaborations between DOE national laboratories and the unconventional Oil & Gas industry. Core elements of the approach taken during the project included: the identification and engagement of a network of national laboratories to optimize the process of enhancing Pioneer awareness of relevant capabilities; identifying existing or emerging DOE activities that could be leveraged to advance both DOE mission goals and industry goals; and streamlining collaboration methods. A number of activities were performed to meet these goals including:

- Webinars exchanging information between DOE subject matter experts and Pioneer subject matter experts
- Workshops conducted at National Laboratories with relevant expertise in geotechnical engineering applicable to subsurface resource extraction
- Facilitation of R&D engagements with national laboratory PIs
- Participation on 1 panel and co-organization of second at the Unconventional Resources Technology Conference (URTeC)
- Screening-level assessments of scientific topics as potential future areas of collaborative investigation

The remainder of this section will summarize the work products associated with each activity.

Webinars

A series of webinars were held in the 2017 – 2018 timeframe to familiarize Pioneer domain experts with ORNL R&D activities and interests and vice versa. These webinars occurred on a nominally bi-monthly basis with topics recommended by both ORNL and Pioneer. Example titles of webinars that took place include: Sensor Activities (ORNL), Neutrons for Geoscience (ORNL), Unconventional Resource Water R&D Interests (Pioneer), Degradable Materials R&D (Pioneer), Novel Atomic Force Microscopy Technique (ORNL), Co-Production of Materials from Produced Water (ORNL). The webinars were generally well attended and often stimulated follow-on discussions between SMEs from each organization. They were largely educational, but in some cases helped initiate R&D activities that will be described later in this report.

Workshops

A series of workshops was held to provide Pioneer with a more in depth understanding of capabilities and R&D activities resident at national laboratories with geotechnical and other subject matter expertise that were thought to be relevant to their R&D interests. Three national laboratories, Sandia National Laboratories (SNL), ORNL and the National Energy Technology Laboratory were visited during the primary period of performance of the project. A fourth visit with Los Alamos National

Laboratory was targeted but not completed before the end of the project due to logistical complications.

SNL Workshop:
Pioneer brought a team of subject matter experts to visit Sandia National Laboratories in Albuquerque, NM on February 21-22, 2017. The agenda shown below highlights the SNL R&D areas and capabilities that were presented.

Following the meeting, Pioneer expressed interest in research performed by Pat Brady on methods for enhancing oil recovery by altering wettability characteristics of rock and engaged.

PIONEER NATURAL RESOURCES

OAK RIDGE National Laboratory

Sandia National Laboratories

Pioneer Natural Resources, Oak Ridge National Laboratories, &
Sandia National Laboratories Workshop
Sandia National Laboratories
February 21 & 22, 2017

Tuesday, February 21, 2017

Time	Topic	Location
8:00 – 8:30 AM	Meet at Sandia Badge Office (IPOC)	IPOC
8:30 – 8:45 AM	Travel to Geomechanics and Downhole Tools Labs	MO293
8:45 – 9:15 AM	Welcome ▪ Leigh Cunningham, *Manager, Geotechnology & Engineering, SNL* Tour of Geomechanics ▪ Mathew Ingraham, *Geomechanics* Tour of Downhole Tools Labs ▪ David Raymond, *Geothermal Research*	MO293
9:15 – 9:30 AM	Travel to National Simulation & Analysis Center (NISAC)	1008

(TRACK A)

Time	Topic	Location
9:30 – 10:15 AM	Introduction and Overview of Technical Interests ▪ Pioneer Natural Resources ▪ Oak Ridge National Laboratories	1008/154
10:15 – 11:30 AM	Theme 1: Unconventional Shale Science D&C and stimulation ▪ Mark Grubelich, *Energetic Stimulation* ▪ Mathew Ingraham, *Efrac Waterless Fracturing Technology* Tight/Shale ER ▪ Pat Brady, *Enhanced Oil Recovery from Tight Formation*	1008/154
11:30 – 12:00 PM	Sandwich Buffet for Working Lunch & Break	1008/154
12:00 – 2:00 PM	Theme 2: Fracking Diagnostics	1008/154

	▪ **Curt Ober**, *Capability and Application Highlights for HPC in the Center for Computing Research* ▪ **Chet Weiss,** *Electromagnetic Imaging of Tagged Proppants for Hydrofrac Monitoring* **Improving Accuracy with Current Methods** ▪ **Tom Dewers**, *Shale Poromechanics: Heterogeneity, Flow, Fracture, and Creep* ▪ **Jason Heath**, *Noble Gas Applications to Monitoring*	
2:00 – 2:15 PM	**Break**	1008/154
2:15 – 3:30 PM	**Theme 3: Induced seismicity** **Field Experiments for Frack Diagnostics & IS Monitoring** ▪ **Hunter Knox,** *Multi-disciplinary Geophysical Monitoring and Imaging for Frack Diagnostics and Induced Seismicity Monitoring* **Trigger Physics** ▪ **Hongkyu Yoon,** *Integrated Geomechanics and Geophysics in Induced Seismicity: Trigger Physics* ▪ **Bart Van Bloemen Waanders,** *Technologies to Control Hydraulic Fracturing to Achieve Optimal Fracture Patterns and Signals from Induced Seismicity*	1008/154
3:30 – 3:45 PM	**Break**	1008/154
3:45 – 4:30 PM	**O&G Landscape** **Pioneer** **Oak Ridge National Laboratories** **Leigh Cunningham,** *Manager, Geotechnology & Engineering, SNL*	1008/154

(TRACK B)

Time	Topic	Location
9:30 – 10:45 AM	**Theme 4: Drilling Technology & Downhole Tools - I** **Overview** ▪ **David Raymond,** *Geothermal Research* **Vibration & High T Tech** ▪ **David Raymond,** *Drilling Vibration Mitigation and High-Temperature Motor Development* **Down-the-Hole Hammers & Microhole Work** ▪ **Jiann Su,** *HT Down-the-Hole Hammers and Microhole Work*	1008/156

10:45 – 11:30 PM	**Theme 4: Drilling Technology & Downhole Tools - II** **Materials Science** ▪ **Ryan Hess,** *Materials Development for Ruggedized Downhole Sensors for Geothermal Reservoirs* ▪ **Somuri Prasad,** *Hard Coating for Drill Bits to Drill through Rocks without Lubrication. Hard Anti-Friction Coating to Operate at 500C Under Corrosive CO2 Environment*	1008/156
11:30 – 12:00 PM	**Sandwich Buffet for Working Lunch & Break**	1008/156
12:00 – 1:15 PM	**Theme 4: Drilling Technology & Downhole Tools - III** **Robotics** ▪ **Jonathan Salton**, *Drilling Automation* ▪ **Stephen Buerger,** *Robotics R&D* ▪ **Jason Wheeler**, *Robotics R&D*	1008/156
1:15 – 2:30 PM	**Theme 5: Air Quality Monitoring & Atmospheric Science** **Monitoring** ▪ **Kate Klise,** *Sensor Placement Optimization for Emissions* **Measurement** ▪ **Mark Ivey,** *Department of Energy Atmospheric Research Facilities on the North Slope of Alaska* **Modeling** ▪ **Erika Roesler,** *High resolution Atmospheric Modeling in the Arctic for Climate Change Research*	1008/156
2:30 – 2:45 PM	**Break**	1008/156
2:45 – 3:00 PM	**Travel to HOT Facility**	
3:00 – 4:15 PM	**Deep Dive Tour of HOT Facility** ▪ **Jiann Su,** *Geothermal Research*	HOT Facility
4:15 – 4:30 PM	**Travel to NISAC**	1008/156

PIONEER NATURAL RESOURCES

OAK RIDGE National Laboratory

Sandia National Laboratories

Pioneer Natural Resources, Oak Ridge National Laboratories, &
Sandia National Laboratories Workshop
Sandia National Laboratories
February 21 & 22, 2017

Wednesday, February 22, 2017

Time	Topic	Location
8:00 – 8:30 AM	Meet at Sandia Badge Office (IPOC)	IPOC
8:30 – 8:45 AM	Travel to Geoscience Building	823
8:45 – 9:45 AM	Porous Media Lab ▪ Tom Dewers, *Geomechanics*	823/B43, 2027
9:45 – 10:45 AM	Geomechanics Lab ▪ Joshua Feldman, *Geomechanics*	823/2243
10:45 – 11:00 AM	Travel to Geomechanics and Downhole Tool Lab	MO293
11:00 – 12:00 PM	Geomechanics Lab ▪ Joshua Feldman, *Geomechanics* ▪ Perry Barrow, *Geomechanics*	MO293
12:00 – 1:00 PM	Drilling Lab ▪ Dennis King, *Geothermal Research*	MO293
1:00 – 1:15 PM	Travel to Sandia Badge Office to Return Badges	IPOC

ORNL Workshop:
Pioneer brought a team of subject matter experts to visit ORNL in Oak Ridge, TN on September 27, 2017. The agenda shown below highlights the Pioneer application interests that were presented.

OAK RIDGE National Laboratory — AGENDA

MANAGED BY UT-BATTELLE FOR THE US DEPARTMENT OF ENERGY

Pioneer/ORNL Project Review Meeting
(Agenda – September 27, 2017)

Event contact	Yarom Polsky, 865-576-0593 (office); 865-244-0260 (mobile); polskyy@ornl.gov			
Time	**Event**	**Lead**	**Attendees**	**Place**
Wednesday, September 27, 2017				
8-8:30 AM	Host Meets Candidate at ORNL Visitor Center			Visitor Center
8:30-9:00 AM	Welcome and Team Introductions	Yarom Polsky Tom Spalding		Building: 4100 Room: C301-P
9:00-9:25 AM	Midland Basin Fractures	Caleb Pollock, Geoscience Advisor		Building: 4100 Room: C301-P
9:25-9:50 AM	Microseismic & Proppant Placement	Rob Hull, Geophysical Advisor		Building: 4100 Room: C301-P
9:50-10:15 AM	Petrophysical Core to Log Calibration	Mriganko Sarkar, Petrophysicist		Building: 4100 Room: C301-P
10:15-10:40 AM	Pipeline Detection, Optical Fiber, 3D Seismic Imaging	Kevin Woller, Geophysical Tech Specialist		Building: 4100 Room: C301-P
10:40-11:00 AM	Break			Building: 4100 Room: C301-P
11:00-11:25 AM	Methane Detection	Carrie Reese		Building: 4100 Room: C301-P

OAK RIDGE National Laboratory **AGENDA**

MANAGED BY UT-BATTELLE FOR THE US DEPARTMENT OF ENERGY

11:25-11:50 AM	Oilfield Corrosion Prevention	Ayman Gazawi		Building: 4100 Room: C301-P
11:50-12:15 PM	Imbedded Sensing, Additive Manufacturing	James Franks		Building: 4100 Room: C301-P
12:15-1:00 PM	Working Lunch			Building: 4100 Room: C301-P
1:00-4:00 PM	Breakouts with PXD & ORNL SMEs			Building: 4100 Room: A157 and Room C301-P
4:00-5:00 PM	Conclusion and Discussion			Building: 4100 Room: C301-P
6:00-8:00 PM	Dinner Discussions, Longhorn Steak House			

NETL workshop:
Pioneer brought a team of domain experts to visit National Energy Technology Laboratory (NETL) sites in Pittsburgh, PA and Morgantown, WV on September 26-27, 2018. The agenda shown below highlights the NETL R&D areas and capabilities that were presented. Two potential areas of interest were identified by Pioneer subsequent to the visit: Microbial ecology for corrosion prevention and Produced water continuous iron monitoring. Follow-on discussions related to these topics were conducted directly between Pioneer and NETL.

U.S. DEPARTMENT OF ENERGY | NETL NATIONAL ENERGY TECHNOLOGY LABORATORY

Pioneer Natural Resources

Wednesday, September 26, 2018
Pittsburgh, PA
12:00 to 5:00 PM

Thursday, September 27, 2018
Morgantown, WV
9:00 AM to 1:00 PM

Wednesday, September 26, 2018
Pittsburgh, PA
12:00 to 5:00 PM
Main Discussions in 83-104A

12:00	Arrive at NETL-Pittsburgh Site – Badging (B95), Introductions and Box Lunch* (B83)
12:30	Operations Overview (Pioneer)
1:00	Geochemistry (Alexandra Hakala)
1:20	Microbial Ecology (Djuna Gulliver)
1:40	Wellbore and Sensors (Barbara Kutchko and Paul Ohodnicki)
2:15	Break
2:30	Atmospheric Emissions (Natalie Pekney)
3:00	Produced Water (Nicholas Siefert)
3:20	Machine Learning (Grant Bromhal)
3:45	Break
4:00	Laboratory Tour – Air Emissions, Environmental Geochemistry and Microbiology, Produced Water, Brine Chemistry and Sensors
5:00	End (1 h 20 minute drive to Morgantown)

**Please complete the box lunch menu and send to Karen.Lockhart@netl.doe.gov by Monday 9/24/2018*

Thursday, September 27, 2018
Morgantown, WV
9:00 AM to 1:00 PM
Discussions and Tour in B-17
Wrap up and Lunch in B-39 Innovation center

9:00	Arrive at NETL-Morgantown Site, Check-in (B-39)
	Core Flooding and Imaging, Geomechanics, Geophysics (Dustin Crandall and Alexandra Hakala)
10:00	Laboratory Tour
12:00	Discussion of Next Steps and Lunch (Pizza)
1:00	End

Facilitation of R&D

One exploratory R&D effort was initiated with ORNL through TIR efforts to investigate the potential applicability of novel ORNL-developed characterization capability. The ORNL PI was Olga Ovchinnikova and the project was supported through the CNMS user program. Below is the description of the main scientific questions addressed in the CNMS user program proposal.

---

1) **What is/are the main scientific question(s) that you plan to address?**

This investigation will attempt to perform simultaneous nanoscale structural and chemical characterization in order to promote the development of improved structure and flow transport models of oil & gas bearing shales that can be used to predict hydrocarbon transport within these materials. While the production of these resources in the last 10 years has triggered an energy revolution in the United States, the understanding of fluid movement within them remains largely a mystery. This is because unlike conventional hydrocarbon bearing rocks, for which internal flow transport is dominated by structural features from the micron to sub-millimeter scale, transport in these rocks is dominated by nanoscale features which are extremely difficult to characterize.

A significant fraction of the stored hydrocarbons in shales occupy pores on the nanometer scale, the materials are highly heterogeneous, and the influence of surface chemistry with structural features, such as pore shape and small scale fractures, combine to create complex flow pathways that cannot be revealed using conventional experimental methods. For example, methods such as Mercury Injection Capillary Pressure have been used to estimate permeability in bulk materials, but when high resolution methods such as X-ray micro computed tomography are employed they severely underestimate permeability because they are not able to resolve features below one micron. Higher resolution techniques, such as Focused Ion Beam - Scanning Electron Microscopy (FIB-SEM), have been used to characterize structural features at the nanoscale, but are performed on samples with size on the order of only one micron. This FIB-SEM method also captures limited chemical information and is not suitable by itself for building a statistically relevant picture of oil and gas bearing shales, which are layered on the centimeter scale. Furthermore, in situ stresses produced by overburden forces, tectonic forces and pore pressure which cause both pore deformation and closure of fractures produce structural changes which must be accounted for in flow transport models. Evaluation of these effects requires mechanical property values, such as elastic moduli, of constituent materials. Such information is not currently obtained at the scale of interest and is typically evaluated only from bulk materials.

There is a need to develop characterization techniques that generate both structural, chemical, and mechanical property information that can be up-scaled to the centimeter level in order to develop a more comprehensive interpretation of the factors that influence flow transport from the nanoscale to the centimeter scale. This research will attempt to utilize the combined AFM/TD-MS instrument developed at ORNL to simultaneously probe structural and chemical features at the nanoscale on shales samples of relevant size (on the order of one centimeter).

During the course of the TIR project, Pioneer initiated R&D efforts or more in-depth conversations related to development of R&D scope with other national laboratories including Lawrence Livermore National Laboratory, SLAC National Accelerator Laboratory, Sandia National Laboratories and National Energy Technology Laboratory. The work or conversations associated with non-ORNL efforts will not be presented in this report.

Increasing the Broader Unconventional Oil & Gas Industry to National Laboratory Capabilities

Efforts were made as part of the project to expose the broader unconventional oil & gas industry to R&D efforts and capabilities within the National Laboratory complex. Pioneer viewed conferences with high industry engagement as a promising opportunity to communicate with many companies at once and submitted a proposed panel, "Shopping for New Ideas from Unconventional Sources", to the 2017 Unconventional Resources Technology Conference (URTeC). ORNL was asked to sit on this panel that also included Battelle, Saudi Aramco Energy Ventures, and ARI and presented a brief overview of the laboratory and emerging technologies from its applied and basic energy science program as part of the panel discussion.

The first year panel was generally viewed as a success and the following year at URTeC 2018 Pioneer submitted a follow-on panel proposal, that was accepted, called "National Labs – Leveraging Basic Science to Advance Subsurface Understanding". This panel expanded the group of national laboratories involved and included Oak Ridge National Lab, Los Alamos National Lab, Lawrence Berkeley National Lab and National Energy Technology Lab.

Screening Level Assessments

A no-cost extension was filed following the official completion of the CRADA period and Pioneer concurrently underwent a restructuring, including assignment of a new TIR lead. For this last phase of the project, ORNL performed a series of 'screening level assessments' on topics recommended by Pioneer to better understand the state of science and technology related to applications of concern to the industry. Four potential screening level assessment topics were identified: 1) Wettability, and wettability alteration, in conventional and unconventional reservoirs, 2) Screening of produced water for rare metals, 3) State of the art for removal of Iodide, Bromide, Tellurium and Gallium from produced water, and 4) Micogrid systems for remote locations. Assessments for topics 1 and 2 were completed during the project and are provided in Appendix A.

5. SUBJECT INVENTIONS (AS DEFINED IN THE CRADA)

No invention disclosures were created during the project.

6. COMMERCIALIZATION POSSIBILITIES

Not applicable based on the project objectives.

7. PLANS FOR FUTURE COLLABORATION

A change in the unconventional Oil & Gas business climate and a 2020 shift in DOE R&D priorities effectively ended direct collaboration with Pioneer. DOE no longer supports R&D related to unconventional oil & gas recovery, limiting opportunities for collaboration that align with current mission priorities. Future collaborative R&D opportunities with this industry will most likely focus on water treatment applications such as produced water treatment and ORNL will attempt to maintain a dialogue with Pioneer on this topic.

8. CONCLUSIONS

The TIR collaboration between Pioneer Natural Resources and Oak Ridge National Laboratory facilitated a large amount of interaction between unconventional oil & gas exploration and production professionals and researchers from multiple national laboratories (ORNL, SNL, NETL, LBNL, SLAC and LANL) to foster mutual awareness of unconventional energy production concerns from an industry perspective and DOE capabilities that could be utilized to address them. The project was particularly successful in taking what is frequently considered to be a complex, opaque network of laboratories more transparent by helping an industry partner efficiently learn about the DOE-related R&D activities and capabilities that might be of interest to them. This involved exploratory educational activities, targeted technical reviews of topics of mutual interest, and facilitation of preliminary R&D efforts involving multiple national laboratories. The project was ended in 2020 after a one year no-cost extension. Changes in the unconventional oil & gas business climate and a shift in DOE R&D priorities halted further collaboration, however, in the opinion of the project team, this TIR project and the TIR program was successful in its goal of promoting more intentional and productive engagement between DOE resources and industries relevant to it’s mission.

APPENDIX A

SCREENING-LEVEL ASSESSMENT OF WETTABILITY, AND WETTABILITY ALTERATION, IN CONVENTIONAL AND UNCONVENTIONAL RESERVOIRS.

Technical Point of Contact:
Josh Brownlow
Senior Geologist, Subsurface Technology
Pioneer Natural Resources USA Inc.
777 Hidden Ridge
Irving, Texas 75038
Phone: 972.969.3908
Email: Josh.Brownlow@pxd.com

Administrative Point of Contact:
Skip Rhodes
Senior Director, Emerging Technology
Pioneer Natural Resources USA Inc.
777 Hidden Ridge
Irving, Texas 75038
Phone: 972.969.3858
Email: Skip. Rhodes@pxd.com

STATEMENT OF WORK

I. Purpose of Study

Pioneer Natural Resources USA, Inc. ("Pioneer") is a large independent oil and gas company focused on evaluating new technologies to enhance its asset portfolio. The purpose of this study is to conduct a screening-level assessment using publicly available data on industry's understanding of wettability, and more specifically wettability alteration, in conventional and unconventional reservoirs.

II. Background

There is enormous incentive to improve oil recoveries in reservoirs from their typically low value of 5% to 10% original oil in place (OOIP). Increased oil recovery would boost reserves while lowering unit operating costs. One control on oil recovery is "wettability" - the ability of a liquid to maintain contact with a solid surface. In an oil reservoir, the liquid can be water or oil (or gas) and the solid phase is the rock mineral assemblage. Affecting a change in wettability, known as wettability alteration, can in some instances increase oil production. We would like to examine how oil recovery in conventional and unconventional reservoirs might increase through wettability alteration by better understanding the mechanisms that control wettability. Different approaches have been taken to adjust the wettability of different types of reservoirs (e.g., carbonate or clastic). We do <u>not</u> seek DOE's engagement on commercially available practices such as the use of surfactants to alter wettability, CO_2 or gas (methane) injection, or chemical flooding with polymers, etc. The screening-level assessment should focus on gathering readily available or obtainable information to better define the controls on wettability in oil reservoirs and, in particular, the mechanisms by which oil can be displaced from porous rock (including shale) using injected water(s) of differing fluid composition(s).

III. Screening-level Assessment

The primary topics for the screening-level assessment are, but not limited to:

- What is an oil-wet reservoir?
- What is a water-wet reservoir?
- And, what naturally occurring mechanisms promote or impede oil migration or flow in each?
- What mechanisms control reservoir wettability (e.g., ionic composition of formation water, reservoir lithology, oil composition, pH and temperature, among others)?
- What are relative permeability and capillary pressure in a reservoir and can either be changed by altering wettability?
- What are the laboratory methods for measuring wettability (e.g., contact angle, Amott-Harvey, etc.)? How have laboratory flotation experiments been used in the mining industry to assess wettability?
- Can DOE identify any significant limitations of the current laboratory methods for evaluating/measuring wettability? If so, can DOE recommend alternate or new laboratory methods for measuring wettability that may mitigate these limitations?
- Examine case histories where wettability alteration is known to enhance oil recovery <u>only by injecting a water</u> with a different fluid chemistry (e.g., salinity, pH, etc.).
- What is the industry's current state of knowledge on controlling the wettability of proppants used during induced fracturing and does the wettability of proppants change during production?

IV. Deliverables

Leverage the knowledge from DOE technical staff and publicly available data including, but not limited to, databases, reports, working papers, white papers, and journal articles. Deliver a written document with a summary of findings including a list of selected references by relevant topic. Delivery of written document to be followed by a presentation of findings to Pioneer staff.

Assessment of Wettability

Lawrence M. Anovitz
Chemical Sciences Division, Oak Ridge National Laboratory

Introduction

What is an oil-wet reservoir? What is a water-wet reservoir?

"Wettability is the tendency of one fluid to spread on, or adhere to, a solid surface in the presence of other immiscible fluids. Wettability refers to the interaction between fluid and solid phases. In a reservoir rock the liquid phase can be water or oil or gas, and the solid phase is the rock mineral assemblage" (Crains Petrophysical Handbook, https://www.spec2000.net/09-wettability.htm).

However, as noted by Haagh et al. (2017) "It is important to point, at the outset of any discussion, to an ambiguity in terminology between physical chemists and the petroleum engineering community in this context: in physical chemistry, "wettability" describes a qualitative measure of the contact angle; "wettability alteration" is therefore equivalent to "contact angle alteration". By contrast, petroleum engineers use the term wettability to express the retention capability of a porous medium in a two-phase flow displacement experiment such as the Amott wettability test; wettability in that sense is therefore a much more complex quantity that is affected by the properties of the aforementioned complex energy landscape and the details of the process parameters such as sample history and flow rates. Throughout this work, we will stick to the generic terminology of physical chemistry, where wettability describes the equilibrium contact angle."

Wettability is governed by a balance between adhesive forces, those between the liquid and the solid, and cohesive forces, those between the liquid and itself although, in general, there are three phases present in such systems (solid - liquid - gas or solid – liquid – liquid). It is, therefore, a function of both

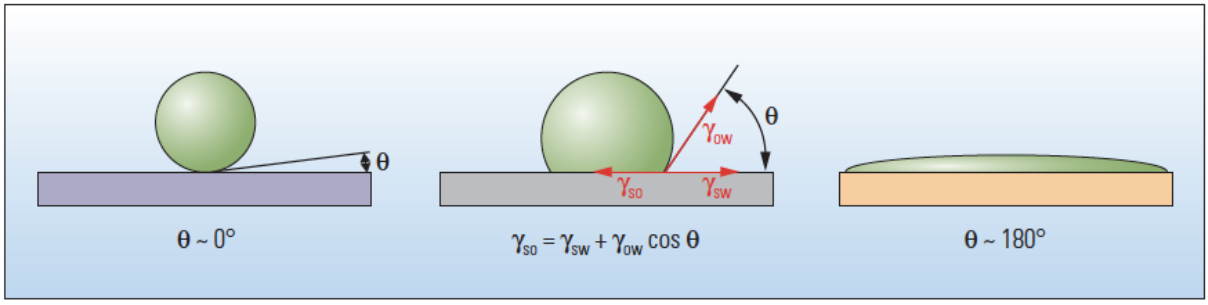

Figure 1: Contact angles for oil as a function of the surface type. An oil drop (green) surrounded by water (blue) on a water-wet surface (left) forms a bead. The contact angle θ is approximately zero. On an oil-wet surface (right), the drop spreads, resulting in a contact angle of about 180°. On an intermediate-wet surface (center) oil also forms a bead, but the contact angle depends on a force balance among the interfacial tension terms, which are γ_{so}, γ_{sw} , and γ_{ow} for the surface-oil, surface-water, and oil-water terms, respectively.(Image and description from Abdallah et al., 2007).

the specific phases involve (mineralogy, liquid composition) and the physical properties of the solid surface (roughness, hydration). While wettability phenomena apply to a wide range of materials systems (polymers, steels), geologic hydrocarbon reservoirs are generally characterized as being either oil-wet, water-wet, intermediate-wet, or mixed-wet.

To discuss wetting we first need to define the important terms.

- Strongly water-Wetting - one end member of a continuum in which the surface strongly "prefers" contact with water

- Strongly oil-wetting – the other end member of the continuum in which the surface strongly "prefers" contact with oil. Note that both water-wet and oil-wet may be history-dependent as well. For instance, pore surfaces that previously contacted by oil may be oil-wet, but those never contacted by oil may be water-wet.
- Intermediate wetting or neutral-wetting – an intermediate state in which the solid does not have a strong "preference" for either oil or water

- Water-saturated or oil-saturated – refers to the fluid actually IN the reservoir. Note that, for example, a surface can be strongly water-wetting, but oil saturated.
- Mixed- (fractional-, or dalmatian-) wet – real rocks are often composed of a variety of materials that may have different wetting properties. Thus, the wetting properties of a given surface may vary from spot to spot.
- Imbibition - formally an increase in the saturation of the wetting phase, whether spontaneous or forced (e.g. waterflood in a water-wet material). Informally a process with increasing water saturation
- Drainage - formally an increase in saturation of the nonwetting phase. Informally. a process with increasing oil saturation.

Background and Theory

The key variable for understanding wettability is surface tension. Surface tension is the tendency of liquid surfaces to shrink to the minimum possible surface area. At liquid–air interfaces, surface tension results from the greater attraction of liquid molecules to each other (cohesion) than to the molecules in air (adhesion). Due to cohesive forces a molecule inside a material is pulled equally in every direction by neighboring molecules, resulting in net zero force. However, the molecules at the surface do not have the same molecules on all sides of them and, therefore, are pulled inward. The net effect is an inward force at the surface of the liquid, and the surface comes under tension from the imbalanced forces. As molecules at the surface have a higher energy state than those in the bulk the surface area is minimized to reduce the total energy of the system. Thus, the surface tension can be defined as the work done in moving a surface divided by the change in area of that surface:

$$\gamma = W/\Delta A \quad (1)$$

Because of the relatively high attraction of water molecules to each other due to hydrogen bonding, water has a relatively high surface tension in air (72.8 millinewtons per meter at 20 °C). By contrast, the values for air-oil and oil-water interface are approximately 24 and 48 millinewtons per meter, respectively (Glover, course notes. Note that this source did not define precisely what was meant by "oil", so real values may vary).

To understand wettability, it is important to realize that surface tension occurs at all boundaries between materials, not just at liquid/gas boundaries. Thus, the surface tension of water (or oil) at a solid interface reflects the balance between the cohesive forces in the water (or oil) itself, and adhesive forces between the water (or oil) and the solid surface (Figure 2). The wetting angle, therefore, represents the balance of these forces. This is expressed via Young's equation (Young, 1805) as:

$$\gamma_{lg} \cos \theta = \gamma_{sg} - \gamma_{sl} \quad (2)$$

Where the γ values are the surface tensions between any two of the three phases (solid (s), liquid (l) and gas (g)) at a given contact, and θ is the angle between the solid and the liquid at that point of contact as shown in Figure 1. For water, a wettable surface may also be termed hydrophilic and a nonwettable surface hydrophobic. Superhydrophobic surfaces have contact angles greater than 150°, showing almost no contact between the liquid drop and the surface. This is sometimes referred to as the "Lotus effect".

If no force acts normal to a surface, the surface must remain flat. However, if the pressure on one side of the surface differs from that on the other side, the pressure difference times the surface area

results in a normal force. In order for the surface tension forces to cancel the force due to pressure, the surface must be curved (Figure 2). The diagram shows how surface curvature

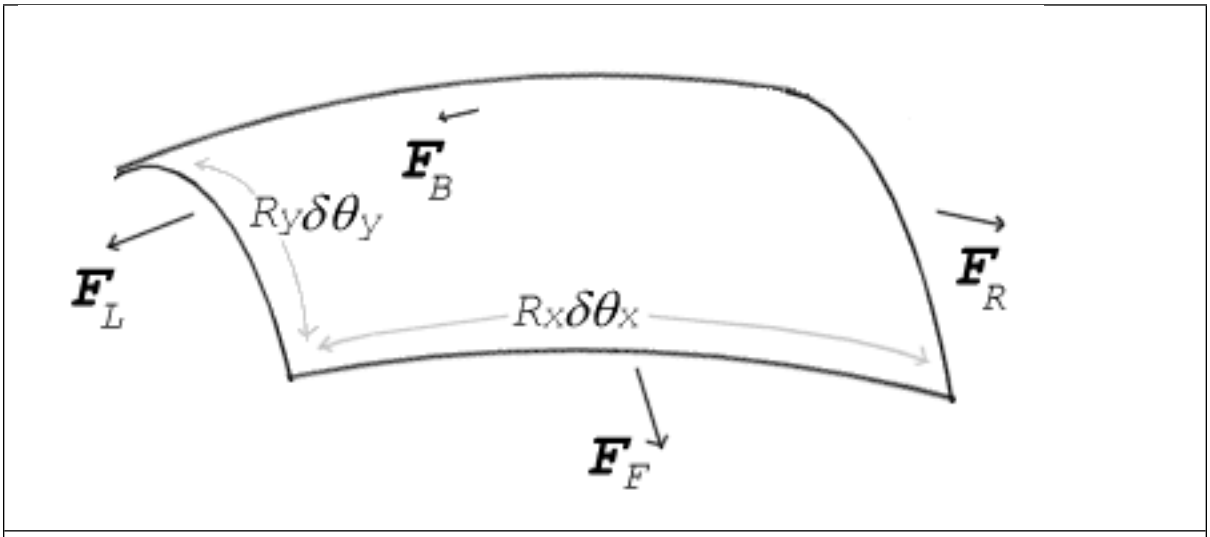

Figure 2: Surface tension forces acting on a differential area of a surface. δθx and δθy indicate the amount of bend over the dimensions of the patch. Balancing the tension forces (F_L, F_R, F_F, F_B) with pressure leads to the Young–Laplace equation. https://en.wikipedia.org/wiki/Surfacetension

of a differential area of the surface leads to a net component of surface tension forces acting normal to the center of the patch. The equation balancing the forces:

$$\Delta p = \gamma\left(\frac{1}{R_X} + \frac{1}{R_Y}\right) \tag{3}$$

is known as the Young–Laplace equation, where: Δp is the pressure difference, the Laplace pressure (Butt et al., 2006), γ is the surface tension, and R_x and R_y are the radii of curvature in each of the axes parallel to the surface. A consequence of this equation is that the internal pressure of a water droplet increases with decreasing radius. This pressure difference becomes very large for nm-sized droplets, leading to changes in freezing point.

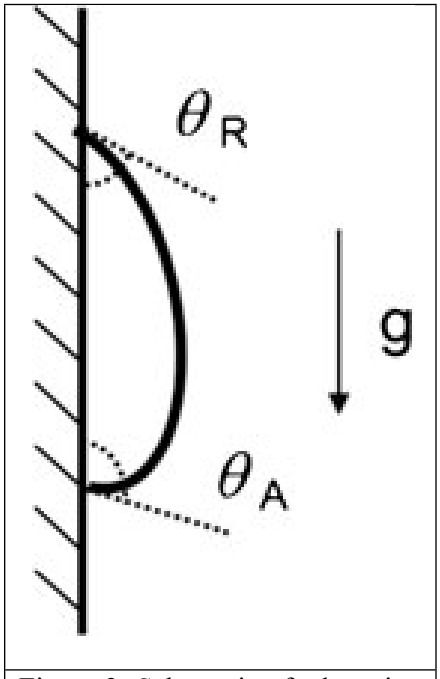

Figure 3: Schematic of advancing and receding contact angles. Eyal et al. (2012)

Addressing the problems of roughness and surface heterogeneity is critical for understanding and predicting wetting in real reservoirs. Unlike ideal surfaces, real surfaces are not perfectly smooth, rigid, or chemically homogeneous. Such deviations from ideality result in a phenomenon called contact-angle hysteresis (cf. Eral et al., 2012), which is defined as the difference between the advancing (θ_a) and receding (θ_r) contact angles (Goode, 1992):

$$H = \theta_a - \theta_r \quad (4)$$

as well as "mixed wet" environments (see below). The advancing contact angle is the maximum stable angle, whereas the receding contact angle is the minimum stable contact angle. Eral et al. (2012) note that this is perhaps most intuitively understood by considering a droplet on a vertical substrate like a raindrop on a window. Gravity pulls on the droplet to move it downward. Contact angle hysteresis, however, tends keep it in place. As a result, the droplet becomes asymmetric - the top of the droplet becomes thin, with a low contact angle, while the bottom becomes thick, with a high contact angle, and the droplet does not move. This is known static hysteresis. Once the droplet reaches a certain size, however, it slides downward while retaining an asymmetric shape, and the difference between its front (in the direction of the driving force in this case gravity) and rear (in the direction opposing the driving force) contact angles is called the dynamic contact angle hysteresis (Joanny and De Gennes, 1984; Dussan and Chow, 1983; Ge Gennes, 1985; Degennes et al., 2004; Extrand, 1998; Bonn et al., 2009, Hyvaluoma et al., 2007). When the contact angle is between the advancing and receding cases, the contact line is considered to be pinned. That is, the drop will not move. When these values are exceeded, displacement of the contact line will take place by either expansion or retraction of the droplet (Shi et al., 2018). Motion of a phase boundary, involving advancing and receding contact angles, is known as dynamic wetting. When a contact line advances, covering more of the surface with liquid, the contact angle increases in proportion to the velocity of the contact line (De Gennes, 1994; Shi et al., 2018).

Rough or heterogeneous surfaces are well-known departures from ideal conditions that also lead to contact angle hysteresis. For a rough surface the wetting regime is homogeneous if the liquid fills the roughness grooves/pits of the surface, and heterogeneous where the surface is a composite of multiple patches. An important example of such a composite surface is one composed of patches of both air and solid. Such surfaces have varied effects on the contact angles of wetting liquids. On a rough surface, contact-angle hysteresis occurs because many different thermodynamically stable contact angles are found on a nonideal solid. These varying thermodynamically stable contact angles are known as metastable states (Johnson, 1993). For a slow-moving drop on a rough surface, static hysteresis will dominate, but for high velocities or low static contact angle hysteresis surfaces (especially on liquids or liquid-soaked solids), dynamic hysteresis becomes extremely important.

The Young equation assumes that the surface on which wetting is being measured is chemically homogenous and topographically smooth. This is not true, however, in the case of real surfaces which, instead of having one equilibrium contact angle value exhibit a range of contact angles between the advancing and receding values. Figure 4 shows schematic illustrations of a liquid droplet on ideal and

real surfaces. On an ideal surface the Young equation applies, and the measured contact angle is equal to the Young contact angle (Figure 4(a)). On a real surface, however, the actual contact angle is that between the tangent to the liquid-vapor interface and the actual, local surface of the solid (Figure 4(b)). However, the measured (apparent) contact angle is that between the tangent to the liquid-vapor interface and a line that represents the apparent solid surface, as seen macroscopically. Because of this fact actual and apparent contact angle values can deviate substantially from each other, but it is the actual contact angles that must be used to calculate the true surface free energies of the solid.

The relationship between roughness and wettability was defined by Wenzel (1936) who showed that adding surface roughness enhance the observed wettability - if the surface is chemically hydrophobic, it will become even more hydrophobic when surface roughness is added. Wenzel's result can be described as (Marmur, 2006).

$$\cos\theta_m = r\cos\theta_Y \quad (5)$$

where θ_m is the measured contact angle, θ_Y is the Young contact angle and r is the roughness ratio. The roughness ratio is the ratio between the actual and projected solid surface area (r=1 for a smooth surface and r > 1 for a rough one). Although Wenzel's equation demonstrates that the contact angle of a rough surface is different from the intrinsic contact angle, it does not describe contact angle hysteresis.

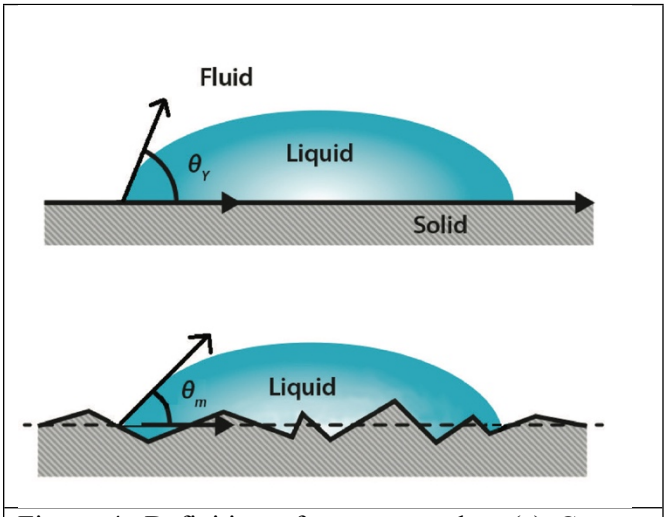

Figure 4: Definition of contact angles, (a) Contact angle on ideal surface is called Young contact angle, (b) Apparent or measured contact angle on rough (Wenzel) surface. https://cdn2.hubspot.net/hubfs/516902/Pdf/Attension/Tech%20Notes/AT-TN-07-Surface-roughness-CA-wettability.pdf

The Wenzel equation is based on the assumption that the liquid penetrates into the roughness grooves (as in Figure 4b). Marmur (2006) stated that if the droplet is larger than the roughness scale by two to three orders of magnitude, the Wenzel equation applies. However, surface roughness is often fractal, so there are a range or roughness scales on any real surface, and both micro and nanoscale roughness have been shown to influence surface wettability. Furthermore, in cases where the liquid does not penetrate into the grooves, the Wenzel equation does not apply. In this case the Cassie equation is used instead. The Cassie or Cassie-Baxter equation was first developed to describe chemically heterogeneous surfaces. In the case of two different chemistries (Cassie and Baxter, 1944) it is given as:

$$\cos\theta_m = x_1 \cos\theta_{Y1} + x_2 \cos\theta_{Y2} \quad (6)$$

where x is the area fraction of each phase and θ_{Yi} are the respective wetting angles (Figure 5a). Thus, the Cassie equation is just an area-weighted expansion of the Wenzel equation. If, instead of having different chemistries on the surface, the second area is air as shown in Figure 5b, then equation (3) can be rewritten as:

$$\cos\theta_m = x_1 (\cos\theta_Y + 1) - 1 \quad (7)$$

This is because the contact angle of a liquid against air can be considered to be 180 ° (thus $\cos\theta_{Y2}$ is -1) and the area fraction $x_2 = 1 - x_1$. It has been found that for the droplet to achieve the real Cassie-Baxter condition (no penetration of the liquid inside the grooves), the geometry of the roughness has to be carefully designed (Tujeta et al., 2007). The most stable contact angle is that associated with the absolute minimum of the Gibbs energy curve. This can be connected to the Young contact angle. The contact angles calculated from the Wenzel and Cassie-Baxter equations have been found to be good approximations of the most stable contact angles (Marmur, 2009). When there are many different fractions of surface roughness, or different phases present, each fraction of the total surface area can be denoted by f_i, where a summation of all f_i is equal to 1 - the total surface. The Cassie–Baxter equation can then be recast as (Whyman et al., 2008):

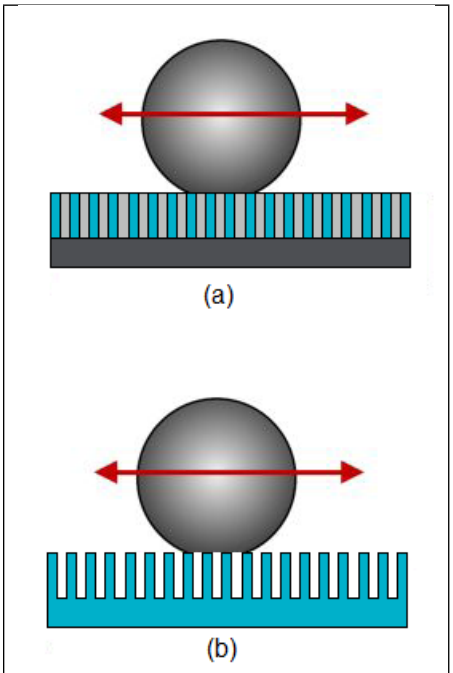

Figure 5: (a) Droplet on a chemically heterogeneous surface (Cassie) (b) Droplet standing on a pillar surface (Cassie-Baxter).

$$\gamma cos\theta_m = \sum_{i=1}^{N} f_i(\gamma_{i,SV} - \gamma_{i,SL}) \quad (8)$$

where γ is the Cassie–Baxter surface tension between liquid and vapor, the $\gamma_{i,sv}$ are the solid/vapor surface tensions of the i^{th} component and $\gamma_{i,SL}$ are the solid/liquid surface tensions of every component.

Liquid drops on rough (monomineralic) surfaces may also undergo a transition from a Cassie-Baxter to a Wenzel state. In the Cassie–Baxter model, the drop sits on top of the textured surface with trapped air underneath. During the wetting transition the air pockets are no longer thermodynamically stable and liquid begins to nucleate from the middle of the drop, creating a "mushroom state" as seen in Figure 6 (Ishino and Okumura, 2008). The penetration condition is given by:

$$\cos\theta_c = \frac{\emptyset - 1}{r - \emptyset} \quad (9)$$

where θ_c is the critical contact angle, ϕ is the fraction of solid/liquid interface with which the drop is in contact, and r is the solid roughness constant (for a flat surface, r = 1). The penetration front propagates to minimize the surface energy until it reaches the edges of the drop, thus arriving at the Wenzel state. This phenomenon is called hemiwicking. The contact angles at which spreading/imbibition occurs are between 0 and 90° (Bico et al., 2002). The Wenzel model is valid between θ_C and 90°. If the contact angle is less than θ_C, the penetration front spreads beyond the drop and a liquid film forms over the surface. The film smooths the surface roughness and the Wenzel model no longer applies. In this state, the equilibrium condition and Young's relation yield (Ishino and Okumura, 2008):

$$\cos(\theta_m) = \phi\cos(\theta_C) + (1 - \phi) \quad (10)$$

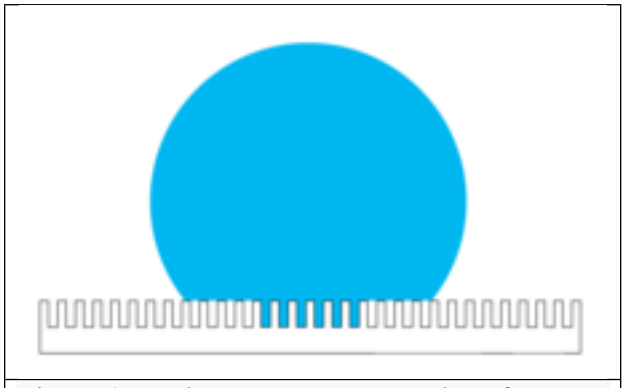

Figure 6: Mushroom state on a rough surface. https://en.wikipedia.org/wiki/Wetting

By fine-tuning the surface roughness, it is possible to achieve a transition between both superhydrophobic and superhydrophilic regions. Generally, the rougher the surface, the more hydrophobic it is.

The Cassie–Baxter and Wenzel approaches are the two main models that attempt to describe the wetting of textured surfaces. However, these equations only apply when the drop size is sufficiently large compared with the surface roughness scale (Marmur, 2003). When the droplet size is comparable to that of the underlying pillars, the effect of line tension, the excess free energy per unit length of the three-phase contact line, must be considered (Chen et al., 2012).

Modifying wetting properties using surfactants

Surfactants are compounds that lower the surface tension (or interfacial tension) between two liquids, between a gas and a liquid, or between a liquid and a solid. Surfactants may act as detergents, wetting agents, emulsifiers, foaming agents, and/or dispersants. They often are composed of a polar head group and a long tail. When a liquid drop is placed on a surface, it can completely wet, partially wet, or not wet the surface. If the surface tension can be reduced using surfactants or some other approach, a nonwetting material can be made to become partially or completely wetting. This is a key to separation by froth floatation and is useful in other industrial processes.

After a drop containing a surfactant is placed onto a surface, the dynamic drop radius can be characterized as the drop begins to spread, and the contact angle changes based on the following equation (Lee et al., 2008)

$$\cos(\theta(t)) = \cos(\theta_0) + (\cos(\theta_\infty) - \cos(\theta_0))\,(1 - e^{-t/\tau}) \qquad (11)$$

where θ_0 is initial contact angle, θ_∞ is final contact angle, and τ is the surfactant transfer time scale. As the surfactants are absorbed, the solid–vapor surface tension increases, and the edges of the drop become hydrophilic. As a result, the drop spreads.

The excess free energy (σ) of a drop on a solid surface is (Lee et al., 2008):

$$\sigma = \gamma S + PV + \pi R^2 (\gamma_{SL} - \gamma_{SV}) \qquad (12)$$

where γ is the liquid–vapor interfacial tension, γ_{SL} is the solid–liquid interfacial tension, γ_{SV} is the solid–vapor interfacial tension, S is the area of liquid–vapor interface, P is the excess pressure inside the liquid, and R is the radius of droplet base. Based on this equation, the excess free energy is minimized when γ or γ_{SL} decreases, or when γ_{SV} increases. Surfactants can be absorbed onto the liquid–vapor, solid–liquid, and solid–vapor interfaces, thus modifying the wetting behavior of hydrophobic materials to reduce the free energy by modifying any of these values. When surfactants are absorbed onto a hydrophobic surface, the polar head groups face into the solution with the tail pointing outward. On more hydrophobic surfaces, surfactants may form a bilayer on the solid, causing it to become more hydrophilic.

Relative permeability and capillary pressure

(What are relative permeability and capillary pressure in a reservoir and can either be changed by altering wettability?)

Relative Permeability

(summary modified after https://en.wikipedia.org/wiki/Relativepermeability. See below for measurement techniques)

Relative permeability is a measure of the ability of a porous system to conduct one fluid when one or more fluids are present. (Craig, 1971; Anderson, 1987b). In multiphase flow in porous media, the relative permeability of a phase is a dimensionless measure of the effective permeability of that phase. It is the ratio of the effective permeability of that phase to its absolute permeability and can be viewed as an adaptation of Darcy's law to multiphase flow.

For two-phase flow in porous media at steady-state conditions, we can write

$$q_i = -\frac{k_i}{\mu_i}\nabla P_i \qquad \text{for i = 1,2} \tag{13}$$

Where, for the i^{th} phase, q_i is the flux, ∇P_i is the pressure drop, μ_i is the viscosity, and ki is the phase permeability (i.e., the effective permeability of the i^{th} phase. The relative permeability of the ith phase, k_{ri} is then defined as:

$$k_{ri} = k_i/k \tag{14}$$

where k is the permeability of the porous medium for single-phase flow, i.e., the absolute permeability. Thus, values for the relative permeability must be between zero and one. In use, relative permeability is often represented as a function of water saturation; however, owing to capillary hysteresis it is often plotted as two functions, one measured under drainage conditions, the other measured during imbibition.

Relative permeability analysis considers the flow of any given phase to be inhibited by the presence of the other phases present. Thus, the sum of relative permeabilities over all phases is less than 1. However, apparent relative permeabilities larger than 1 can be measured, because the Darcean approach disregards viscous coupling effects derived from momentum transfer between the phases (see assumptions below). This coupling can, rather than inhibit, the flow. This has been observed in heavy oil petroleum reservoirs when the gas phase flows as bubbles or disconnected patches (Bravo and Araujo, 2008).

The above form for Darcy's law (Equation 13), sometimes also called Darcy's extended law, is formulated for horizontal, one-dimensional, immiscible multiphase flow in homogeneous, isotropic porous media. As just mentioned, interactions between the fluids are neglected, so this model assumes that the combination of the solid porous media with the other fluids present forms a new porous matrix through which a given phase flows. This implies that fluid-fluid interfaces remain static during steady-state flow, which is not true. The model also assumes that the saturation of each phase is larger than the irreducible saturation. This is the maximum water saturation a formation with a given permeability and porosity can retain without producing water. This water, although present, is held in place by capillary forces and will not flow. Each phase is also assumed to be continuous within the porous medium.

To further discuss relative permeability, we must first analyze saturation. Water saturation (S_w) and oil saturation (So) are simply the fractions of the pore volume that are filled with water or oil (Note: not all sources use consistent abbreviations for these parameters and those that follow.). Thus, these saturations are scaled properties. For an oil/water system

$$S_w + S_o = 1 \Leftrightarrow S_w = 1\text{-}S_o \tag{15}$$

This being the case, model functions or correlations for relative permeabilities in an oil-water system can be written as functions of the water saturation alone. If we let S_{wir} (also denoted S_{wc}, S_{wr} and S_{wcr}) be the irreducible (minimal or connate) water saturation, and S_{orw} be the residual (minimal) oil saturation after water flooding (imbibition), then the flowing water saturation window in a water invasion / injection / imbibition process is bounded by a minimum value of S_{wir} and a maximum of

$$S_{wor} \text{ (also } S_{owcr}) = 1 - S_{orw} \tag{16}$$

Thus, the flowing saturation window can be written as

$$S_{wir} \leq S_w \leq S_{wor} (= 1 - S_{orw}) \tag{17}$$

Then, by scaling the water saturation to the flowing saturation window, we obtain a water saturation value normalized to the range of possible saturations as:

$$S_{wn} = S_{wn}(S_w) = \frac{S_w - S_{wir}}{1 - S_{wir} - S_{orw}} = \frac{S_w - S_{wir}}{S_{wor} - S_{wir}} \tag{18}$$

and a normalized oil saturation value

$$S_{on} = 1 - S_{wn} = \frac{S_0 - S_{orw}}{1 - S_{wir} - S_{orw}} \tag{19}$$

Having defined saturation values, we can now define values for relative permeability. First, let K_{row} be the relative permeability for oil, and let K_{rw} be the relative permeability for water. There are two ways of scaling permeability in order to quantify the effective permeability of the phase. If we scale phase permeability with respect to absolute water permeability (i.e. $S_w = 1$), this yields the same endpoint for the relative permeability of both oil and water. Alternatively, if we scale phase permeability with respect to the permeability for oil with irreducible water saturation present, then the K_{row} endpoint is one, and we are left with only the K_{rw} endpoint parameter as a variable. In order to satisfy both options, it is common to

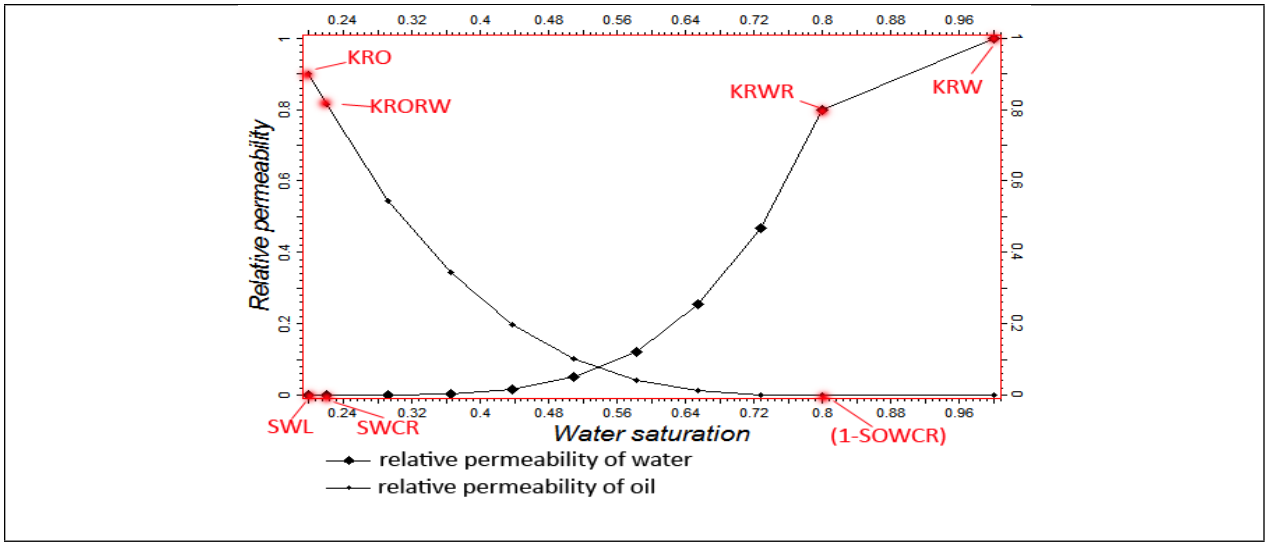

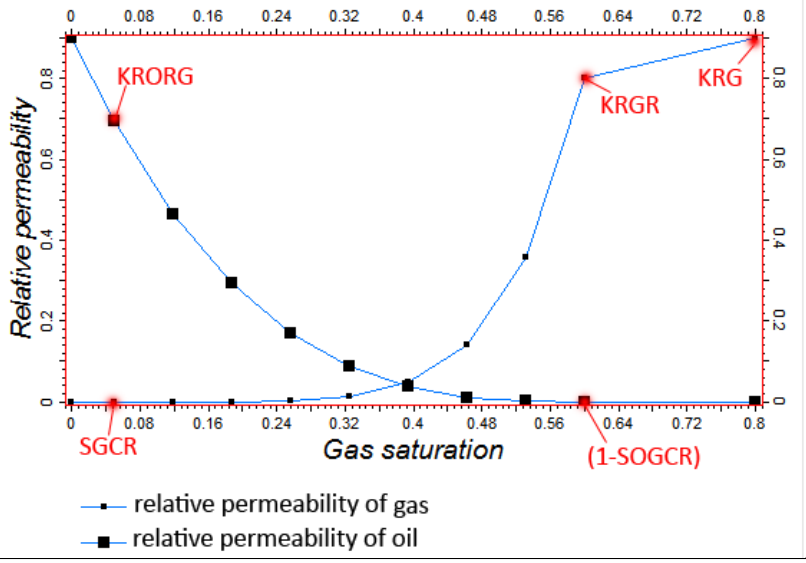

Figure 7: definitions of saturation and relative permeability reference points.

Upper (oil/water)
SWCR (= S_{wir}) - critical water saturation (the largest water saturation for which the water relative permeability is zero)
SOWCR (= S_{wor}) - critical oil-in-water saturation (the largest oil saturation for which the oil relative permeability is zero in an oil-water system)
SWL - connate water saturation (the smallest water saturation in a water saturation function table)
KRW - relative permeability of water at maximum water saturation
KRO - relative permeability of oil at maximum oil saturation
KRWR - relative permeability of water at residual oil saturation (or residual gas saturation in a gas-water run)
KRORW (= K_{rot}) - relative permeability of oil at critical water saturation

Oil/gas
SGCR - critical gas saturation (that is the largest gas saturation for which the gas relative permeability is zero)
SOGCR - critical oil-in-gas saturation (that is the largest oil saturation for which the oil relative permeability is zero in an oil-gas-connate water system)

Relative permeability end-point scaling (KRW, KRG, KRO, KRWR, KRGR, KRORG, KRORW)
KRG - relative permeability of gas at maximum gas saturation parameter
KRGR - relative permeability of gas at residual oil saturation (or critical water saturation in a gas-water run) parameter
KRORG - relative permeability of oil at critical gas saturation parameter

http://petrofaq.org/wiki/Saturationandrelativepermeabilityend-pointsscaling

use two endpoint symbols in models of two-phase relative permeability. The endpoints / endpoint parameters for the relative

permeabilities of oil and water are: 1) the permeability for oil relative to that at irreducible (minimal) water saturation

$$K_{row}(S_{wir}) = K_{rot} \quad (20)$$

and 2) the relative permeability for water relative to that of water with residual (minimal) oil saturation after water flooding

$$K_{rw}(S_{wor}) = K_{rwr} \quad (21)$$

These symbols have merits and limitations. Use of the symbol K_{rot} emphasizes that it represents the maximum (top) point of K_{row}. That is, it occurs at irreducible water saturation, and is thus the largest possible value of K_{row} that can occur for initial water saturation. The competing endpoint symbol K_{rwr}

occurs in imbibition flow in oil-gas systems. If the permeability basis is oil with irreducible water present, then K_{rot}=1. The symbol K_{rwr} emphasizes that it is the relative permeability for water occurring at residual oil saturation. Figure 7 shows the positions of these reference points for oil-water systems, and similar points for oil-gas systems.

Having defined these endpoints, oil and water relative permeability models can now be written as

$$K_{row} = K_{rot} \bullet K_{rown}(S_{wn}) \tag{22}$$

for the relative permeability of oil, and

$$K_{rw} = K_{rwr} \bullet K_{rwn}(S_{wn}) \tag{23}$$

for the relative permeability of water. The functions K_{rwon} and K_{rwn} are called normalized relative permeabilities or shape functions for oil and water, respectively. The endpoint parameters K_{rot} and K_{rwr} (which is a simplification of K_{rwor}) are physical properties obtained either before or together with the optimization of shape parameters present in the shape functions, providing equations for the relative permeability as a function of normalized water saturation.

An often-used approximation of relative permeability is the Corey correlation (Corey, 1954; Brooks and Corey, 1964; Goda and Behrehbruch, 2004), which is a power law in saturation. The Corey correlations of the relative permeability for oil and water are:

$$K_{row}(S_w) = K_{rot}(1-S_{wn})^{No} \tag{24}$$

and

$$K_{rw}(S_w) = K_{rot} S_{wn}^{N_w} \tag{25}$$

If the permeability basis is normal oil with irreducible water present, then K_{rot} = 1. The empirical parameters N_o and N_w are called curve shape parameters or simply shape parameters and can be obtained from measured data either by analytical interpretation, or by optimization using a core flow numerical simulator to match the experiment (often called history matching). In some cases, $N_o = N_w = 2$ is an appropriate choice. The physical properties K_{rot} and K_{rwr} are obtained either before or while optimizing N_o and N_w. There are also Corey correlations similar to the oil-water relative permeabilities correlations shown above for gas-water and gas-oil systems.

One limitation of the Corey model is that it has only one degree of freedom for the shape of each relative permeability curve, the shape parameters N_o and N_w. The LET-correlation (Lomeland, 2005, 2018) adds more degrees of freedom in order to accommodate the shape of relative permeability curves in SCAL (special core analysis laboratory) experiments (McPhee et al., 2015) and in 3D reservoir models adjusted to match historic production. These adjustments frequently include relative permeability curves and endpoints. The LET-type approximation is described by 3 parameters L, E, and T. The correlations for water and oil relative permeabilities with water injection are:

$$K_{rw} = \frac{K_{rwr} S_{wn}^{Lw}}{S_{wn}^{Lw} + E_w(1 - S_{wn})^{Tw}} \tag{26}$$

and

$$K_{row} = \frac{K_{rot}(1 - S_{wn})^{L_0}}{(1 - S_{wn})^{L_0} + E_0 S_{wn}^{T_0}} \tag{27}$$

written using the same S_w normalization as for Corey. Only S_{wir}, S_{orw}, K_{rot} and K_{rwr} have direct physical meaning. The parameters L, E and T are empirical. Parameter L describes the lower part of the curve and is comparable to the appropriate Corey parameter. The parameter T describes the upper part (or the top part) of the curve, and E describes the position of the slope (or the elevation) of the curve. A value of one for E is a neutral value, leaving the position of the slope governed by the L- and T-parameters. Increasing the value of E pushes the slope towards the high end of the curve. Decreasing the value of E pushes the slope towards the lower end of the curve. Experience using the LET correlation indicates the following reasonable ranges for the parameters L, E, and T: $L \geq 0.1$, $E > 0$ and $T \geq 0.1$. Again, there are similar LET correlations for gas-water and gas-oil systems. Sakhaei et al. (2016) evaluated 10 common and widely used relative permeability correlations for gas/oil and gas/condensate systems and found that LET showed the best agreement with experimental values for both gas and oil/condensate relative permeability.

It should be noted that relative permeability is just one of the factors that affect fluid flow dynamics and, therefore, can't fully capture dynamic flow behavior in porous media (Mirzaei-Paiaman et al., 2018, 2019, 2020). A criterion/metric that has been established to characterize dynamic characteristics of rocks is known as the True Effective Mobility or TEM-function (Mirzaei-Paiaman et al., 2019, 2020). The TEM-function is a function of relative permeability, porosity, permeability and fluid viscosity, and can be determined for each fluid phase separately. The TEM-function, derived from Darcy's law for multiphase flow, is written as:

$$TEM = \frac{kk_r}{\phi\mu} \tag{28}$$

where k is the permeability, k_r is the relative permeability, φ is the porosity, and μ is the fluid viscosity. Rocks with better fluid dynamics (i.e., those experiencing a lower pressure drop in conducting a fluid phase) have higher TEM versus saturation curves.

Capillary Pressure

(summary modified after https://en.wikipedia.org/wiki/ Capillarypressure, and Anderson, 1987a)

In fluid statics, the capillary pressure (p_c) is the pressure between two immiscible fluids in a thin tube. This results from the interactions of forces between the fluids and the solid walls of the tube (i.e. the surfacer tensions/wettability). Capillary pressure can serve as either an opposing or a driving force for fluid transport and is a significant property for analysis of oil extraction from porous rock.

Capillary pressure is defined as:

$$p_c = p_{\text{non-wetting phase}} - p_{\text{wetting phase}} \tag{29}$$

where p_c is the capillary pressure, $p_{non\text{-}wetting\ phase}$ is the pressure of the non-wetting phase, and $p_{wetting\ phase}$ is the pressure of the wetting phase. The wetting phase is identified by its ability to preferentially diffuse along the capillary walls before the non-wetting phase. As we have discussed above, the wettability of a solid by a fluid depends on the surface tension. This is measured by determining the contact angle of the fluid and can be controlled by varying surface properties (e.g. roughness, hydrophilicity).

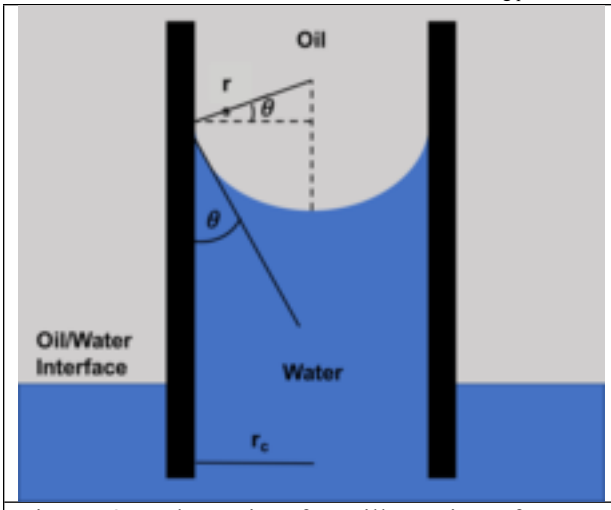

Figure 8: Schematic of capillary rise of water to demonstrate measurements used in the Young-Laplace equation. https://en.wikipedia.org/wiki/Capillarypressure see also Anderson (1987a)

The pressure difference leading to capillary pressures arises at the resulting curved interface between the two fluids (Tiab and Donaldson, 2015). Capillary pressure formulas are derived from a balanced pressure relationship between two fluid phases in the capillary tube at equilibrium. That is, "force up" must equal "force down" (cf. Fanchi, 2006). The upward force is equal to the interfacial tension of the fluid(s) acting along the perimeter of the capillary tube, while the downward force is given as

force down = (density gradient difference) x (cross-sectional area) x (capillary rise height) (30)

These forces can be described by the interfacial tension and contact angle of the fluids, and the radius of the capillary tube (Figure 8).

There are two general equations that describe the force up and force down relationships of two fluids in equilibrium. The Young–Laplace equation (Eqn. 3) is the force up description of capillary pressure, and the most commonly used variation of the capillary pressure equation. Written in terms of the wetting angle θ for a capillary with a circular cross-section, the Young-Laplace equation is given as:

$$p_c = \frac{2\gamma cos\theta}{r_c} \tag{31}$$

where: γ is the interfacial tension and r is the effective radius of the interface. The downward force for capillary pressure is given as:

$$p_c = \frac{\pi r^2 h(\Gamma_w - \Gamma_{nw})}{\pi r^2} = h(\Gamma_w - \Gamma_{nw}) \tag{32}$$

Where h is the height of the capillary rise, Γ_w is the density gradient of the wetting phase, and Γ_{nw} is the density gradient of the non-wetting phase.

A relationship between capillary pressure and the pore structure is provided by the Leverett J-function, a dimensionless function of water saturation describing the capillary pressure (Leverett, 1941).

$$J(S_w) = \frac{p_c(S_w)\sqrt{k/\phi}}{\gamma} \tag{33}$$

where S_w is the water saturation measured as a fraction, p_c is the capillary pressure (in pascals), k is the permeability (measured in m^2), ϕ is the porosity (range = 0-1), γ is the surface tension (in N/m). This equation is also given as:

$$J(S_w) = \frac{p_c(S_w)\sqrt{k/\phi}}{\gamma cos\theta} \tag{34}$$

Where θ is the contact angle. The function is important in that it is constant for a given saturation within a reservoir, thus relating reservoir properties for neighboring beds. As noted by Anderson (1987a), however, the cos θ relationship is not valid for the effects of wettability on capillary pressure in reservoir cores. Hence the original J function without the cos θ term should be used. However, as long as all of the measurements are made with reservoir fluids on cores with the reservoir wettability, the cos θ term will simply act as a constant multiplier and not affect the results. Problems arise, however, when different fluids are used, or when the core is cleaned.

The Leverett J-function is an attempt at extrapolating capillary pressure data for a given rock to similar rocks with differing permeability, porosity and wetting properties. It assumes that the porous rock can be modelled as a bundle of non-connecting capillary tubes, where the factor $\sqrt{k/\phi}$ is a characteristic length of the capillaries' radii. In many cases, all of the capillary pressure data from a formation will be reduced to a single curve when the Leverett J function is plotted vs. the saturation.

There are two basic types of capillary pressure processes: drainage and imbibition (Anderson, 1987a). In a drainage process, the non-wetting fluid displaces the wetting fluid (e.g. air replacing water), while the reverse occurs for imbibition (e.g. water uptake into a "dry" rock). Generally, however, there is hysteresis in capillary pressure as the saturation is varied, leading to differences in the drainage and imbibition curves. To establish a drainage capillary pressure curve, the wetting-phase saturation is reduced from its maximum to the irreducible minimum (S_{wir}) by

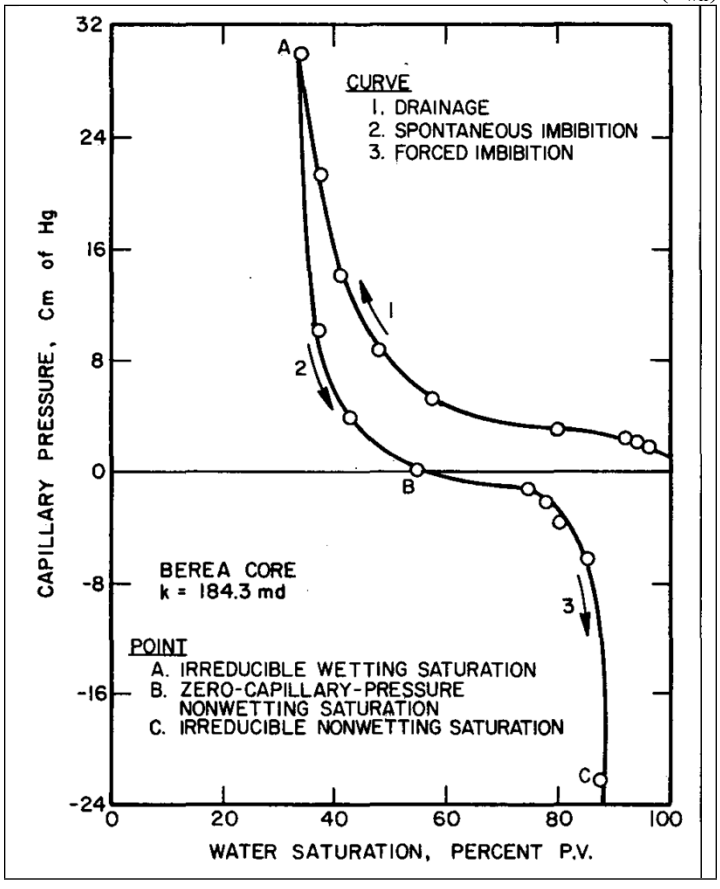

Figure 9: Oil/water capillary pressure curve measured on a water-wet core of Berea Sandstone (Killins et al., 1953; Anderson, 1987a)

increasing the capillary pressure from zero to a large positive value. To develop an imbibition capillary pressure curve, the wetting-phase saturation is increased.

Two distinctly different portions of the imbibition curve can be measured. The first is the spontaneous imbibition curve, which is determined immediately after measurement of the drainage capillary pressure. The capillary pressure ($Pc=P_{NW}-P_{WET}$) is then decreased to zero, allowing the wetting phase to imbibe into the rock. The second portion is the forced imbibition curve, where the capillary pressure is decreased from zero to a large negative value, forcing further fluid into the rock.

As noted above, there is often significant hysteresis between the drainage and imbibition curves. One cause of this effect is contact-angle hysteresis (Figure 3). During drainage, the nonwetting fluid displaces the wetting fluid from the core. The wetting fluid is being pushed back from surfaces it previously covered, so the contact angle between the fluids will be the receding angle, θ_{rec}. During imbibition the contact angle is the advancing contact angle, θ_{adv}, because then the wetting-phase saturation increases, and it displaces the non-wetting phase from the pore walls. Changing the wetting properties of the surface, therefore, will change the imbibition and drainage curves.

An example of the three sections of the capillary pressure curve is shown in Figure 9 for a water-wet system (Killins et al., 1953; Anderson, 1987a). Initially, when the capillary pressure is zero, all of the brine is contiguous and at the same pressure. The drainage capillary pressure (Curve 1) is measured by gradually increasing the capillary pressure from zero to a large positive value, which reduces the saturation of the wetting phase (water). As the saturation is decreased, portions of the wetting phase become disconnected from the bulk of that phase. Eventually, when the externally applied capillary pressure is sufficiently high, all of the wetting phase remaining in the core will be in disconnected segments and the capillary pressure curve will be almost vertical as no more water can be drained by increasing pressure. This saturation, where hydraulic continuity of the wetting phase is lost, is the irreducible wetting-phase saturation (S_{wir}) (Morrow, 1971; Dullien, 1979, Anderson, 1987a).

Curve 2 in Figure 9 is the spontaneous imbibition curve. This is determined after the drainage capillary pressure curve is measured. The capillary pressure, initially at a large positive value, is gradually decreased to zero, allowing the wetting phase (water) to imbibe. The nonwetting residual saturation reached when $P_c = 0$ is referred to as the zero-capillary-pressure nonwetting saturation. In general, some of the oil (nonwetting phase) is still connected at thie point when the capillary pressure is zero, so the non-wetting phase residual saturation defined in this fashion is not irreducible. Curve 3 of Figure 9 is the forced imbibition curve, where the capillary pressure, P_o-P_w, is decreased from zero to a large negative value. When the capillary pressure is negative, the pressure in the wetting phase (water) is greater than the pressure in the nonwetting phase (oil), forcing water into the core. (Note that the fact that the water pressure is greater than the oil pressure does not imply that oil is the wetting fluid at these saturations. If the core were a bundle of cylindrical capillary tubes, then negative capillary pressures would be possible only if the core were oil-wet. However, the interaction of pore structure and wettability allows negative capillary pressures even for strongly water-wet cores (Purcell, 1950).) Much of the oil (the nonwetting phase) is still connected at the end of the spontaneous imbibition curve when the capillary pressure is zero because additional oil is produced as the capillary pressure becomes negative. The oil saturation decreases, and the oil gradually disconnects as the capillary pressure becomes increasingly negative until the capillary pressure curve is almost vertical. This saturation, where hydraulic continuity of the nonwetting phase is lost, is referred to as the irreducible non-wetting phase saturation. In general, different residual nonwetting-phase saturations will be measured after the spontaneous and forced imbibition curves unless the core is very strongly wetted (Morrow, 1971; Dullien, 1979, Anderson, 1987a).

Wetting Effects

The qualitative question of the effects of wetting on capillary pressure and relative permeability is, in part, obvious from the descriptions above. As the capillary pressure is a function of the interfacial tension, which is the force leading to wettability, the capillary pressure must, similarly, be a function of wettability. The details of this relationship are, however, more complex. The effects of wettability on capillary pressure were discussed in detail by Anderson (1987a). That discussion is summarized here.

Before discussing how changes in wettability affect capillary pressure, we must examine capillary pressure curves measured on strongly water-wet and strongly oil-wet systems. In contrast to Figure 9, above, which shows the capillary pressure measured on a water-wet core of Berea sandstone, Figure 10 shows data for a strongly water-wet core of Venango sandstone (Killins et al., 1953; Anderson, 1987a). The change in water wetness causes the areas under the drainage (Curve 1) and forced imbibition (Curve 3) curves to differ significantly. Because of the favorable free energy change, little or no work must be done during imbibition, when the preferentially wetting fluid (water) displaces the nonwetting fluid
(oil). Conversely, a great deal of work is required during drainage when the non-wetting fluid (oil) displaces the wetting one from the core. It can be shown that the work required for one fluid to displace the other is related to the area under the capillary pressure curve. For oil displacing water (drainage curve in a water-wet core, Curve 1), the external work required is (Leverett, 1941; Morrow, 1970; Anderson 1987a):

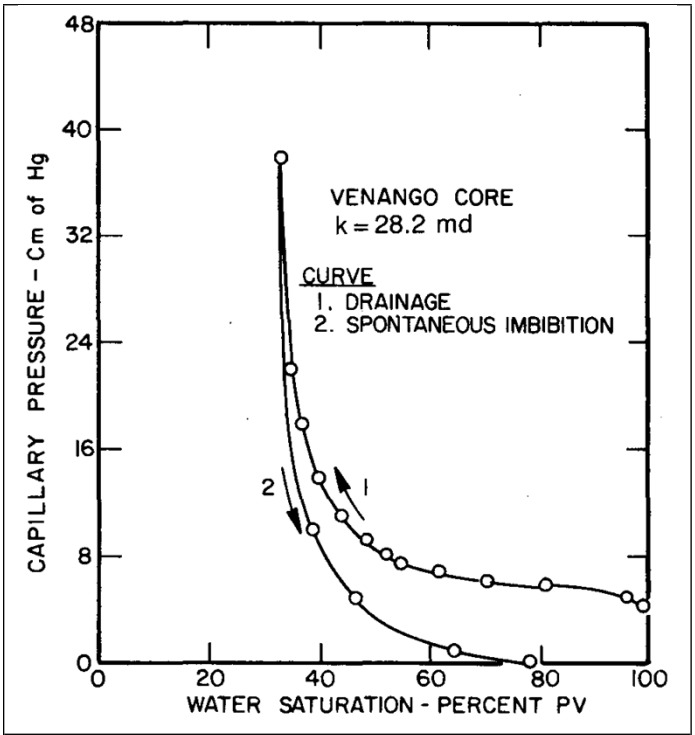

Figure 10 - Oil/water capillary pressure curve measured on a strongly water-wet core of Venango sandstone

$$\Delta W_{ext} = -\phi V_b \int_{S_{w1}}^{S_{w2}} P_c dS_w, \ldots. \quad (35)$$

where V_b is the bulk volume of the core, ø is the porosity, and S_w is the water saturation. Similarly, the work required for water to displace oil (forced imbibition curve for a water-wet core) is

$$\Delta W_{ext} = -\phi V_b \int_{S_{o1}}^{S_{o2}} P_c dS_o, \ldots. \quad (36)$$

The area under the drainage capillary pressure curves (curve 1) in Figures 9 and 10 is relatively large because a great deal of work is necessary for the oil to displace the water. The Venago core shown in Figure 10 can be seen to be very strongly water-wet because a great deal of the water imbibes back spontaneously, and the residual oil saturation is approached at zero capillary pressure. The water saturation after spontaneous imbibition is almost 80% PV. The Berea core shown in Figure 9 can be seen to be less strongly water-wet because after spontaneous imbibition, the water saturation is only about 55 % PV, and additional water can be forced into the core (Curve 3, Figure 9). The area under the imbibition curve, however, is much smaller than the area under the drainage curve, so more work is necessary for oil to displace water than for the reverse.

Figure 11 shows the capillary pressure measured in a strongly oil-wet systems – a Berea plug core treated with Drifilm TM, an organochlorosilane, to render it strongly oil-wet (Anderson, 1986a). The core was first saturated with oil, then the drainage capillary pressure curve (Curve 1) was measured by increasing the capillary pressure, Po -Pw, to a large, negative value. Because oil is the wetting fluid, a large amount of work is necessary to force water into the core, as shown by the large area under Curve

1 (see Equation 36). When oil is the strongly wetting fluid, the roles of oil and water are reversed from the strongly water-wet case. If Figure 11 for the oil-wet Berea plug were inverted, it would resemble the capillary pressure curve shown in Figure 9 for the water-wet Berea plug. Curve 2 in Figure 11 is the spontaneous imbibition curve, measured as the capillary pressure is reduced to zero. Because oil is the wetting fluid, it imbibes spontaneously, just as water imbibed in the water-wet plugs. Curve 3 in Figure 11 is the forced imbibition curve. The capillary pressure, Po - Pw, is increased to a large positive value, forcing additional oil into the core. Again, the areas under the capillary
pressure curves show that the work required for this displacement is much smaller than the work for the reverse displacement, where the nonwetting fluid displaces the wetting fluid from the core. Curve 4 in Figure 11 shows that no water is imbibed as the capillary pressure is reduced to zero.

The reasons for some of the differences between the behavior of strongly oil-wet and water-wet rocks are illustrated as a cartoon in Figure 12. As the rock/oil/brine system becomes more neutrally wetted, the transition zone and the area under the drainage capillary pressure curve are reduced. This occurs because less work is necessary for drainage as the preference of the rock surface for the wetting phase decreases. Consider a weakly water-wet system compared with a strongly water-wet one; more water would be displaced by oil at any given capillary pressure, giving a lower water saturation. Another way of stating this is that at any given capillary pressure, the nonwetting fluid (oil) would be able to enter smaller and smaller pores as the water wetness of the system was reduced. In addition, the amount of wetting fluid (water) imbibed during spontaneous imbibition would also decrease as the system becomes more neutrally wet because the driving force is reduced. The behavior in an oil-wet system is analogous. As the system moves from strongly oil-wet to neutrally wet, the area under the drainage capillary pressure curve
decreases, as does the amount of spontaneous oil imbibition. Finally, drainage capillary pressure curves can be measured even if the contact angle is 90°. In general, external work will still be necessary for one fluid to displace the other, causing a finite area under the capillary pressure curve. This disagrees with the capillary tube model.

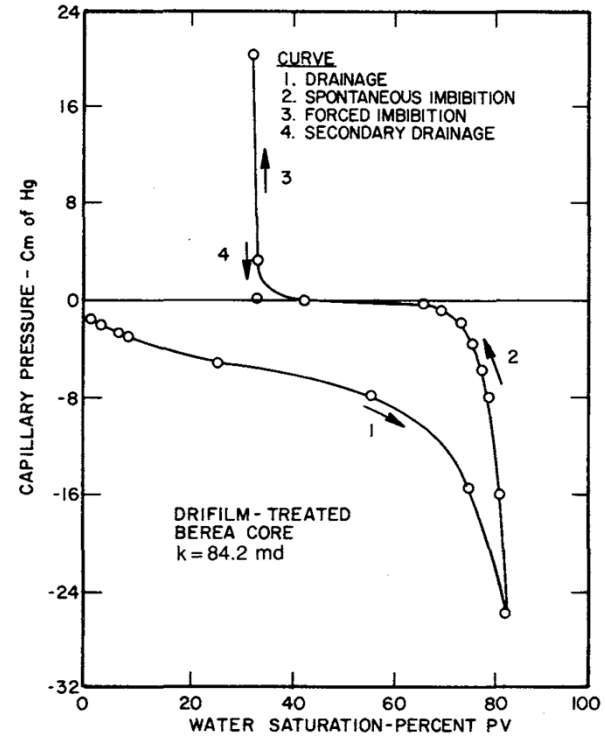

Figure 11: Oil/water capillary pressure curve measured on an oil-wet Berea core treated with Drifilm (Anderson et al., 1986a, 1987a)

Further examples of the effects of wetting on capillary pressure are provided by Anderson (1987a), and he drew the following conclusions.

1. While the capillary-pressure/saturation relationship depends on the interaction of wettability, pore structure, and saturation history, no simple relationship exists that relates capillary pressures determined at two different wettabilities. In particular, a porous medium can generally not be modeled as a set of capillary tubes. Because there is no simple relationship, an apparent contact angle calculated from either the displacement capillary pressure or the complete capillary pressure curve is only a rough estimate of the actual contact angle.

2. In a uniformly wetted porous medium, the drainage capillary pressure is insensitive to the wettability when the contact angle is less than 50°. This has been demonstrated in measurements with

uniformly wetted Teflon cores and by use of mercury capillary pressure measurements with reservoir cores, and is a result of pore geometry surface roughness, which
makes the effective contact angle zero. Similarly, the spontaneous imbibition capillary pressure curve (positive capillary pressure) measured in a uniformly wetted core is insensitive when the contact angle is less than about 20°.

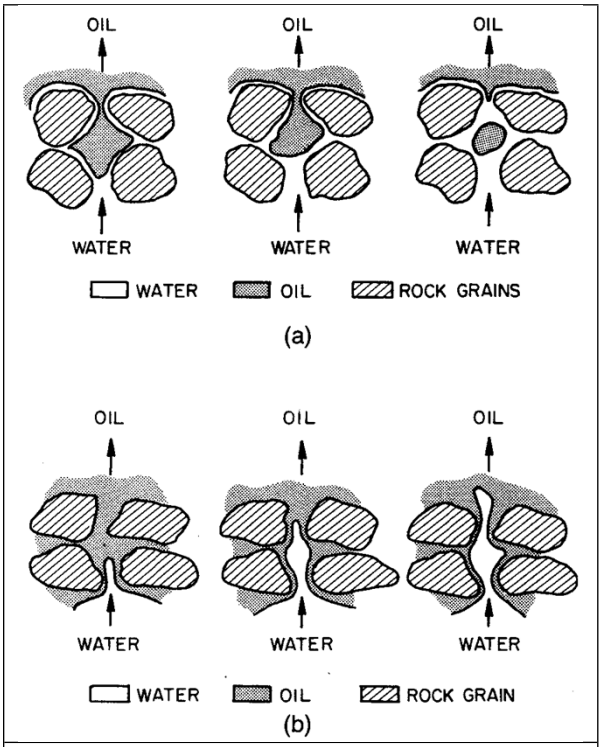

Figure 12: Water displacing oil from a pore during a waterflood. A) strongly water-wet rock, B) strongly oil-wet rock (Raza et al., 1968; Anderson et al. 1987b)

3. The most accurate capillary pressure measurements are made on native- or restored-state cores with crude oil and water because these conditions best match those in the reservoir. While measurements with cleaned cores or with other fluids such as air/water or mercury/vacuum can be made, there is no simple relationship (cosine or otherwise) to convert to native-state oil/water capillary pressure curves. Generally, measurements with fluids like air/water or mercury/vacuum where one of the fluids is strongly wetting will give accurate results only in strongly water-wet reservoirs. The contact angle should be neglected when converting to oil/brine capillary pressures, as shown by experiments in uniformly wetted porous media.

4. The minimum residual oil saturation (ROS) occurs when a uniformly wetted system is slightly oil-wet to neutrally wet. This residual saturation correlates well with that in waterflooding after many pore volumes of water have flowed through the system. If the reservoir has a fractional or mixed wettability, then residual saturations depend on both the amount and distribution of the water-wet and oil-wet surfaces.

5. When a system is strongly wetted, the preferentially wetting fluid will spontaneously imbibe into the core, displacing the nonwetting fluid. The amount and rate of spontaneous imbibition depends on the wettability, viscosity, interfacial tension, pore structure, and initial saturation of the core. Wettability (surface energy) considerations alone would indicate that at least some imbibition would occur when the contact angle is less than 90°. There is no free imbibition, however, in an initially dry, uniformly wetted Teflon core when the contact angle is as low as 49°. This implies that in a uniformly wetted reservoir core, there is a large range of contact angles where neither oil nor water will imbibe spontaneously.

6. In a fractional- or mixed-wet core, it is possible for either fluid to imbibe freely when the core is initially at the irreducible saturation for that fluid.

7. If the reservoir is intermediate- or oil-wet and a clean water-wet core is used, the shape of the capillary pressure curve will not be representative of the reservoir. This causes an overestimation of the height of the transition zone and an inaccurate estimation of the interstitial water.

8. Measurements made with a clean water-wet core will overestimate the amount and rate of oil recovered by imbibition when waterflooding a non-water-wet reservoir, especially a fractured one.

Permeability

Wettability also has a significant impact on relative permeability. Wettability affects relative permeability because it is a major factor in the control of the location, flow, and spatial distribution of fluids in the core (cf. Raza et al., 1968; Craig, 1971; Anderson, 1987b; Falode and Manuel, 2014).

Because relative permeability is a function of saturation history, hysteresis is often observed when comparing relative permeabilities measured with increasing vs. decreasing wetting-phase saturations. In general, the shapes of the relative permeability curves are altered by changing wetting such that the relative permeability curve for a wetting fluid is concave upwards whereas that for non-wetting fluid has an "s" shape. In the case where there is no interfacial tension between the fluid phases, the relative permeability curves simplify to straight lines between the endpoints. These effects have been discussed in detail by Anderson (1987b), whose results will be summarized here.

Consider a strongly water-wet rock initially at irreducible water saturation. Water, the wetting phase, will occupy the small pores and form a thin film over all the rock surfaces (Moore, and Slobod, 1956; Pirson, S.1., 1958; Mattax, and Kyte, 1961; Marsden, 1965a,b; Donaldson and Crocker, 1977). Oil, the nonwetting phase, will occupy the centers of the larger pores. This occurs because it is the most energetically favorable situation. Any oil placed in the small pores would be displaced into the center of the large pores by spontaneous water imbibition, because this lowers the energy of the system.

During a waterflood of a water-wet system, water moves through the porous medium in a fairly uniform front (Craig, 1971). The injected water tends to imbibe into small- or medium-sized pores, moving oil into the large pores where it is easily displaced. Only oil is moving ahead of the front. In the frontal zone, each fluid moves through its own network of pores, but with some wetting fluid located in each pore (Craig, 1971). In this zone, where both oil and water are flowing, a portion of the oil exists in continuous channels with some dead-end branches, while the remainder is trapped in discontinuous globules. Figure 12, taken from Raza et al. (1968), shows water displacing oil from a water-wet pore. The rock surface is preferentially wetted by the water, so water will advance along the walls of the pore, displacing oil in front of it. At some point, the neck connecting the oil in the pore with the remaining oil will become unstable and snap off, leaving a spherical oil globule trapped in the center of the pore. After the water front passes, almost all the remaining oil is immobile. Because of such immobility in this water-wet case, there is little or no oil production after water breakthrough (Chatenever, 1955; Moore, and Slobod, 1956; Mattax and Kyte, 1961; Morris, and Wieland, 1963; Craig, 1971; Donaldson and Thomas, 1971; Donaldson and Crocker, 1977). The disconnected, residual oil exists in two basic forms: (1) small, spherical globules in the center of the larger pores, and (2) larger patches of oil-extending over many pores that are completely surrounded by water.

In a strongly oil-wet rock, the rock is preferentially in contact with the oil, and the location of the two fluids is reversed from the water-wet case. Oil generally will be found in the small pores and as a thin film on the rock surfaces, while water will be located in the centers of the larger pores. The interstitial water is located as discrete droplets in the centers of the pore spaces (Raza et al., 1968). A waterflood of a strongly oil-wet rock is much less efficient than one in a water-wet rock because, when the waterflood is started, the water forms continuous channels through the centers of the larger pores, pushing oil in front of it (see Figure 12), but oil is left in the smaller crevices and pores. As water injection continues, water invades the smaller pores to form additional continuous channels, and the water to oil ratio of the produced fluids gradually increases. When sufficient waterfilled flow channels form to permit nearly

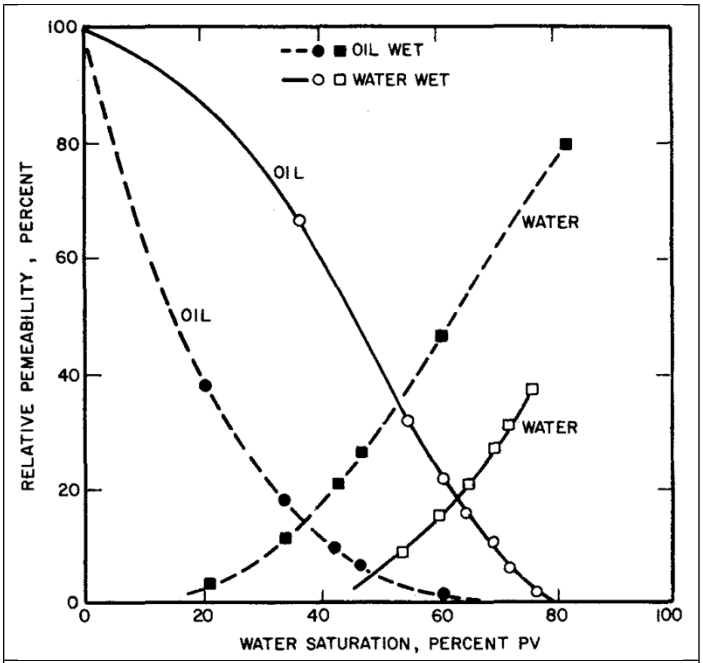

Figure 13: Steady state oil/water relative permeabilities measured with heptane and brine in water- and oil-wet synthetic alundum cores (Jennings, 1957)

unrestricted water flow, oil flow practically ceases (Craig, 1971). The remaining oil is found (1) filling the smaller pores, (2) as a continuous film over the pore surfaces, and (3) as larger pockets of oil trapped and surrounded by water (Moore and Slobod, 1956; Donaldson and Thomas, 1971; Donaldson and Crocker, 1977). Because much of this oil is still continuous through the thin oil films and can be produced at a very slow rate (Moore and Slobod, 1956; Mattax and Kyte, 1961; Morris and Weiland, 1963; Hjelmeland, and Torsaeter, 1981), the residual oil saturation is not well-defined.

Before discussing how changes in wettability affect relative permeability, we will examine relative permeability curves measured on strongly water-wet and strongly oil-wet systems. In general, at a given saturation, the relative permeability of a fluid is higher when it is the nonwetting fluid. This occurs because the wetting fluid tends to travel through the smaller, less permeable pores, while the nonwetting fluid travels more easily in the larger pores. In addition, at a low nonwetting-phase saturation, the nonwetting phase can become trapped as discontinuous globules in the larger pores that block pore throats, lowering its relative permeability. At low wetting-phase saturations the effective permeability of the nonwetting-phase often approaches the absolute permeability, demonstrating that the wetting phase does not greatly restrict the flow of the nonwetting phase (Geffen et al., 1951; Von Engelhardt and Lübben, 1957; Raza et al., 1968)

Figure 13 shows experimental relative permeabilities (normalized to the absolute oil permeability at 100 % oil saturation) for water-wet and oil-wet synthetic Alundum ™ (sintered aluminum oxide) cores with brine and heptane (Jennings, 1957). At any given saturation, the water permeability is higher and the oil permeability lower in the oil-wet core when compared with the water-wet one. Note that the relative permeability curves for the oil-wet and water-wet cores are in good agreement if they are plotted vs. wetting phase saturation (oil for the oil-wet system, water for the water-wet system), indicating the reversal of the positions and flow behavior of the oil and water (Kamath and Marsden, 1966). Generally (Craig, 1971) the water saturation at which the water and oil relative permeabilities are equal is greater than 50% in a strongly water-wet core and less than 50% in a strongly oil-wet one.

Relative permeability curves can be normalized to either (1) the absolute permeability of the core saturated with a single phase, usually brine or air, or (2) the effective permeability of the core at a specified initial saturation. The choice of normalizing permeability affects how the shape of the relative permeability curves changes as the wettability changes. Relative permeability curves normalized to absolute permeability explicitly show the decline in relative

(effective) oil permeability as the core becomes more oil-wet, whereas curves normalized to the effective oil permeability have already factored out this effect and all the curves start at the same point.

In considering the effects of wettability on relative permeability we must consider both uniform and heterogeneously wetted samples. Figure 14 (Owens and Archer, 1971) shows the effects of wettability on relative permeability for a uniformly wetted sample of Torpedo sandstone. At any given water saturation, the water relative permeability increases as the system becomes more oil-wet, and the oil relative permeability simultaneously decreases, causing a gradual reduction in the waterflooding efficiency. Owens and Archer normalized their curves with the effective oil permeability at the initial water saturation. The effective oil permeability decreases as wettability is varied from water-wet to oil-wet. At a contact angle of 0° (measured for water), the water has only a small influence on the effective oil permeability, which is almost equal to the absolute (air) permeability, because the initial 20% water saturation in the water-wet core is close to the irreducible water saturation. At this condition, the water is present in the smallest pores and as a thin film on the rock surfaces, allowing oil to flow through the larger pores. At a 180° contact angle, however, water forms blobs that can block pore throats, substantially reducing the effective oil permeability.

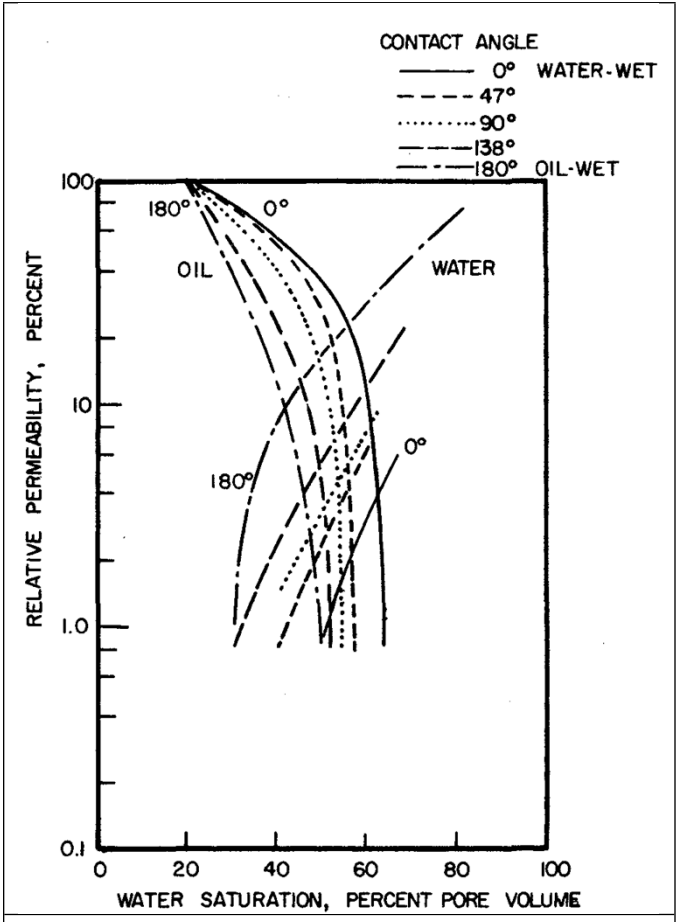

Figure 14: -Effects of wettability on relative permeability-outcrop Torpedo sandstone, brine, and barium dinonyl-naphthalene sulfonate (BDNS)-treated mineral oil. The contact angle was measured through the water. Relative permeabilities are based on the effective oil permeability, at the initial water saturation. (From Owens and Archer, 1971)

Unlike the above example, however, the wettability of many reservoir rocks is heterogeneous. This non-uniformity leads to additional wettability effects as portions of the surface are strongly water-wet, while the remainder are strongly oil-wet (Brown and Fatt, 1956; Anderson et al., 1986a; Salathiel, 1973) Such non-uniformity may also affect relative permeability. For instance, Salathiel (1973) introduced the term "mixed" wettability for a special type of fractional wettability in which the oil-wet surfaces form continuous paths through the larger pores. The small pores remain water-wet, containing no oil. The main distinction between mixed and fractional wettability is that the latter does not imply either specific locations for the oil-wet and water-wet surfaces or

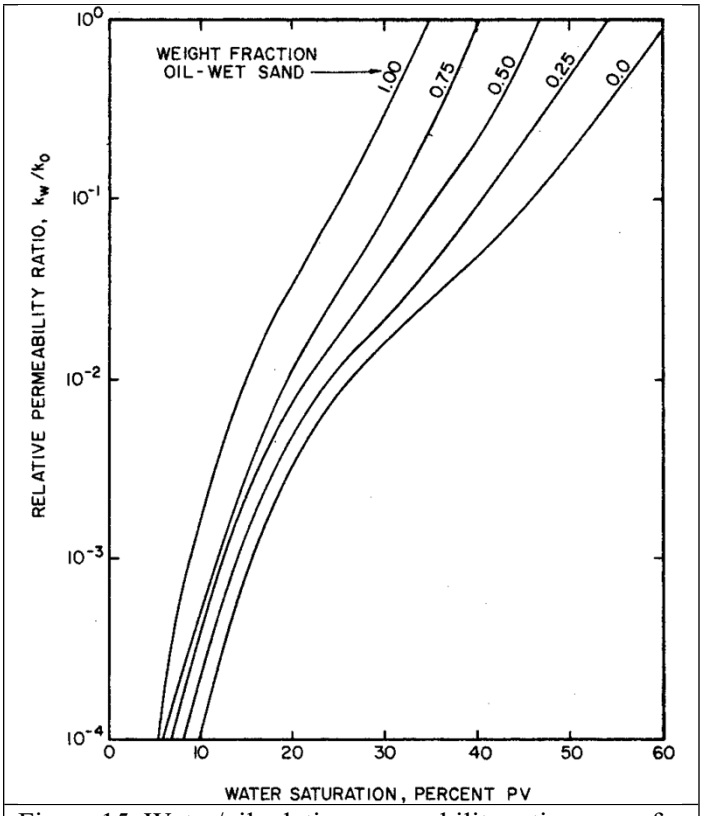

Figure 15: Water/oil relative permeability ratio curves for fractionally-wetted sandpacks. (From Fatt and Klikoff, 1959)

continuous oil-wet paths. In fractionally wetted systems, the individual water-wet and oil-wet surfaces have sizes on the order of a single pore.

Figure 15 shows the relative permeability ratios for a fractionally wetted sandpack (Fatt and Klickoff, 1959) calculated from a constant-rate waterflood data using Welge's method (Welge, 1952) as a function of the weight fraction of oil-wet sand in the pack, The changes in the relative permeability were similar to those observed when the wettability of a uniformly wetted core is changed from water-wet to oil-wet The relative permeability for waterflooding an oil-wet pack was greater than that for the water-wet one. The remaining curves lie between the two extremes. Fatt and Klikoff state that the relatively small difference between the 100% water-wet and 100% oil-wet sandpacks results from the relatively narrow pore-size distribution of the sandpack. The oil recovery decreased as the system become more oil-wet.

By contrast, Figure 16 shows changes in the relationship between water saturation and the relative permeability ratio, k_w/k_o, in a core of East Texas Woodbine sandstone that was repeatedly oil- and water flooded. (Richardson et al., 1955). This core was later shown by to have mixed wettability (Salathiel, 1973). Run 1, the initial waterflood of the native-state core, had a very low residual oil saturation, which averaged about 12 % of pore volume for the nine samples tested after the injection of roughly 40 pore volumes of water (Richardson et al., 1955; Salathiel, 1973). Three of the cores had residual oil saturations on the order of 2 % of pore volume. During repeated cycles of oil flooding followed by waterflooding, the water/oil relative permeability ratio increased for a given water saturation, as did the residual oil saturation. The relative permeability ratio for cleaned cores increased even more, and imbibition tests showed that the cleaned core was more water-wet than the native-state core.

The behavior of the relative permeability ratio as the core was cleaned and rendered water-wet contrasts with that for uniformly and fractionally wetted systems, where the relative permeability ratio at a given water saturation was lowest for a strongly water-wet system (wetting fluid displacing nonwetting fluid), and the more oil-wet curves were to the left of the strongly wet curve. In Figure 16 the water-wet curve lies to the left of the native-state curve because the native-state core has mixed wettability. At the same time that the residual oil was increasing during the repeated floods, the IWS was decreasing. The native-state core generally had a high irreducible water saturation after the first oilflood, but this dropped with repeated cycles or cleaning.

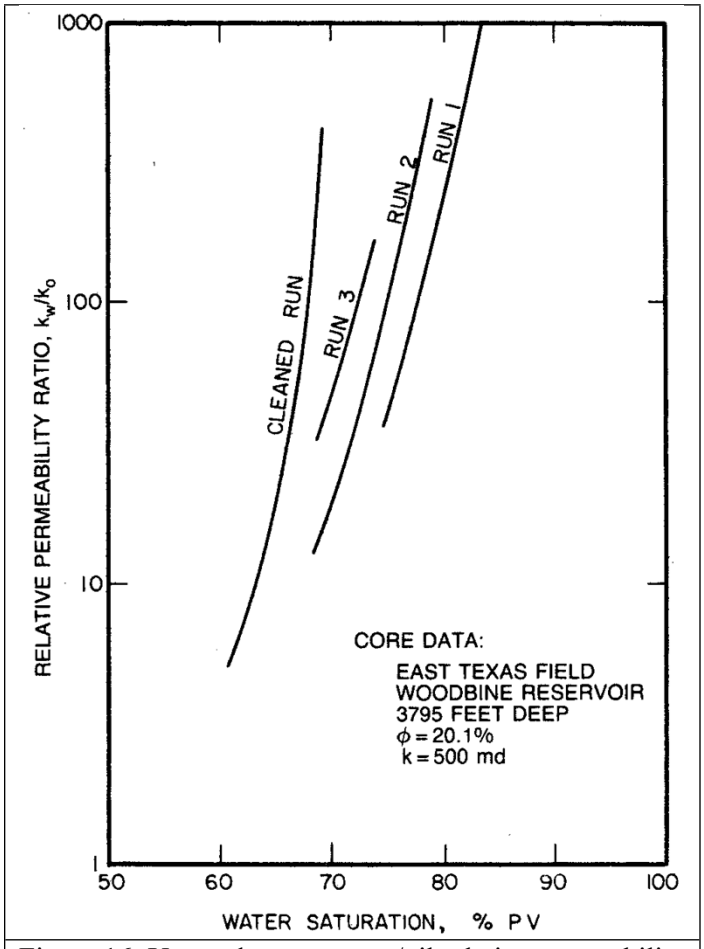

Figure 16: Unsteady-state water/oil relative permeability ratios, k_w/k_o, measured during a series of waterfloods of a native-state East Texas Woodbine core that Initially had a mixed wettability. (Richardson et al., 1955s)

Further details concerning the effects of wettability on relative permeability were provided by Anderson (1987b), from whom much of this summary has been taken. However, he drew the following conclusions concerning the effect of wettability on relative permeability.

1. Relative permeabilities are a function of wettability, pore geometry, fluid distribution, saturation, and saturation history. Wettability affects relative permeability by controlling the flow and spatial distribution of fluids in a porous medium.

2. In a uniformly wetted core, the effective oil permeability at a given initial water saturation decreases as the wettability is varied from water-wet to oil-wet. In addition, the water relative permeability increases, and the oil relative permeability decreases as the core becomes more oil wet.

3. In fractionally wetted sandpacks, where the size of the individual water- and oil-wet surfaces are on the order of a single pore, relative permeabilities appear to be similar to those in uniformly wetted systems. The water relative permeability increases, and the oil relative permeability decreases as the fraction of oil-wetted surfaces increases.

4. In a mixed-wettability core, the larger, oil-filled pores are oil wet, while the smaller, water-filled pores are water-wet. The continuous oil-wet paths in the larger pores change the relative permeability curves when compared with a uniformly or fractionally wetted system and allow the mixed-wettability system to be waterflooded to a very low residual oil saturation by the injection of many pore volumes of water.

5. The most accurate relative permeability measurements are made on native-state cores, where the reservoir wettability is preserved. When such cores are unavailable, the core should be cleaned and restored. Serious errors can result when measurements are made on cores with altered wettability, such as cleaned core or core contaminated with drilling-mud surfactants.

6. The effective water permeability of a cleaned core at the residual oil saturation (ROS) will vary, depending on the effectiveness of the core cleaning method.

7. The wetting-phase drainage and imbibition relative permeabilities show little hysteresis in many strongly wetted systems. However, several unsteady-state experiments have shown little hysteresis in the nonwetting phase, but significant hysteresis in the wetting phase.

8. In many strongly wetted systems, the wetting-phase relative permeability is primarily a function of its own saturation and is very similar for both two- and three-phase relative permeability measurements.

9. Some researchers recommend that the unsteady-state Johnson-Bossler-Naumann (JBN, Johnson et al., 1959) relative permeability method not be used in strongly water-wet cores because of insufficient time for the fluids to come to wetting equilibrium. Unfortunately, very few data are available either to prove or to disprove this hypothesis.

Experimental Wettability Analysis

What are the laboratory methods for measuring wettability (e.g., contact angle, Amott-Harvey, etc.)?

As we have just described, wettability and surface tension are closely linked phenomena. Thus, wettability can either measured directly or the three relevant surface tension pairs can be measured, and the wetting angle calculated.

There are, in fact. A large number of methods available for measuring wettability, contact angle (cf. Krishnan et al., 2005) and surface tension. These are summarized below.

Surface tension measurements (liquid/gas)

There are a number of ways in which surface tension can be measured. The optimal approach depends upon the nature of the material being analyzed, the conditions under it is to be measured, and the stability of the surface. An instrument that measures surface tension is called tensiometer.

Table 1: Methods of surface tension measurement	
Measurement Technique	Physical observation
Liquid/Gas interfaces	
Bubble Pressure (Jaeger's)	Gas pressure
Capillary Rise	height
Drop Volume	volume
Du Noüy ring	force
Du Noüy - Padday	force
Pendant drop	image
Resonant Oscillations	lasar
Spinning drop	image
Stalagmometric	volume
Vibrational frequency	frequency
Wilhelmey Plate	force
Solid/Liquid Interfaces	
Sessile drop	angle
Capillary/Fracture uptake	Position vs. time

Bubble pressure method (Jaeger's method): This approach measures the pressure required to force a gas bubble out of a capillary that is vertically immersed in the liquid to be investigated. It is performed increasing the pressure forcing gas down a tube just touching the liquid and recording the value just before the bubble emerges from the capillary tube into the liquid. Thus, the gas pressure just overcomes the capillary and hydrostatic pressures in this experiment as:

$$\gamma = \frac{r}{2}(P_{max} - hpg) \quad (37)$$

Where r is the internal radius of the capillary tube, h is the immersion depth of the capillary tube in the liquid, ρ is the density of the liquid, g is the acceleration due to gravity, and P_{max} is the pleasured bubble pressure. This technique allows measurement at short surface ages. It is clearly easy to change the gas and the liquid in this approach. Changing confining pressure or temperature is more difficult. Further details are provided at (http://www.phywe.fr/index.php/fuseaction/download/lrnfile/versuchsanleitungen/P3040101/e/p3040101e.pdf)

Capillary rise method: In this method the end of a capillary tube is immersed into a solution. The height that the solution reaches inside the capillary is related to the surface tension as: [http://mysite.du.edu/~jcalvert/phys/surftens.htm]

$$h = \frac{2\gamma cos\theta}{\rho g r} \quad (38)$$

this method is clearly somewhat dependent on the liquid-solid and gas/solid surface tensions as well.

Drop volume method: In the drop volume method, a liquid is introduced into a bulk phase through a capillary. A drop, which tries to move upwards due to buoyancy, forms at the tip of the capillary. The reverse arrangement, in which drops of the heavy phase drop from the tip of the capillary, is also possible. As a result of the interfacial tension the drop tries to keep the interface with the bulk phase as small as possible. As a new interface comes into being when the drop detaches from the capillary outlet, it is necessary to overcome the corresponding interfacial tension. The drop does not detach until the lifting force or weight compensates for the force resulting from the interfacial tension on the wetted length of the capillary, the circumference. The formula for this relationship is:

$$\gamma = \frac{\Delta\rho V g}{\pi d} \quad (39)$$

Where g is the acceleration due to gravity, V is the drop volume, d is the inside diameter of the capillary, and Δp is the difference in density between the phases. Conventionally, the measurement consists of determining the number of drops into which a given total volume divides, or in measuring the mass of the collected drops (stalagmometer, see below). As a rule, it is not possible to specify the flow rate. This results from the viscosity and height of the liquid column of the stored volume, as a result of which it changes during the measurement. With a drop volume tensiometer, the time between two detaching drops at a set flow rate can be measured by means of a light barrier. This enables the interface age (time from the start of drop formation to the moment of detachment) to be predetermined by varying the flow rate, and the interfacial tension can be measured as a function of the interface age. [https://www.kruss-scientific.com/services/education-theory/glossary/drop-volume-tensiometer/]

Du Noüy ring method: This is the traditional method used to measure surface or interfacial tension. The method involves slowly lifting a ring, often made of platinum, from the surface of a liquid. The force, F required to raise the ring from the liquid's surface is measured and related to the liquid's surface tension, γ as:

$$F = w_{ring} 2\pi(r_i + r_a)\gamma \quad (40)$$

where r_i is the radius of the inner ring of the liquid film pulled, r_a is the radius of the outer ring of the liquid film, and w_{ring} is the weight of the ring minus the buoyant force due to the part of the ring below the liquid surface. When the ring's thickness is much smaller than its diameter, this equation can be simplified to:

$$F = w + 4\pi R\gamma \quad (41)$$

where R is the average of the inner and outer radius of the ring. This technique was proposed by the French physicist Pierre Lecomte du Noüy (1883–1947) (du Noüy, 1919, 1925). The measurement is performed with a force tensiometer, which typically uses an electrobalance or a torsion wire balance to measure the excess force caused by the liquid being pulled up. The maximum force is used for the calculations, and empirically determined correction factors are required to remove the effect caused by the finite diameter of the ring:

$$F = w + 4\pi R\gamma f \quad (42)$$

with f being the correction factor. The most common correction factors are those of Zuidema and Waters (1941, for liquids with low interfacial tension), Huh and Mason (1975, which covers a wider range than Zuidema-Waters), and Harkins and Jordan (1930, which is more precise than Huh-Mason while still covering the most widely used liquids) (Udeagbara, 2010).

Du Noüy–Padday method: This is a minimized version of Du Noüy method that uses a small diameter metal rod (needle) instead of a ring, in combination with a high sensitivity microbalance to record maximum pull. The advantage of this method is that very small sample volumes (down to few tens of microliters) can be measured with very high precision, without the need to correct for buoyancy (for a rod with proper geometry). Further, the measurement can be performed very quickly, nominally in about 20 seconds.

The du Noüy Padday rod is often made from a composite metal that may be roughened to ensure complete wetting. The rod is cleaned with water, alcohol and a flame or with strong acid to ensure complete surfactant removal. It is attached to a scale or balance via a thin metal hook. The maximum force is recorded as the probe is first immersed approximately one mm into the solution and then slowly withdrawn. The primary other forces acting on a probe are the buoyancy (due to the volume of liquid displaced by the probe) and the mass of the meniscus adhering to the probe. This is an old, reliable, and well-documented technique (Harkins and Jorday, 1930; Freud and Freud, 1930; Padday et al., 1974; Fischer et al., 1998; Christian et al., 1998). No correction factors are required, the rod can be used in high throughput instruments, and the Padday technique offers low operator variance and does not need an anti-vibration table, which makes it good for use in the field. In a typical experiment, the rod is lowered to the surface being analyzed until a meniscus is formed, and then raised so that the bottom edge of the rod lies on the plane of the undisturbed surface. One disadvantage of this technique is that one cannot bury the rod into the surface to measure interfacial tension between two liquids. The surface tension is given in these measurements as:

$$\gamma = \frac{F_{Max}}{\tau_P} \tag{43}$$

Where F_{max} is the maximum measured force, and τ_p is the perimeter of the probe. https://en.wikipedia.org/wiki/DuNoüy–Paddaymethod

Pendant drop method (Figure 17): The pendent drop method has the advantage that surface tension can be measured by this technique, even at elevated temperatures and pressures. In this approach an image is obtained of a liquid drop that hangs on a dosing needle, and the shape of the drop is analyzed. Surface tension and gravitation determine the shape of the pendant drop. Surface tension seeks to minimize the surface area make the drop spherical. However, gravity stretches the drop from this spherical shape, generating the typical pear-shaped results. Gravitation also causes a pressure difference along the z-axis according to Pascal's law (hydrostatic pressure). The analysis of the drop shape is based on the Young-Laplace equation. The Laplace pressure $\Delta P(z)$ at a distance z from an arbitrary reference plane with Laplace pressure ΔP_0 is:

$$\Delta P(z) = \Delta P_0 + \rho g z \tag{44}$$

For a pendant drop the principal radii of curvature at the vertex (lowest point of the drop) are: $R_1=R_2=R$.

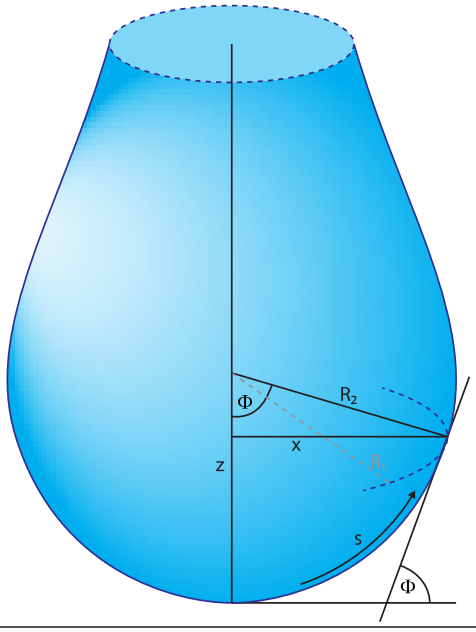

Figure 17: Schematic of the pendant drop method

Thus, it is convenient to place the reference plane in this point. For every point above it

$$R_2=x/\sin\Phi \quad (45)$$

Which, combined with equation (10) and the Young-Laplace Equation (3) this leads to:

$$\frac{1}{R_1}+\frac{sin\phi}{x}=\frac{2}{R}\pm\frac{\Delta\rho gz}{\gamma} \quad (46)$$

The introduction of a parametrization using the arc length s of the drop shape results in the following set of three first-order differential equations and three boundary values, which are solved numerically to fit the shape of the drop recorded optically:

$$\frac{d\phi}{ds}=-\frac{sin\phi}{x}+\frac{2}{R}\pm\frac{\Delta\rho gz}{\gamma} \quad (47)$$

$$\frac{dx}{ds}=cos\phi \quad (48)$$

$$\frac{dz}{ds}=sin\phi \quad (49)$$

$$0=x(s=0)=z(s=0)=\phi(s=0) \quad (50)$$

This method can also be applied when the surrounding phase is not air but another liquid. https://www.dataphysics-instruments.com/us/knowledge/understanding-interfaces/pendant-drop-method/

Resonant oscillations of spherical and hemispherical liquid drop method: The technique is based on measuring the resonant frequency of spherical and hemispherical pendant droplets driven in oscillations by a modulated electric field. It is applicable to all kinds of liquids and solutions including non-conductive, isolating liquids. The oscillations are detected optically, with the help of a laser beam. The measured resonant frequency modes and resonance half-widths may be used to obtain information about the surface properties of the droplet (surface tension and surface charge, in particular). The surface tension and viscosity can be evaluated from the resonant curves obtained. For the main mode at n = 2, the surface tension can be expressed as:

$$\gamma=\frac{\rho a^3\omega_2^2}{8}+\frac{Q^2}{16\pi a^3} \quad (51)$$

Where r is the fluid density, a is the radius of a spherical droplet w is the frequency of the oscillation, and Q is the surface charge (Tankovsky and Zografov, 2011, 2103; Zografov and Tankovsky, 2013, 2014).

Spinning drop method (Figure 18): This technique is ideal for measuring low interfacial tensions. It involves measuring the diameter of a liquid drop suspended within a heavier phase while both are rotated. Measurements are carried out in a rotating horizontal tube which contains a dense fluid. A drop of a less dense liquid or a gas bubble is placed inside the fluid. Since the rotation of the horizontal tube creates a centrifugal force towards the tube walls, the liquid drop will start to deform into an elongated shape; this elongation stops when the interfacial tension and centrifugal forces are balanced. The surface tension between the two liquids (for bubbles: between the fluid and the gas) can then be derived from the shape of the drop at this equilibrium point. The spinning drop method is usually preferred for accurate measurements of surface tensions below 10^{-2} mN/m. An approximate theory was developed by Bernard Vonnegut (1942). This assumes that the droplet's length L is much greater than its radius R, so that it may be approximated as a straight circular cylinder. This results in the equation:

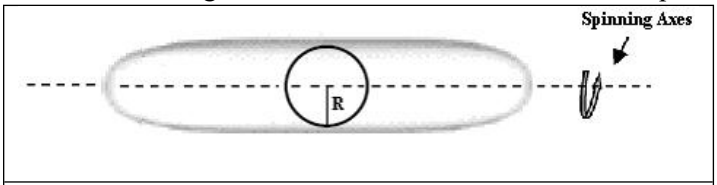

Figure 18: Geometry of the spinning drop method. https://en.wikipedia.org/wiki/Spinningdropmethod

$$\gamma = \left(\frac{\Delta\rho\omega^2}{4}\right)R^3 \qquad (52)$$

Where Δρ is the difference between the densities of the droplet and of the surrounding fluid, ω is the angular velocity of the rotating tube, and R is the internal radius of the rotating tube. A complete mathematical analysis of the shape of spinning drops was done by Princen et al. (1967). This required solving non-linear equations, but modern algorithms make these soluable. The spinning drop method is convenient because contact angle measurement is not required, and it is not necessary to estimate the curvature at the interface However, it is not expected to give accurate results for high surface tension measurements, since a much higher centrifugal force is required to maintain the drop in a cylindrical shape. (https://en.wikipedia.org/wiki/Spinningdropmethod)

Stalagmometric method (Figure 19): This method involves weighing drops of a fluid of interest falling from a capillary glass tube. A stalagmometer is a capillary glass tube whose middle section is widened (Figure 19). The volume of a drop is predetermined by the design of the stalagmometer. The lower end of the tube is narrowed to force the fluid to fall out of the tube as a drop. In an experiment, the drops of fluid hanging on the bottom of the tube fall when the volume of the drop reaches a maximum value dependent on the characteristics of the solution. At the moment a drop falls, its weight is in equilibrium state with the surface tension described by Tate's law (Tate, 1864):

$$mg = 2\pi r\gamma f \qquad (53)$$

Where m is the mass of the drop, g is the acceleration due to gravity, and r is the radius of the drop, and f is a correction factor for the fraction of the drop left on the tip of the capillary, which depends on both the tip design and the liquid being measured. In the case of a liquid which wets the stalagmometer's tip the r value is that of the outer radius of the capillary and if the liquid does not
wet the tube the r value is that of the inner radius of the capillary. If the appropriate tip shape is used the f value can be eliminated by ratioing the results to those of a known material (i.e. water. Further details can be found at
http://zzm.umcs.lublin.pl/Wyklad/FGF-Ang/2A.F.G.F.%20Surface%20tension.pdf
https://en.wikipedia.org/wiki/Stalagmometricmethod

Vibrational frequency of levitated drops method : Proposed by Trinh et al. (1988), the natural frequency of vibrational oscillations of magnetically levitated drops has been used to measure the surface tension

of superfluid ^{4}He. This value is estimated to be 0.375 dyn/cm at T = 0 K. (Vicente et al., 2002). Viscosity can also be measured in this way (Kremer et al., 2018). The frequencies of the resonant modes of shape oscillation for a free spherical inviscid liquid drop in air were first investigated by Rayleigh (1945), and the results for the case of small amplitude of oscillations (i.e., where the deviations from a spherical shape are small) with axial symmetry may be expressed as:

$$f_L^2 = \frac{L(L+2)(L-1)\gamma}{\rho R^3} \qquad (54)$$

for the L^{th} resonant mode, where γ is surface tension, ρ is the density, and R is the equilibrium radius of the spherical drop. For moderately viscous liquids, the oscillation frequency is very weakly dependent on the viscosity. In practice, however, some of the conditions required by the derivation of equation (54) might be violated. In particular, the initial shape of the sample may be oblate spheroidal rather than spherical due to action of some body force (e.g. gravity), or the amplitude of the shape oscillation may not be small compared to the drop size. The effect of translational motion and deformation of drops on their shape oscillation frequencies has been theoretically investigated by Subramanyam (1969).

Figure 19: Stalagmometer, straight form. https://en.wikipedia.org/wiki/Stalagmometricmethod

In the experiment described by Trinh et al. (1988) an ultrasonic transducer, the source of the ultrasonic wave, was placed below the sample, and a reflector was placed above the driver at a distance of three half-wavelengths. This creates the standing wave in air in the gap. The spatial acoustic pressure distribution allowed the levitation of samples slightly below any of the pressure nodes and centered on the driver/reflector axis. The shape oscillations of the levitated drop were excited by modulating the acoustic force by either amplitude modulation of the transducer drive signal, or by adding an additional signal in phase quadrature (a second, time offset sign wave). Detection of resonant shape oscillations was carried out by either monitoring the magnified shadow of a backlighted drop with a video camera and varying the modulation frequency to maximize the oscillation amplitude or using a "pseudo-extinction of light" method that allowed the detection of very small amplitude oscillations (Marston and Trink, 1985).

Wilhelmy plate method (Figure 20): This is a universal method especially suited for checking surface tension over long time intervals. A vertical plate of known perimeter is attached to a balance, and the force due to wetting is measured. This can be used to measure the surface tension of a liquid relative to a known liquid, or of the liquid relative to a known solid. The Wilhelmy plate consists of a thin plate usually on the order of a few square centimeters in area. The plate is often made from filter paper, glass or platinum which may be roughened to ensure complete wetting. The results do not depend on the

material used, as long as the material is wetted by the liquid. The plate is cleaned thoroughly and attached to a balance with a thin metal wire. The force on the plate due to wetting is measured using a tensiometer or microbalance and used to calculate the surface tension as:

$$\gamma = \frac{F}{l\cos\theta} \qquad (55)$$

where l is the wetted perimeter and θ is the contact angle between the liquid phase and the plate. In practice the contact angle is rarely measured, instead either literature values are used, or complete wetting (θ = 0) is assumed.

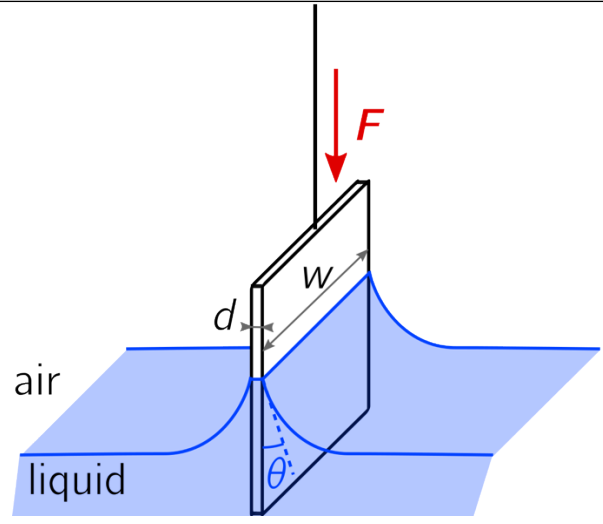

Figure 20: Illustration of Wilhelmy plate method. The magnitude of the capillary force F on the plate is proportional to the wetted perimeter l = 2w + 2d and the surface tension γ. https://en.wikipedia.org/wiki/Wilhelmyplate

Solid/liquid surface tension measurements

Sessile drop method: This is a method for determining surface tension and density by placing a drop on a substrate and measuring the contact angle. The main premise of the method is that by placing a droplet of liquid with a known surface energy on a solid surface, the contact angle and the known surface energy of the liquid can be used to calculate the surface energy of the solid. The liquid used for such experiments is referred to as the probe liquid, and several different probe liquids are required if the components of the surface energy are of interest. However, the contact angle is affected not only by surface chemistry but by surface roughness. As noted above, the Young equation (Equation 2), assumes a homogeneous, smooth surface. In case surface roughness is present, the droplet can be in a Wenzel state (homogeneous wetting), a Cassie-Baxter state (heterogeneous wetting) or in some intermediate state. The surface roughness amplifies the wetting behavior caused by the surface chemistry.

The simplest way to measure the contact angle of a sessile drop is with a contact angle goniometer, which allows the user to measure the contact angle visually. A droplet is deposited by a syringe positioned above the sample surface, and a high-resolution camera captures the image from the profile or side view. The image can then be analyzed either by eye (with a protractor) or measured using image analysis software. This type of measurement is referred to as a static contact angle measurement.

In order to measure contact angle hysteresis, the sessile droplet can be increased gradually in volume. The maximum possible contact angle is referred to as the advancing contact angle. The receding contact angle can be measured by removing volume from the drop until dewetting occurs. The minimum possible contact angle is referred to as the receding contact angle. The contact angle hysteresis is the difference between the two.

The advantages of this method are that it is relatively straight forward, and with a large enough solid surface, multiple droplets can be deposited to determine heterogeneity. The reproducibility of the contact angle reflects the surface's heterogeneity. However, if the sample is only large enough for one droplet, heterogeneity is difficult to determine. In addition, there is inherent subjectivity as to the placement of the lines to measure the contact angle, leading to a certain amount of unavoidable imprecision. https://en.wikipedia.org/wiki/Sessiledroptechnique.

Capillary/Fracture uptake – neutron imaging: this method was developed by DiStefano et al. (2017, in prep) here at ORNL using facilities at ORNL and NIST/NCNR. In this approach wettability is measured as a variable controlling spontaneous imbibition in a synthetic, planar fracture in a rock or other material. Neutron imaging, sometimes at rates up to 10 ms/image, is used to record the location of a wetting front during spontaneous imbibition of water or any other H-bearing fluid of interest into the fracture with time (Figures 11, 12). Fracture dimensions can be measured at higher resolution using X-ray computed tomography either separately or simultaneously depending on the systems available. The images also provide details of the shape fo the wetting front, which can be fitted to a suitable equation (an error function in this case) and a reference point selected to quantify the location of the front as a function of time. Because neutrons interact with the nucleus of an atom rather than its electron cloud (as X-rays do), they are quite penetrating. They are, however, scattered strongly by hydrogen, and thus see water quite well. One advantage of this technique, therefore, is that, unlike most of the techniques described above, it can be done inside a heated pressure vessel, allowing measurements to be made under reservoir conditions.

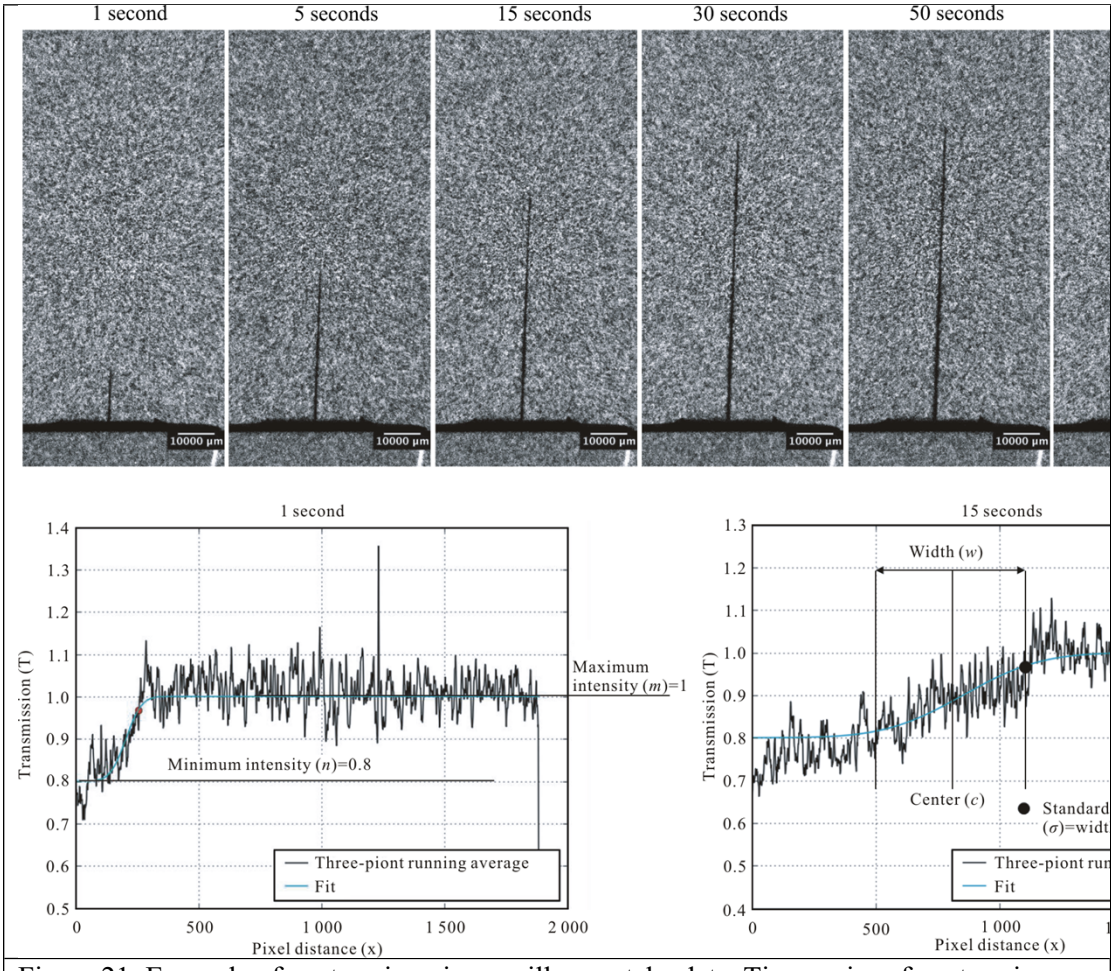

Figure 21: Example of neutron imaging capillary uptake data. Time series of neutron images that show water imbibition into EF 19 with fitted plots. Plots also show parameters for fitting. (Distefano et al., 2017)

Spontaneous imbibition occurs when a wetting fluid displaces a nonwetting fluid, such as air, under the influence of capillary suction (Gao and Hu, 2016). This has been shown to strongly affect the production of oil and gas by water blockage of oil and gas escape pathways (Cheng, 2012; Pordel Shahri et al., 2012; Li, 2007). The rate of imbibition, however, is strongly dependent on the multiscale properties of

the rock matrix. It depends on mineralogy of the source rock, total organic carbon, distribution of pore throat sizes and fractures, and wettability.

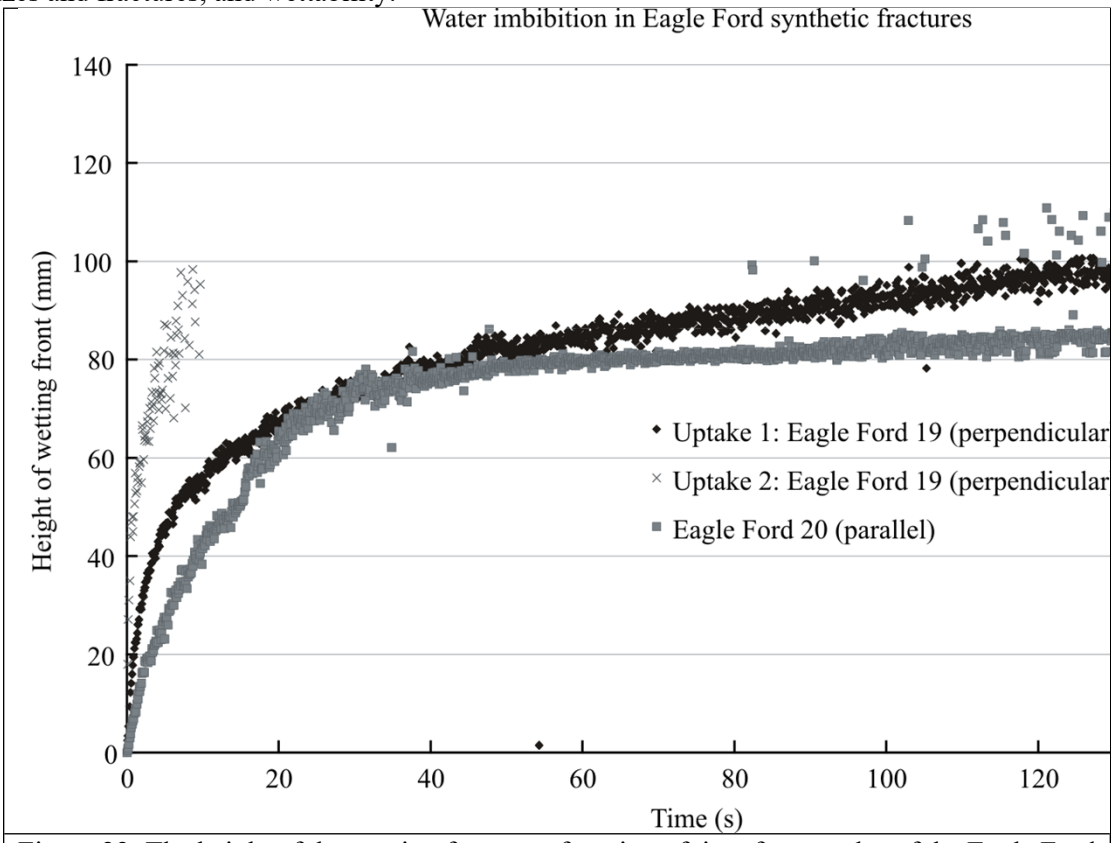

Figure 22: The height of the wetting front as a function of time for samples of the Eagle Ford shale. The visible outliers are not significant but are where the least squares algorithm failed to fit the data. (DiStefano et al., 2017)

In the simplest case, fluid in a narrow, smooth, cylindrical capillary with diameter, D, the Washburn-Lucas Equation, provides a measure of the height of the wetting front due to capillary forces as a function of time (Washburn, 1921; Lucas, 1918)

$$h = \left(\frac{\gamma D cos\theta}{4\eta}\right)t \qquad (56)$$

where h is the height of the water in the capillary, t is time, γ is surface tension, and η is viscosity. Wettability is measured by the contact angle, θ. While this equation is insufficient to describe capillary uptake in real-world fractures, or even two-dimensional planar fractures, the relation of wetting angle to the uptake process of capillary uptake is clear.

Both the work of Handy (1960), and the Washburn- Lucas model, indicate that the height of the fluid column should increase as a linear function of the square root of time. That is, that capillary uptake is, essentially, a diffusive process. The results of DiStefano et al. (2017), however, demonstrated that this was not the case, possibly due to combined effects from gravity, differential wetting along the fracture surface, roughness, and other important variables. Instead, they were able to use this approach to directly calculate changes in wetting angle. Improvements in this approach are in progress.

Wettability measurements

There are a number of methods of directly measuring the wettability of solids or, more specifically rock cores (Table 2). However, whichever methods are used, the comment of Anderson (1986a) on the treatment of the material to be measured should be kept in mind:

"Wettability is a major factor controlling the location, flow, and distribution of fluids in a reservoir. The wettability of a core will affect almost all types of core analyses, including capillary pressure, relative permeability, waterflood behavior, electrical properties, and simulated tertiary recovery. The most accurate results are obtained when native- or restored-state cores are run with native crude oil and brine at reservoir temperature and pressure. Such conditions provide cores that have the same wettability as the reservoir. The wettability of originally water-wet reservoir rock can be altered by the adsorption of polar compounds and/or the deposition of organic material that was originally in the crude oil. The degree of alteration is determined by the interaction of the oil constituents, the mineral surface, and the brine chemistry."

Table 2: Methods of measuring wettability

Measurement Technique	**Physical observation**
Macroscopic observation	Measurement of wetting angles of a liquid on a solid surface.
Amott and Amott-Harvey	Amounts of oil and water imbibed by a sample spontaneously and by force.
US Bureau of Mines (USBM)	Work required to imbibe oil and water.
Nuclear Magnetic Resonance (NMR)	Changes in longitudinal relaxation time.
Microscopic Evaluation	Microscopic examination of the interaction between the fluids and the rock matrix.
Glass Slide	Displacement of the non-wetting fluid from a glass slide.
Imbibition	Core submerged in water or oil
Relative Permeability	Shape and magnitudes of K_{ro} and K_{rw} curves.
Capillary Presssure curves	Areas under capillary pressure curves
Capillarimetric method	Measurement in a glass capillary
Displacement capillary pressure	Uses the threshold capillary pressure to calculate an apparent contact angle
Permeability/saturation relationship	Statistical. Connate water saturation vs air permeability curves
Reservoir Logs	Resistivity logs before and after injection of a reverse wetting agent.
Dye adsorption	Adsorption of a dye in an aqueous solvent.
Floatation	The distribution of grains at water/oil or air/water interfaces.

Macroscopic observation method - Direct macroscopic observation is probably the simplest, most direct method of wettability determination. It involves the direct observation and measurement of wetting angles on small rock samples or other solids of interest. One of the most popular methods for measuring the contact angle is the 'sessile drop method', which involves depositing a liquid drop on a smooth solid surface and measuring the angle between the solid surface and the tangent to the drop profile at the drop edge. In most cases the drop is small enough that the effect of gravity can be neglected. During the measurement the deposited drop deforms from its initial spherical shape, flattens to form a small cap of liquid and eventually reaches its equilibrium state. Figure 23 shows a schematic diagram of a liquid drop spreading on a solid surface. During the spreading process, the liquid drop forms a 'dynamic contact angle' with the solid surface, $\theta c(t)$, and spreads out along the horizontal axis. With the increase of the contact radius of the drop, R(t), the drop becomes thinner and its central height h(t), decreases in order to maintain a constant volume. The spreading process continues until the

'equilibrium contact angle' is achieved. This contact angle represents the wettability of the solid–liquid–fluid system and can be related to the interfacial tensions of the system by the Young equation.

While conceptually simple, these measurements are difficult to do in a consistent manner, and good results may rely more on luck than judgment. There are several issues that must be addressed when measuring contact angles in this manner:

1) Surface roughness – as discussed above, roughness can significantly affect the measured contact angle
2) Surface history - which fluid first contacted the surface will affect the measured value of the contact angle.

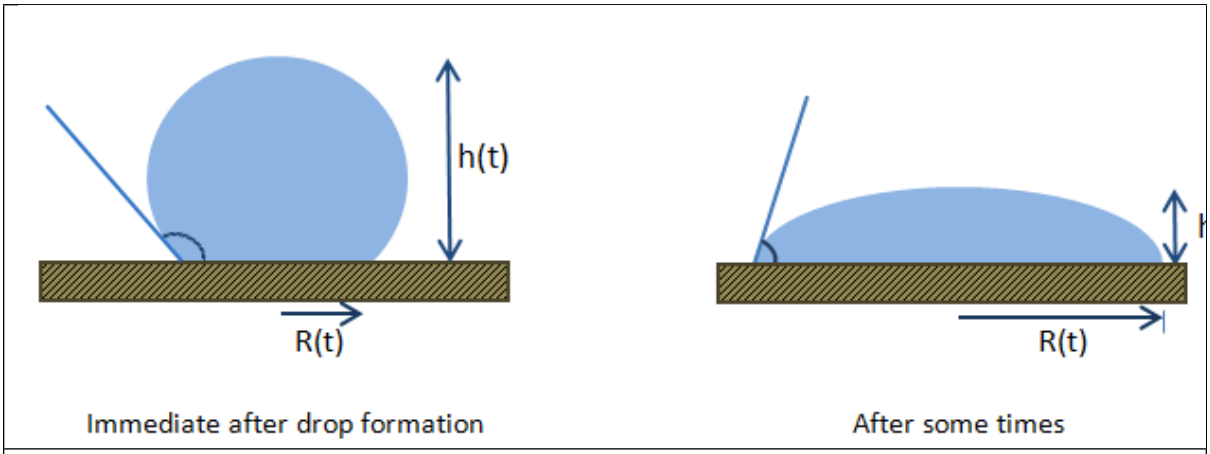

Figure 23: Liquid drop spreading on a solid surface. https://perminc.com/resources/ fundamentals-of-fluid-flow-in-porous-media/chapter-2-the-porous-medium/multi-phase-saturated-rock-properties/wettability/laboratory-determination-wettability/

3) Fluid-Rock interactions (e.g. solubility, pH, ions in the aqueous phase, reaction, polar groups in crude oil, etc.) will affect the value of the contact angle. This may change over time as the two surfaces react.
4) Polished solid surfaces may not be representative of solid surfaces in porous media.
5) Time to reach equilibrium (the point when the contact angle is independent of time) may vary from seconds to days or years. Consequently, the contact angle measured in the laboratory may not represent the natural wettability of the system under examination.

On the other hand, the direct measurement approach does have the advantage that experiments can be performed at reservoir conditions, using pressure vessels with appropriate viewing ports. Wan and colleagues, for instance (e.g. Wan et al., 2014) have used this approach to measure contact angles in supercritical CO_2-water-mineral systems using two methods: captive drop and sessile drop. In the captive-drop method, a mica plate was clipped onto the stage, the chamber was filled with water and pressurized, then a CO_2-saturated brine was used to completely displace the water. Water-saturated $scCO_2$ was then used to displace 10 volume percent of the water in the chamber. A $scCO_2$ (pre-water-saturated) droplet was then formed at the tip of a syringe from the bottom of the chamber and released upward onto the mica plate. Dynamic images of the droplet were taken, and a selected static contact angle was measured.

In the sessile drop method, the chamber was set upside down. After clip-mounting the mica sample, 5 ml of DI water was injected into the chamber to insure the water saturation of the CO_2. Then the chamber was filled with CO_2 to the desired pressure. About 1 hour after a stable P/T was obtained, a water droplet (estimated 8 µl) was generated and released onto the mica plate. High-resolution time-lapse photographs (video recordings for the dynamic CA measurements) were taken.

Regardless of the method used, however, an important conclusion of this study was that reaction of the mica with the water-saturated supercritical (sc) CO_2 phase severely roughened the muscovite surfaces, increased contact angle hysteresis and CO_2 adhesion. Although some methodological influences on contact angle uncertainty can be reduced, the high surface-energies of clean and pristine aluminosilicate minerals have a strong tendency to adsorb oppositely changed molecules and particles to reduce their surface energy, resulting in less reproducible contact angle values. Giving the fact that such mineral surfaces do not exist in real reservoirs, the utility of these results is uncertain.

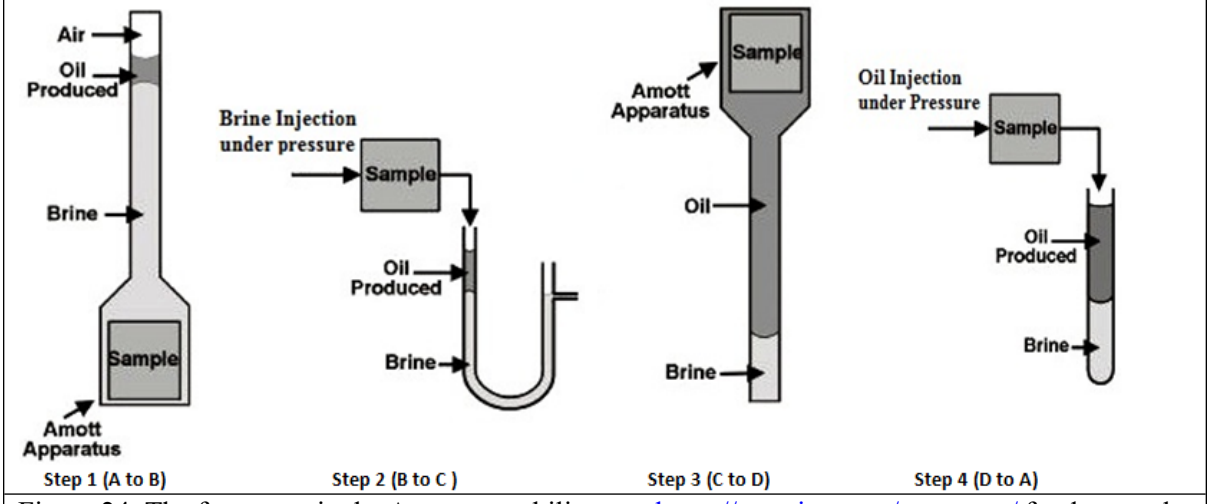

Figure 24: The four steps in the Amott wettability test. https://perminc.com/resources/ fundamentals-of-fluid-flow-in-porous-media/chapter-2-the-porous-medium/multi-phase-saturated-rock-properties/wettability/laboratory-determination-wettability/

Amott method (Figure 24)- This is a macroscopic measurement of the mean wettability of a rock by a given fluid. Wettability measurements by the Amott method provide a guide to the relative oil or brine wetting tendencies of reservoir rocks. This can be crucial in the selection of relative permeability test methods to generate data relevant to the reservoir situation. The method combines two spontaneous imbibition measurements and two forced displacement measurements (Figures 24 and 25). That is, it is a measurement of capillary imbibition. This

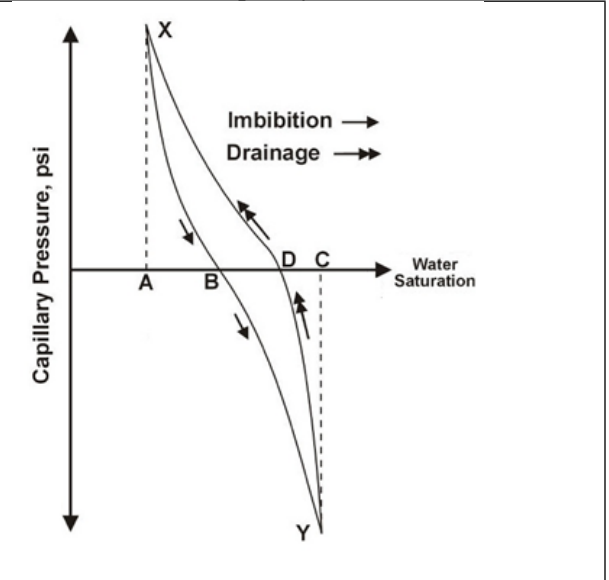

Figure 25: Calculation of the Amott index.

https://perminc.com/resources/fundamentals-of-fluid-flow-in-porous-media/chapter-2-the-porous-medium/multi-phase-saturated-rock-properties/wettability/laboratory-determination-wettability/

approach is qualitative but is an industry standard for comparing the wettability of various core plugs. In general use, the samples to be measured are centrifuged or flooded with brine, and then flooded or centrifuged in oil to obtain an S_{wir} state (irreducible water saturation, the minimum water saturation obtainable in a rock. Water is usually the wetting fluid in oil or gas reservoirs, so a film of water covers each pore surface. The surface area thus defines the irreducible water saturation. This is point A on the x-axis of Figure 25). The standard Amott method is then followed. This test defines two indices: the Amott water index and the Amott oil index.

The Amott method involves four measurements. These are shown in Figure 24, and their interpretation in Figure 25.

- Step 1: The amount of water or brine spontaneously imbibed = the amount of produced oil (AB in Figure 25).
- Step 2: The amount of water or brine forcibly imbibed = the amount of produced oil (BC in Figure 25).
- Step 3: The amount of oil spontaneously imbibed = the amount of produced water (CD in Figure 25)
- Step 4: The amount of oil forcibly imbibed = the amount of produced water (DA in Figure 25)

Initially, then the recovered core sample is saturated with oil at some initial water saturation (point X in Figure 25). Then spontaneous imbibition measurements are carried out by placing the sample in a container submerged in a known volume of the fluid to be imbibed (steps 1 and 3 in Figure 24 for imbibition of water and oil respectively). The volume of the fluid displaced by the imbibing fluid is then measured (step 1 and step 3 of Figure 24). Forced imbibition measurements are performed by injecting the imbibing fluid through the rock and measuring the amount of fluid displaced (steps 2 and 4). The important measurements are the spontaneous and total (spontaneous and forced) imbibitions of oil and water. Water-wet samples only spontaneously imbibe water, oil-wet samples only spontaneously imbibe oil, and those that spontaneously imbibe neither are called neutrally-wet. The wettability ratios for oil (AB/AC) or water (CD/CA) are the ratios of the spontaneous imbibition to the total imbibition of each fluid. A water-wet system should have an Amott Index for water close to 1 and its Amott Index for oil close to zero. An oil-wet system should have an Amott index to water close to zero, an Amott index to oil close to one.

At the end of the experiment the Amott-Harvey wettability indices are calculated as:

$$Oil\ Index = \frac{Spontaneous\ Oil\ Imbibition}{Total\ Oil\ Imbibition} = \frac{CD}{CA} \quad (57)$$

$$Water\ Index = \frac{Spontaneous\ Water\ Imbibition}{Total\ Water\ Imbibition} = \frac{AB}{AC} \quad (58)$$

$$Wettability\ Index = Water\ Index - Oil\ Index = \frac{AB}{AC} - \frac{CD}{CA} \quad (59)$$

USBM (US Bureau of Mines) Method - This method is very similar to the Amott method, but measures the work required to do the imbibitions. It is usually done using a centrifuge, and the wettability index W is calculated from the areas under the capillary pressure curves A1 and A2 as shown in Figure 26:

$$W = log\left(\frac{A1}{A2}\right) \quad (60)$$

where, A1 and A2 are defined in Figure 26. Note that in this case the initial conditions of the rock are S_w=100%, and an initial oil flood down to S_{wi} is required (shown as step 1 in Figure 26). Figure 27 shows typical USBM test curves for water-wet, oil-wet and neutrally-wet cores. Note that, while both the Amott and USBM methods are common within the oil industry, they can yield remarkably different results especially for samples near the neutral wettability region. In general, the Amott method is probably the most reliable and accurate especially in the neutral wettability region. A comparison of the two methods, together with contact angles, is given in Table 3.

Table 3: Comparison of the Amott and USBM Wettability Methods

	Oil Wet	**Neutral Wet**	**Water Wet**
Amott wettability index water ratio	0	0	0
Amott wettability index oil ratio	>0	0	0
Amott-Harvey wettability index	-1.0 to -0.3	-0.3 to 0.3	0.3 to 1.0
USBM wettability index	About -1	About 0	About 1
Minimum contact angle	105° to 120°	60° to 75°	0°
Maximum contact angle	180°	105° to 120°	60° to 75°

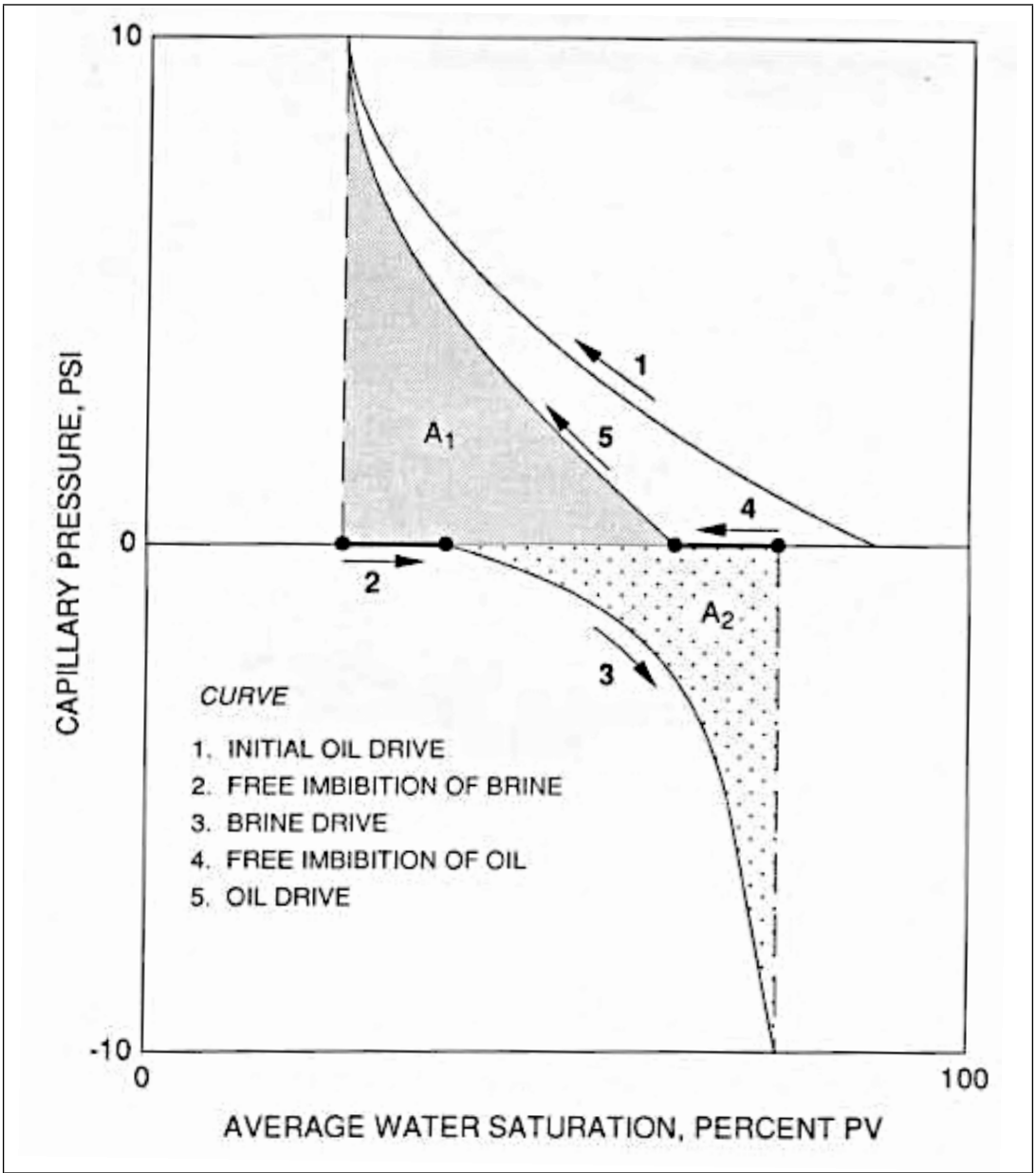

Figure 26: USBM test capillary pressure curve. Numbers indicate the progress of the test from Sw = 100%.

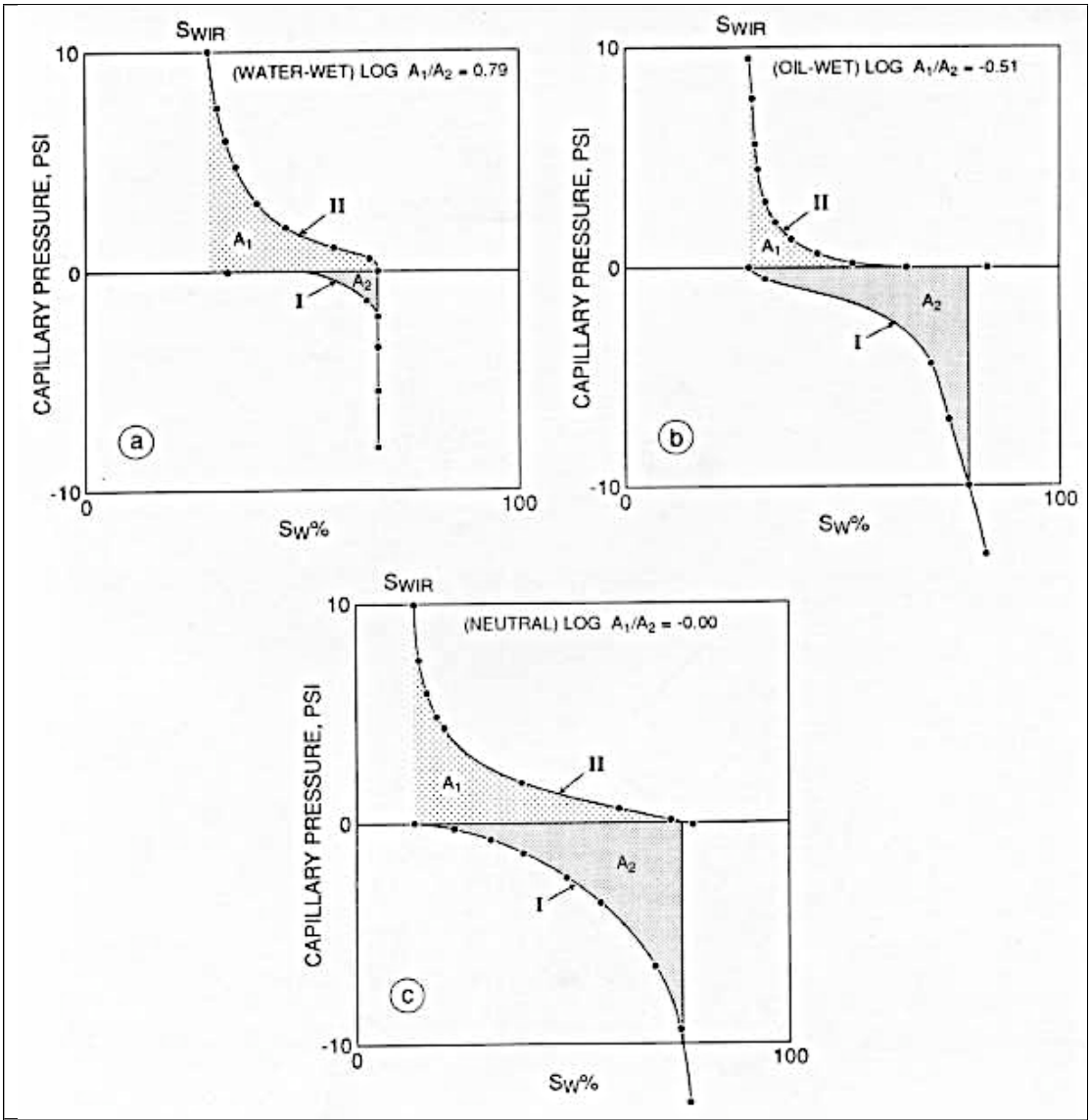

Figure 27: USBM test capillary pressure curves for: a) water wet, b) oil wet, and c) neutrally wet samples. Figure probably originally from Donaldson et al., 1969, see also Anderson (1986b)

http://homepages.see.leeds.ac.uk/~earpwjg/PGEN/CD%20Contents/Formation%20Evaluation%20English/Chapter%207.PDF

Nuclear Magnetic Resonance (NMR) - NMR is another method for measuring wettability (e.g. Brown and Fatt, 1956; Saraf et al., 1970; Hsu et al., 1992; Oren et al., 1994; Howard, 1994, 1998; Zhang et al., 2000; Freedman et al., 2001a,b; Al-Mahrooqi et al., 2003; Venkataramanan et al., 2014; Anovitz and Cole, 2015; Shikhov et al., 2019). Unlike the measurements above, however, it does not directly provide a surface tension, contact angle or wettability index, but a measurement of the relative oil/water wetting in the sample and how that changes with the fluid composition.

Anderson (1986b) summarized the technique, noting that Brown and Fatt (1956) and others (Devereauz, 1967; Kumar et al., 1969) proposed the nuclear magnetic resonance (NMR) method for determining the fraction of the core that is oil-wet vs. water-wet in a core with fractional wettability. This approach uses the nuclear magnetic thermal relaxation time for water protons (hydrogen) in porous media. To measure the relaxation time, the sample is first exposed to a strong magnetic field, which

makes the nuclei of the hydrogen atoms line up with the field. The core is then exposed to a much weaker field. The nuclear magnetic relaxation time, which is the time it takes for the hydrogen nuclei to adjust (relax) to the new field, is measured. There are two relaxation times: relaxation of the component parallel to the field is called "thermal relaxation," (this was later called T1, see below) and relaxation of the component perpendicular to the field is called' 'transverse relaxation (Brown et al., 1960, this was later called T2, see below).” The thermal relaxation time is the time used to measure fractional wettability. The T1 relaxation is called thermal relaxation because, for thermal relaxation to occur after the magnetic field is changed, the protons must dissipate some of their energy to random thermal motion of the molecules. The protons are only loosely coupled to their environment, so they require a time on the order of seconds to adjust to the new magnetic field, which is a very long time for atomic processes.

The use of nuclear magnetic relaxation times to measure wettability is based on the observation that the surfaces of porous media can significantly reduce the measured relaxation time (Brown et al., 1960; Brown and Fatt, 1956). When a proton is near a surface, it can become temporarily bound to the surface, relaxing much faster than in the bulk fluid. The wettability of the surface can, therefore, influence the relaxation time (Brown et al., 1960; Brown and Fatt, 1956; Devereauz, 1967; Kumar et al., 1969). Oil-wet surfaces cause a smaller reduction in relaxation time than water-wet surfaces.

Brown and Fatt (1956) examined 100% water-saturated sand packs in which a fraction of the sand grains were water-wet and the remainder had been treated with an organochlorosilane to render them oil-wet. They found a linear relation between the relaxation rate and the fraction of oil-wet surface area. (The relaxation rate is the inverse of the relaxation time.) The greater the fraction of oil-wet grains, the longer the relaxation time, and the slower the relaxation rate. Kumar et al. (1969) measured relaxation times with 100% water-saturated bead packs composed of water-wet glass beads and non-water-wet polymethylmethacrylate beads. The relaxation time increased linearly as the fraction of non-water-wet beads was increased.

Brown and Fatt (1956) and Kumar et al. (1969) applied their method only to sandpacks and beadpacks. Devereaux (1967) found that asphaltene adsorption in sandstone cores could also increase the relaxation time. In one set of experiments, clean sandstone plugs were saturated with crude oil, then aged for several days. The bulk of the oil was removed by flushing with cyclohexane, leaving behind a film of asphaltenes on the rock surfaces. The plugs were saturated with water, and the relaxation time measured. The adsorbed film increased the relaxation time when compared with the time for clean plugs. In another experiment, a plug was saturated with water and crude oil, aged, flushed with cyclohexane, then saturated with water. The nuclear magnetic relaxation curve for this sample had three components: (1) a fast component for water in the small pores, (2) an intermediate component for water in the large pores, and (3) a slow component for water in the large pores that had been filled with oil and coated with asphaltenes. However, Devereaux (1967) did not suggest any way to use this to measure the wettability.

Brown and Fatt (1956) also proposed a nuclear magnetic relaxation method to measure the wettability of reservoir cores, which apparently has not actually been used (as of the review by Anderson, 1986b). The method compares the nuclear magnetic thermal relaxation rate of the untreated core with reference measurements on the same core in both strongly water-wet and strongly oil-wet states. The core is first flushed with toluene or hexane to displace all of the brine and oil. After vacuum drying, the core is saturated with distilled water, and the thermal relaxation rate is measured. It is assumed that the preparation procedure above has not altered the wettability of the core. Next, the core is made strongly water-wet by flushing with methanol and chloroform or by firing at 950°F [510°C] to remove all of the adsorbed surface material. The nuclear magnetic thermal relaxation rate of the core in this water-wet reference state is then measured. Finally, the core is treated with an organochlorosilane, which renders it strongly oil-wet, and the thermal relaxation rate is measured. The reference relaxation rates for the core when it is strongly water-wet and oil-wet are plotted vs. the percent of oil-wet surface, and a straight line is drawn between them. Assuming a linear relationship between fractional wettability

and relaxation rate, the fractional wettability of the native-state untreated core is then found by plotting its relaxation rate on this straight line.

Unfortunately, this proposed procedure suffers from several problems. First, the functional relationship between relaxation rate and fractional wettability is not clear. Brown and Fatt (1956) found a linear relationship between fractional wettability and reaction rate, while Kumar et al. (1969) found a linear relationship using reaction time (the inverse of reaction rate). Second, as discussed in Anderson (1986a) the methods that Brown and Fatt (1956) suggest for preparing the original core will generally alter the native-state wettability. Finally, it is not possible to tell whether the cleaning method has rendered the core totally water-wet or the organochlorosilane treatment has rendered the core totally oil-wet. In some cases, cores treated with an organochlorosilane are only neutrally wet Anderson (1986a).

More recent laboratory studies of fluids in rock usually use a low-field NMR approach. If laboratory data are to be used for log calibration, the measurements must be based on consistent spin physics. Consequently, the industry standard for laboratory NMR core analysis has been set at an ^{1}H resonance frequency of $\nu_0 = 2$ MHz, corresponding to a magnetic field strength of $B_0 = 0.05$ T. The low field also limits the influence of internal gradients, enabling quantitative analysis (Mitchell et al. 2010). Low-field NMR measures the response of hydrogen protons in an external magnetic field. Therefore, the signal comes from water or oil in the rock and not the rock itself (Bryan et al. 2013). In the NMR experiment the protons in the oil or water are polarized in the direction of a static magnetic field, called the longitudinal direction. Another magnetic field is then applied as a radio frequency pulse to “tip” the protons perpendicular to the transverse plane, where they rotate in phase. As the protons lose energy to one another and their surroundings, the magnetic signal decays. T_1, the spin-lattice relaxation time, is a measure of how quickly the net magnetization vector (NMV) recovers to its ground state in the direction of B_0. The return of excited nuclei from the high energy state to the low energy or ground state is associated with loss of energy to the surrounding nuclei. Nuclear magnetic resonance was originally used to examine solids in the form of lattices, hence the name "spin-lattice" relaxation. T_2 relaxation, also known as spin-spin relaxation or transverse relaxation, refers to the progressive dephasing of spinning dipoles resulting in decay of the magnetization in the transverse plane

In homogeneous magnetic fields such as those generated in NMR instruments, two types of relaxation exist in fluids: bulk and surface (Straley et al. 1997). When a bulk fluid is placed in the NMR the measured transverse relaxation is bulk relaxation, or energy transferred between protons in the fluid. Bulk relaxation is a property of the fluid, related to local motions such as molecular tumbling and diffusion (Kleinberg and Vinegar 1996; Straley et al. 1997). If solids are present, surface relaxation occurs at the fluid–solid interface where the hydrogen protons are constricted by the grain surfaces and transfer energy to these surfaces. When samples of saturated porous media are measured, the amplitude of T_2 is directly proportional to porosity, and the decay rate is related to the pore sizes and the fluid type and its viscosity in the pore space. Short T2 times generally indicate small pores with large surface-to-volume ratios and low permeability.

Most published NMR studies into rock wettability have focused on the spin-lattice relaxation time T1. However, significant advances in NMR techniques have improved NMR measurements in most NMR laboratory instruments, and logging tools are able to process the NMR signals into T1 and T2 relaxation time distributions. The measurement of T2 relaxation is preferred as it is faster and usually provides similar distributions to T1.

In strongly water-wet rocks, the wetting films prevent the oil from interacting with the pore surfaces. T_2 for this non-wetting oil is governed by the interaction between the oil hydrogen nuclei, so it produces a relaxation distribution close to the bulk oil response. Any water present will be in contact with the pore walls and its T_2 relaxation will be related to the size of the pores. In a strongly oil-wet rock, the signal for oil and water will be reversed (i.e., water relaxes at bulk and oil relaxes according to pore sizes). As the bulk relaxation times for oil and water usually have different values, by analyzing the location of peaks within the T_2 distribution at different saturations, the wettability of the rock fluid system can be deduced.

The T_2 cutoff is used to define a transition point between mobile and capillary bound water. This value depends on the pore structure and surface relaxivity, which is influenced by fluid–solid interactions. Use of a single cutoff implies pores below a certain size are considered completely saturated. The T_2 cutoff can be determined in the laboratory by obtaining the T_2 distribution at two saturations, fully brine saturated and irreducible water saturation. The T_2 cutoff is defined as the relaxation time at the point where the cumulative porosity of the fully saturated sample equals the irreducible water saturation when air is used as the displacing phase:

$$Sw_{irr} = \sum_{T2=0.1ms}^{T2\ cuttoff} A(T_2) \tag{61}$$

where A is the signal amplitude in the brine saturated T_2 distribution and S_{wir} is the irreducible water saturation after desaturation to end point. An example dataset is shown in Figure 28 (Al-Marooqui et al., 2003)

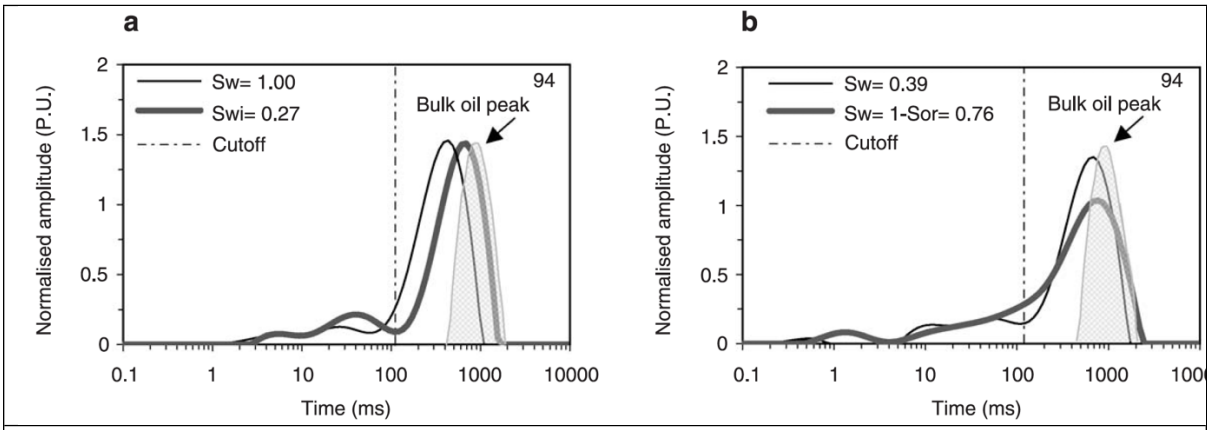

Figure 28: T_2 distributions for sample 94 at different water saturations from Al-Marooqi et al., 2004. The vertical line is the T_2 cutoff and the shadowed area is the T_2 distribution for bulk oil. (left, thin line $S_w = 1$, thick line $S_{wi} = 0.27$; right, thin line $S_w = 0.39$, thick line $S_w = S_{or} = 0.76$

Rise in Core Method

The rise in core (RIC) method is a reservoir wettability characterization method described by S. Ghedan and C. H. Canbaz in (2014). It enables estimation of all wettin regions relatively quickly and accurately in terms of contact angle rather than wettability index. The method is applicable for any set of reservoir fluids, on any type of reservoir rock at any heterogeneity level and characterizes wettability from strongly water to strongly oil wet conditions (Gheden and Canbaz, 2010). This approach is based on a modified form of the Washburn equation given as

$$cos\theta_{12} = \frac{(\mu_1\rho_1^2) - (\mu_2\rho_1^2)}{\rho_1^2\rho_2^2 C\gamma_{L1L2}} \bullet \left(\frac{m^2}{t}\right) \tag{62}$$

Where θ_{12} is the contact angle of liquid/liquid/rock system, μ_1 is the viscosity of the oil phase, μ_2 is the viscosity of the water phase, ρ_1 is density of oil phase in g/cm³, ρ_2 is density of water phase in g/cm³, m is the mass of fluid that penetrated into the porous rock, t is time in min, γ_{L1L2} is the surface tension between oil and water in dyne/cm, and C is a characteristic constant of the porous rock.

To make these measurements core plugs are divided into 3–4 core samples. The lateral area of each core sample is sealed by epoxy resin to ensure one-dimensional liquid penetration into the core by imbibition. A hook is mounted on top of the core sample with which to suspend it in a beaker of the

imbibing fluid. The core sample is suspended below a high-precision balance and positioned with its bottom barely touching the imbibing fluid in the beaker. A computer connected to a balance continuously monitors the mass of the core sample as a function of time, the slope of which generates the second part of the RIC equation (Ghedan and Canbaz, 2014, Canbaz and Gheden, 2014).

The first step is to determine the C constant. To do so the RIC experiment is performed with an n-dodecane–air–rock system. N-dodecane imbibes into one of the core samples and the imbibition curve is recorded. Dodecane is an alkane that has a low surface energy and very strongly wets the rock sample in the presence of air, with a contact angle θ equal to zero. The C constant is determined as:

$$C = \frac{\mu}{\rho^2 \gamma_{LV} cos\theta} \bullet \frac{m^2}{t} \tag{63}$$

The second step of the RIC process is to saturate samples with crude oil and subjected the sample to water imbibition. Applying the slopes of the RIC curves, the fluid properties of the oil/brine system (ρ,μ,γ) and the C value yields the calculate the contact angle, θ.

Other Methods of Measuring Wettability

While the first three methods described above are the most common and quantitative methods of determining wettability, a number of others exist. These are mostly older, and far less discussed. In fact, many sources just list them with little explanation. Many of the following descriptions are taken, in whole or in part, from Anderson (1986b).

Microscope examination - Microscope examination is sometimes used in laboratory flow visualization studies. The wettability is determined from a description of flow on a single pore level in an idealized porous medium during waterflooding (Donaldson and Thomas, 1971; Cooke et al., 1974). This description includes the structure of the residual oil and the changes in the location of the oil and water. If the system is strongly water-wet, the water surrounds the grains as a thin film. The large pools of residual oil rest on a water film, while smaller spherical drops of residual oil form in the center of the pores. If the system is intermediately wet, both oil and water are in contact with the rock surfaces, and both can be found in the small pores. Finally, if the system is oil-wet, the roles of the oil and water are reversed. The oil forms a film around the grain surfaces and is found in the small pores, while the water rests on an oil film or forms small spheres. The method of qualitatively determining the wettability by microscope examination was particularly important in the study of wettability reversals (Michaels and Timmins, 1960; Morris and Wieland, 1963; Michaels et al., 1964; Michaels and Porter, 1965; Cooke et al., 1974; Castor et al., 1981) one of the proposed mechanisms for EOR that occurs during alkaline waterflooding (Cooke et al., 1974). In these experiments, a chemical that changes the wettability is injected into the porous medium during a waterflood, causing a zone of wettability reversal to propagate through the core. A microscope is used to follow wettability changes and to determine whether EOR will occur by this mechanism.

Glass Slide Method - Another early qualitative wettability measurement technique is the glass slide method (Nutting, 1925; Reisberg and Doscher, 1956), which assumes that a glass surface is representative of the reservoir rock. In this approach a clean, dry, glass microscope slide is suspended in a layer of crude oil floating on water in a transparent container and aged. The glass slide is then lowered into the water. If the slide is water-wet, the water quickly displaces the oil on the slide. On the other hand, if the slide is oil-wet, a stable oil-wet film is formed, and the oil is very slowly displaced. Reisberg and Doscher (1956) aged slides in crude oil and found that it took up to 30 days for the final

wettability to be reached. Cooke et al. (1974) used a simple variation of the glass slide method as a quick, qualitative test to screen different acidic-oil/alkaline-water combinations for use in alkaline waterflooding experiments. They placed oil and water without mixing in a glass vial and waited to see whether a stable oil-wet film formed on the vial. This was determined by tilting the vial and seeing how the water and oil behaved on the previously oil-covered surface.

Imbibition - The most commonly used qualitative wettability measurement is the imbibition method (Bobek et al., 1958; Denekas et al., 1959; Handy, 1960; Kyte et al., 1961; Gimatudinov, 1963; Ehrlich et al., 1974). This gives a quick but rough idea of wettability without requiring complicated equipment. The original imbibition apparatus tested wettability at room temperature and pressure (Bobek et al., 1958). Kyte et al. (1961) described a modification that allows wettability to be measured at reservoir conditions. In an imbibition test, a core at IWS (irreducible water saturation) is first submerged in brine underneath a graduated cylinder, and the rate and amount of oil displaced by brine imbibition are measured. The core is strongly water-wet if large volumes of brine are rapidly imbibed, while lower rates and smaller volumes imply a more weakly water-wet core. If no water is imbibed, the core is either oil wet or neutrally wet. Non-water-wet cores are then driven to ROS (Remaining Oil Saturation) and submerged in oil. The imbibition apparatus is inverted, with the graduated cylinder below the core to measure the rate and volume of water displaced by oil imbibition. If the core imbibes oil, it is oil-wet. The strength of oil-wetness is indicated by the rate and volume of oil imbibition. If neither oil nor water is imbibed, the core is neutrally wet. Finally, some cores will imbibe both water and oil (Burkhardt et al., 1958; Mohanty and Salter, 1983; Sharma and Wunderlich, 1985). These cores have either fractional or mixed wettability. One problem with the imbibition method is that, in addition to wettability, imbibition rates also depend on relative permeability, viscosity, IFT (interfacial tension), pore structure, and the initial saturation of the core (Dullien, 1979; Anderson, 1987a). Frequently, this dependence on other variables is reduced by comparison of the measured imbibition rate with a reference rate measured when the core is strongly water-wet. To do this, the core is cleaned by heating at 750°F [400°C] for 24 hours to oxidize all of the organic material, leaving the core strongly water-wet. The core is then resaturated to its original oil saturation with a refined white oil having the same viscosity as the crude oil, and the reference imbibition rate is measured. Denekas et al. (1959) reported wettability changes in terms of the "relative rate" of imbibition:

$$R = \frac{\dot{m}}{\dot{m}_r} \tag{64}$$

where R = relative rate of imbibition, $\dot{m}$ = initial imbibition rate of the core just after it is submerged (cm^3/s), and $\dot{m}_r$ = initial imbibition rate of the cleaned, strongly water-wet core (cm^3/s). If the core is water-wet, $\dot{m}$ is the initial water imbibition rate. If the core is oil-wet, $\dot{m}$is the initial oil imbibition rate, and the relative imbibition rate, R, is reported as a negative number. Note, however, that while the use of a reference rate reduces the effect of other variables, the imbibition method still suffers from the same problem as the Amott method - insensitivity near neutral wettability. Bobek et al. (1958) also suggested an imbibition test for unconsolidated cores. In this test, a thin layer of sand is spread on a microscope slide, after which the oil saturation is increased by addition of a refined mineral oil. Droplets of water are then placed on the surface of the sand, and the movement of the fluid is observed by microscope. If the sample is water-wet, the water will move readily into the sand, displacing oil from the surface of the sand grains. In addition, the oil will form spherical droplets, indicating that it is the nonwetting phase. A similar procedure is used to test for oil wettability. This test is similar to the microscope examination method.

Relative permeability curves - A number of qualitative methods are based on the effects of wettability on relative permeability. However, they are all suitable only for discriminating between strongly water-wet and strongly oil-wet cores. A smaller change in wettability-e.g., between strongly and moderately

water-wet-may not be noticed by these methods. AS discussed above, relative permeability is the ratio of the effective permeability of that phase to its absolute permeability. That is, its permeability in single-phase flow. Relative permeability must, therefore, be between zero and one.

One method developed by Ehrlich and Wygal (1977) is based on the rules of thumb given by Craig (1971) to differentiate between strongly water-wet and strongly oil-wet cores. Craig's (Bobek et al., 1958; Kamath and Marsden, 1966; Raza et al., 1968) rules of thumb are as follows.

1. Connate water saturations are usually greater than 20 to 25% PV (pore volume) in a water-wet rock, but less than 10% PV in an oil-wet rock.

2. The water saturation at which oil and water relative permeabilities are equal is generally greater than 50% for water-wet cores and less than 50% for oil-wet ones.

3. The relative permeability to water at floodout (maximum water saturation) is generally less than 30% in water-wet rocks, but from 50 to 100% in oil-wet ones (see Figure 29).

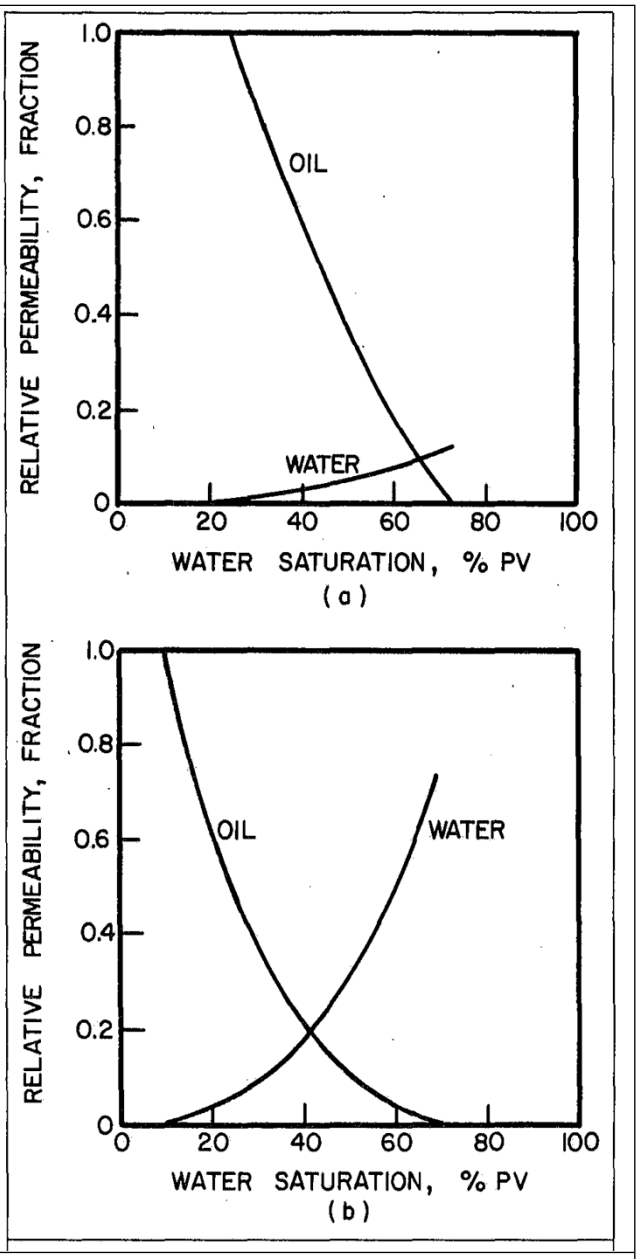

Figure 29: Typical water/oil relative permeability curves bases on the effective permeability to oil at the reservoir connate water saturation. A) strongly water-wet rock, b) strongly oil-wet rock. From Anderson (1986b) after Craig (1971).

These relative permeabilities are based on (relative to) the oil permeability at the connate water saturation. Examples of relative permeability curves in strongly water-wet and oil-wet cores taken from Craig (1971) are shown in Figure 29. Note that Raza et al. (1968) state that there are exceptions to the general rule that the connate water saturation is higher for a water-wet rock than for an oil-wet one.

Treiber et al. (1972) proposed a second qualitative technique for strongly wetted rocks. The method compares the oil/water, gas/oil, and gas/water relative permeabilities and takes advantage of the fact that relative permeability of the strongly wetting phase is a function only of its own saturation (Schneider and Owens, 1970; Craig, 1971; Owens and Archer, 1971). For example, if the sample is strongly water-wet, the relative permeability to oil (the preferentially wetting phase with respect to the gas) in the gas/oil relative permeability test should be a continuation of the relative permeability to the water (the wetting phase) in the water/oil relative permeability test (Owens and Archer, 1971). If significant differences are observed, the sample is not strongly water-wet.

An example of the comparison of the relative permeability curves in a strongly water-wet core taken from Owens and Archer (1971) is shown in Figure 30. The gas/oil drainage relative permeability, where the oil is the strongly

wetting fluid, is shown as the dotted lines. The water/oil relative permeability, where the water is the strongly wetting fluid, is shown as the solid lines. Note that the water relative permeability, where the wetting fluid saturation is increasing, is a continuation of the oil relative permeability, where the wetting fluid saturation is decreasing. This demonstrates that the core is water-wet. An example of the same test for an oil-wet formation (Treiber et al., 1972) is shown in Figure 31.

Batycky et al. (1981) developed a third wettability measurement technique based on unsteady-state relative permeability. Their method uses the capillary end effect that occurs when a core initially at IWS (Irreducible Water Saturation) is water flooded at a constant, slow injection rate. The end effect is the accumulation of wetting phase near the outlet end of the core caused by the discontinuity between the porous medium and the outlet pipe (Richardson et al., 1952). An increased pressure drop can occur because of this wetting fluid accumulation. Batycky et al. 's (1981) relative-permeability/ wettability tests are run at very slow flow rates, so end effects are very important in determination of the pressure drop across the core. In contrast, standard unsteady-state relative permeability measurements use high flow rates to minimize the end effect.

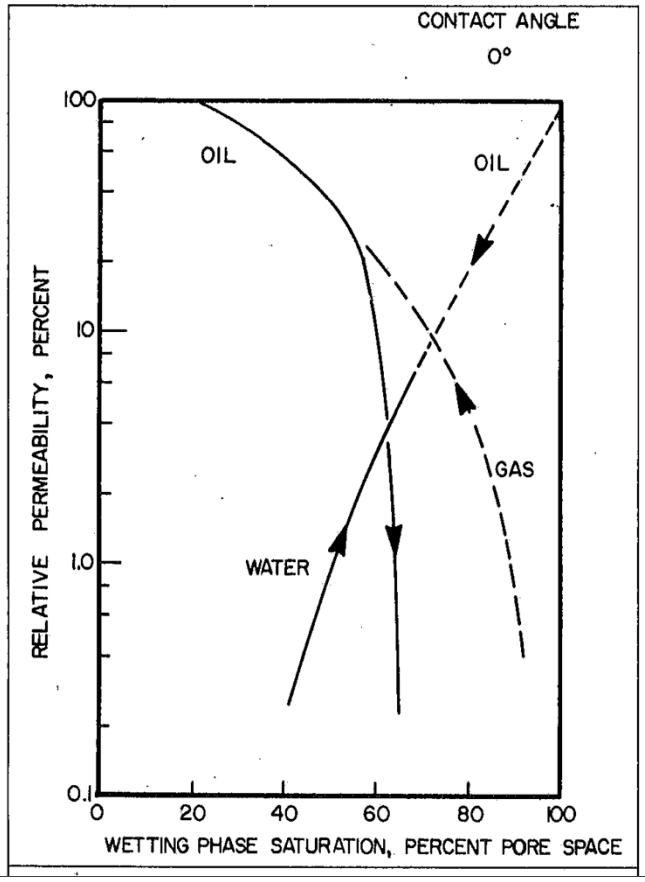

Figure 30: Comparison of gas/oil drainage and water/oil imbibition relative permeability relationships – water-wet Torpedo Sandstone. From Anderson (1986b) after Owens and Archer (1971)

Batycky et al. (1981) determined the wettability by waterflooding the core at very low rates until the ROS (residual oil saturation) was reached. The flow was then stopped to allow the fluid to redistribute, then restarted in the reverse direction. The core is water-wet if there is no change in the pressure drop after the flow reversal and oil-wet if the pressure drop is reduced immediately after the reversal. In a water-wet core at ROS, the wetting fluid saturation will be high throughout the core, with no additional water accumulation at the outlet end (Batycky et al., 1981; Marle, 1981). There will be no redistribution of fluids when the flow is stopped; consequently, the pressure drop will not change. On the other hand, if the core is oil-wet, capillary forces will cause oil (the wetting phase) to accumulate near the outlet. The pressure drop caused by this oil accumulation is detected by stopping the flow, thereby allowing capillary forces to redistribute the oil evenly throughout the core. When flow is started in the reverse direction, the pressure drop will initially be lower, gradually rising to its original value as the end effect is re-established on the opposite end of the core.

Capillary pressure curves - Calhoun (1951) suggested that the entire capillary pressure curve should be used to measure the wettability of the core. Gatenby and Marsden (1957) were the first to examine the use of the areas under the capillary pressure curves for this purpose. The capillary pressure curves used were the complete drainage and imbibition curves for both positive and negative capillary pressures measured by the porous plate method. The two areas that they examined were the total area

surrounded by the drainage and imbibition capillary pressure curves and the area under the oil-drive curve. They found that neither of these areas correlated well with the wettability of the core. However, Donaldson et at. (1969) later showed that the areas that should be measured were the areas under both the oil-drive and brine-drive curves. This is the basis of the quantitative USBM method discussed earlier.

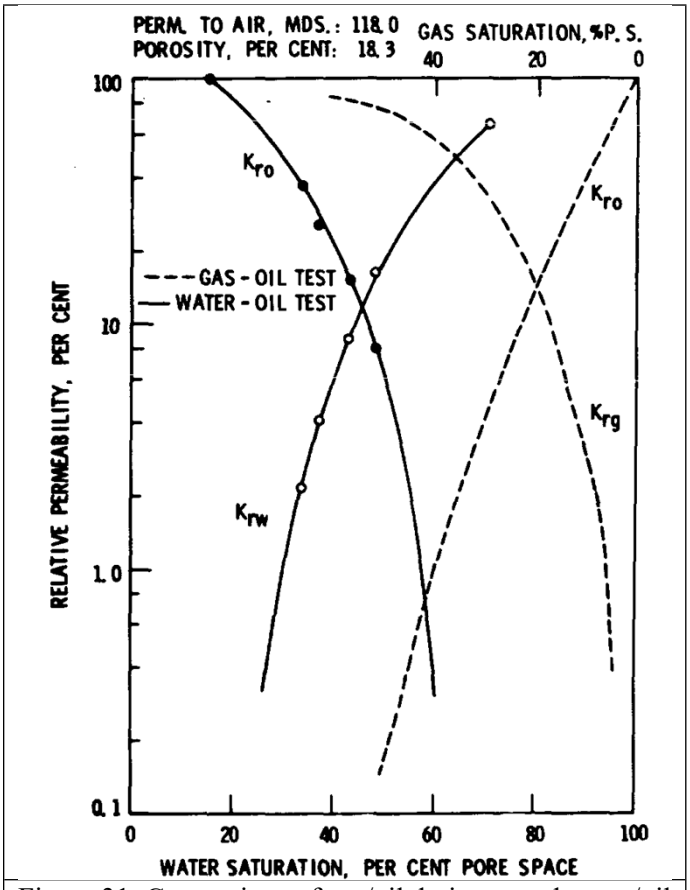

Figure 31: Comparison of gas/oil drainage and water/oil imbibition relative permeability relationships – oil-wet Miocene Kareem Formation, United Arab Republic (Egypt). From Treiber et al. (1972)

Capillarimetric method - Dunning and Johansen (Dunning and Johansen, 1958; Johansen and Dunning, 1959, 1961) developed a qualitative wettability technique that measured the adhesion tension, $\sigma\cos\theta$, in a glass capillary tube. In this method, the top of the tube is connected to a column filled with oil, while the bottom is connected to a column filled with water (see Figure 32). The top of the water column can be raised or lowered relative to the oil column, changing the hydrostatic head. As the hydrostatic head is changed, the oil/water interfaces rise or fall in the tube until the capillary forces balance the gravitational forces:

$$P_c = \frac{2\sigma cos\theta}{r} = g(\rho_o h_o - \rho_w h_w) \quad (65)$$

where r = radius of the capillary tube, ρ_o = oil density, ρ_w = water density, h_o = height of the oil column above the oil/water interface, and h_w = height of the water column above the oil/water interface. Equation 63 can be rearranged to calculate the product of σ and $\cos\theta$, which Johansen and Dunning called the displacement energy (adhesion tension).

$$E_D = \sigma cos\theta = \frac{rg}{2}(\rho_o h_o - \rho_w h_w) \quad (66)$$

The displacement energy is positive if water wets the glass and negative if oil wets the glass. If one of the liquids completely wets the glass, then the contact angle is zero, $\cos\theta$ is unity, and the displacement energy is equal to the IFT (interfacial tension). Johansen and Dunning usually
changed the height of the water column so that the interface moved over an area previously covered by oil; hence the contact angle in Equation 64 is water advancing. The capillarimetric method assumes that glass is representative of the reservoir rock and, therefore, is generally qualitative at best. Because this method measures the product $\sigma\cos\theta$, the problems discussed in the section on measuring contact angles also hinder this method.

Displacement capillary pressure - One of the earliest wettability measurements was the displacement capillary pressure method, which uses the threshold capillary pressure to calculate an apparent contact

angle (Bartell and Osterhof, 1927; Bartell and Miller, 1928; Benner et al., 1942, 1943; Slobad and Blum, 1952; Warren and Calhoun, 1955; Singhal and Dranchuk, 1975).

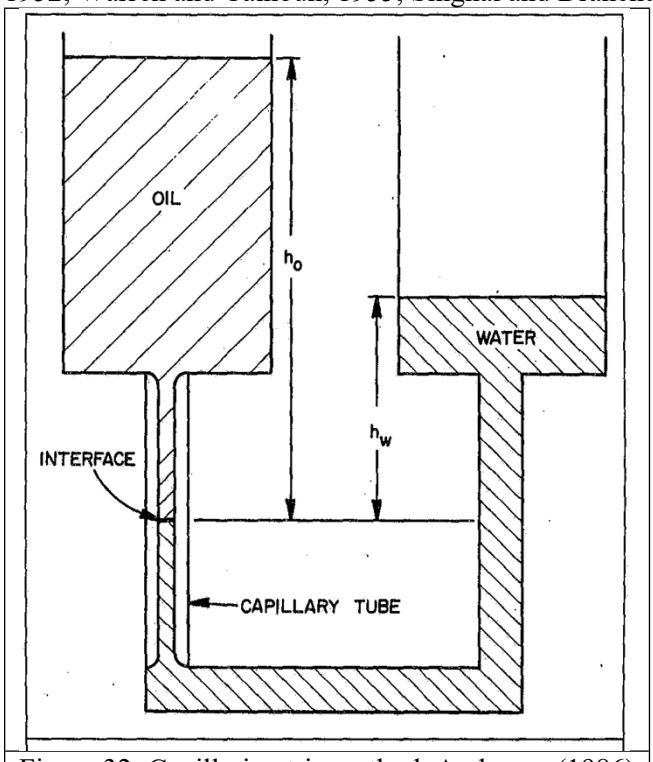

Figure 32: Capillarimetric method. Anderson (1986)

This method is now used infrequently because pore geometry effects can cause the calculated contact angle to differ significantly from the contact angle measured on a flat plate (Anderson, 1987a). The displacement (or threshold) capillary pressure is the capillary pressure at which a nonwetting fluid will first enter a core initially 100% saturated with the preferentially wetting fluid. An apparent contact angle is calculated from the threshold capillary pressure by modeling the rock as a straight, cylindrical capillary tube (Adamson, 1982; Dullien, 1979):

$$P_T = \frac{2\sigma cos\theta_a}{r_{max}} \qquad (67)$$

where P_T is the displacement capillary pressure, σ is the IFT, θ_a is the apparent contact angle, and r_{max} is the radius of the pore through which the nonwetting fluid begins to enter the core. Because the capillary pressure needed to inject nonwetting fluid is reduced as the pore radius is increased, r_{max} is an average of the radii of the largest pores in the core. Note that one limitation of this method is that it examines the wettability of only the largest pores. Because Equation 67 has two unknowns, θ_a and r_{max}, the only way to solve for the apparent contact angle is to make additional assumptions. It is usually assumed that some fluid exists that will completely wet the core, so $\cos\theta=1$, and r_{max} can be calculated. This allows the contact angle to be computed for other fluid pairs. Slobod and Blum (1952) proposed two semiquantitative wettability measurements based on the displacement capillary pressure, the wettability number, and the apparent contact angle. The wettability number is calculated by carrying out two displacement experiments - first, water by oil, and second, oil by air. Equation 67 for the oil/water/rock system becomes:

$$P_{(o-w)T} = \frac{2\sigma_{o-w}cos\theta_{o-w}}{r_{max}} \qquad (68)$$

and for the air/oil/rock system,

$$P_{(a-o)T} = \frac{2\sigma_{a-o}cos\theta_{a-o}}{r_{max}} \qquad (69)$$

In both equations, the radius of the pore is assumed to be the same. The wettability number, N, is determined by solving Equation 69 for the ratio of the cos θ terms:

$$N = \frac{cos\theta_{o-w}}{cos\theta_{a-o}} = \frac{\sigma_{a-o}P_{(o-w)T}}{\sigma_{o-w}P_{(a-o)T}} \qquad (70)$$

Slobod and Blum (1952) stated that if it were assumed that the oil is completely wetting in the oil/air/rock system, then cos $\theta_{a\text{-}o}$ is unity. An apparent contact angle for the oil/water system can then be computed from Equation 70:

$$cos\theta_{(o-w)_a} = \frac{\sigma_{a-o}P_{(o-w)T}}{\sigma_{o-w}P_{(a-o)T}} \quad (71)$$

Slobod and Blum (1952) realized that their assumptions were only approximately true and that the contact angle that could be calculated from the displacement pressure was, at best, only semiquantitative. In general, the apparent contact angle measured from the displacement pressure is not equal to the contact angle measured on a smooth surface because of pore geometry effects. Morrow and his coworkers (Morrow and Mungan, 1971; Morrow, 1976; Morrow and McCaffery, 1978) compared apparent contact angles computed in sintered Teflon cores using pure fluid with the true contact angles measured on a smooth Teflon plate. They found that there was no change in the apparent contact angle when the true conflict angle was varied from 0 to 22° [0 to 0.4 rad]. In addition, when θ was greater than 22° [0.4 rad], the apparent contact angle was always less than the true contact angle. Finally, in some cases, the apparent contact angle calculated from the displacement pressure can show the wrong fluid to be the wetting phase. Positive displacement pressures for both fluids, particularly when the core is initially 100 % saturated with the other fluid, have been frequently reported in the literature (Brenner et al., 1942; Stahl and Nielsen, 1950; Kinney and Nielsen, 1950, 1951; Calhoun, 1951; McCaffery, 1973; Morrow and McCaffery, 1978; Singhal and Dranchuk, 1975). When a positive displacement pressure is required for both fluids, the fluid with the lower displacement pressure is the preferentially wetting fluid because less energy is required to force it into the core (Calhoun, 1951; Kinney et al., 1951). Anderson (1987a) provides further discussion.

Permeability/saturation relationships - Two qualitative methods of measuring wettability based on air permeability and fluid saturations have been proposed. Both are statistical, require a relatively large number of samples, and give only a very rough idea of the wettability. The advantage of the methods is that only routine core analysis techniques are required, but the reliability of these methods is unknown. They are also limited to core samples without significant fractures or vugs, in which the pore structure determines the air permeability.

The first of these was suggested by Raza et al. (1968), who proposed an empirical method to determine reservoir wettability based on connate water saturation and air permeability. To obtain the connate water saturation, cores are obtained with an oil-based drilling fluid, and the freshly cut cores are then analyzed for their water content. The cores are extracted and dried, and the air permeability is then measured. A qualitative measure of the wettability is obtained by plotting the connate water saturation vs. the air permeability, Figure 23 shows examples of the plot for strongly oil-wet and strongly water-wet conditions (Raza et al., 1968). For the oil-wet case, the average connate water saturation is generally relatively low. The curve is nearly vertical and extends over only a small saturation interval. Conversely, for the water-wet reservoir, the curve has a gentler slope and extends over a large saturation interval.

Frehse (1973) proposed a second statistical method based on the assumption that low-permeability core samples will have a higher wetting-phase saturation than high permeability cores. For a uniformly wetted rock, the small pores are filled with the wetting fluid, while the large pores contain both the wetting and nonwetting fluids. In comparison to higher-permeability samples, a low-permeability sample will generally have a pore structure containing a larger

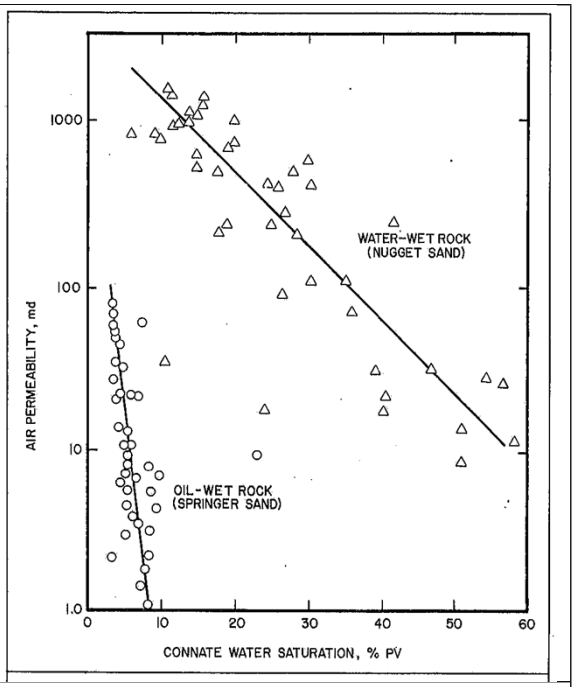

Figure 33: Relationship between connate water saturation and air permeability for water-wet and oil-wet sands. From Anderson (1986b) after Raza et al. (1968)

number of small pores that are filled with the wetting fluid. To determine the wettability, Frehse (1973) classified routine core analysis samples into different permeability ranges. The saturation distributions for the highest and lowest permeability ranges are then compared. For example, consider a core taken with a water-based mud, where the residual oil saturations are known. The reservoir is assumed to be oil-wet if the low-permeability samples have a higher average ROS and water-wet if the high-permeability samples have a higher oil saturation. Currently, this method appears to be only theoretical. No tests comparing the results of this method with more standard wettability measurements, such as the Amott or USBM indices have been published.

Anderson (1986b) felt that wettability evaluations based on air permeability and fluid saturations should not be used at that time. Raza et al. 's (1968) method is empirical, and it is not known whether it is generally valid. Frehse's (1973) method had not been tested. Until these-methods are evaluated by comparison with standard wettability measurements, Anderson (1986b) felt they should be considered unreliable.

Grigor'ev (1980) proposed a theoretical method for determining an apparent contact angle based on the IWS and ROS. The method is probably not generally valid. It is based on a large number of unproven assumptions about the behavior of the water/oil/rock system. In addition, there do not appear to be any tests comparing this method with other wettability measurements.

Reservoir Logs - Graham (1958) proposed a method for measuring the wettability of *in-situ* reservoir rock from well-log data based on the fact that the electrical resistivity of an oil-wet rock is higher than that of a water-wet rock at the same saturation. In Graham's method, the formation is injected with brine, and resistivity logs are run. The formation is then injected with the same brine containing a reverse wetting agent, which will change a water-wet formation to an oil-wet one; if the formation is already oil-wet, the reverse wetting agent will not alter the wettability. After logs are rerun, the wettability of the formation can be determined by comparing the two resistivity measurements. If the formation was originally water-wet, the change to oil-wet will increase the resistivity. If the formation was oil-wet, no change in resistivity will be observed. Holmes and Tippie (1977) proposed a second method that Compares logs with core data. The saturation in a formation is first measured with logs and the data, converted into a capillary pressure curve. Next, the capillary pressure is measured in a clean water-wet core where it is assumed that the contact angle is zero, and the two capillary pressure curves are compared. If they agree the reservoir is strongly water-wet. If they do not agree, Holmes and Tippie (1977) model the porous medium as a series of straight cylindrical capillaries and determine the apparent contact angle with equations similar to those discussed in the section on displacement capillary pressure. Because of the number of approximations, this apparent contact angle will provide only a rough estimate of the actual reservoir wettability.

Dye adsorption - Holbrook and Bernard (1958) used the adsorption of methylene blue from an aqueous solution injected into a core to measure fractional wettability. This method successfully measured the

wettability of fractionally-wetted sandpacks containing mixtures of oil-wet and water-wet sands. However, the method will probably not work for reservoir cores containing large amounts of clay.

In the dye adsorption method, water-covered rock surfaces are assumed to be water-wet, while oil-covered ones are assumed to be oil-wet. The technique is based on the observation that a rock surface covered with water will adsorb a large amount of methylene blue, whereas one covered with oil will not. The dye adsorption of the test core is measured at ROS (residual oil saturation), where essentially all of the wetting phase is continuous (Brown, 1957; Raymondi et al., 1961; Salter and Mohanty, 1982; Jones, 1985). This enables the dye to adsorb on essentially all of the water-covered, water-wet surfaces. A reference dye adsorption measurement is made on an adjacent core plug that is cleaned to render it totally water-wet. The cleaned reference plug is saturated with brine, so the entire rock surface is water covered. The fractional wettability is then established by dividing the dye adsorption of the test core by that of the 100 % water-wet reference core. When this method was tested on fractionally wetted sandpacks containing mixtures of oil-wet and water-wet sands, a linear relationship between the fractional wettability and the dye adsorption was found.

The dye adsorption test actually measures the fraction of the total surface area of the core that is contacted by the injected water. Because of this, both oil and water must be present in the core when the dye adsorption is measured. The dye adsorption method makes two additional assumptions: the water phase is continuous at ROS, so the dye contacts all of the water-covered surfaces; and the thin films of oil and water coating the rock surfaces are not affected by large changes in saturation. Tracer experiments have shown that essentially all of the water is continuous at ROS for both water-wet and oil-wet cores (Salter and Mohanty, 1982). The assumption that the thin films of oil and water are not affected by large changes in saturation seems reasonable because the amount of liquid in the thin films is very small in comparison with the bulk fluids. Shankar and Dullien (1981) examined how dye adsorption varied with water saturation in Berea sandstone cores. They injected oil and brine at constant rates and allowed the saturations in the core to reach equilibrium. The injection was then switched from brine to dyed brine, and the dye adsorption was measured. They found that the dye adsorption was almost constant when the water saturation was greater than 40% PV (pore volume). The dye adsorption decreased at lower saturations, where the water started to lose continuity. These measurements show that the wettability of a core measured by dye adsorption is not dependent on the saturation, except possibly at water saturations near IWS.

Although the fractionally wetted sandpacks that were used by Holbrook and Bernard (1958) did not contain clays, they realized that clays would strongly affect dye adsorption in reservoir cores. This occurs because the surface area and dye adsorption capacities of clays are much larger than those of sand grains (Hang and Brindley, 1970; Shankar and Dullien, 1981). Holbrook and Bernard stated that their test would measure the fraction of the clay surface that was water-wet in a reservoir core. However, they had problems when measuring the dye adsorption and fractional wettability of cores containing a significant amount of montmorillonite. Irreversible changes in the clay structure of the water-wet reference core resulting from extraction and drying caused them to calculate relative water wettabilities that were greater than 100 %. Note, however, that Anderson (1986b) suggested that it may be possible to use supercritical drying to avoid these problems (Heaviside et al., 1983).

Floatation

How have laboratory flotation experiments been used in the mining industry to assess wettability?

The basics of using the floatation method to measure wettability were also summarized by Anderson (1986b). He noted that these flotation methods are fast but work only for strongly wetted systems. In the simplest method, water, oil, and sand are placed in a glass bottle. The bottle is shaken, and the experimenter observes the fate of the sand grains (Nutting, 1925; Bartell and Osterhof, 1933; Rust, 1957; API, 1977). This method was recommended by API for determining the effects of surfactants on wettability (API, 1977). If the system is strongly water-wet, clean sand grains will settle to the bottom

of the bottle. Sand grains placed in the oil will aggregate and form small clumps of grains surrounded by a thin layer of water. If the system is oil-wet, some of the grains can be suspended at the oil/water interface. Oil-wet sand grains in the water will clump together, forming small oil globules coated with sand. This flotation system is qualitative and works only for strongly wetted systems. Several experimenters (Celik and Somasundaran, 1980; Clementz,1982) have used more elaborate flotation tests developed in the mining industry that were based on liquid/liquid extraction (Lai and Fuerstenau, 1968; Popiel, 1978). In these tests, particles are initially suspended in water. A second fluid, either oil or air, is bubbled from below. The particles that are water-wet remain in the water, while the hydrophobic, oil-wet particles adhere to the oil (air) and rise to the surface. The fraction of particles in each phase can then be measured. Clementz (1982) used the flotation method to measure the wettability of small clay particles, which cannot be conveniently measured in any other way. Untreated, strongly water-wet particles would not float. After exposure to crude oil, the clay particles floated, demonstrating that their wettability had been altered. Flotation tests based on liquid/liquid extraction appear to divide particles into two categories: strongly water-wet, and mildly water-wet to strongly oil-wet (Gaudin, 1957; Glembotskii et al., 1972). Besides the wettability, flotation of a particle also depends on particle size, particle density, and IFT. A small particle with low density and high IFT might float if the contact angle was greater than about 30° [0.5 rad]. On the other hand, the minimum contact angle for flotation of a large, dense particle could be 90° [1.6 rad] (Gaudin, 1957; Glembotskii et al., 1972).

Since the summary by Anderson (1986b) a great deal of additional work on froth floatation has been undertaken in the mining industry. It is also an important technique in waste water treatment and paper recycling. The Critical Materials Institute, a DOE funded project at ORNL, has specifically been working on using and improving this approach to purify rare earth minerals from US deposits.

They key process in froth flotation is selective separation of hydrophobic materials from hydrophilic. While it dates back to ancient times (Nelson, 2012), in the 20th century it became "the single most important operation used for the recovery and upgrading of sulfide ores" (Jameson, 1992). The basic procedure for froth floatation is as follows. (https://en.wikipedia.org/wiki/Frothflotation) First, the ore to be treated is reduced to fine particles by crushing and grinding (a process known as comminution) so that the various minerals exist as physically separate grains (liberation). The particle sizes are typically less than 0.1 mm (100 μm), but sometimes sizes smaller than 7–10 μm are required (Nihill et al., 1998). The ground ore is mixed with water to form a slurry and the desired mineral is rendered hydrophobic by the addition of a surfactant or collector chemical (although some mineral surfaces are naturally hydrophobic). The particular chemical depends on the mineral to be recovered and, perhaps, those that are not wanted. For example, sodium ethyl xanthate may be added as a collector in the selective flotation of galena (lead sulfide) to separate it from sphalerite (zinc sulfide). A great deal of research my go into determining the best collectors, as is the case for the ongoing work on rare earth mineral production. As the main purpose of this process is to modify which phases are hydrophobic, and which hydrophilic, it is this work, potential modifying water-wet vs oil-wet behavior in a reservoir, which may be of interest here, rather than the froth floatation process itself.

The slurry (called the pulp) is then introduced to tanks known as flotation cells that are aerated to produce bubbles. The hydrophobic particles attach to the air bubbles, which rise to the surface, forming a froth (Williams, 1991). The froth is removed from the cell, producing a concentrate. Frothing agents, known as frothers, may be introduced to promote the formation of a stable froth on top of the flotation cell. The minerals that do not float into the froth are referred to as the flotation tailings or flotation tails. These may be subjected to further stages of flotation to recover valuable particles that did not float the first time. This is known as scavenging. The final tailings after scavenging may be pumped for disposal or treated separately (e.g. the in sphalerite/galena example above both the lead and zinc are valuable).

Froth flotation efficiency is determined by a series of probabilities: those of particle–bubble contact, particle–bubble attachment, transport between the pulp and the froth, and froth collection (Atkinson et al., 1993) In a conventional, mechanically-agitated cell, the void fraction (i.e. volume occupied by air bubbles) is low (5 to 10 percent) and the bubble size is usually greater than 1 mm

(Atkinson et al., 1995). This results in a relatively low interfacial area and a low probability of particle–bubble contact (Atkinson et al., 1995; Pease, 2007) To be effective on a given ore slurry, the collectors are chosen based upon their selective wetting of the types of particles to be separated. A good collector will adsorb, physically or chemically, with one of the types of particles, and not with others. This provides the thermodynamic requirement for the particles to bind to the surface of a bubble. The wetting activity of a surfactant on a particle can be quantified by measuring the contact angles that the liquid/bubble interface makes with it. Another important measure for attachment of bubbles to particles is induction time. The induction time is the time required for the particle and bubble to rupture the thin film separating the particle and bubble. This rupturing is achieved by the surface forces between the particle and bubble.

The mechanisms for the bubble-particle attachment consists of three steps, collision, attachment and detachment. The collision is achieved by particles being within the collision tube of a bubble and this is a function of the velocity and radius of the bubble. The collision tube is the region in which a particle will collide with the bubble, with a perimeter corresponding to the grazing trajectory.

Attachment of the particle to the bubble is controlled by the particle/bubble induction time. The particle and bubble need to bind, and this occurs if the time in which the particle and bubble are in contact is larger than the required induction time, which is a function of the fluid viscosity, particle and bubble size and the forces between the particle and bubbles. The air bubbles will attach to more hydrophobic particles. The attachment of the bubbles to the surface is determined by the interfacial energies between the solid, liquid, and gas phases and, as we have been discussing, this is determined by the Young-Dupré Equation and, therefore, is a wetting phenomenon.

Detachment of a particle and bubble occurs when the force exerted by surface tension is exceeded by shear and gravitational forces. These forces vary within the cell. High shear will be experienced close to the impeller of a mechanical flotation cell and gravitational forces are most important in the collection and cleaning zone of a flotation column.

Significant issues of entrainment of fine particles occurs as these particles experience low collision efficiencies as well as sliming and degradation of the particle surfaces. Coarse particles show a low recovery of the valuable mineral due to the low liberation and high detachment efficiencies.

A key factor is that minerals targeted for separation can be, and often are chemically surface-modified with collectors so that they are more hydrophobic. Collectors are a type of surfactant that increase the natural hydrophobicity of the surface, increasing the separability of the hydrophobic and hydrophilic particles. Collectors either chemically bond via chemisorption to the mineral or adsorb onto the surface via physisorption. As noted above, they must be selected to bond to specific minerals being separated and not to others. For instance, Tall oil fatty acids are a common collector used for separation of rare-earth minerals (cf. Satur et al., 2016). However, significant work has been ongoing to find better materials to improve the separation, in part because one typical ore mineral, bastnaesite, is a carbonate, which is, therefore difficult to separate cleanly from calcite in the matrix (Cui and Anderson, 2017; Everly et al., 2018; Owens et al., 2018). For applications to oil recovery, therefore, the key would be the selection of an appropriate collector (see discussion of surfactants above) that is highly selective for the minerals present in the reservoir without being cost-prohibitive.

Can DOE identify any significant limitations of the current laboratory methods for evaluating/measuring wettability? If so, can DOE recommend alternate or new laboratory methods for measuring wettability that may mitigate these limitations?

It is clear from the above descriptions of methods for the measurement of surface tension and wettability that methods for measuring either value under reservoir conditions, while not lacking, are limited. This primarily reflects the underlying requirement in all cases that measurements be made through a window. Thus, they are essentially identical to, if more complex to complete, room pressure/temperature experiments, and suffer from the paired limitations inherent in each applicable low-pressure technique and those involved in using high pressure windows. What is needed is an approach that can be

performed accurately and precisely without physical optical observation from outside the pressure vessel. This might include non-optical observations, such as neutron imaging, or a wholly independent approach such as dielectric spectroscopy or resistivity measurements that do not require direct optical observation.

It is also clear from several of the papers mentioned above that when the fluid composition changes wetting properties can be time-dependent due to surface interactions/reactions between the new fluid and the mineral or organic surface. This is a poorly understood phenomenon. Reflectometry (X-ray or neutron) and other approaches could be used to understand this at a molecular scale in order to better predict how such changes (i.e. during CO_2 flooding, hydraulic fracturing fluids, surfactants etc.) may affect wettability and recovery.

An important consideration in wettability is mixed and fractional wetting. This clearly happens on a grain-by-grain scale but is difficult to analyze. We have been in discussions with an AFM company, and currently have a proposal in, to develop an instrument that would allow this to be studied at and below this scale. **

Wettability in Real Reservoir Rocks

• What mechanisms control reservoir wettability (e.g., ionic composition of formation water, reservoir lithology, oil composition, pH and temperature, among others)?

As discussed above, wettability is a function of the surface tension at water-gas-rock interfaces. It is, therefore, a function of the surface chemistry at that interface (cf. Abdallah et al., 2007; Purswani et al., 2017). Because of its relationship to both capillary uptake and wetting angle, wettability is also a function of surface roughness (AlRatrout et al, 2018). Reservoir rocks are complex structures, often comprised of a variety of mineral types, each of which may have a different wettability, making the wetting character of the composite rock difficult to describe. In addition, the saturation history of the material may influence surface wetting, such that pore surfaces that had been previously contacted by oil may be oil-wet, but those never contacted by oil may be water-wet. Thus, wettability is a function of mineralogy, fluid chemistry, and local geometry and history.

Wetting forces lead to an equilibrium condition between at least three substances: a solid and two fluids. The constituents and conditions for all three substances influence the wetting preference. Thus, to understand the wetting properties of a formation we must consider the oil components, brine chemistry and the mineral surface, both mineralogy and roughness, as well as system temperature, pressure and saturation history (Buckley et al., 1998; Abdallah et al., 2007). In addition, wettability may be adjusted in the field by changes in either oil or water chemistry.

To understand the variables the affect wettability we must first consider the nature of the mineral surface. The surface of a water-wet material is coated by a film of water. The part of this water film that is closest to the surface forms what is commonly known as an electrical double layer. In this model (Helmholtz, 1853; Gouy, 1910; Chapman, 1913; Stern, 1924; Grahame, 1947; Bokris et al., 1963) excess charges on the solid surface are countered by electrolyte ions of opposite charge. The first layer of water with these ions is static, and the second layer exchanges ions with the bulk water. In fact, more recent work (cf. Mamontov et al., 2007, 2008, 2009, 2012; Wesolowski et al., 2012) has found that this surface may be yet more complex, consisting of an inner “layer 1” of water chemisorbed as either hydroxyl groups or molecular water that have little or no translational motion, a second physisorbed layer that is strongly structured but more mobile, and a third “layer 3” that is yet more mobile and whose structure is more disordered, trending towards that of bulk water with distance from the surface. In addition, depending on the surface and solution chemistry, cations or anions may be attracted to the surface, often to specific binding sites, depending on the structure of the brine itself (e.g. ion pairing, solvation spheres etc.). Specific cations and anions may also change the structure of the

bulk water (e.g. structure making vs. structure breaking, cf. Frank and Wen, 1957; Markus, 1988, 2009; Collins, 1997; Plumridge and Waigh, 2002; Salis and Ninham, 2014)

For components of an oil to alter wetting, the oil phase must displace brine from the surface. The surface of a water-wet material is coated by a water film. This is almost always present on a water-wet material. It can be removed at high temperature but soaking in water or condensation from humid air will usually replenish it, although treatment at suitably high temperature can cause a silicate surface to become hydrophobic (Iler, 1979). The part of this film that is closest to the surface forms an electrical double layer: excess charges on the solid surface are countered by electrolyte ions of opposite charge. The first layer of water with these ions is largely static, and the second layer exchanges ions with the bulk water. The thickness of such a wetting film is governed by a balance of repulsive short-range and/or electrostatic forces and attractive long-range dispersion forces (Hirasaki, 1991).

When two interfaces—such as the solid-water and water-oil interfaces—are in proximity, the forces acting to keep them separated or draw them together include van der Waals, electrostatic, and structural or solvation interactions (Hirasaki, 1991). The net force (per unit area) is often termed the disjoining pressure. A positive disjoining pressure holds the interfaces apart; a negative one is attractive. The composition of crude oil, and the pH and composition of brine influence the disjoining pressure. Measurements of these quantities have been used to predict water film stability, and the general trends are upheld by experiment. When the film destabilizes, polar components of the crude oil can adhere to the surface and make the surface more oil-wetting, and dissolved divalent ions, such as Ca^{2+}, can destabilize the film. Because of the presence and nature of ionized sites on the solid surface, the range of pH leading to instability is different for different phases such as carbonates and sandstones. This is because the point of zero charge (pzc), the pH at which the surface of the phase is electrically neutron, varies with mineralogy. Silica surfaces are negatively charged above a pH of about 2, so positively charged ions (base chemical species) can adsorb. Conversely, calcite surfaces may be positively charged below pH 9.5, so negatively charged ions (acidic species) can adsorb (Buckley et al., 1998). Carbonate wettability is also influenced by specific interactions with carboxylic acids and by the reactivity of carbonate minerals (Thomas et al., 1993). Thus, surface complexation models can be very useful for understanding brine/oil/solid interfaces (cf. Bonto et al., 2019).

Haagh et al. (2017) analyzed the role of divalent cations on salinity-dependent contact angle alteration in oil/brine/silicate systems. As noted above, the effectiveness of water flooding for oil recovery depends significantly on the competitive wetting of oil and water on the solid rock matrix. The typically rather low overall efficiency of waterflooding, often leaving between half and two-thirds of the oil in the ground (Cordiner et al., 1972) is caused to an important extent by the microfluidic two-phase flow processes that occur when oil is displaced by the injected brine at the pore scale. These two-phase flows are controlled to a large extent by the wettability of oil and water in the complex geometry of the porous rock material.

Empirical evidence suggests that water flooding oil recovery with brines of reduced salinity gives rise to significant increases in recovery (Sheng, 2014; Myint and Firoozabadi, 2015; Jackson et al. 2016). Wettability alteration from more oil-wet toward more water-wet has become the predominant

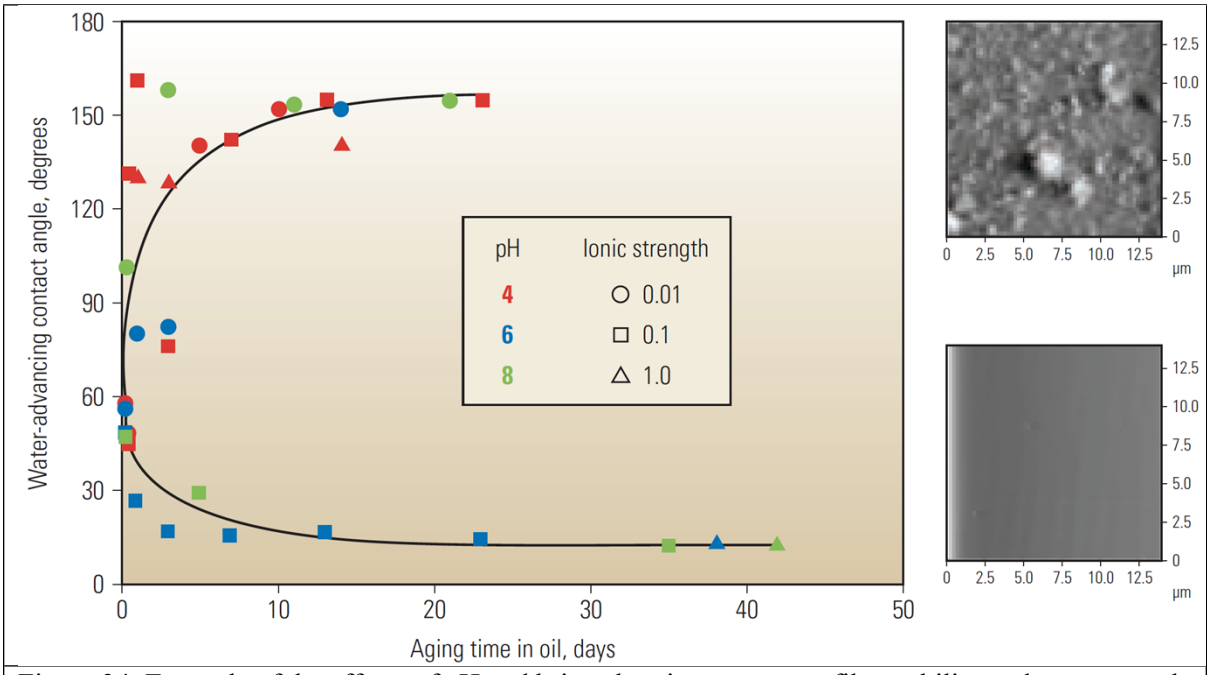

Figure 34: Example of the effects of pH and brine chemistry on water film stability and contact angle (Abdallah et al., 2007). A glass surface was conditioned in water with a salt [NaCl] concentration of 0.01, 0.1 or 1.0 mol/m^3, and a pH of 4, 6 or 8. This water-wet surface was then aged in a crude oil known to contain components that can alter wettability. Contact angle measurements (left) showed oil-wetting behavior (low water contact angle) at low salt concentrations and at low pH, and water wetting behavior (high water contact angle) at high concentrations and at high pH. Thus, the surface-water film retained its stability at high salt concentrations and high pH (the surface remained water wet). In related tests (right), freshly cleaved mica surfaces were aged in various NaCl solutions and then in crude oil for 11 to 14 days. Top right: when the brine conditions (0.01 mol/m^3, pH = 4, i.e., low salt concentration and low pH) allowed a change to oil-wetting state, a surface image from atomic-force microscopy (AFM) shows a complex of micron-sized surface irregularities deposited on the surface. These were thought to be asphaltic material because the irregularities were insoluble in decane. Bottom right: A similar image of a mica surface aged in brine (1.0 mol/m^3, pH = 8, i.e. high salt concentration and high pH) that retains a water wetting surface film indicated no deposits.

paradigm for explaining this change (Sheng, 2014; Myint and Firoozabadi, 2015). The microscopic mechanisms causing this wettability alteration, however, are uncertain. Whereas the situation in carbonate reservoirs is particularly complex due to the strong chemical activity of the rock (Rezaei-Doust et al., 2009; Yousef et al., 2012), the discussion for sandstone reservoirs largely focuses on two specific competing mechanisms: double-layer expansion (DLE) upon salinity reducuction, (Tang and Morrow, 1999; Ligthelm et al., 2009; Hilner et al., 2015) and multicomponent ion exchange/complex formation (Laer et al., 2008; Austad et al., 2010). Haagh et al. (2017) note that, while the existence of a water film is very plausible, its existence in experiments is usually only inferred from indirect evidence such as sample history and pretreatment. Direct proof for the existence of these layers has been provided only in very few cases either using neutron reflectivity (Stocker et al., 2014) or imaging ellipsometry in model systems (Mugele et al., 2015). Haagh et al. (2017) analyzed the effect of brine composition on the contact angle of a multicomponent brine droplet in ambient decane with fatty acid on muscovite and oxidized silicon wafers. They showed that, although some specific cation effects, beyond valence, were observed for muscovite substrates, reducing the ionic strength while keeping the divalent cation

concentration constant had little effect on wettability, whereas reducing the divalent cation concentration while keeping the ionic strength constant significantly decreased the contact angle of the droplets. Dilution of artificial seawater leads essentially to the same behavior. By contrast, for oxidized silicon surfaces, dilution had little effect on water wettability. This difference is consistent with experiments that suggest a correlation between the efficiency of low salinity water flooding and clay content. These experiments showed that the expansion of the electric double-layer is primarily a collateral effect, not the cause of the wettability (i.e., contact angle) alteration, which seems to be driven by the removal of divalent cations. An experimental example of combined ionic strength and pH effects is shown in Figure 34. This interaction was modelled in much greater detail as a surface complexation model by Bonto et al. (2019). Although they note that their approach does not work well at high ionic strengths, this is not an uncommon phenomenon, and may be associated with the so-called "Kirkwood reversal", where solution structures begin to dominate over interfacial processes (Kirkwood, 1936).

The existence of double layers in the water phase at the water/mineral interface explains why there is a difference between a material whose pores are saturated with crude oil and one whose surfaces are wetted by oil. So long as the water film is stable, components of the crude oil cannot attach to the solid surface and alter the wetting tendency of that surface toward oil wet. One result of this surface interaction is contact angle hysteresis. The water-advancing contact angle, which is present when bulk water displaces bulk oil from a surface, can be much larger than the water-receding angle, which occurs when bulk oil displaces bulk water. Descriptions of the surface layers under these two conditions may be complex (Hirasaki, 1991). This also explains the influence of saturation history on wetting. In an oil-bearing formation, wettability can vary with depth, with a greater water-wetting preference near the bottom of the transition zone and a greater oil-wetting preference near the top (Okasha et al., 2007). The higher zones have a greater capillary pressure, which can counteract the disjoining pressure and destabilize the water film, allowing surface-active components in the oil to contact the solid. Lower in the structure, the solid surfaces mostly retain the water film. However, saturation in a reservoir is not static. Multiple phases of oil migration, development of a gas cap, leakage of oil and gas from the reservoir and tectonic activity can all affect the saturation state of a reservoir. These changes will result in different fluid saturations based in part on the wettability of the surface at the time. This dependence of saturation on history applies not only over geologic time, but also at drilling and production time scales. Drilling fluids, particularly oil-base muds, contain surfactants that can invade pore spaces. This can alter wettability in the near-well region, affecting flow when the well is put into production. Fluids used in workover operations can have a similar near-well impact on wettability. During production, injected fluid can alter formation wetting either deliberately or inadvertently. This may result in improved or damaged injectivity or productivity. An injected brine whose dissolved solid content or pH differs from that of the formation brine can also induce wetting changes, and surfactants, including those generated by microbial action, can decrease the interfacial tension between fluids and change the contact angle.

Changes in temperature, such as those caused by thermal recovery methods (Mahani et al., 2015), can also affect wettability. Quartz tends to become more oil-wet at higher temperatures, but calcite tends to become more water-wet (Nasralla and Nasr-El-Din, 2014). Lu et al. (2017) reported the results from a systematic investigation of the effect of temperature on the wettability of oil/brine/rock systems. They found that, when using an oil sample produced from a sandstone reservoir on sandstone-like substrates (i.e., mica and quartz) in NaCl and $MgCl_2$ solutions with concentrations ranging from 0 to 3 M, raising the temperature from 25 to 50 °C had no discernible effect on the contact angle, regardless of substrate type, brine type, or salt concentration. However, when an oil sample obtained from a carbonate reservoir was examined on carbonate-like substrates (i.e., calcite) in NaCl and $MgCl_2$ solutions ranging from 0−1 M, contact angles decreased as the temperature increased from 25 to 65 °C, and this effect depended strongly on brine type and salt concentration.

As discussed above, surface roughness also plays a significant role in wettability. The interaction of fluids with a rough surface is traditionally described using the approaches of Wenzel (1936) or Cassie and Baxter (1944) to calculate an effective contact angle on a rough surface (Hirasake,

1991; Lafuma and Quéré, 2003). This approach has been used to interpret the transition from water-wet to hydrophobic conditions (Sanchez et al., 2005; Sun et al., 2005, Nychka and Gengleman, 2010; Bromberg et al., 2017). However, in porous rocks, where portions of the solid surface have undergone wettability alteration by direct contact of surface-active components with the solid (Buckley et al., 1989), it has been suggested that separated water- and oil-wet regions are present (Kovscek et al., 1993; Blunt, 2017). That is, the surface is fractionally- or mixed-wet. This has been observed using atomic force microscopy in chalk (Hassenkam et al., 2009). In addition, high-resolution X-ray microtomography has shown a wide distribution of contact angles, both above and below 90°, at temperatures and pressures representative of deep underground reservoirs, even in mineralogically homogeneous rocks (Berg et al., 2013; Pak et al., 2015; Andrew et al., 2014; Khishvand et al., 2016, 2017; Alhammadi et al., 2017). These have local variations over a pore scale of around 100 μm (AlRatrout et al., 2018), allowing both oil and water to remain connected in wetting layers that can flow over a wide range of saturation. This is favorable for oil recovery (Blunt, 2017, Alhammadi et al., 2017). It has been suggested that the range of observed contact angles is likely to be a result of the roughness of the rock surfaces.

The relationship between wettability in complex porous materials, the mixed-wet state, to surface roughness has recently been examined by AlRatrout et al. (2018). They used X-ray microtomography to examine three cores from "a giant multibillion barrel carbonate oil reservoir in the Middle East." In this study CO_2 was first injected into clean, dry samples to displace air. This was followed by brine injection to saturate the rock. Subsurface conditions were established (60°C or 80°C, 10 MPa), following the method of Alhammadi et al (2017) and primary drainage (crude oil injection) was performed followed by aging over 3 weeks to restore rock wettability. During brine injection, the flow was reversed, brine was injected, ~ 3.4 mm^3 of the sample was imaged with 2 μm voxel sizes, and the images were segmented into three phases (oil, brine, rock). The results showed that, in water wet media, the interfacial curvature did not depend on surface roughness. However, where there was significant wettability alteration, the range of the of contact angle and curvature distribution increased with the degree of roughness, with the correlation being more obvious in larger pores. The contact angle tended to be lower on rougher surfaces due to accumulation of water in crevices, which made the surface effectively less oil wetting. This yielded a mixed-wet state with a wide range of local contact angles that facilitated the flow of both phases. This was deemed favorable for oil recovery (Alhammadi et al., 2017). While it is well understood that, by using surfactants or changing the brine salinity, oil recovery can be improved through changing the wettability (Morrow, 1990; Jerauld and Rathmell, 1997), they suggested that a mixed wet state is ideal, and hypothesized that a mixed-wet state derived from a combination of wettability alteration and surface roughness, in which a naturally water-repellent surface has range of effective contact angles, allows both liquid and gas phases to flow over a wide range of saturations, improving oil recovery.

- **What is the industry's current state of knowledge on controlling the wettability of proppants used during induced fracturing and does the wettability of proppants change during production?**

It is clear that there is a limit to how well this question can be answered. Obviously, much of the industry's knowledge in this area is proprietary and we cannot necessarily say what the current state of their knowledge with respect to this question may be. Nonetheless, we can examine what is available in the open literature and note a few of the commercial products and patents available.

Proppants materials can be grouped into three main categories (Figure 35): rounded silica sand, resin coated sands, and sintered and/or fused synthetic ceramic materials (Droppert et al., 2002). The most commonly used materials are sand, ceramic, sand-lined resin and sintered bauxite (McLin et al., 2010; Liang et al., 2016). Materials such as walnut shell, Brandy and Ottawa sand, glass. Kaolin and molten zirconia have also been used as proppants (Hellmann et al., 2014), and steel shot, aluminosilicates, zirconia, plastic pellets, glass beads, aluminum pellets and ash have also been tested

(O'Driscoll and Clarke, 2015). Unless purposely altered, Mora et al. (2010) note that most commercially available proppants are generally water-wet, although relative permeability to oil, and thus fluid conductivity, may be enhanced by weakening the adhesive forces between the proppant surface and the aqueous phase.

The earliest study of the effects of proppant wettability on flow and oil recovery of which we are aware is that of Mora et al. (2010). They performed a series of core flood experiments using porous packs with varying degrees of wettability (water-wet, oil-wet, and intermediate-wet) to evaluate the potential benefits of wettability alteration. These used spherical beads ranging between 0.43 and 0.60 mm in diameter (30–40 U.S. sieve with 80% roundness) composed of: soda–lime silica glass (hydrophilic or water-wet), acrylic polymer (hydrophobic or oil-wet), and treated glass beads (intermediate wettability). The treated beads were coated using a silanization method to decrease their surface affinity to water. This was done by dip-coating the glass surfaces using 3-animopropyltriethoxysilane (APS). Glass coated with APS has shown intermediate wettability (Pantano, 2001). Sequences of oil and water

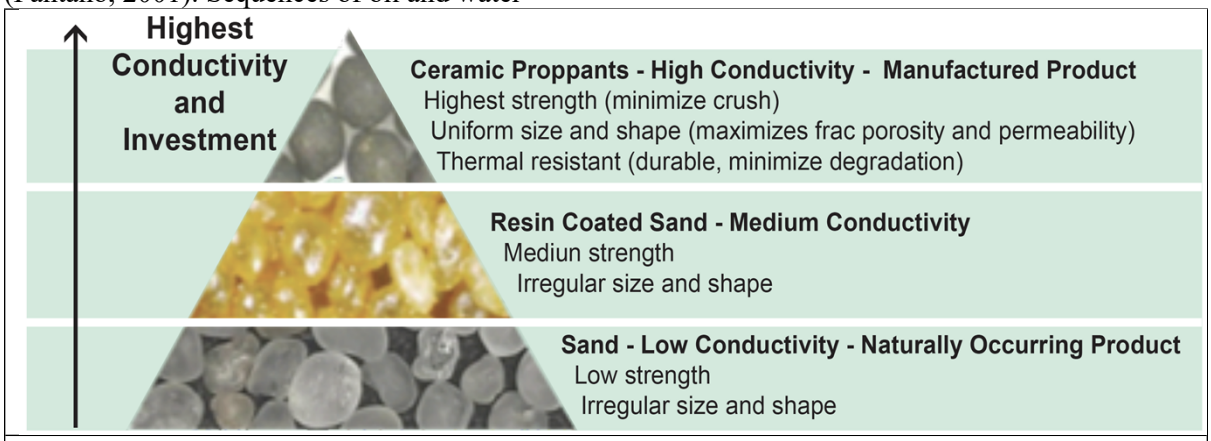

Figure 35: Proppant pyramid (Campos et al., 2018; adapted from Kullman (2011))

injections were used to monitor saturation changes inside a horizontal bead pack and analyze the relative difference in oil displacement. The oil phase in these experiments was kerosene with a surface tension of 26.69 mN/m, density of 0.797 g/cm^3, and viscosity of 2.43 cP. The water phase was a brine solution with 8 weight % NaI. Contact angles measurements were performed using the Washburn method by capillary uptake with a Krüss FL12 cell, and n-hexane to determine a necessary material constant (Rulison, 2008). Comparing the various bead types, the trend for kerosene contact angles was Glass > Treated glass > Polymer. The glass beads thus had the highest surface energy, indicating an increased affinity for water/brine - a tendency to be water-wet. In addition, the higher surface tension of the brine, relative to distilled water, gave it greater adhesion energy to the solid beads and larger contact angles. By contrast, the lower contact angles for distilled water meant it had a lesser adhesion energy to each bead, making it less resistant to displacement by the kerosene. Using these materials for flow tests, Mora et al. (2010) concluded that their results demonstrated competition between permeability and wettability in which the latter had a diminished impact on displacement efficiency at high permeability values.

The second study of this effect is that of Parmar (2013), who included an analysis of the effects of proppant wettability in a master's thesis at the University of Alberta. In order to study the effect of surface tension and proppant wettability on frac fluid recovery, experiments were performed in which the interfacial tension of the frac-fluid and wettability of the glass beads used as proppant were altered. The fluids were water and water containing 1% isopropanol, which had interfacial tensions of 72 and 42 dynes/cm, respectively. The beads were glass (hydrophobic), and glass treated using the procedure of Shahidzadeh-Bonn et. al (2004 – wrong reference number given in thesis) to make them hydrophobic. They then studied the displacement of water by gas in packed cells where they could watch the displacement and quantify "wormhole" formation during the process (Figures 36 and 37)

In the experiments of Parmar (2013) the ultimate recovery of frac-fluid from the hydrophobic pack (18.61%) was more than two times higher than that from hydrophilic pack (8.01%). As shown in Figure 37, channels of gas are observed to be formed with hydrophobic glass beads. The diameter of these channels was larger than that of the fingers observed in the hydrophilic pack (Figure 36). This indicates that the sweep efficiency is likely to be better in porous media packed with hydrophobic proppants and shows the strong effect of proppant surface properties on sweep efficiency during fracture clean-up. However, these experiments suggest that the effect of gravity is still dominant, as the ultimate recovery did not exceed 20 %.

Parmar (2013) notes that, in a previous study (Glass et al., 2000), done by draining proppant packed columns saturated with water, an increase in water recovery was observed by changing the wettability of glass beads from hydrophilic to hydrophobic. In another (Dehghanpour et al., 2010), water flooding experiments conducted in oil saturated cores showed higher oil recovery rates in water-wet

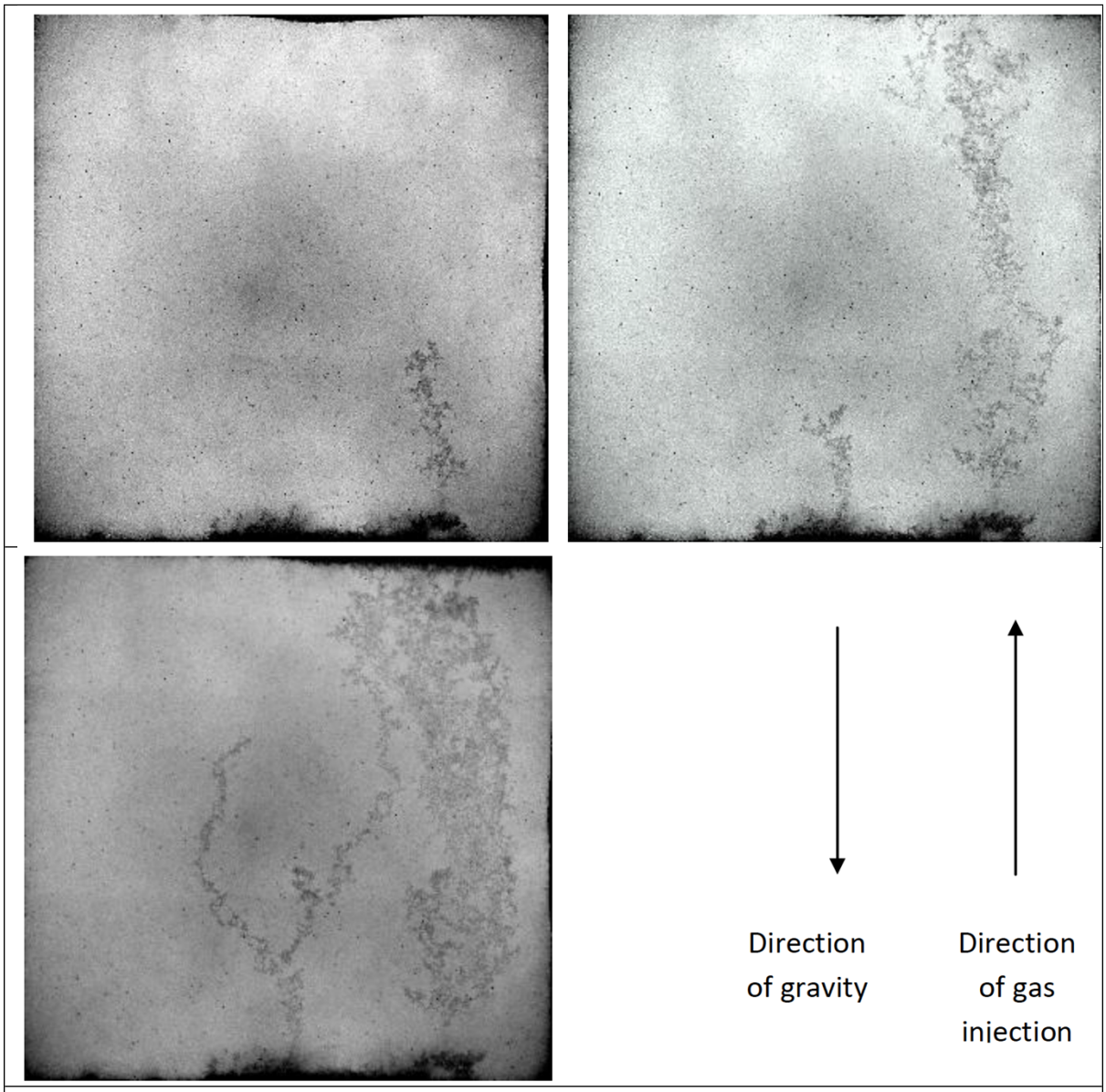

Figure 36: Drainage pattern at time interval t1, t2 and t3 in experimental cell packed with hydrophilic glass beads and saturated with 1 wt. % isopropanol solution (Parmar, 2013 test2 of set3)

cores as compared with oil-wet cores. For oil-wet cores, the instability was higher which resulted in early breakthrough of water and lower

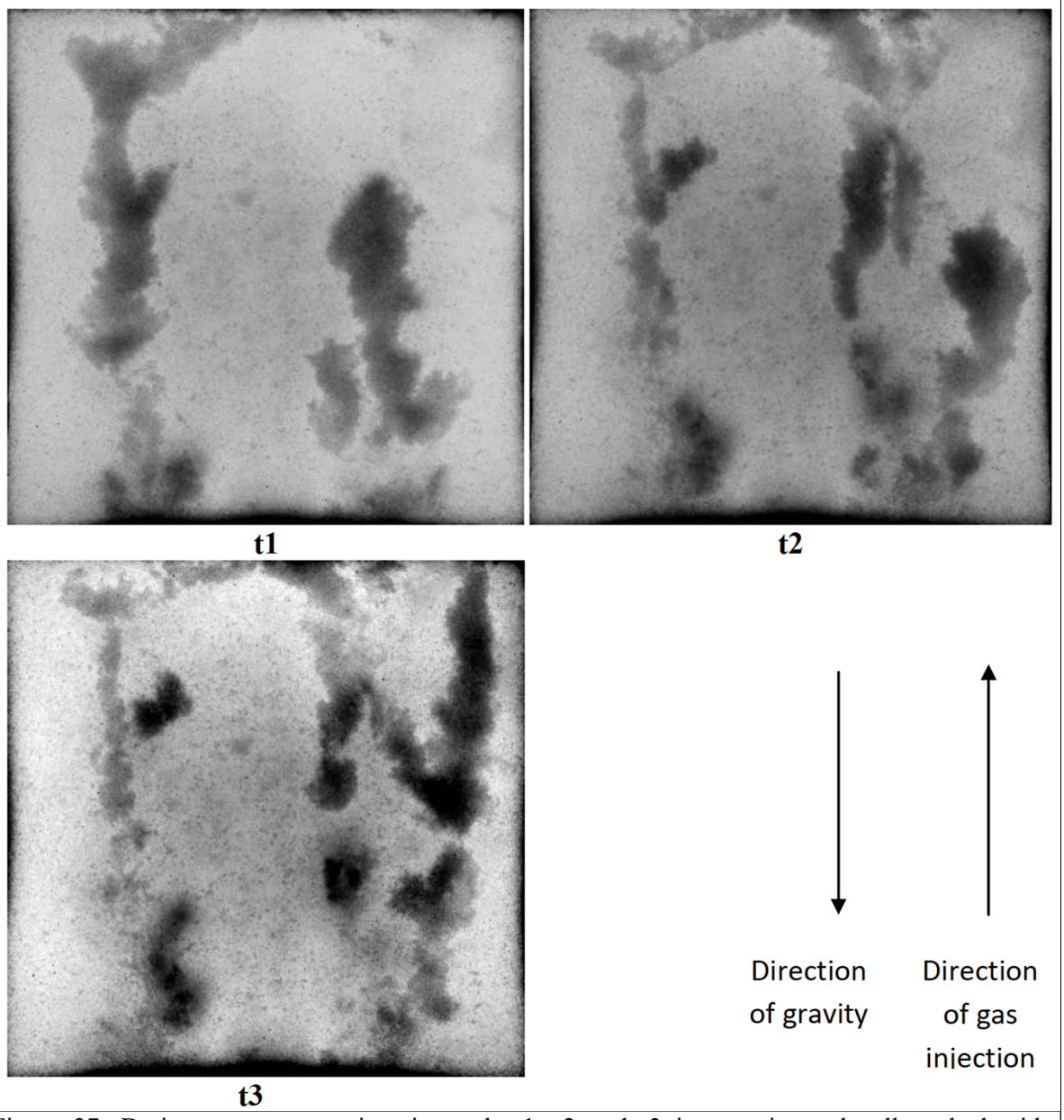

Figure 37: Drainage pattern at time intervals t1, t2 and t3 in experimental cell packed with hydrophobic glass beads and saturated with water (Parmar, 2013, test3 of set3)

oil recovery. From these studies, Parmar (2013) concluded that the porous media should be preferentially wetted by displacing fluid rather than displaced fluid for better sweep efficiency.

When using hydrophobic glass beads, they also observed discontinuous gas lumps, which move upward and displace water rather than traveling in continuous fingers. These disappeared when they reached the production end of the pack, and new lumps were formed at the gas injection end.

Parmar (2013) suggested that there are two ways of looking at this phenomenon.

(a) At the microscopic scale, imbibition and drainage occur simultaneously. When a new gas lump is formed, it drains the water and creates an are of low water saturation. Water from the surrounding highly water-saturated area then imbibes into the drained area and replaces the gas.

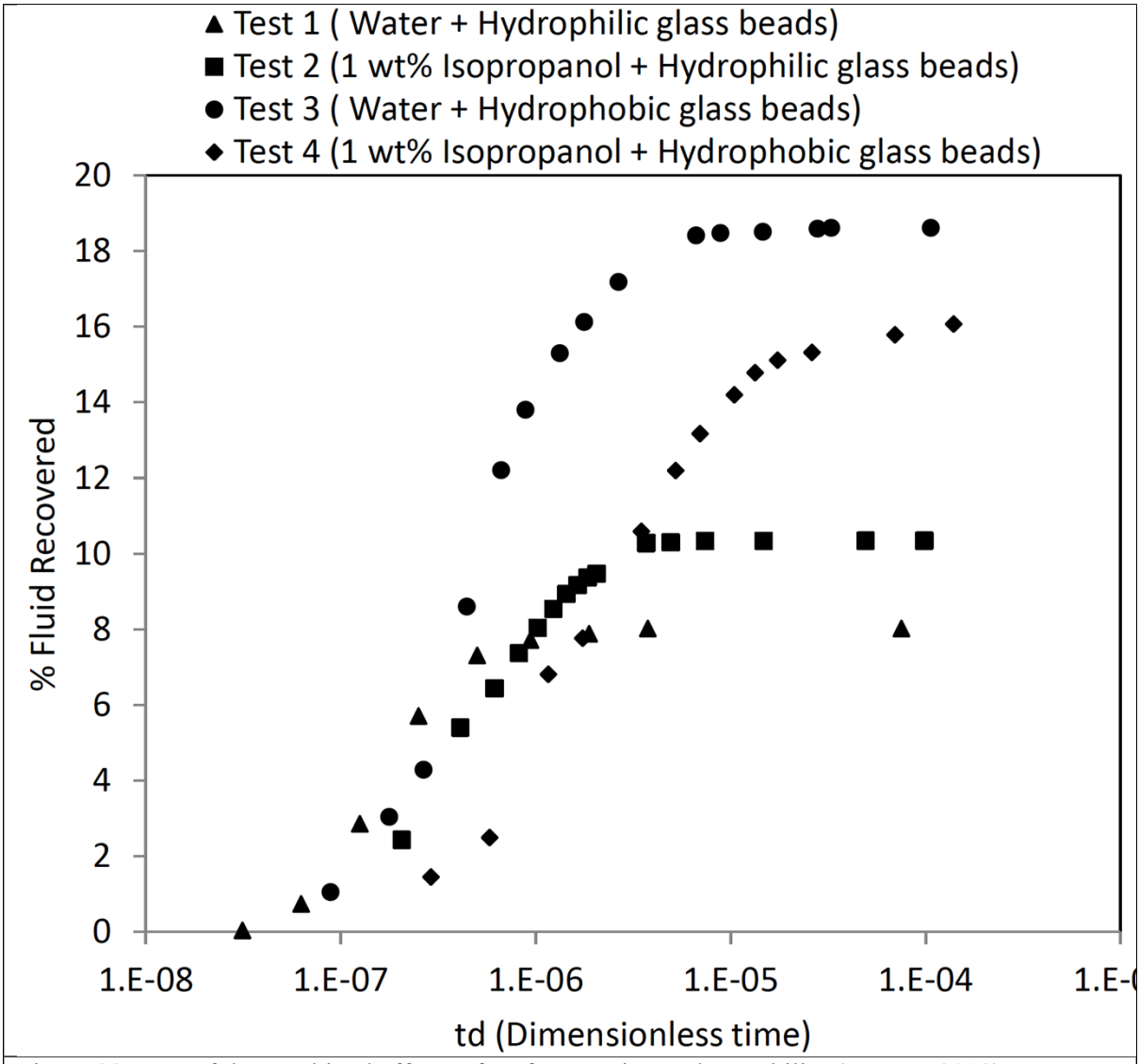

Figure 38: Test of the combined effects of surface tension and wettability (Parmar, 2013).

(b) At macroscopic scale, counter current flow of water and gas occur due to the buoyancy effect. Gas with a lower density moves upward due to buoyancy and water drains downwards.

Parmar (2013) also examining the combined effects of surface tension and wettability. The results of this test are shown in Figure 38, which shows the fraction of the fluid recovered by gas input. Recovery in test 4 (Isopropanol solution (lower interfacial tension) + hydrophobic proppants) was higher than that in test 1 (Water (higher interfacial tension) + hydrophilic proppants) and test 2 (isopropanol solution + hydrophilic proppants) but slightly less than that in test 3 (water + hydrophobic proppants). Wide channels were formed in test 4, similar to those for water and hydrophobic proppants shown in Figure 37, which resulted in a higher water recovery.

The next study of the effects of proppant wettability on oil recovery was that of Palisch et al. (2015), who noted that the oil-wet proppants tried to that time had yielded poor recovery in the laboratory. They, therefore, designed a new proppant with a neutrally-wet surface that would not promote entrapment of either water or oil in the proppant pack. The specific nature of the coating used was not, however, given, and is assumed to be proprietary. Both laboratory and field tests were performed with this material coating a ceramic proppant. The laboratory results suggested an increase in permeability, and a decrease in pressure drop relative to an uncoated proppant. The field tests were

performed in several locations given as “north Louisiana (DeSoto Parish), south Texas, and the Permian Basin.” The treated wells reported earlier gas production and greater gas and oil production than the untreated wells.

Wang et al. (2016) reported on the effects of a “proprietary chemical” applied to silica sand to change its wettability. This treatment was selected to make the sand surface hydrophobic. It was applied at a concentration of 0.8 liters per metric ton of sand. Both Tier 1 (clean, consistently sized, spherical, monocrystalline quartz sand, often from Wisconsin or Illinois) and Tier 2 (often polycrystalline and containing impurities, especially feldspar) type sands were tested. Their results suggested that this treatment led to greater conductivity to flowback, reduced fines generation on crushing, and improved airborne dust control. The qualitative effects of this treatment on sand wettability are shown in Figure 39.

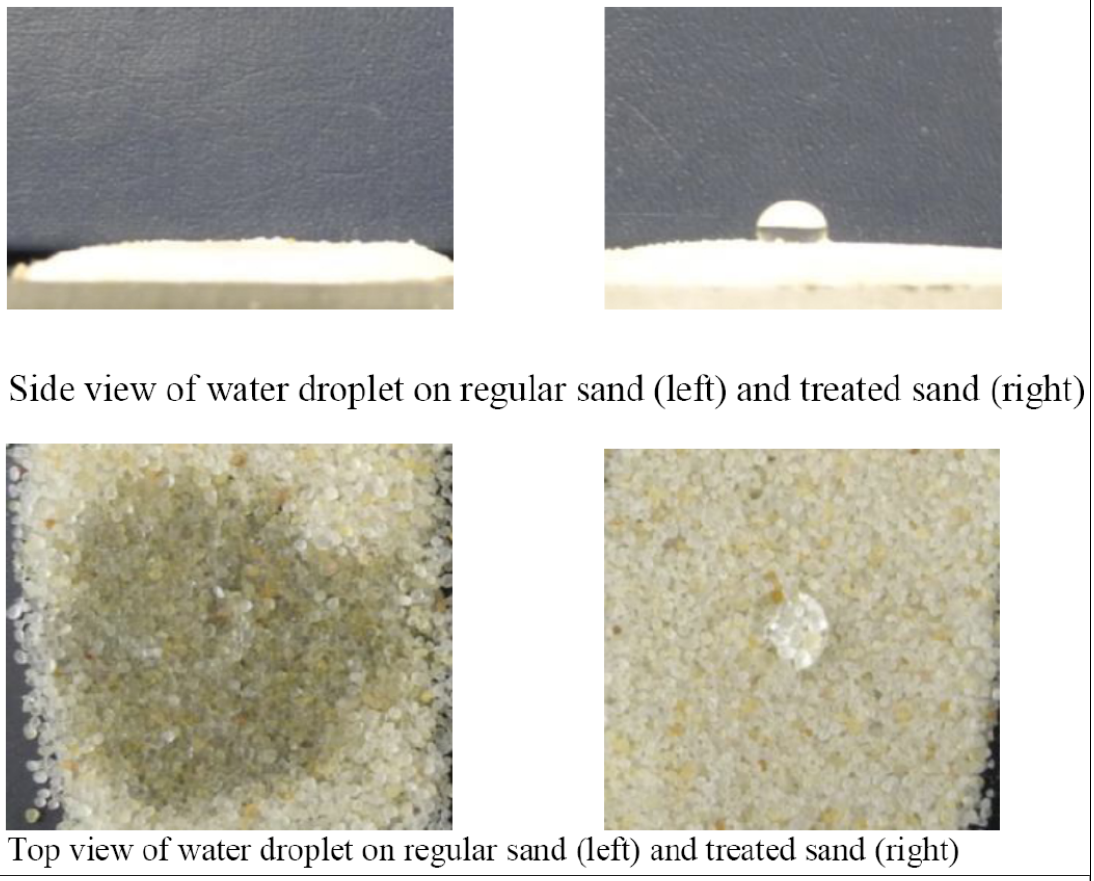

a) Side view of water droplet on regular sand (left) and treated sand (right)

b) Top view of water droplet on regular sand (left) and treated sand (right)

Figure 39: Effects of the treatment proposed by Wang et al. (2016) on sand wettability.

Aggarwal (2016) studied the effects of wettability alteration using a fluorinated nano-silica in a master’s thesis at the University of Oklahoma, Mewbourne School of Petroleum and Geological Engineering. The wettability modifiers investigated were fluorinated nano-silica particles, which can permanently bond to quartz and carbonate substrates, and to carbon atoms in organic molecules. Fluoro-organics can be extremely hydrophobic, with high thermal and oxidative stability, weak intermolecular interactions, low surface energy and biological inertness (Pagliaro and Ciriminna, 2005). Fluoroalkylsilanes contain alkyl groups with all their hydrogen atoms replaced by fluorine and silanes with the first base unit, SiH_4. These can form long chain polymeric networks. Fluorine atoms on the outer edges of these molecular structures impart hydrophobicity. Hydroxyl groups attached to silicon atoms (silanes), bond strongly with rock substrates, generating chemical and thermal stability. The

primary active compounds utilized were Tetraethylorthosilicate [TEOS, $Si(OC_2H_5)_4$] and Triethoxy-1H,1H,2H,2Hperfluorodecylsilane [PFDS, $CF_3(CF_2)_7(CH_2)_2Si(OCH_2CH_3)_3$] reacted using a sol-gel process (Sharifzadeh et al., 2013). Two different treatment mixtures were used, although the first, containing more PFDS and TEOS, was later abandoned, as observed permeability reductions (25 % for treatment A, 10% for treatment B) were deemed too large. Measurements were made on samples of Berea Grey sandstone and Indiana limestone, as well as glass plates and a sand proppant pack. The selected PFDS+TEOS treatment was successfully tested for thermally durability by immersing it in a water bath at 80°C for over 24hrs. Treatment with this material significantly increased contact angles on both glass and sandstone. These were capillary uptake experiments, characterized as recovery fraction – the fraction of the pore volume filled by the incoming fluid. As the aim was to reduce wetting, this implies a reduced recovery fraction. For both sandstone and limestone water recovery fractions dropped significantly, indicating increased hydrophobicity. Decane recovery fractions increased, however, indicating a slight increase in the oil-wet character of the rock. It is not clear whether they applied their treatment in the proppant tests, however, instead comparing sand (water wet) and a resin-coated sand. These showed similar absolute permeabilities, but water wet sand had better water mobility, with a higher irreducible water saturation. Oil/neutral wet resin-coated sand had better oil mobility, with a much lower irreducible water saturation.

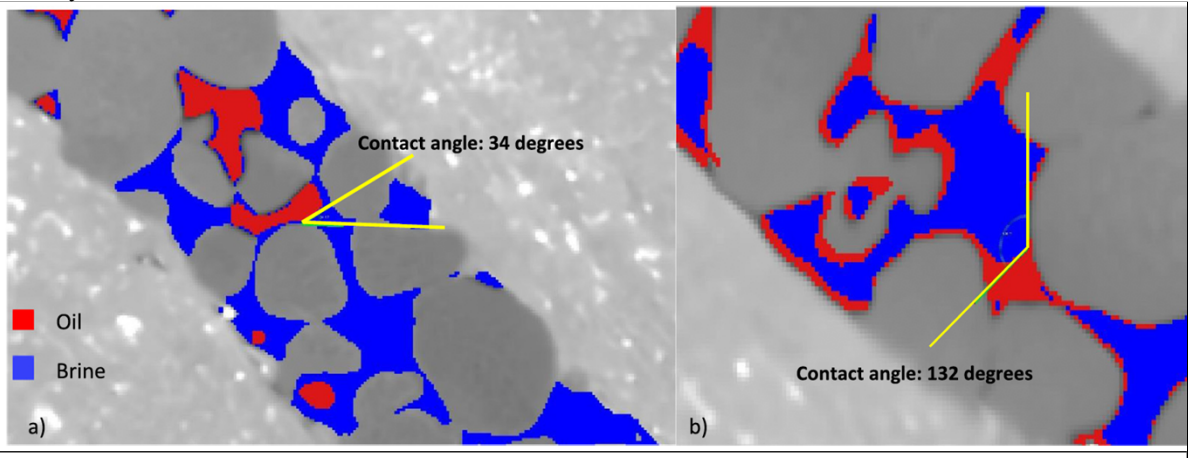

Figure 40: In-situ contact angle measurements from Arshadi et al. (2017): a), water-wet; and b), oil-wet.

The study of Arshadi et al. (2017) was not primarily focused on the effects of the wetting properties of proppants, but on the effects of deformation on two-phase flow through proppant-packed fractured shales. However, *in-situ* contact angles measured using micro-CT images showed that proppant grains experienced a drastic alteration of wettability (from strong water-wet to weakly oil-wet) after the medium was subjected to a flow of oil and brine for several weeks (Figure 40). The proppants were water-wet sand grains of a type used in fracturing operations in Bakken shale oil formations of North Dakota They suggested that this alteration may have been caused by one or both of the following factors: 1) interactions of polar components that may have been present in the mineral oil used in the experiments with the surface of the sand grains. (They suggested this was a low probability mechanism as most of polar contaminants of the mineral oil were removed); and 2) small shale fragments, removed from the surface of the shale, may have contained polar components that deposited on the proppants after coming in contact with mineral oil (cf. Graue et al., 2001).

Arshadi et al. (2018) further explored these changes in a micro-scale experimental investigation of two-phase gas/brine flow through proppant- packed fractured shale samples under increasing effective stresses of up to 5000 psi using a miniature core-flooding apparatus integrated with a high-resolution X-ray micro-CT scanner. Wettability alteration of the proppant pack from water-wet to strongly oil-wet was observed. This occurred non-uniformly and was thought to be due to deposition of shale-derived organic matter released after significant proppant embedment. Similarly, to their previous

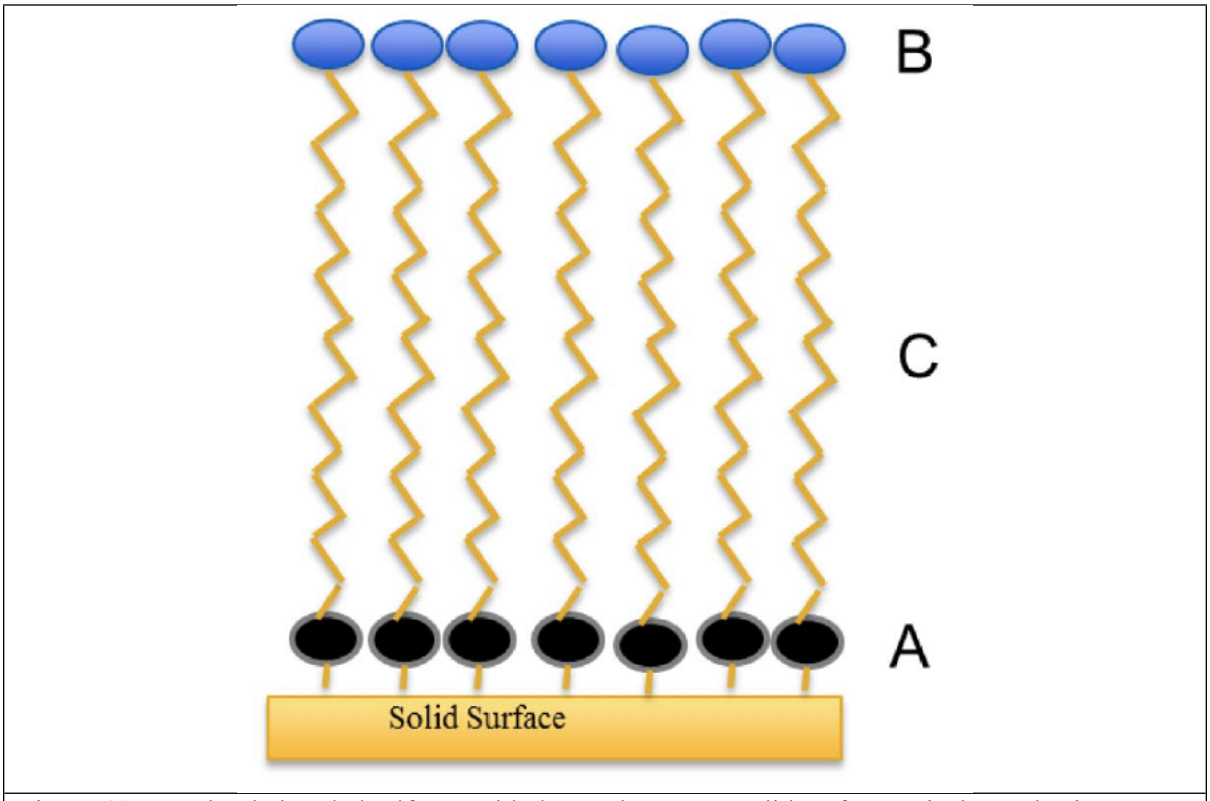

Figure 41: Covalently bonded self-assembled monolayer on a solid surface. A is the anchoring group, B is the group that provides the surface with special wettability characteristics, and C is a spacer group. A self-assembled monolayer can provide a surface with permanent non-native wettability properties (from Bestaoui-Spurr et al., 2017a).

work, they hypothesized that severe proppant embedment into the shale matrix under 5000 psi confining stress released organic matter, including its polar components, from the matrix, which eventually deposited on the surface of the proppant grains causing wettability alteration Such wetting characteristics aggravated multi-phase trapping within the fractures, which in turn lead to dramatic reductions in effective gas permeability.

Bestaoui-Spurr et al. (2017a) noted that reduction in water saturation of surfaces during the working life of a well reduces its relative permeability to oil and gas and hydrocarbon recovery. Addition of strong water-wet surfactants temporarily improves the situation, but these are eventually washed out. In order to obtain a more permanent solution they considered modifying silica and ceramic proppant surfaces to see how this effected fluid recovery. These were self-assembled monolayers of "hydrophobic/oleophobic moieties" covalently bonded to the surface (Figure 41). Several possibilities were tested, but the specifics of these treatments were not provided. Wettability was tested with a drop of liquid on a treated glass slide and the proppant was tested with a dyed kerosene and in a column. It was found that if the proppant became hydrophobic-only it became oil wet and would retain oil and potentially reduce oil flow. However, a hydrophobic/oleophobic surface caused neither oil nor water to be retained in the pores of the proppant pack. If the contact angle was close to 90 degrees, the proppant could be mixed with the fracturing fluid and pumped.

Bestaoui-Spurr et al. (2017b) reported some results of using the coated proppant reported by Bestaoui-Spurr et al. (2017a) at several completions in the Gulf of Mexico, as well as in the laboratory. This was a light-weight ceramic proppant with a permanently modified neutrally wet surface. The new proppant was found to reduce water saturation and improve oil mobility. It had a viscosity similar to the untreated proppant, indicating that it was compatible with the fracturing fluid and did not aggregate. Significant details are given of the case study, but the key result was that all of the stimulation fluids pumped into the completions(s) were recovered at the end of the treatment and the time to first oil recovery was reduced by 43 percent.

Bestaoui-Spurr et al. (2018) continued the work reported in their previous two papers. They began by noting that stimulation fluids left in the fracture may leak off into the formation or block part of the proppant pack, impairing hydrocarbon production. They suggested that using a proppant that is neither oil- nor water-wet may help these issues. To do so they created a neutral wet lightweight ceramic (LWC) proppant (30/50 mesh) by modifying a commercial product (water wet) using molecules with both hydrophobic and oleophobic properties. They do not describe exactly what was used or how it was applied in this paper, but do reference the two previous works (Bestaoui-Spurr et al., 2017a,b). This paper reproduces some of the data in those papers but provides greater detail as to the oil recovery with time in the Gulf of Mexico studies. Production data for the first 100 days show a lower draw down pressure, and thus a higher productivity index with the treated proppants, and data for the first 150 days show a higher productivity index than an offset well using a similar proppant with untreated surfaces. Their overall conclusion was that their newly enhanced proppant neutralized the inherent wettability of the untreated material, so that the new surfaces repel both oil and water and allow both to flow more readily

Zhang (2018) studied the effect of proppant wettability on two-phase flow efficiency in fractured, water-wet sandstone for a master's thesis in the Department of Petroleum Engineering at the University of Louisiana at Lafayette. The materials used included the following components: Berea Sandstone Core Samples, Parker Sandstone Core Samples, 50° API Light Crude Oil, and Carbo Ceramics proppants. The proppants included 20/40 mesh CC water-wet proppant, 20/40 mesh CC oil-wet proppant, and a 12/18 mesh SL oil-wet proppant (20/40 = 420 μm - 840 μm, CC – Carbolite ceramic). The proppants had bulk densities and specific gravities similar to sand, crush resistances superior to sand, and consistent roundness and sphericity. Three tasks were performed, each with four experiments: water- and oil-wet proppants and two-phase flow with 100% and initial water saturation: 1) Proppant wettability in low-water-saturation oil reservoirs using 20/40 proppants with a fluid containing 40% water, 2) proppant wettability in high-water-saturation oil reservoirs using 20/40 proppants with a fluid containing 70% water, and 3) investigation of proppant size on the effectiveness of oil-wet proppants using 20/40 and 12/18 proppants. The results showed that oil-wet proppants were more effective at improving oil flow efficiency than water-wet proppants in both low-water saturation cores and high-water saturation cores, and that small oil-wet proppants had better performance than large oil-wet proppants.

Dong (2018) and Dong et al. (2019a,b) also studied the effects of proppant wettability on oil recovery (note: the author of the masters thesis just discussed, Chi Zhang, is a co-author on one of these papers. Some of the results reported by Dong (2018) are very similar.). Dong (2018) reported the results of nine experiments on the effect of ceramic proppant wettability on oil flow efficiency from core samples into proppant-filled "fractures." These experiments used a two-foot-long core holder containing a 2-inch diameter core sample with a slot cut along its length filled with proppants, simulating a propped fracture. The experiments used Parker and Berea sandstone cores CC20/40 —water-wet, CC20/40 —oil-wet, and SL12/18 —oil-wet ceramic proppants, 48~50° API gravity crude oil, and tap water. The results showed that oil-wet ceramic proppants promote oil flow efficiency from sandstone core samples to proppant packs and thus should promote oil well productivity. The mechanism behind this phenomenon was believed to be formation of oil flow channels across the fracture face due to oil imbibition from the core onto the oil-wet proppant surface, promoting oil flow from the core into the fracture. Oil-wet proppants were more effective in improving oil flow efficiency

in low-water saturation cores than in high-water saturation cores. Larger oil-wet proppants helped improve oil flow efficiency, possibly due to greater adhesion/affinity of oil to the narrow corners of the solid surface in large-size proppant packs.

Dong et al. (2019a) extended the work of Dong (2018) to analysis of the effect of ceramic proppant surface wettability on oil flow in hydraulic fractures. Parker sandstone cores 22 inches long and 2 inches in diameter, with a relatively low permeability of 15-30 mD were used to simulate a low-permeability reservoir. Each core had a planar cut at one end with a slot width of 0.10 inches and a length of 6 inches that was used to mimic a fracture. Three kinds of proppants were used to fill the fracture: a 20/40 mixed-wet proppant (MP), a 20/40 oil-wet proppant (OP-1), and a 12/18 oil-wet proppant (OP-2). It should be noted that the definition of mixed-wet used in this paper, a material that can absorb both water and the oil droplets, is not necessarily consistent with that given above, where "mixed wet" is a type of fractional wettability that implies continuous water-wet and oil-wet pathways.

Dong et al. (2019a) summarized the results of their experiments as follows:

1. For a proppant pack with a small proppant size, the surface wettability plays an essential role in determining the flow efficiency of oil and water. Increasing the proppant size diminishes the effect of surface wettability on hydrogen transfer due to high permeability.

2. The mixed-wet proppants did better than the same-size oil-wet proppants at increasing oil flow efficiency and blocking the water inside the proppant pack.

3. Waterflooding can reduce the oil flow efficiency through large-size oil-wet proppants but increase the same through small-size oil-wet proppants. It does not significantly affect oil flow efficiency with mixed-wet proppants.

4. Combining proppant wettability with the microscopic structures of the proppant surface, an interconnective fluid channel mechanism was proposed caused by the preferential affinity of the proppant surface.

In the third paper in this series Dong et al. (2019b) considered the effect of ceramic proppant wettability in guar gum solutions on oil flow efficiency in fractures. In this case, eight experiments were conducted using traditional guar gum fracturing fluid. They found that, whereas oil-wet ceramic proppants should promote oil flow efficiency from sandstone to proppant packs and promote oil well productivity due to formation of oil flow channels across the fracture face from the core onto the oil-wet surface of the proppant, after guar gum was added the results inverted and water-wet proppants were more efficient. This was believed to be due to increased fracture fluid viscosity, which promoted oil flow from the core to the fracture. Inside the proppant matrix filled with guar gum fracturing fluid, oil can be blocked as a discontinuous phase while the aqueous phase can mix easily with the guar gum fluid and be transferred out.

Some references to commercial products and patents (note: not a comprehensive list)

https://multimedia.3m.com/mws/media/1116639O/3m-engineered-surface-treatment-for-proppants-pst-100.pdf

Baker-Hughes Neutraprop. https://www.bakerhughes.com/integrated-well-services/integrated-well-construction/completions/stimulation-fracturing/specialty-proppants-and-engineered-systems/neutraprop-neutralwettability-proppant

Droppert, D., P. Fiore, Y. Dessureault, F. Cardarelli (2002) High strength, heat- and corrosion-resistant ceramic granules for proppants, Canadian Patent CA 2 329 834 (2002).

Green J., Terracino J. M., Borges J. F., Spillars S., Edward and Mah S. H. (2011) proppant materials and methods of tailoring proppant material surface wettability. *Momentfve Specialty Chemicals Inc.*, Patent number **WO 2013/049235 Al,** 1-46.

Hexion, Inc. (2018) Resin coated proppants for water-reducing application Jul 24, 2015 - HEXION INC. Patent number: 10017688 Filed: Jul 24, 2015, Date of Patent: Jul 10, 2018, Assignee: HEXION INC. (Columbus, OH), Inventors: John W. Green (Cypress, TX), Silje V. Nordas (Richmond, TX), Mark D. Leatherman (Stamford, CT) https://patents.justia.com/patent/10017688

TENEX, Nanoclear, https://www.tenextechnologies.com/nanoclear-cec

Vincent M.C. (2004) Coating and/or treating hydraulic fracturing proppants to improve wettability, proppant lubrication, and/or to reduce damage by fracturing fluids and reservoir fluids. **U.S.A.**, patent WO 2005/100007 A2, 29p.

- **Examine case histories where wettability alteration is known to enhance oil recovery only by injecting a water with a different fluid chemistry (e.g., salinity, pH, etc.).**

Low-Salinity water injection is a potential method for increasing oil recovery. In 1995, Tang and Morrow (1995) were the first to publish coreflood results which indicated that lowering brine salinity increases oil recovery. Webb (2004) was the first to publish results from a single-well test, which demonstrated that lowering brine salinity increases oil recovery in sandstone reservoirs. Seccombe, et. al. (2010), reporting on a study of the Endicott Field on the North Slope of Alaska were the first to publish a comprehensive inter-well field trial. As discussed above in the section on proppant wettability, our access to case history data is likely to be limited as such tests are often proprietary. Many published studies are, therefore, experimental (e.g. Katende and Sagala, 2019; Hosseini et al., 2020; Song et al., 2020), not field case studies. However, several published field studies exist, and numerous laboratory and field-based studies of low-salinity water flooding were summarized and analyzed by Katende and Sagala (2019). Table 4, taken from Katende and Sagala (2019), summarizes the available studies on low-salinity water flooding.

Katende and Sagala (2019) noted that several factors affect, or may affect, oil recovery during LSW.

Fines migration – Mixed-wet clay release was the first mechanism proposed to explain the additional oil recovery that resulted from low-salinity water injection (Tang and Morrow, 1999; Yu et al., 2019; Al-Sarihi et al., 2018; Song and Kovscek, 2016). Experiments were performed on several Berea sandstone cores. In tests were these were fired and acidized oil recovery results were insensitivity to salinity. This was also the case when a refined oil was used instead of crude oil and when the cores were initially 100% saturated with crude oil. The authors concluded that the presence of potentially mobile fines (clay minerals), initial water saturation and adsorption from crude oil are all necessary to achieve an increase in oil recovery with a decrease in salinity. Tang and Morrow (1999) also reported a reduction in brine permeability caused by fines migration and confirmed that the presence of potentially mobile fines, such as kaolinite, played a key role in increased oil recovery.

More recently, several contradictory results have been reported. Larger et al. (2008) did not notice any fines migration during numerous low salinity experiments but did observe additional oil recovery. Zhang et al. (2007) found no evidence of clay content in the production stream or at the oil/brine interface in their experiments. Berg et al. (2010) proposed that fines migration is not the main mechanism behind LSW, and no fines migration was observed during increased oil recovery in their experiments, and Cissokho et al. (2010) indicated a substantial incremental LSW recovery in kaolinite-free cores.

Changes in pH - Austad et al. (2010) proposed that the desorption of organic material from the surface of clays by a local increase in pH at the clay-water interface plays an important role in low-salinity-enhanced oil recovery. This was based on three experimental observations:

1. clay must be present in the sandstone,
2. polar components (acidic and/or basic material) must be present in the crude oil,
3. the formation water must contain active ions such as Ca^{2+}.

This model suggests that the clays act as a cation exchanger with a relatively large surface area. Initially, both basic and acidic organic materials are adsorbed onto the clay together with inorganic cations, especially Ca^{2+}, from the formation water, establishing a chemical equilibrium with respect to, temperature, pressure, and fluid composition. When the low-saline water invades the porous medium with an ion concentration much lower than that in the formation connate water the equilibrium is disturbed, and cation desorption occurs. To compensate for the loss of cations, protons from the water adsorb onto the clay. This creates a local increase in pH close to the clay surface as:

$$Ca^{2+}\ Clay + H_2O = H+\ Clay + Ca^{2+} + OH^- \quad (72)$$

This pH change, in turn, causes reactions between adsorbed basic and acidic components of the fluid as an ordinary acid-base proton transfer reaction, as:

$$NHR^{+3}\ Clay + OH^- = R_3N\ Clay + H_2O \quad (73)$$

$$RCOOH\ Clay + OH^- = RCOO^-\ Clay + H_2O \quad (74)$$

Both acidic and basic crude oil components are thus partly desorbed from the clay surface, making it more water-wet after flooding (Vledder et al., 2010).

Multicomponent Ionic Exchange (MIE) - Multicomponent ionic exchange (MIE) was suggested by Larger et al. (2010) as a mechanism to explain LSW effects, especially desorption of both positively and negatively charged organic compounds. Their investigations showed that additional oil recovery occurs in the tertiary mode only if the connate brine contains divalent cations (Ca^{2+}), and eight adsorption mechanisms were, therefore, proposed for different organic compounds Schroth and Sposito, (1997). Studies of the adsorption of marine pore water onto montmorillonite suggested that van der Waals interactions, ligand exchange and cation bridging are the dominant mechanisms amongst these eight. According to DLVO theory, electrostatic repulsion forces between particles decrease in high-ionic-strength fluids, and particles tend to aggregate due to van der Waals forces (Anovitz and Weston, 2021). Ligand exchange occurs when the carboxylate groups of acidic materials substitute hydroxyl groups onto the surface (Doust et al., 2011; Xie et al., 2019; Amiri and Gandomkar, 2019; Wilmott et al., 2018), and cation bridging occurs when a negatively charged surface and functional groups of the organic material are connected by a cation acting as a bridge - a weak adsorption mechanism.

As noted above, it has been observed that the presence of divalent cations in the formation brine, especially Ca^{2+}, is essential to a recovery increase during LSW Lager et al., 2006). In addition, the effluents from low-salinity tests showed a strong reduction in Mg^{2+} concentration during LSW. This indicates that it is strongly adsorbed to the rock matrix and suggests that increased oil recovery is due to competition between the ions in the brine for with the rock surface. Polar components may adsorb onto the clay with multivalent cations and form an organometallic complex, or by direct adsorption in which the most labile cations are displaced at the clay surface (Cissokho et al., 2010). The latter is a bridging mechanism whereby the negatively charged clay surface and negatively charged molecules in the oil are bridged together by divalent cations (Buckley and Liy, 1998).

Extension of the electrical double layer – The electrical double layer is a well-known phenomenon describing the state and distribution of charges around a mineral surface. Winsauer and McCardell (1953) introduced the concept of ionic double layer conductivity in reservoir rock. Their results showed that excess double layer conductivity is dependent on the particular ions in the electrolyte as well as their concentration. Alias (2013) demonstrated the relation between the electrical double layer and the

zeta potential, showing that oppositely charged ions (counterions) are preferentially attracted toward the surface and where ions of the same charge (coions) tend to be repelled. In light of this, Ligthelm et al. (2009) proposed that wettability modification toward water wetness was the main mechanism of LSW and results from extension of the electrical double-layer in a low-salt solution. Knott (2009) suggested that, when a negatively charged clay particle in a porous, oil-bearing reservoir its double layer consists of an inner adsorbed layer of positive ions and an outer diffuse layer of mainly negative ions. The thickness of this layer, however, depends on the ion concentration in the surrounding water. At high-salinity the double layer is more compact, but when low-salinity water is introduced during LSW, the double layer tends to expand. The adsorbed layer of positive ions contains divalent calcium (Ca^{2+}) or magnesium (Mg^{2+}), which act as tethers between the clay and oil droplets. Expansion of the diffuse layer enables monovalent ions such as sodium (Na^{+}), carried in the injection water, to penetrate the double layer, displacing the divalent ions, and increasing the electrostatic repulsion between clay particles and oil. Once the repulsive forces exceed the binding forces caused by multivalent cation bridges, the tethers between oil and clay particles are broken, and the oil can be desorbed. This changes the wetting state and allows the oil to be swept out of the reservoir.

Ligthelm et al. (2009) made several observations supporting the proposed mechanism. During flooding experiments, after oil production with high-salinity brine containing sodium, calcium and magnesium had stopped, the flooding brine composition was changed to include only sodium chloride with the same ionic strength, and a small increase in oil recovery was observed. This is consistent with the proposed cation exchange mechanism, suggesting the pure sodium chloride brine stripped the divalent cations from the rock surface. The brine was then diluted to a 100-times-lower salinity, and a subsequent large increase in recovery was observed. This was believed to be related to the expansion of the electrical double layer and suggested that the contribution of the cation exchange mechanism to oil release was small compared to that from expansion of the electrical double layer.

Nasralla and Nasr-El-Din (2012, 2014) also deduced that expansion of the electrical double layer is a dominant mechanism of oil recovery improvement by LSW. However, a recent molecular simulation by Mehana and Fahes (2018) on double-layer expansion during LSW was inconsistent with this conclusion.

Wettability alteration – As discussed above, making a rock more oil wet tends to release oil held by capillary trapping, and making it more water wet enhances water imbibition and oil counter-current production. Cassie and Baxter (1944), Buckley et al. (1989), and Chen et al. (2004) suggested that the water film separating crude oil from the mineral surface is not always stable and that the original water wetness of the rock can be altered by destabilizing the water film. To do so, the disjoining pressure must be overcome by altering the wettability. Zhang et al. (2007) examined the role of calcium and magnesium, and sulphate ions on wettability alteration in carbonates. The results revealed that divalent anions have a stronger effect on wettability alteration than their monovalent counterparts. The ratio of Ca^{2+}/SO_2^{-4} was found to have a more pronounced effect on wettability alteration and hence recovery than individual anions. Mohammed and Babadagli (2015), Saikia et al. (2018) and Ding and Rahman (2018) provided a comprehensive review of the various methods for wettability alteration during LSW.

Osmosis - Buckley (2009) hypothesized that osmosis may be a mechanism for enhanced oil recovery during LSW. In this model clays separating brines with different salinities create an osmotic pressure that can enhance the water drive. Later, studies by Yousef and Ayirala (2014), Callegaro et al. (2014), Rotondi et al. (2014), Fredriksen et al. (2016), Sandengen et al. (2016), Fredriksen et al. (2016), and Pollen and Berg (2018), supported these findings.

Salting effect - Salting in refers to a process where increasing the ionic strength of a solution increases the solubility of a solute, often a polar molecule. This effect tends to be observed when the ionic strength of the water is low. Salting out, on the other hand, also known as salt-induced precipitation, implies the reduced solubility of polar components in high ionic strength solutions (Austad, 2012). This is often

used as a purification technique for large biomolecules. RezaeiDoust et al. (2009) evaluated salting as a mechanism for LSW by performing adsorption and desorption studies of quinoline onto kaolinite at room temperature. Their assumption was that low-salinity effects are linked to the improved water wetness of the clay. There have, however, been very few studies supporting the salting-in mechanism in relation to LSW, although Austad et al. (2010), Nasralla and Nasr-El-Din (2014), and Kakati and Sangwai (2017), argue that there is a need for additional experiments to validate the possible importance of this effect.

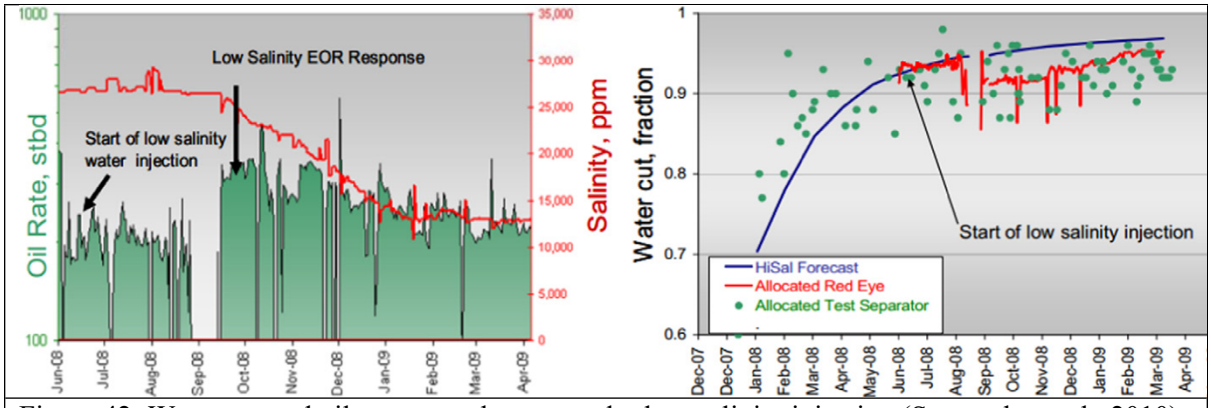

Figure 42: Water cut and oil recovery changes under low-salinity injection (Seccombe et al., 2010)

As noted above, Katende and Sagala, (2019) summarized several examples of LSW case histories. One was an extensive field test conducted at the Endicott field on the north slope of Alaska by British Petroleum, a pioneer in LSW (Seccombe et al., 2010). Endicott core measurements, field single-well chemical tracer tests (SWCTT) and simulation studies were reported by Seccombe et al. (2008). From 2004 through 2006, SWCTTs were performed to evaluate reduced-salinity EOR including the impact of clay content and slug size on incremental oil recovery. The reduced-salinity pilot was designed in 2007 and operated in 2008 and 2009. The Endicott trial was implemented in a single reservoir zone (subzone K3A, composed of braided-stream sands with discontinuous shales, in an area with an average permeability of 100 md and an average porosity of 20 percent) with the injector and producer wells spaced 1040 ft. apart. The dominant framework grain in this sub-zone is quartz, and the most common cement is siderite. A significant amount of the porosity at Endicott is secondary porosity formed by the leaching of siderite. Kaolinite is the dominant clay, followed by illite. The reservoir water at Endicott was alumina-rich and authigenic kaolinite crystals formed in the available interstitial space in preference to other clays. The producer was monitored for changes in water cut and ionic water composition after injection of low-salinity water.

The goal of this pilot was to determine the incremental benefit of tertiary-low-salinity EOR water flooding over secondary high-salinity water flooding. To accomplish this, the pilot was pre-flooded with high-salinity produced water. Reduced salinity water injection did not commence until the pilot producer watercut reached 95% and the associated tracers indicated that enough water had been injected to completely fill the pore volume in the region where fluids were flowing between the two wells. Data from the wellhead infrared water cut meter and test separator confirmed a decrease in water cut from 95% to 92% after injection. In addition, 10% of the additional oil was recovered from the zone swept with low-salinity water and, in the pilot area, a significant drop in residual oil saturation of 41% to 28% was observed (Seccombe et al., 2010). Based on Endicott corefloods and SWCTTs, it was determined that incremental low-salinity oil recovery is a function of clay content.

Figure 42 presents the water cut and oil recovery profiles. A slight drop in water cut from 95% to 92% after a few months of injection, followed by a gradual rise to the previous value. This was attributed to formation of a second oil bank ahead of the flooded zone. As shown in Figure 42 (right-hand side), reducing the salinity of the injected water improved daily production significantly.

Based on the results from the Endicott test, Seccombe et al. (2010) concluded that:

1. The area swept by reduced-salinity water resulted in additional oil recovery in agreement with that observed in Endicott corefloods and single-well tracer tests. After injection of 1.6 pore volumes of reduced-salinity water, incremental oil recovery from both the pilot and the coreflood (scaled for clay content) was ten percent of the total pore volume swept.

2. The pilot demonstrated that low-salinity waterflooding works equally well at inter-well distances as it does in corefloods and single well tests. Using an Endicott coreflood and SWCTTs a linear relationship between reduced-salinity and clay content was defined. Based on clay content in the pilot area, it was predicted that final pilot oil recovery would be 13 percent of the total pore-volume swept with reduced-salinity water. Actual pilot recovery after 1.6 pore volumes of reduced-salinity water injection was 10% of the total pore-volume swept. Comparison of the pilot recovery profile with the scaled core-flood recovery profile indicated that the pilot was on-track to recover 13%.

3. The pilot showed that mixing reduced-salinity and high-salinity brines did not affect the EOR process at inter-well distances.

4. Viscous fingering of reduced-salinity water into the oil bank was not evident.

5. The three aspects of the pilot that confirm the validity of the low-salinity EOR mechanism are:

• Right Time: Incremental oil recovery came when reduced-salinity water broke through at the producer.

• Right Size: The incremental oil recovered agreed with predictions from the coreflood and from tracer tests.

• Right Shape: The incremental oil recovery profile overlays the coreflood profiles when scaled for clay content.

Conversely, a number of unsuccessful field cases studies of LSW recovery have been reported. These include the: Bastrykskoye Field in Russia (Khisamov et al., 2017; Ahmetgareev et al., 2015; Zeinijahromi et al., 2015; Bedrikovetsky et al., 2015) where the insignificant IOR due to LSW was as due to the large volume of high salinity water produced before the start of LSW; the Sijan Field in Syria [8] where the insignificant response was due to a strong buoyancy effect caused by the high permeability of the block, and injectant mixing with the highly saline aquifer; and the Snorre Field in the North Sea of Norway (Skrettingland et al., 2011; Reinholdtsen et al., 2011), where the lack of response to LSW was related to the pH of the formation brine.

On the basis of their analysis of the available studies, Katende and Sagala (2019) concluded that, “despite the promising potential justified by both laboratory studies and field applications, there exists a large number of unsuccessful field case studies. LSW is viewed as an immature EOR technique with many ambiguities because definitive conclusions about which mechanism(s) is responsible for improving oil recovery remains elusive and a bewilderment to the oil industry. They noted that “Significant work investigating LSW has been conducted by major oil field companies and research institutes for the past 20 years. These studies have covered laboratory core floods, single-well reactive chemical tracer tests (SWCTTs) and well-to-well pilots of tertiary LSW. In addition, data on earlier low-salinity secondary water floods have been analyzed.

The main conclusions to be drawn from this study are as follows.

1. LSW is an immature EOR technique with considerable potential for increasing oil recovery, as verified through various laboratory studies and field applications. The incremental recovery reported in the literature ranges from 0 to 15% OIIP depending on the rock and fluid properties and reservoir conditions.
2. Several recovery mechanisms have been proposed by various researchers; however, no consensus exists as to which mechanisms are dominant in improving oil recovery during low-salinity water injection. Therefore, prior to any field-scale application, extensive laboratory studies should be conducted on the representative rocks and fluid samples to investigate the potential of LSW to increase oil recovery.
3. The provision of a low-salinity water supply in a field can act synergistically with other water-based EOR processes such as alkaline/surfactant/polymer flooding with the potential for even greater

incremental recoveries. The injection of low salinity water can also help in overcoming conventional problems such as souring and scaling.

4. Although not yet proven, LSW either alone or in conjunction with other water-based EOR techniques has the potential to be a "game changer" in both offshore and onshore reservoirs, and therefore, the potential benefits of switching to LSW should be studied for all fields in which water flooding is ongoing or planned. Such research should be undertaken systematically and consistently through independent laboratories."

Table 4: Summary of previous studies on low-salinity water flooding (Katende and Sagala (2019).

Reference	Porous medium	Pressure and temperature	Injected water salinity (ppm)	Reservoir formation salinity (ppm)	Proposed mechanism of oil recovery	Remarks
Bernard (1967)	Sandstone (Berea)	Ambient conditions	100–15,000	15,000	– Wettability alteration	1. If the fresh waterflood does not develop a high-pressure drop, no additional oil is produced. 2. A higher recovery is achieved in water-sensitive cores with a fresh waterflood than with brine largely because hydratable clays are present. 3. A decrease in salinity causes an increase in oil recovery.
Jadhunaiidan (1990)	Sandstone (Berea)	Ambient conditions at 26, 50 and 80 °C	200–18,000	18,814	– Wettability alteration	1. Temperature and initial water saturation are dominant variables with respect to wettability. 2. Intermediately wet systems show the lowest residual oil saturation and the greatest amount of oil recovered by water flooding.
Yildiz and Morrow (1996)	Sandstone (Berea)	Ambient conditions at 110 °C	6370	63,700	– Wettability alteration	1. Rock-brine interactions are responsible for the wettability changes. 2. Oil recovery is dependent on the initial and injected brine composition.
Tang and Morrow (1997)	Sandstone (Berea)	Ambient pressure at 75 °C	<8000	24,168	– Wettability alteration	1. The transition toward a more water-wet system occurs when the temperature is increased during the course of dispersement, although the wettability changes with thermodynamic conditions in the reservoir.
Tang and Morrow (1999)	Sandstone (Berea)	2000 psi and 55 °C	36,960	15,150	– Fines mobilization. – Limited release of mixed wet particles.	1. Recovery of crude oil at a high water cut could be initiated or curtailed based on the composition of the injection brine. 2. Changes in oil recovery with salinity can be partly ascribed to the effect of brine chemistry on the forces needed to strip these particles from the pore walls during the course of waterflooding.
McGuire et al. (2005)	Sandstone (Berea)	Ambient conditions at 40 °C	1500	15,000	– Saponification	1. Low-salinity water flooding appears to be effective at salinity levels of approximately 5000 ppm TDS or less. 2. The EOR mechanisms underlying low-salinity water flooding appear to be similar to those of alkaline flooding, i.e. the, generation of surfactants, changes in wettability, and reductions in the interfacial tension; in addition, the detachment of clay particles may also be involved.
Lager et al. (2006)	Sandstone	Ambient and Reservoir Conditions	1550	20,000	– Cation exchange	1. Cation-exchange explains why low-salinity water flooding is not effective when a core is acidized and fired as the cation exchange capacity of the clay minerals is destroyed. 2. Cation-exchange explains why low-salinity water injection has no effect on mineral oil, as no polar compounds are present to strongly interact with the clay minerals. 3. Cation exchange explains why low-salinity water flooding is not effective on carbonate reservoirs.
Zhang and Morrow (2006)	Sandstone (Berea)	Ambient conditions	Not mentioned	Not mentioned	– Increased pH – Saponification	1. The properties of sandstone influence oil recovery via the injection of low-salinity water. 2. Effluent pH influences oil recovery.
Zhang et al. (2007)	Sandstone	Ambient conditions at 60 °C	1479	29,690	– Wettability alteration – Cation exchange	1. The effluent pH is clearly dependent on the crude oil and its role in the crude oil/brine/rock interactions, but there was no obvious relationship between effluent pH and oil recovery 2. Additional recovery is obtained via the addition of divalent ions to the injection brine. 3. For mixed wet cores, there was little or no oil recovery as a result of injection of low-salinity brine.
Loahardjo et al. (2007)	Sandstone	Ambient conditions at 60 °C	<5000	35,000	– Wettability Alteration – Cation exchange	1. Low-salinity water flooding changes core properties during several flood cycles.
Seccombe et al. (2008)	Carbonates	Ambient and Reservoir conditions	3983	54,720	– Multicomponent Ion Exchange – Expansion of the electrical double layer	1. A 40% low-salinity water flooding is expected to be fully effective based on coreflood studies, single-well chemical tracer tests in multiple wells, numerical simulations and geochemical modelling.

Table 4 (*continued*)

Reference	Porous medium	Pressure and temperature	Injected water salinity (ppm)	Reservoir formation salinity (ppm)	Proposed mechanism of oil recovery	Remarks
Lebedeva et al. (2009)	Sandstone (Tensleep)	Ambient Conditions	1316.3	38,651	– Cation exchange	1. The application of DLVO (Derjaguin-Landau-Verwey-Overbeek) theory at the salinity seen in most reservoirs is questionable because of the very high concentrations of the brine.
Soraya et al. (2009)	Sandstone	Ambient conditions at 90 $^{\circ}$ C	1170	58,320	– Multicomponent ion exchange – Increase in pH – Influence of temperature	1. The multicomponent ion exchange proposed by Larger et al. [95] , can be used for screening different types of adsorption mechanisms of organic compounds on mineral surfaces and to explain how salinity can influence oil/rock interactions. 2. There was no direct relationship between the pH of the effluent and additional oil recovery. 3. Low-salinity injection is sensitive to initial wettability.
Ligthelm et al. (2009)	Sandstone (Berea)	Ambient Conditions	100 times diluted Dagang brine	240,000	– Wettability altertaion toward increased water-wet conditions.	1. Designer waterflooding in mixed wet/oil wet sandstones causes wettability modification toward an increased water-wet state and in abscence of an efficient water/oil gravity drainage process, application on the reservoir scale may yield an increased displacement sweep efficiency of several magnitudes.
RezaiDoust et al. (2009)	Sandstone and Carbonates	High pressure and temperature > 90 $^{\circ}$ *C*	<5000	25,000	– Wettability alteration – Salting out effect – Multicomponent Ion Exchange	1. For carbonates, salinity water is able to improve water wetness at high temperature. 2. For sandstones, improved water wetness is associated with the presence of clay materials. 3. The adsorption strength of organic materials in both carbonates and sandstones is attached to the rock. 4. The MIE mechanism for low-salinity flooding in sandstones only occurs under low salinity conditions. 5. The MIE in carbonates is dependent on the ions Ca^{2+} , Mg^{2+} and SO_4^{2-}
Lee et al. (2010)	Clay	Not mentioned	<4000	Not mentioned	– Expansion of the electrical double layer	1. Expansion of the double layer supports the theory presented by Lager et al. [95] .
Austad et al. (2010)	Sandstone	Ambient conditions at 40 $^{\circ}$ C	Not mentioned	Not mentioned	– Wettability alteration toward increased water wetness – Cation Exchange	1. At low water-wet conditions, a substantail increase in oil recovery of 75% by low-salinity water flooding can be obtained in the laboratory if the core
Sorbie and Collins (2010)	Pore-Scale Modelling	Not mentioned	Not mentioned	Not mentioned	– Wettability alteration toward increased water wetness.	1. The wetting change in the oil wet pores from some degree of oil wetness to a more water-wet state may be affected by any of the precise surface chemistry mechanisms that may occur.
Vledder et al. (2010)		Ambient contions	2200	90,000	– Wettability Alteration	A change in wettability leads to a significant increase in recovery of the STOIIP.
Alotaibi et al. (2010)	Carbonates	Ambient temperature at 1000 psi and 500 psi	5436	54,000	– Wettability Alteration	1. The effect of pressure on wettability is not significant. 2. There is a lower contact angle for acquifer water (TDS 5436 ppm) than formation water (TDS 54,000 ppm).
Berg et al. (2010)	Montmorillonite clay	Ambient Conditions	2000	29,950	– Wettability Alteration	1. Experiments were not specific enough to determine whether the actual weakening of the adhesion forces is caused by the double-layer expansion or the ion exchange reactions. 2. Interfacial tension, fines migration and the selective plugging of water-bearing pores using clay swelling are not relevant mechanisms for the low-salinity water flooding effect. 3. Oil is released under very low salinity.
Cissokho et al. (2010)	Clayey Sandstone	Ambient conditions at 90 ◦C, 60 ◦C and 35 ◦C	2500	50,000	– Increase in temperature – Cation exchange	1. Temperature has a significant effect on oil recovery, and the recovery occurs even if no divalent ions are present in the low-salinity brine. 2. Experimental results show that additional oil recovery can be obtained without the presence of kaolinite as proposed by Tang and Morrow [18] .

Reference	Porous medium	Pressure and temperature	Injected water salinity (ppm)	Reservoir formation salinity (ppm)	Proposed mechanism of oil recovery	Remarks
Wang and Alvarado (2010)	Sandstone	1000 psi and 30 ° C	5749.1	57,491	– Interfacial effect through analysis of capillary hysteresis. – Wettability alteration	1. The low-salinity effect can still act in the abscence of wettability alteration. 2. At low temperatures, low-salinity brine suppresses capillary hysteresis.
Morrow (2011)	Sandstone (Berea)	Ambient conditions	<5000	24,168	– Cation exchange and wettability alteration	1. Significant clay fraction 2. Presence of connate water 3. Exposure to crude oil to create mixed-wet conditions
Yousef et al. (2011)	Carbonates (Chalk)	1804 psi and 212 ° *F*	Twice, 10, 20, 100-times-diluted formation water	213,000	– wettability alteration – Significant pressure drops were related to fine particle migration.	1. Approximately 7–8.5% additional oil recovery for twice-diluted water. 2. 10 times diluted 9–10% additional oil. 3. 20 times diluted 1–1.6%. 4. 20 times diluted 1–1.6%. 5. Tertiary oil was obtained after 0.5–0.7 PV. 6. No noticeable IFT reduction; hence, LSW has no effect on IFT reductions.
Nasralla et al. (2011)	Sandstone (Berea)	500 psi and 100 ° C	5000–174,000	174,156	– Cation exchange resulting from wettability alteration. – Reduction of electrostatic forces between oil and rock.	1. Additional 22% in the secondary mode but no recovery in tertiary mode. 2. Recommend LSW for secondary flooding injection.
Li (2011)	Sandstone (Berea)	Room temperature and pressure	1780	33,540	– Increased pH – and reduced IFT similar to alkaline flooding.	1. In either secondary or tertiary oil recovery, the EOR associated with the injection of low-salinity water is obtained under a negative pressure gradient higher than that during the brine injection at the same flow velocity, as the water permeability is reduced because of the blockage of pore networks by swelling clay aggregates or migrating clay particles and crystals. 2. For the injection of low-salinity water, the EOR is strongly dependent on flow velocity and flow acceleration.
Alotaibi et al. (2011)	Sand stone (Sciot o and Berea)	2000 psi and Temperatures from (50 ° C, 90 ° C and 132.2 ° C)	5,436	174,156	– Wettability Alteration	1. For Berea Sandstone, the interfacial energies of solid/fluid and fluid/fluid interfaces are affected by different ion strength solutions, and as such, the wettability and contact angle are altered. 2. For Scioto sandstone rocks, the wettability was not affected by low-salinity water.
Hassenkam et al. (2011)	Sandstone	Ambient Conditions	1400	36,500	– Wettability alteration to a more water wet system. – Expansion of the double layer	1. The pH of the solution did not play a critical role in the low-salinity effect. 2. The response to changes in salinity is not uniform.
Sandengen et al. (2011)	Sandstone	~20 bar and 124 C	1741	40,075	– Wettability alteration to a more oil wet system because of ion exchange	1. Experimental core flooding shows that the introduction of low-salinity water yields an end to oil production as a result of capillary end effects and a significant change in the capillary pressure curve that parallels the wettability alteration toward a more oil-wet system.
Suijkerbuijk et al. (2012)	Sandstone (Berea)	Ambient conditions at 60oC	1,681	237,858	– Wettability alteration	1. Increasing the concetration of divalent cations in the formation brine makes the crude/oil/brine/rock system oil wet. 2. When the imbibing phase was either higher or lower in salinity than the formation brine, there was an increase in oil recovery.
Fjelde et al. (2012)	Sandstone (Berea)	725 psi and 80◦C	Prepared by diluting FW 100 times using distilled water	105,096	– Low-salinity water altered the wetting state of the rock. – Cation exchange.	1. Oil was produced over much longer periods in LSW. 2. Estimated permeability and capillary curves indicated that the rock was water wet in the high-salinity floods and mixed wet in the low-salinity floods.
Zahid et al. (2012)	Carbonates (Chalk)	Ambient conditions and at 90 ◦C	20-timesdiluted formation water	213,734	– Fine particle migration – Dissolution of the rock material – Wettability alteration based on contact angle measurements	1. No oil recovery under ambient conditions 2. Increased pressure drops detected over the core plugs 3. At 90 ◦C, more oil was recovered. 4. Pressure drops were attributed to fine particle migration. 5. Substitution reactions seem to not be a mechanism that controls oil recovery in chalk.

Table 4 (*continued*)

Reference	Porous medium	Pressure and temperature	Injected water salinity (ppm)	Reservoir formation salinity (ppm)	Proposed mechanism of oil recovery	Remarks
Romanuka et al. (2012)	Carbonates	Ambient conditions at85 ° C	<5000	230,000	– Wettability alteration	1. Oil recovery for carbonates can be increased by lowering the ionic strength of the brine. 2. Information on water and oil relative permeability curves is vital before and after wettability alteration for determining the benefit of low-salinity waterflooding on a field scale. 3. Conditions under which wettability alteration takes place are not identified.
Mahani et al. (2013)	Sandstone	Ambient conditions	6487.5	25,950	– Wettability alteration toward a more water-wet state.	1. The kinetics of wettability change are slow, and the time scales observed were approximately10–20 times longer than expected by diffusion only.
Suijkerbuijk et al. (2013)	Sandstone	Ambient Conditions	Not mentioned	Not mentioned	– Wettability alteration– Expansion of thedouble layer	1. Multicomponent ion exchange is not an economically viable mechanism behind low-salinity water flooding because it occurs at the retardation front, which requires several magnitudes of the injection of low salinity brine to result in a significant production. 2.Low-salinity water flooding leads to wettability alteration toward a more water-wet system; however, it requires a longer time scale.
Nasralla and Nasr-El-Din (2014)	Sandstone (Berea)	Ambient conditions at212 ° F	5000	174,156	– Expansion of the double layer – Salt in effect	1. The behavior of the rock wettability versus the brine salinity and pH was correlated to the change in the double layer thickness based on the *ζ*–potential results. 2. The high-salinity seawater resulted in an intermediate-wet mica surface, whereas 10% AQ and 5000 mg/L NaCl conditions made the mica surface water wet, which demonstrates the effect of water salinity on wettability alteration and hence the potential for oil recovery improvement.
Xie et al. (2014)	Core plugs extracted from theChang-8 formation of the ChangQing Oilfield	Ambient Conditions at65 ° C	2777	58,430	– Expansion of the double layer.	1. Ions tuning water flooding showed a high potential to improve oil recovery in both secondary and tertiary injection modes for low-permeability reservoirs in the ChangQing oilfield. 2.Multi-component might be one of the mechanisms in recovering additional oil.
Bartels et al. (2014)	Micro-models with active clays as a model system for sandstone.	Ambient Conditions	6393	25,574	– Wettability alteration	1. Low-salinity effect is not driven by a change in interracial tension. 2.The role of osmosis is not the primary mechanism behind the occurrence of the low salinity effect.
Mahani et al. (2015)	Carbonate	Ambient conditions at 25 °C	1759 and 2540	43,731	– Wettability alteration	1. The low-salinity change causes a wettability shift to a more water-wet state
Brady et al. (2015)	Sandstone	Ambient Conditions	<5000	24,000	– Simultaneous effect of pH and ion exchange on oil and mineral surface electrostatics	1. This DLVO approximation omits, among other things, short-range, repulsive, and structural forces. 2.Linking reservoir morphology, surface chemistry, wettability, and crude oil/brine/rock interactions tooil recovery can be readily utilized to predict waterflood recoveries in sandstone reservoirs containing clays other than kaolinite and to carbonates.

Table 4 (*continued*)

Reference	Porous medium	Pressure and temperature	Injected water salinity (ppm)	Reservoir formation salinity (ppm)	Proposed mechanism of oil recovery	Remarks
Mahani et al. (2015)	Carbonate	Ambient conditions at 25 °C	1759	179,855	– Wettability alteration toward a more oil-wet system. – Impact of mineral dissolution.	1. Low-salinity effect occurs even in the absence of mineral dissolution and depends on electrostatic interactions between the crude oil and the rock.
Ouden et al. (2015)	Carbonate	Ambient conditions	1000–5000	33,390	– Mineral Dissolution – Wettability alteration	1. pH increase has a significant effect on calcite dissolution 2. Increase in salinity of the injected brines caused by calcite dissolution makes low-salinity waterflooding effective.
Xie et al. (2016)	Sandstone (Berea)	Ambient Conditions	2000	174,000	– Cation exchange – Expansion of the double layer	1. Low-salinity water triggers positive disjoining pressure in a system of crude oil/brine/rock as a result of double layer expansion. 2. The cation type dominates the disjoining pressure of the oil/brine/rock system instead of the salinity level. 3. Removing divalent cations from the injected brine is essential to observing the low-salinity effect. 4. The disjoining pressure based on extended DLVO theory could be applied to preliminary screen the candidate reservoirs for low-salinity water flooding.
Sandengen et al. (2016)	Sandstone	Ambient conditions	Not mentioned	Not mentioned	– Osmosis	1. Osmotic gradients are present across oil films, and the increase in oil production is largely caused by osmosis rather than a wettability change.
Torsaeter et al. (2016)	Sandstone (Berea)	45 bar and 60 °C	3106	31,061	– Wettabilility alteration	1. Low-salinity water flooding with only NaCl resulted in a more water-wet system with divalent cations.
Fredriksen et al. (2016)	Sandstone and Carbonates	Ambient temperature and pressure	Not mentioned	Not mentioned	– Osmotic pressure – Wettability alteration	1. The growth of water in emulsions is a result of osmosis. 2. The low-salinity effect is more relevant under oil-wet conditions, and there are a variety of circumstances under which the low-salinity effect may or may not be observed, which suggests that more than one mechanism is at play.
Xie et al. (2017)	Sandstone	20 MPa, 30 MPa, 40 MPa, 50 MPa and temperatures of 60 °C, 100 °C and 140 °C	1424.31	142,431	– Wettability alteration variation with temperature. – Expansion of the double layer.	1. Water chemistry, temperature and pressure affect the contact angle; however, water chemistry plays a dominant role in determining the contact angle and thus the wettability. 2. Low-salinity water flooding can be applied to high-temperature (> 100 °C.) reservoirs
Kakati and Sangwai (2017)	Sandstone	Ambient conditions at 25 °C, 40 °C and 55 °C	1900	19,000	– Wettability alteration	1. The ageing time has a considerable effect on the contact angle in a sense that the contact angles increase with the ageing time, while quartz surfaces become more oil wet when the temperatures increase.
Salehi et al. (2017)	Sandstone	1700 psi and 80 °C	up to 200,000	200,000	– Wettability alteration	1. Oil recovery increases with the injection of salinity, while the interfacial tension decreases with salinity.
Kim and Lee (2017)	Sandstone	Ambient conditions at 60 °C	3000	30,000	– Wettability alteration	1. The shift in relative permeability curves is proportional to the clay contents in kaolinite, and thus, low-salinity water flooding should be considered an EOR scheme for reservoirs with a high kaolinite content.
Xie et al. (2018)	Carbonate	Ambient conditions at 25 °C, 60 °C and 100 °C	10-times-diluted formation brine	252,244	– Increased pH combined with wettability alteration.	1. pH scales with contact angle and the oil/brine/rock system wettability.

Table 4 (*continued*)

Reference	Porous medium	Pressure and temperature	Injected water salinity (ppm)	Reservoir formation salinity (ppm)	Proposed mechanism of oil recovery	Remarks
Nasralla et al. (2018)	Carbonates (Chalk)	400 psi and 100 ° C	10 times diluted Salinity water	239,000	– Reduction in residual oil saturation – Dilution of sea water	1. Spontaneous imbibition tests showed minimal oil production with FW, which indicates that the rock wettability of the tested samples is non-water wet. 2. Secondary mode Amott tests showed higher oil production by seawater than formation brine, which demonstrates the wettability alteration by SW. 3. Diluted seawater gave higher spontaneous imbibition than both FW and SW, which proves that diluting seawater has a greater potential to improve oil recovery than FW or SW. 4. Tertiary mode Amott tests and qualitative USS tests confirmed the wettability alteration by LS brines and the greater potential of diluted SW to improve oil recovery than seawater.
Suleimanov et al. (2018)	Sandstone	16 MPa and 62 ° C	3587.45	18,738.24	– Cation exchange – Wettability alteration	1. There are slight differences in ionic adsorption caused by LHAW and LSW; however, the changes in contact angle for the LHAW were greater than for LSW, as were the changes in interfacial tension, suggesting that the LHAW waters will release more oil than LSW. 2. In a tertiary treatment model, LHAW-2 and LHAW-1 as displacement agents increased oil recovery (%OOIP) by 13% and 10% respectively in comparison with LSW.
Chen et al. (2018)	Carbonates	2000 psi and 60 ° C	<5000	100,000	– Multicomponent ion exchange – pH increase	1. Multicomponent ion exchange triggers a pH increase during low-salinity water flooding in the presence of basal-charged clays, and a more water-wet system is obtained.
Chen et al. (2018)	Carbonate	2000 psi and 60 ° C	10-times-diluted formation brine and 100-times-diluted formation brine	252,244	– Wettability alteration Increased pH	1. Conventional dilution triggers an oil-wet system at a lower pH 2. pH plays a fundamental role in the surface chemistry of oil/brine interfaces and wettability.
Pooryousef et al. (2018)	Sandstone	200 bar at 50 ° C and 100 ° C	2000	50,000	– Wettability alteration Influence of temperature	1. Wettability shifts from oil wet to slightly water wet with increasing temperature. 2. A low concentration of Ca^{2+} produces an oil-wet system, and a high concentration of Ca^{2+} produces a water-wet system. 3. Contact angle varies with increasing temperature in the presence of softened brine. 4. Zeta potential of brine/muscovite increases with increasing salinity 5. Wettability alteration does not support the theory of multicomponent ion exchange proposed by Lager et al. [95] .
Sharma and Mohanty (2018)	Carbonate	Ambient conditions at 120 ° C	511 and 1,600	149,160	– Wettability alteration – Mineral dissolution	1. Wettability of the surface is dependent on surface concentration of the acids. 2. Mineral dissolution is important for determining the wettability alteration
AlHammadi et al. (2018)	Carbonate	1000 psi and 80 ° C	1000–35,000	208,600	Wettability alteration Micro-dispersion formation	1. Additional recovery is predominantly controlled by the formation of micro-dispersions and is linked to the interaction between polar components with brine molecules. 2.
Saiia et al. (2018)	Carbonate	700psi and 82 ° F	2 times, 10 times, 50 times and 100 times diluted formation brine	10,780	– Wettability alteration	1. Wettability of carbonates depends on the iso-electric point of the carbonate rock surface, pH and inter-facial energy between the aqueous brine solution and the rock surface. 2. Reducing the interfacial energy manifests as a wettability change.
Pollen and Berg (2018)	Sandstone	Ambient Conditions at 22 ° C and elevated temperatures of 70 ° C	Not mentioned	Not mentioned	– Osmosis	1. At ambient conditions, no clear correlation was found between IOR and the surface-to-volume ratio. However, there is a correlation between IOR and the pore volume. 2. Elevated temperatures result in low values of IOR which do not correlate with either surface are or pore volume.

*** the sections below have not been completed/answered***

- **What naturally occurring mechanisms promote or impede oil migration or flow in oil-wet and water-wet reservoirs?**

***

Acknowledgements

As the purpose of this report is to provide a summary of measurement methods and answer a number of specific questions posed by Pioneer Natural Resources, I have freely borrowed and edited prose from whatever sources could be found. References to these sources are found in each part of this manuscript as necessary, along with those they quoted. Other parts of this report are new prose. However, this report should not be published in any form as some of it is not new work.

References

Abdallah W., Buckley J. S., Carnegie A., Edwards J., Herold B., Fordham E., Graue A., Habashy T., Seleznev N. and Signer C. (2007) Fundamentals of wettability. *Technology* **38**, 1125-1144.

Adamson, A.W. (1982) Physical Chemistry of Surfaces, fourth edition, John Wiley and Sons Inc., New York City (1982) 332-68.

Aggarwal S. (2016) Wettability alteration using fluorinated nano-silica for near wellbore region. **M.S.**, University of Oklahoma, 72p.

Aggarwal S. (2016) Wettability alteration using fluorinated nano-silica for near wellbore region. **M.S.**, University of Oklahoma, 72p.

Ahmetgareev, V., A. Zeinijahromi, A. Badalyan, R. Khisamov, P. Bedrikovetsky (2015) Analysis of low salinity waterflooding in Bastrykskoye Field, Pet. Sci. Technol. 33 (5), 561–570. https://doi.org/10.1080/10916466.2014.997390.

Al-Mahrooqi S. H., Grattoni C. A., Moss A. K. and Jing X. D. (2003) An investigation of the effect of wettability on NMR characteristics of sandstone rock and fluid systems. *Journal of Petroleum Science and Engineering* **39**, 389-398.

Al-Sarihi, A., A. Zeinijahromi, L. Genolet, A. Behr, P. Kowollik, P. Bedrikovetsky (2018) Effects of fines migration on residual oil during low-salinity waterflooding, Energy Fuels 32 (8), 8296–8309. https://doi.org/10.1021/acs. energyfuels.8b01732.

Alhammadi AM, AlRatrout A, Singh K, Bijeljic B, Blunt MJ (2017) In situ characterization of mixed-wettability in a reservoir rock at subsurface conditions. Sci Rep 7:10753.

AlHammadi, M., P. Mahzari, M. Sohrabi (2018) Fundamental investigation of underlying mechanisms behind improved oil recovery by low salinity water injection in carbonate rocks, Fuel 220, 345–357. https://doi.org/10.1016/j.fuel. 2018.01.136

Alias, A. (2013) Emulsion Stability, https://www.slideshare.net/akarim717/emulsion-stability, Accessed date: 19 April 2018.

Alotaibi, M.B., R. Azmy, H.A. Nasr-El-Din (2010) Wettability Challenges in Carbonate Reservoirs, SPE Improved Oil Recovery Symposium, 24–28 April, Tulsa, Oklahoma, USA, https://doi.org/10.2118/129972-MS.

Alotaibi, M.B., R.A. Nasralla, H.A. Nasr-El-Din (2011) Wettability studies using low salinity water in sandstone reservoirs, SPE Reserv. Eval. Eng., 1–13. https://doi.org/10.2118/149942-PA.

AlRatrout A., Blunt M. J. and Bijeljic B. (2018) Wettability in complex porous materials, the mixed-wet state, and its relationship to surface roughness. *Proc Natl Acad Sci U S A* **115**, 8901-8906.

AlRatrout AAM, Blunt MJ, Bijeljic B (July 2, 2018) Spatial correlation of contact angleand curvature in pore-space images. Water Resour. Res.

Amiri, S., A. Gandomkar (2019) Influence of electrical surface charges on thermodynamics of wettability during low salinity water flooding on limestone reservoirs, J. Mol. Liq. https://doi.org/10.1016/j.molliq.2018.12.069.

Anderson W. G. (1986a) Wettability Literature Survey-Part 1: Rock/Oil/Brine interactions and the Effects of Core Handling on Wettability. *Journal of Petroleum Technology* **38**, 1125-1144.

Anderson W. G. (1986b) Wettability Literature Survey-Part 2: Wettability Measurement. *Journal of Petroleum Technology* **38**, 1246-1262.
Anderson W. G. (1986c) Wettability Literature Survey-Part 3: The Effects of Wettability on the Electrical Properties of Porous Media. *Journal of Petroleum Technology* **38**, 1371-1378.
Anderson W. G. (1987b) Wettability Literature Survey-Part 5: The Effects of Wettability on Relative Permeability. *Journal of Petroleum Technology* **39**, 1453-1468.
Anderson, W.G. (1987a) Wettability Literature Survey-Part 4: The Effects of Wettability on Capillary Pressure," paper SPE 15271 available at SPE, Richardson, TX.
Andrew M, Bijeljic B, Blunt MJ (2014) Pore-scale contact angle measurements at reservoir conditions using x-ray microtomography. Adv Water Resour 68:24–31.
Anovitz L. M. and Cole D. R. (2015) Characterization and Analysis of Porosity and Pore Structures. *Reviews in Mineralogy and Geochemistry* **80**, 61-164.
Anovitz, LM and Weston, J. (2021) **
API (1977) API Recommended Practices for Laboratory Testing of Surface Active Agents for Well Stimulation, American Petroleum Inst., API RP 42, second edition, Dallas (Jan. 1977).
Arshadi M., Piri M. and Sayed M. (2018) Proppant-packed fractures in shale gas reservoirs: An in-situ investigation of deformation, wettability, and multiphase flow effects. *Journal of Natural Gas Science and Engineering* **59**, 387-405.
Arshadi M., Zolfaghari A., Piri M., Al-Muntasheri G. A. and Sayed M. (2017) The effect of deformation on two-phase flow through proppant-packed fractured shale samples: A micro-scale experimental investigation. *Advances in Water Resources* **105**, 108-131.
Atkinson, B W, C J Conway and G J Jameson (1995) High-efficiency flotation of coarse and fine coal, in: High-efficiency Coal Preparation: An International Symposium, (Society of Mining, Metallurgy and Exploration: Littleton, Colorado, 1995).
Atkinson, BW, C J Conway and G J Jameson (1993) Fundamentals of Jameson Cell operation including size–yield response, Archived 2012-03-17 at the Wayback Machine in: Sixth Australian Coal Preparation Conference, Mackay, Queensland, 6–9 September 1993 (The Australasian Institute of Mining and Metallurgy: Melbourne, 1993).
Austad, T. (2012) Water Based EOR in Carbonates and Sandstones: New Chemical Understanding of the EOR-potential Using Smart Water.
Austad, T., A. Rezaeidoust, T. Puntervold (2010) Chemical Mechanism of Low Salinity Water Flooding in Sandstone Reservoirs, SPE Improved Oil Recovery Symposium, 24–28 April, Tulsa, Oklahoma, USA, https://doi.org/10.2118/129767-MS.
Austad, T.; Rezaeidoust, A.; Puntervold, T. (2010) Chemical Mechanism of Low Salinity Water Flooding in Sandstone Reservoirs; Society of Petroleum Engineers, 2010.
Bartell, F.E. and Miller, F.L. (1928) Degree of Wetting of Silica by Crude Petroleum Oils, Ind. Eng. Chem. (July 1928) 20, No. 7, 738-42.
Bartell, F.E. and Osterhof, H.J. (1927) Determination of the Wettability of a Solid by a Liquid: Relation of Adhesion Tension to Stability or Color Varnish and Lacquer Systems, Ind. Eng. Chem. (1927) 19, 1277-80.
Bartell, F.E. and Osterhof, H.J. (1933) Adhesion Tension: Pressure of Displacement Method, J. Phys. Chem. (1933) 37, No.5, 543-52.
Bartels, W.-B., H. Mahani, S. Berg, R. Menezes, J.A. van der Hoeven, A. Fadili (2014) Double-layer expansion: is it a primary mechanism of improved oil recovery by low-salinity waterflooding? SPE Reserv. Eval. Eng., 1–11. https://doi. org/10.2118/154334-PA.
Batycky, J.P. et al. (1981) Interpreting Relative Permeability and Wettability from Unsteady State Displacement Measurements, SPEJ (June 1981) 296-308.
Bedrikovetsky, P., A. Zeinijahromi, A. Badalyan, V. Ahmetgareev, R. Khisamov (2015) Fines-Migration-Assisted Low-Salinity Waterflooding: Field Case Analysis, SPE Russian Petroleum Technology Conference, 26–28 October, Moscow, Russia pp. 1–14. https://doi.org/10.2118/176721-MS.

Benner, F.C., Dodd, C.G., and Bartell, F.E. (1942) Displacement Pressures for Petroleum Oil-Water-Silica Systems, Oil & Gas J. (Nov. 12, 1942) 41, No. 27, 199-208.
Benner, F.C., Dodd, C.G., and Bartell, F.E. (1943) Evaluation of Effective Displacement Pressures for Petroleum Oil-Water-Silica Systems, Fundamental Research on Occurrence and Recovery of Petroleum, API, New York City (1943) 85-93.
Berg S et al. (2013) Real-time 3d imaging of haines jumps in porous media flow. Proc Natl Acad Sci USA 110:3755–3759.
Berg, S., A. Cense, E. Jansen, K. Bakker (2010) Direct Experimental Evidence of Wettability Modification By Low Salinity, Society of Petrophysicists & Well Log Analysts. https://www.onepetro.org/journal-paper/SPWLA-2010-v51n5a3.
Bernard, G.G. (1967) Effect of Floodwater Salinity on Recovery Of Oil from Cores Containing Clays, SPE California Regional Meeting, 26–27 October, Los Angeles, California, pp. 1–8. https://doi.org/10.2118/1725-MS.
Bestaoui-Spurr N., Langlinais K., Stanley D., Usie M. and Li C. (2018) Controlling Proppant Wettability Leads to Increase Flowback Recovery and Flow in Frac-Packs. *Society of Petroleum Engineers Journal* **SPE-189476-MS**, 1-8.
Bestaoui-Spurr N., Stanley, D., Wiulliams, V., Usie, M., Nugyen, H., and Hoffpauir, E. (2017b) OTC-27897-MS, Offshore Technology Conference, Houston, TX, May 1-4, 2017.
Bestaoui-Spurr N., Sun, S., Williams, V., Volk, A., Nguyen, S, (2017a) Using properties in nature to modify proppant surfaces and increase flow, SPI-184543-MS, SPE International Symposium on Oilfield Chemistry, Montgomery, TX, Apr-13-15 2017.
Bico J., Thiele U. and Quéré D. (2002) Wetting on textured surfaces. *Colloids and Surfaces A: Physicochemical and Engineering Aspects* **206**, 41-46.
Blunt MJ (2017) Multiphase Flow in Permeable Media: A Pore-Scale Perspective (Cambridge Univ Press, Cambridge, MA), p 500.
Bobek, J.E., Mattax, C.C., and Denekas, M.A. (1958) Reservoir Rock Wettability-Its Significance and Evaluation, JPT (July 1958) 155-60; Trans., AIME, 213.
Bockris, J. O'm., Devanathan, M. A. V., and Müllen, K. (1963). On the structure of charged interfaces. *Proceedings of the Royal Society of London. Series A. Mathematical and Physical Sciences*. **274** (1356): 55–79.
Bonn D, Eggers J, Indekeu J, Meunier J, Rolley E (2009) Wetting and spreading. Rev Mod Phys 81(2):739–805. doi:10.1103/RevModPhys.81.739
Bonto M., Eftekhari A. A. and Nick H. M. (2019) An overview of the oil-brine interfacial behavior and a new surface complexation model. *Sci Rep* **9**, 6072.
Brady, P.V., N.R. Morrow, A. Fogden, V. Deniz, N. Loahardjo, A. Winoto (2015) Electrostatics and the low salinity effect in sandstone reservoirs, Energy Fuels, 666–677. https://doi.org/10.1021/ef502474a.
Bravo, M.C.; Araujo, M. (2008) Analysis of the Unconventional Behavior of Oil Relative Permeability during Depletion Tests of Gas-Saturated Heavy Oils. International Journal of Multiphase Flow. 34 (5): 447–460. doi:10.1016/j.ijmultiphaseflow.2007.11.003
Bromberg L et al. (2017) Control of human skin wettability using the ph of anionic surfactant solution treatments. Colloids Surf B Biointerfaces 157:366–372.
Brooks, R.H.; Corey, A.T. (1964) Hydraulic properties of porous media. Hydrological Papers. 3.
Brown, R.I.S.and Gamson, B.W. (1960) Nuclear Magnetism Logging, Trans., AIME (1960) 219, 199-207.
Brown, R.J.S., Fatt, I., (1956) Measurements of fractional wettability of oilfield rocks by the nuclear magnetic relaxation method. Trans. AIME 207, 262– 264.
Brown, W.O. (1957) The Mobility of Connate Water During a Waterflood, JPT (July 1957) 190-95; Trans., AIME, 210.
Buckley JS, Liu Y and Monsterleet S (1998) Mechanisms of Wetting Alteration by Crude Oils, paper SPE 37230, SPE Journal 3, no. 1 (March 1998): 54–61.

Buckley JS, Takamura K, Morrow N (1989) Influence of electric surface charges on the wetting properties of crude oils. SPE Res Eng 4:332–340.
Buckley, J. (2009) Low Salinity Waterflooding — An Overview of Likely Mechanisms, https://www.uwyo.edu/eori/_files/eorctab_jan09/buckley_mechanisms. pdf, Accessed date: 19 April 2018.
Buckley, J., K. Takamura, N. Morrow (1989) Influence of electrical surface charges on the wetting properties of crude oils, SPE Reserv. Eng., 1–9. https://doi.org/10.2118/16964-PA.
Buckley, J.S., Y. Liu (1998) Some mechanisms of crude oil/brine/solid interactions, J. Pet. Sci. Eng. 155–160. https://doi.org/10.1016/S0920-4105(98) 00015-1.
Burkhardt, J.A., Ward, M.B., and McLean, R.H. (1958) Effect of Core Surfacing and Mud Filtrate Flushing on Reliability of Core Analysis Conducted on Fresh Cores, paper SPE 1139G presented at the 1958 SPE Annual Fall Meeting, Houston, Oct. 5-8.
Butt, Hans-Jürgen; Graf, Karlheinz; Kappl, Michael (2006). Physics and Chemistry of Interfaces. Wiley. p. 9. ISBN 978-3-527-60640-5.
Calhoun, J.C. (1951) Criteria for Determining Rock Wettabllity, Oil & Gas J. (May 10, 1951) 50, No. I, 151.
Callegaro, C., M. Bartosek, F. Masserano, M. Nobili, V.P.P. Parracello, C.S. Pizzinelli, A. Caschili (2014) Opportunity of Enhanced Oil Recovery Low Salinity Water Injection: From Experimental Work to Simulation Study up to Field Proposal, EAGE Annual Conference & Exhibition incorporating SPE Europec, 10–13 June, London, UK, https://doi.org/10.2118/164827-MS.
Campos V. P. P. D., Sansone E. C. and Silva G. F. B. L. E. (2018) Hydraulic fracturing proppants. *Cerâmica* **64**, 219-229.
Canbaz, C.H., Ghedan, S.G. (2014) Theory and Experimental Setup of the New Rise in Core Reservoir Wettability Measurement Technique. IPTC #17659, IPTC, Doha, Qatar, January 2014.
Cassie, A. B. D. and Baxter, S. (1944) Wettability of porous surfaces, Transactions of the Faraday Society 40, 546.
Cassie, A.B.D., S. Baxter (1944) Wettability of porous surfaces, Trans. Faraday Soc. 40, 546–551. https://doi.org/10.1039/TF9444000546.
Castor, T.P., Somerton, W.H., and Kelly, J.F. (1981) Recovery Mechanisms of Alkaline Flooding, Surface Phenomena in Enhanced Oil Recovery, D.O. Shah (ed.), Plenum Press, New York City (1981) 249-91.
Celik, M.S. and Somasundaran, P. (1980) Wettability of Reservoir Minerals by Flotation and Correlation with Surfactant Adsorption, paper SPE 9002 presented at the 1980 SPE Inti. Symposium on Oilfield and Geothermal Chemistry, Stanford, CA, May 28-30.
Chapman DL (1913) A contribution to the theory of electrocapillarity. Philos Mag 25:475–481.
Chatenever, A. (1955) Microscopic Behavior of Fluids in Porous Systems Final Report on Research Project 47b, Research on Occurrence and Recovery of Petroleum, API, New York City (1955) 69-80.
Chen X., Ma R., Li J., Hao C., Guo W., Luk B. L., Li S. C., Yao S. and Wang Z. (2012) Evaporation of droplets on superhydrophobic surfaces: surface roughness and small droplet size effects. *Phys Rev Lett* **109**, 116101.
Chen, J., G. Hirasaki, M. Flaum (2006) NMR wettability indices: effect of OBM on wettability and NMR responses, J. Pet. Sci. Eng. 52, 161–171. https://doi.org/10.1016/j.petrol.2006.03.007.
Chen, Y., Q. Xie, A. Sari, P.V. Brady, A. Saeedi (2018) Oil/water/rock wettability: influencing factors and implications for low salinity water flooding in carbonate reservoirs, Fuel 215, 171–177. https://doi.org/10.1016/j.fuel.2017.10. 031.
Chen, Y., Q. Xie, W. Pu, A. Saeedi (2018) Drivers of pH increase and implications for low salinity effect in sandstone, Fuel 218, 112–117. https://doi.org/10.1016/ j.fuel.2018.01.037.
Christian, S. D., Slage, A. R., Tucker, E. E., and Scamehorn, J. F. (1998) Inverted Vertical Pull Surface Tension Method, Langmuir, 14(X), 3126–3128.

Cissokho, M., H. Bertin, S. Boussour, P. Cordier, G. Hamon (2010) Low Salinity Oil Recovery On Clayey Sandstone: Experimental Study, Society of Petrophysicists and Well-Log Analysts. https://www.onepetro.org/journal-paper/SPWLA-2010-v51n5a2.

Clementz, D. M. (1982) Alteration of Rock Properties by Adsorption of Petroleum Heavy Ends: Implications for Enhanced Oil Recovery, paper SPE 10683 presented at the 1982 SPE/DOE Symposium on Enhanced Oil Recovery, Tulsa, OK, April 4-7.

Collins, K. D. (1997), Biophys. J., 72, 65–76.

Cooke, C.E., Williams, R.E., and Kolodzie, P.A. (1974) Oil Recovery by Alkaline Waterflooding, JPT (Dec. 1974) 1365-74.

Cordiner, F. S.; Gordon, D. T.; Jargon, J. R. (1972) Determination of Residual Oil Saturation After Waterflooding; Society of Petroleum Engineers, 1972.

Corey, A.T. (Nov 1954) The Interrelation Between Gas and Oil Relative Permeabilities. Prod. Monthly. 19 (1): 38–41.

Craig, F.F. (1971) The Reservoir Engineering Aspects of Waterflooding, Monograph Series, SPE, Richardson, TX (1971) 3, 12-44.

Cui H. and Anderson C. G. (2017) Alternative flowsheet for rare earth beneficiation of Bear Lodge ore. *Minerals Engineering* **110**, 166-178.

De Gennes PG (1985) Wetting—statics and dynamics. Rev Mod Phys 57(3):827–863

De Gennes PG, Brochard-Wyart F, Quéré D (2004) Capillarity and wetting phenomena. Springer, New York

De Gennes, P. G. (1994) Soft Interfaces. Cambridge, UK: Cambridge University Press. ISBN 978-0-521-56417-5.

Dehghanpour, H., DiCarlo,D.A, Aminzadeh.B., and Mirzaei,M. (2010) Two-Phase and Three-Phase Saturation Routes and Relative Permeability During Fast Drainage, SPE Improved Oil Recovery Symposium, SPE 129962-MS, DOI: 10.2118/129962-MS

Denekas, M.A., Mattax, C.C., and Davis, G.T. (1959) Effect of Crude Oil Components on Rock Wettability, JPT (Nov. 1959) 330-33; Trans., AIME, 216.

Devereaux, O.F. (1967) Effect of Crude Oil on the NMR Relaxation of Water Protons in Sandstone, Nature (Aug. 5, 1967) 215, 614-15.

Ding, H., S. Rahman (2018) Experimental and theoretical study of wettability alteration during low salinity water flooding — a state of the art review, J. Pet. Sci. Eng., 622–639. https://doi.org/10.1016/j.colsurfa.2017.02.006.

Donaldson, E.C. and Crocker, M.E. (1977) Review of Petroleum Oil Saturation and Its Determination, Bartlesville Energy Research Center, U.S. DOE, report BERC/RI-77/15 (Dec. 1977).

Donaldson, E.C., and Thomas, R.D. (1971) Microscopic Observations of Oil Displacement in Water-Wet and Oil-Wet Systems, paper SPE 3555 presented at the 1971 SPE Annual Meeting, New Orleans, Oct. 3-6.

Donaldson, E.C., Thomas, R.D., and Lorenz, P.B. (1969) Wettability Determination and Its Effect on Recovery Efficiency, SPEJ (March 1969) 13-20.

Dong K. (2018) Effect of Ceramic Proppant Surface Wettability on Oil Flow Efficiency in Hydraulic-Fractured Wells. *International Journal of Engineering Research and Development* **14**, 13-22.

Dong K., He W. and Wang M. (2019a) Effect of surface wettability of ceramic proppant on oil flow performance in hydraulic fractures. *Energy Science & Engineering* **7**, 504-514.

Dong K., Wang M. and Zhang C. (2019b) Effect of wettability of ceramic proppant surface in guar gum solution on the oil flow efficiency in fractures. *Petroleum* **5**, 388-396.

Doust, A.R., T. Puntervold, T. Austad (2011) Chemical verification of the EOR mechanism by using low saline/smart water in sandstone, Energy Fuels 25, 2151–2162. https://doi.org/10.1021/ef200215y.

Droppert, D., P. Fiore, Y. Dessureault, F. Cardarelli (2002) High strength, heat- and corrosion-resistant ceramic granules for proppants, Canadian Patent CA 2 329 834 (2002).

Du Nouy P. Lecomte (1919) A new apparatus for measuring surface tension", Gen. Physio.,1, 521-524.

du Noüy, Pierre Lecomte (1925) An Interfacial Tensiometer for Universal Use. The Journal of General Physiology. 7 (5): 625–633. doi:10.1085/jgp.7.5.625. PMC 2140742. PMID 19872165.
Dullien, F.A.L. (1979) Porous Media: Fluid Transport and Pore Structure, Academic Press, New York City (1979).
Dunning, H.N. and Johansen, R.T. (1958) Capillarimetric Method for Measurement of Crude Oil Wetting Tendency, Pet. Eng. (July 1958) 30, No.7, B26-B27.
Dussan EB, Chow RTP (1983) On the ability of drops or bubbles to stick to non-horizontal surfaces of solids. J Fluid Mech 137 (Dec):1–29
Ehrlich, R. and Wygal, R.I. (1977) Interrelation of Crude Oil and Rock Properties with the Recovery of Oil by Caustic Waterflooding, SPEJ (Aug. 1977) 263-70.
Ehrlich, R., Hasiba, H.H., and Raimondi, P. (1974) Alkaline Waterflooding for Wettability Alteration-Evaluating a Potential Field Application, JPT (Dec. 1974) 1335-43.
Eral H. B., 't Mannetje D. J. C. M. and Oh J. M. (2013) Contact angle hysteresis: a review of fundamentals and applications. *Colloid and Polymer Science* **291**, 247-260.
Everly D., Anderson C., Bryantsev V. S. and Jansone-Popova S. (2018) Improved Collectors for Flotation of Bastnaesite. *Research & Development in Material Science* **5(2)**, RDMS.000610.2018. DOI: 10.31031/RDMS.2018.05.000609.
Extrand CW (1998) A thermodynamic model for contact angle hysteresis. J Colloid Interface Sci 207(1):11–19
Falode O. and Manuel E. (2014) Wettability Effects on Capillary Pressure, Relative Permeability, and Irreducible Saturation Using Porous Plate. *Journal of Petroleum Engineering* **2014**, 1-12.
Fanchi, John R. (2006). Principles of Applied Reservoir Simulation (3rd Edition). Elsevier.
Fatt, I. and Klikoff, W.A. (1959) Effect of Fractional Wettability on Multiphase Flow Through Porous Media, Trans., AIME (1959) 216, 426-32.
Fischer, H., Gottschlich, R., Seelig, A. (1998) Blood-Brain Barrier Permeation: Molecular Parameters Governing Passive Diffusion, J. Membrane Biol. 165, 201–211.
Fjelde, I., S.M. Asen, A.V. Omekeh (2012) Low Salinity Water Flooding Experiments and Interpretation by Simulations, SPE Improved Oil Recovery Symposium, 14–18 April, Tulsa, Oklahoma, USA, https://doi.org/10.2118/154142-MS.
Frank, H. S., Wen, W. Y. (1957) Structural aspects of ion-solvent interaction in aqueous solutions: a suggested picture of water structure. Disc. Faraday Soc. 24: 133± 140
Fredriksen, S., A. Rognmo, K. Sandengen, M. Fern. (2016) Wettability Effects on Osmosis as an Oil Mobilization Mechanism During Low Salinity Waterflooding, International Symposium of the Society of Core Analysts held in Snowmass, Colorado, USA, 21–26 August, 2016, http://jgmaas.com/SCA/2016/SCA2016-011.pdf.
Fredriksen, S., A. Rognmo, M. Fern. (2016) Pore-scale Mechanisms During Low Salinity Waterflooding: Water Diffusion and Osmosis for Oil Mobilization, SPE Bergen One Day Seminar, 20 April, Grieghallen, Bergen, Norway https://doi.org/10.2118/180060-MS.
Freedman, R., Heaton, N., Flaum, M. (2001a) Field applications of a new nuclear magnetic resonance fluid characterisation method. SPE 71713, SPE Annual Tech. Conf. and Exhibition, New Orleans, LA.
Freedman, R., Lo, S., Flaum, M., Hirasaki, G.J., Matteson, A., Sezginer, A. (2001b) A new NMR method of fluid characterization in reservoir rocks: experimental confirmation and simulation results. SPE J. 6, 452– 464.
Frehse, W. (1973) Method for Determining the State of Wetting of Oil Reservoir Rocks, Zeitschrijt jar Angewandte Geologie (Feb. 1973) 19, No.2, 86-88. English translation available from the John Crerar Library, translation no. 74-10424-08G.
Freud, B. B., and Freud H. Z. (1930) A theory of the ring method for the determination of surface tension, J. Am. Chem. Soc., 52(5), 1772–1782.
Gatenby, W.A. and Marsden, S.S. (1958) Some Wettability Characteristics of Synthetic Porous Media, Producers Monthly (Nov. 1957) 22, No.1, 5-12.

Gaudin, A.M. (1957) Flotation, second edition, McGraw Hill Book Co. Inc., New York City.
Geffen, T.M. et al. (1951) Experimental Investigation of Factors Affecting Laboratory Relative Permeability Measurements, Trans., AlME (1951) 192, 99-110.
Ghedan, S.G. and Canbaz, C.H. (2014) Theory and Experimental Setup of the New Rise in Core Reservoir Wettability Measurement Technique. Paper presented at the International Petroleum Technology Conference, Doha, Qatar, January 2014. Paper Number: IPTC-17659-MS doi:10.2523/iptc-17659-ms. ISBN 9781613993224.
Ghedan, S.G.; Canbaz, C.H, Boyd, D. A., Mani, G.M., Haggag, M.K. (2010) Wettability Profile of a Thick Carbonate Reservoir by the New Rise in Core Wettability Characterization Method. Abu Dhabi International Petroleum Exhibition and Conference. doi:10.2118/138697-ms. ISBN 9781555633158.
Gimatudinov, Sh. K. (1963) The Nature of the Surface of Minerals of Oil-Bearing Rocks, lzv. Vyssh. Ucheb. Zavedenii, Neft i Gaz (1963) 6, No.7, 37-42. English translation available from Associated Technical Services, translation no. 23R75R.
Glass, R.J., Conrad, S.H., Peplinski, W. (2000) Gravity-destabilized nonwetting phase invasion in macroheterogeneous porous media: Experimental observations of invasion dynamics and scale analysis, Water Resources Research, Vol 36 Issue 11 http://dx.doi.org/ 10.1029/2000wr900152
Glembotskii, V.A., Klassen, V.I., and Plaksin, LN. (1972) Flotation, Primary Sources, New York City.
Goda, H.M.; Behrenbruch, P. (2004) Using a Modified Brooks-Corey Model to Study Oil-Water Relative Permeability for Diverse Pore Structures. Paper SPE-88538-MS Presented at SPE Asia Pacific Oil and Gas Conference and Exhibition, Perth, Australia. doi:10.2118/88538-MS. ISBN 978-1-55563-979-2.
Good, R. J. (1992) Contact angle, wetting, and adhesion: a critical review. Journal of Adhesion Science and Technology. 6 (12): 1269–1302. doi:10.1163/156856192X00629.
Gouy M (1910) Sur la constitution de la charge électrique a la surface d'un électrolyte. J Phys 9:457–468.
Graham, J.W. (1958) Reverse-Wetting Logging, Trans AIME (1958) 213, 304-09.
Grahame, David C. (1947) The Electrical Double Layer and the Theory of Electrocapillarity. *Chemical Reviews*. **41** (3): 441–501.
Grigor'ev, S.N. (1980) Procedure for Evaluating Relative Wettability of Reservoir Rock of Producing Deposits, Izv. Vyssh. Ucheb. Zavedenii, Nefti Gaz (Nov. 1980) No. 11,33-38. English translation available from Associated Technical Services, translation no. 59L169R.
Haagh M. E., Siretanu I., Duits M. H. and Mugele F. (2017) Salinity-Dependent Contact Angle Alteration in Oil/Brine/Silicate Systems: the Critical Role of Divalent Cations. *Langmuir* **33**, 3349-3357.
Handy, L.L. (1960) Determination of Effective Capillary Pressures for Porous Media from Imbibition Data, Trans., AIME (1960) 219, 75-80.
Hang, P.T. and Brindley, G.W. (1970) Methylene Blue Adsorption by Clay Minerals. Detenrunationof Surface Areas and Cation Exchange Capacities, Clays and Clay Minerals 18, 203-12.
Harkins, W. D., and Jordan H. F. (1930) A method for the determination of surface and interfacial tension from the maximum pull on a ring, J. Am. Chem. Soc., 52(5), 1751–1772.
Hassenkam T, Skovbjerg L, Stipp S (2009) Probing the intrinsically oil-wet surfaces of pores in North Sea chalk at subpore resolution. Proc Natl Acad Sci USA 106:6071– 6076.
Hassenkam, T., C.S. Pedersen, K. Dalby, T. Austad, S.L.S. Stipp (2011) Pore scale observation of low salinity effects on outcrop and oil reservoir sandstone, Colloids Surf. A Physicochem. Eng. Asp. 390, 179–188. https://doi.org/10.1016/j. colsurfa.2011.09.025.
Heaviside, J., Langley, G.O. and Pallatt, N. (1983) Permeability Characteristics of Magnus Reservoir Rock, Proc., European Formation Evaluation Symposium, London (March 1983).
Hellmann, J.R., B.E. Scheetz, W.G. Luscher, D.G. Hartwich, R.P. Koseski (2014), Am. Ceram. Soc. Bull. **93**, 1 (2014) 29.

Helmholtz, H. (1853), Ueber einige Gesetze der Vertheilung elektrischer Ströme in körperlichen Leitern mit Anwendung auf die thierisch-elektrischen Versuche, Annalen der Physik und Chemie (in German), 165 (6), pp. 211–233, Bibcode:1853AnP...165..211H, doi:10.1002/andp.18531650603

Hilner, E.; Andersson, M. P.; Hassenkam, T.; Matthiesen, J.; Salino, P. A.; Stipp, S. L. S. (2015) The effect of ionic strength on oil adhesion in sandstone: The search for the low salinity mechanism. Sci. Rep. 2015, 5, 9933.

Hirasaki GJ (1991) Wettability: Fundamentals and Surface Forces, SPE Formation Evaluation 6, no. 3 (June 1991): 217–226.

Hjelmeland, O. and Torsaeter, 0. (1981) Wettability, The Key to Proper Laboratory Waterflooding Experiments, Proc., IntI. Energy Agency Workshop on Enhanced Oil Recovery, Bartlesville Energy Technology Center, April 24, 1980, U.S. DOE, CONF-8004140 (Feb. 1981) 1-24.

Holbrook, O.C. and Bernard, G.C. (1958) Determination of Wettability by Dye Adsorption, Trans., AIME (1958) 213, 261-64.

Holmes, M. and Tippie, D.B. (1977) Comparison Between Log and Capillary Pressure Data to Estimate Reservoir Wetting, paper SPE6856 presented at the 1977 SPE Annual Technical Conference and Exhibition, Denver, Oct. 9-12.

Hosseini, E., Chen, Z., Sarmadivaleh, M., and Mohammadnazar, D. (2020) Applying low-salinity water to alter wettability in carbonate oil reservoirs: an experimental study. *Journal of Petroleum Exploration and Production Technology*.

Howard, J.J. (1994) Wettability and fluid saturations determined from NMR T1 distributions. Magn. Reson. Imaging 12, 197– 200.

Howard, J.J. (1998) Quantitative estimates of porous media wettability from proton NMR measurements. Magn. Reson. Imaging 16, 529– 533.

Hsu, W.F., Li, X., Flumerfelt, R.W., 1992. Wettability of porous media by NMR relaxation methods. SPE 24761, 67th Annual Tech. Conf. and Exhibition, Washington, DC.

Huh C. and S.G. Mason (1975) A Rigorous Theory of Ring Tensiometry. Colloid Poly. Sci.,253, 566-580.

Hyvaluoma J, Koponen A, Raiskinmaki P, Timonen J (2007) Droplets on inclined rough surfaces. Eur Phys J E 23(3):289–293. doi:10.1140/epje/i2007-10190-7.

Iler, R. K (1979) The Chemistry of Silica: Solubility, Polymerization, Colloid and Surface Properties and Biochemistry of Silica. Wiley, ISBN: 978-0-471-02404-0, 896 Pages

Ishino, C.; Okumura, K (2008) Wetting transitions on textured hydrophilic surfaces (PDF). European Physical Journal. 25 (4): 415–424. Bibcode:2008EPJE...25..415I. doi:10.1140/epje/i2007-10308-y. PMID 18431542.

Jackson, M. D.; Vinogradov, J.; Hamon, G.; Chamerois, M. (2016) Evidence, mechanisms and improved understanding of controlled salinity waterflooding part 1: Sandstones. Fuel 2016, 185, 772−793.

Jadhunaiidan, P.P. (1990) Effects of Brine Composition, Crude Oil and Aging Conditions on Wettability and Oil Recovery, PhD dissertation. New Mexico Institute of Mining and Technology Socorro New Mexico 87801.

Jameson, G J (1992) Flotation cell development, in: The AusIMM Annual Conference, Broken Hill, New South Wales, 17–21 May 1992 (The Australasian Institute of Mining and Metallurgy: Melbourne, 1992), 25–31.

Jennings, H.Y. Jr. (1957) Surface Properties of Natural and Synthetic Porous Media, Prod. Monthly (March 1957) 21, No.5, 20-24.

Jerauld G, Rathmell J (1997) Wettability and relative permeability of Prudhoe Bay: A case study in mixed-wet reservoirs. SPE Reservoir Eng 12:58–65.

Joanny JF, De Gennes PG (1984) A model for contact-angle hysteresis. J Chem Phys 81(1):552–562

Johansen, R.T. and Dunning, H.N. (1959) Relative Wetting Tendencies of Crude Oil by the Capillarimetric Method, Producers Monthly (Sept. 1959) 23, No. 11, 20-22.

Johansen, R.T. and Dunning, H.N. (1961) Relative Wetting Tendencies of Crude Oils by Caplllarimetric Method, U.S. Dept. of the Interior, USBM, report RI 5752 (1961).
Johnson, E.F., Bossler, D.P., and Naumann, V.O. (1959) Calculation of Relative Permeability from Displacement Experiments, Trans., AlME (1959) 216, 370-72.
Johnson, R. E. (1993) in Wettability Ed. Berg, John. C. New York, NY: Marcel Dekker, Inc. ISBN 0-8247-9046-4
Jones, S.C. (1985) Some Surprises in the Transport of Miscible Fluids in the Presence of a Second Immiscible Phase, SPE.T (Feb. 1985) 101-12.
Kakati, A., J.S. Sangwai (2017) Effect of monovalent and divalent salts on the interfacial tension of pure hydrocarbon-brine systems relevant for low salinity water flooding, J. Pet. Sci. Eng. 157, 1106–1114. https://doi.org/10.1016/j.petrol.2017.08.017.
Kakati, A., J.S. Sangwai (2017) Wettability alteration of mineral surface during low salinity water flooding: role of salt type, pure alkanes, and model oils containing polar components, Energy Fuels 32 (2017) 3127U″ -3137. https://doi.org/10. 1021/acs.energyfuels.7b03727.
Kamath, LS.K. and Marsden, S.S. (1966) A Wettability Scale for Porous Media, preprint 14D presented at the 1966 AIChE Natl. Meeting, Dallas, Feb. 6-9.
Katende, A., and Sagala, F. (2019) A critical review of low salinity water flooding: Mechanism, laboratory and field application. *Journal of Molecular Liquids*, *278*, 627-649.
Khanamiri, H.H., I.B. Enge, M. Nourani, J.A. Stensen, O. Tors.ter, N. Hadia (2016) EOR by Low Salinity Water and Surfactant at Low Concentration: Impact of Injection and in Situ Brine Composition, Energy Fuels 30, 2705–2713. https://doi. org/10.1021/acs.energyfuels.5b02899.
Khisamov, V., V. Akhmetgareev, T. Shilova (2017) Core Tests and Field Case Studies of Successful and Unsuccessful Low-Salinity Waterfloods from Four Oil Fields, 79th EAGE Conference and Exhibition 2017 - Workshops, pp. 1–7. https://doi.org/10.3997/2214-4609.201701703.
Khishvand M, Alizadeh AH, and Piri M (2016) In-situ characterization of wettability and pore-scale displacements during two- and three-phase flow in natural porous media. Adv Water Resour 97:279–298.
Khishvand M, Alizadeh AH, Kohshour IO, Piri M, Prasad RS (2017) In situ characterization of wettability alteration and displacement mechanisms governing recovery enhancement due to low-salinity waterflooding. Water Resour Res 53:4427–4443.
Killins, C.R., Nielsen. R.F., and Calhoun, J.E (1953) Capillary Desaturation and Imbibition in Porous Rocks. Producers Monthly (Dec. 1953) 18, No.2, 30-39.
Kim, C., J. Lee (2017) Experimental study on the variation of relative permeability due to clay minerals in low salinity water-flooding, J. Pet. Sci. Eng. 151, 292– 304. https://doi.org/10.1016/j.petrol.2017.01.014.
Kinney, P.T. and Nielsen, R.F. (1950) The Role of Wettability in Oil Recovery, Producers Monthly (Jan. 1950) 14, No. 3,29-35.
Kinney, P.T. and Nielsen, R.F. (1951) Wettability in Oil Recovery, World Oil (March 1951) 132, No.4, 145-54.
Kinney, P.T., Killins, C.R., and Nielsen, R.F. (1951) Some Applications of Capillary Pressure Measurements on Pennsylvania Sands, Bull., Technical Conference on Petroleum Production, Mineral Industries Experiment Station, Pennsylvania State U. (Oct. 24-26, 1951) No. 59, 52-61.
Kirkwood, J. G. (1936) ** Chem Rev. 19, 275-**.
Knott, T. (2009) Less Salt, More Oil, BP Magazine of Technology and Innovation. 1–12.
Kovscek A, Wong H, Radke C (1993) A pore-level scenario for the development of mixed wettability in oil reservoirs. Environ Energy Eng 39:1072–1085.
Kremer J., Kilzer A. and Petermann M. (2018) Simultaneous measurement of surface tension and viscosity using freely decaying oscillations of acoustically levitated droplets. *Rev Sci Instruments* **89**, 015109.

Krishnan, A., Liu, Y.-H., Cha, P.,Woodward, R., Allara, D., and Vogler, E. A. (2005). An evaluation of methods for contact angle measurement. Colloids and Surfaces B: Biointerfaces 43:95–98.

Kullman, J. (2011) The complicated world of proppant selection, South Dakota Sch. Mines Techn., Dakota (2011).

Kumar, J., Fatt, 1., and Saraf, D.N. (1969) Nuclear Magnetic Relaxation Time of Water in a Porous Medium with Heterogeneous Surface Wettability, J. Appl. Physics (Sept. 1969) 40, No. 10, 4165-71.

Kyte, J.R., Naumann, V.O., and Mattax, C.C. (1961) Effect of Reservoir Environment on Water-Oil Displacements, JPT (June 1961) 579-82.

Lafuma A, Quéré D (2003) Superhydrophobic states. Nat Mater 2:457–460.

Lager, A., K. Webb, C. Black, M. Singleton, K. Sorbie (2008) Low Salinity Oil Recovery — An Experimental Investigation1, Society of Petrophysicists and Well-Log Analysts. https://www.onepetro.org/journal-paper/SPWLA-2008-v49n1a2.

Lager, A., K.J. Webb, C.J.J. Black, M. Singleton, K.S. Sorbie (2006) Low Salinity Oil Recovery — An Experimental Investigation, International Symposium of the Society of Core Analysts held in Trondheim, Norway 12–16 September, 2006, pp. 1–8. https://www.scaweb.org/abstracts/880.html.

Lager, A.; Webb, K.; Black, C.; Singleton, M.; Sorbie, K. (2008) Low Salinity Oil Recovery:An Experimental Investigation. Petrophysics; Society of Petrophysicists and Well-Log Analysts, 2008; Vol. 49 (1).

Lai, R.W.M. and Fuerstenau, D.W. (1968) Liquid-Liquid Extraction of Ultrafine Particles, Trans., AIME (1968) 241, 549-56.

Lebedeva, E., T.J. Senden, M. Knackstedt, N. Morrow (2009) Improved Oil Recovery from Tensleep Sandstone Studies of Brine-Rock Interactions by Micro-CT and AFM, IOR 2009 - 15th European Symposium on Improved Oil Recovery, https://doi.org/10.3997/2214-4609.201404879.

Lee, K. S.; Ivanova, N.; Starov, V. M.; Hilal, N.; Dutschk, V. (2008) Kinetics of wetting and spreading by aqueous surfactant solutions. Advances in Colloid and Interface Science. 144 (1–2): 54–65. doi:10.1016/j.cis.2008.08.005. PMID 18834966.

Lee, S.Y., K.J. Webb, I. Collins, A. Lager, S. Clarke, M.O. Bapos Sullivan, A. Routh, X. Wang (2010) Low Salinity Oil Recovery: Increasing Understanding of the Underlying Mechanisms, SPE Improved Oil Recovery Symposium, 24–28 April, Tulsa, Oklahoma, USA, pp. 1–11. https://doi.org/10.2118/129722- MS.

Leverett, M.C. (1941) Capillary behavior in porous solids. Transactions of the AIME (142): 159–172.

Li, Y. (2011) Oil recovery by low salinity water injection into a reservoir: a new study of tertiary oil recovery mechanism, Transp. Porous Media (2011) 333U-362. https://doi.org/10.1007/s11242-011-9788-8.

Liang, F., M. Sayeda, G.A. Al-Muntasheria, F.F. Chang, L. Lia, (2016) ** Petroleum **2**, 1 (2016) 26.

Ligthelm, D. J.; Gronsveld, J.; Hofman, J.; Brussee, N.; Marcelis, F.; van der Linde, H. (2009) Novel Waterflooding Strategy By Manipulation Of Injection Brine Composition; Society of Petroleum Engineers, 2009.

Ligthelm, D.J., J. Gronsveld, J. Hofman, N. Brussee, F. Marcelis, H. van der Linde (2009) Novel Waterflooding Strategy By Manipulation Of Injection Brine Composition, EUROPEC/EAGE Conference and Exhibition, 8–11 June, Amsterdam, The Netherlands, https://doi.org/10.2118/119835-MS.

Loahardjo, N., X. Xie, P. Yin, N.R. Morrow (2007) Field and laboratory observations of remaining oil saturations in a light oil reservoir flooded by a low salinity aquifer, International Symposium of the Society of Core Analysts held in Calgary, Canada, 10–12 September, 2007, http://jgmaas.com/SCA/2007/29.pdf.

Lomeland, F. (2018) Overview of the LET Family of Versatile Correlations for Flow Functions. Proceedings of the 2018 International Symposium of the SCA, Trondheim, Norway, 27 - 30 August, 2018.

Lomeland, F.; Ebeltoft, E.; Thomas, W.H. (2005) A New Versatile Relative Permeability Correlation. Proceedings of the 2005 International Symposium of the SCA, Abu Dhabi, United Arab Emirates, October 31 - November 2, 2005.

Lu Y., Najafabadi N. F. and Firoozabadi A. (2017) Effect of Temperature on Wettability of Oil/Brine/Rock Systems. *Energy & Fuels* **31**, 4989-4995.

Mahani, H., A.L. Keya, S. Berg, W.-B. Bartels, R. Nasralla, W. Rossen (2015) Driving Mechanism of Low Salinity Flooding in Carbonate Rocks, EUROPEC 2015, 1–4 June, Madrid, Spain, https://doi.org/10.2118/174300-MS.

Mahani, H., A.L. Keya, S. Berg, W.-B. Bartels, R. Nasralla, W.R. Rossen (2015) Insights into the mechanism of wettability alteration by low-salinity flooding (LSF) in carbonates, Energy Fuels 29, 1352–1367. https://doi.org/10.1021/ ef5023847.

Mahani, H., S. Berg, D. Ilic, W.-B. Bartels, V. Joekar-Niasar (2013) Kinetics of the Low Salinity Waterflooding Effect Studied in a Model System, SPE Enhanced Oil Recovery Conference, 2–4 July, Kuala Lumpur, Malaysia, pp. 1–14. https://doi.org/10.2118/165255-MS.

Mahani, H.; Keya, A. L.; Berg, S.; Bartels, W.-B.; Nasralla, R.; Rossen, W. R. (2015) Insights into the Mechanism of Wettability Alteration by Low-Salinity Flooding (LSF) in Carbonates. Energy Fuels 2015, 29, 1352−1367.

Mamontov E., O'Neill H., Zhang Q., Wang W. and wesolowski D. J. (2012) Common features in the microscopic dynamics of hydration water on organic and inorganic surfaces. *Journal of Physics-Condensed Matter* **24**, 064104.

Mamontov E., Vlcek L., wesolowski D. J., Cummings P. T., Wang W., Anovitz L. M., Rosenqvist J., Brown C. M. and GarciaSakai V. (2007) Dynamics and Structure of Hydration Water on Rutile and Cassiterite Nanopowders Studied by Quasielastic Neutron Scattering and Molecular Dynamics Simulations. *Journal of Physical Chemistry C* **111**, 4328-4341.

Mamontov E., Vlcek L., Wesolowski D., Cummings P., Rosenqvist J., Wang W., Cole D., Anovitz L. and Gasparovic G. (2009) Suppression of the dynamic transition in surface water at low hydration levels: A study of water on rutile. *Physical Review E* **79**,

Mamontov E., Wesolowski D. J., Vlcek L., Cummings P. T., Rosenqvist J., Wang W. and cole D. R. (2008) Dynamics of Hydration Water on Rutile Studied by Backscattering Neutron Spectroscopy and Molecular Dynamics Simulation. *Journal of Physical Chemistry C* **112**, 12334-12341.

Marcus Y. (1988) Ionic Radii in Aqueous Solutions. *Chemical Reviews* **88**, 1475-1498.

Marcus Y. (2009) Effect of ions on the structure of water: structure making and breaking. *Chem Rev* **109**, 1346-1370.

Marle, C.M. (1981) Multiphase Flow in Porous Media, Gulf Publishing Co., Houston (1981) 42-64.

Marmur, A. (2003) Wetting of Hydrophobic Rough Surfaces: To be heterogeneous or not to be, Langmuir 19 (20), 8343–8348. doi:10.1021/la0344682

Marmur, A. (2006) Soft contact: Measurement and interpretation of contact angles, Soft Matter 2, 12.

Marmur, A. (2009) Solid-surface characterization by wetting, Annual Review of Materials Research 39, 473.

Marsden, S.S. (1965a) Wettability-Its Measurement and Application to Waterflooding, J. Jpn. Assoc. Pet. Tech. (Jan. 1965) 30, No.1, 1-10.

Marsden, S.S. (1965b) Wettability: The Elusive Key to Waterflooding, Petroleum Engineer (April 1965) 37, No.4, 82-87.

Marston, P. L., and Trinh, E. H., J. (1985), Acoust. Soc. Amer., Suppl. 1, 77, $20 (1985).

Mattax, C.C. and Kyte, J.R. (1961) Ever See a Waterflood? Oil & Gas J. (Oct. 16, 1961) 59, No. 42, 115-28.

McCaffery, F.G. (1973) The Effect of Wettability on Relative Permeability and Imbibition in Porous Media, PhD thesis, U. of Calgary, Calgary, Alberta (1973).
McGuire, P.L., J.R. Chatham, F.K. Paskvan, D. Sommer, F. Carini (2005) Low Salinity Oil Recovery: An Exciting New EOR Opportunity for Alaska's North Slope, SPE Western Regional Meeting, 30 March–1 April, Irvine, California, pp. 1–15. https://doi.org/10.2118/93903-MS.
McLin, K., D. Brinton, P. Mandalaparty, C. Jones, J. Moore, (2010) ** Trans. Geotherm. Resour. Counc. **1**, 34 (2010) 365.
McPhee, C.; Reed, J.; Zubizarreta, I. (2015) Core Analysis: A Best Practice Guide. Elsevier. ISBN 978-0-444-63533-4.
Mehana, M., M.M. Fahes (2018) Investigation of Double Layer Expansion in Low salinity Waterflooding: Molecular Simulation Study, SPE Western Regional Meeting, 22–26 April, Garden Grove, California, USA, pp. 1–17. https://doi.org/10.2118/190106-MS.
Michaels, A.S. and Porter, M.E. (1965) Water-Oil Displacements from Porous Media Using Transient Adhesion Tension Alterations, AIChE J. (July 1965) 11, No.4, 617-24.
Michaels, A.S. and Timmins, R.S. (1960) Chromatographic Transport of Reverse-Wetting Agents and Its Effect on Oil Displacement in Porous Media, Trans., AIME (1960) 219,150-57.
Michaels, A.S., Stancell, A., and Porter, M.E. (1964) Effect of Chromatographic Transport in Hexylamine on Displacement of Oil by Water in Porous Media, SPEJ (Sept. 1964) 231-39: Trans., AIME, 231.
Mirzaei-Paiaman, Abouzar; Asadolahpour, Seyed Reza; Saboorian-Jooybari, Hadi; Chen, Zhangxin; Ostadhassan, Mehdi (2020) A new framework for selection of representative samples for special core analysis. Petroleum Research. doi:10.1016/j.ptlrs.2020.06.003.
Mirzaei-Paiaman, Abouzar; Ostadhassan, Mehdi; Rezaee, Reza; Saboorian-Jooybari, Hadi; Chen, Zhangxin (2018) A new approach in petrophysical rock typing. Journal of Petroleum Science and Engineering. 166: 445–464. doi:10.1016/j.petrol.2018.03.075. hdl:20.500.11937/66997.
Mirzaei-Paiaman, Abouzar; Saboorian-Jooybari, Hadi; Chen, Zhangxin; Ostadhassan, Mehdi (2019) New technique of True Effective Mobility (TEM-Function) in dynamic rock typing: Reduction of uncertainties in relative permeability data for reservoir simulation. Journal of Petroleum Science and Engineering. 179: 210–227. doi:10.1016/j.petrol.2019.04.044.
Mohammed, M., T. Babadagli (2015) Wettability alteration: a comprehensive review of materials/methods and testing the selected ones on heavy-oil containing oil wet systems, Adv. Colloid Interf. Sci. 220, 54–77. https://doi.org/10.1016/j.cis.2015.02.006.
Mohanty, KK and Salter, S.J. (1983) Multiphase Flow in Porous Media: III. Oil Mobilization, Transverse Dispersion, and Wettability, paper SPE 12127 presented at the 1983 SPE Annual Technical Conference and Exhibition, San Francisco, Oct. 5-8.
Moore, T.F. and Slobod, R.L. (1956) The Effect of Viscosity and Capillarity on the Displacement of Oil by Water, Prod. Monthly (Aug. 1956) 20, No. 10, 20-30.
Mora T., Orogbemi O. A. and Karpyn Z. T. (2010) A Study of Hydraulic Fracture Conductivity and Its Dependence on Proppant Wettability. *Petroleum Science and Technology* **28**, 1527-1534.
Morris, E.E. and Wieland, D.R. (1963) A Microscopic Study of the Effect of Variable Wettability Conditions on Immiscible Fluid Displacement, paper SPE 704 presented at the 1963 SPE Annual Fall Meeting, New Orleans, Oct. 6-9.
Morrow NR (1990) Wettability and its effect on oil recovery. J Pet Technol 42:1476–1484.
Morrow, N., J. Buckley (2011) Improved oil recovery by low-salinity waterflooding, J. Pet. Technol. (2011) 1–7. https://doi.org/10.2118/129421-JPT.
Morrow, N.R. (1970) Physics and Thermodynamics of Capillary Action in Porous Media, Ind. Eng. Chem. (June 1970) 62, No.6, 32-56.
Morrow, N.R. (1971) The Retention of Connate Water in Hydrocarbon Reservoirs, J. Cdn. Pet. Tech. (Jan.-March 1971) 10, No. 1, 38-55.
Morrow, N.R. (1976) Capillary Pressure Correlations for Uniformly Wetted Porous Media. J. Cdn. Pet. Tech. (Oct.-Dec. 1976) 15, No.4, 49-69.

Morrow, N.R. and McCaffery, F.G. (1978) Displacement Studies in Uniformly Wetted Porous Media, Wetting, Spreading, and Adhesion, G.F. Padday (ed.), Academic Press, New York City (1978), 289-319.

Morrow, N.R. and Mungan, N. (1971) Wettability and Capillarity in Porous Media, Petroleum Recovery Research Inst., Calgary, report RR-7 (Jan. 1971).

Mugele, F.; Bera, B.; Cavalli, A.; Siretanu, I.; Maestro, A.; Duits, M.; Cohen-Stuart, M.; van den Ende, D.; Stocker, I.; Collins, I. (2015) Ion adsorption-induced wetting transition in oil−water−mineral systems. Sci. Rep. 2015, 5, 10519.

Myint, P. C.; Firoozabadi, A. (2015) Thin liquid films in improved oil recovery from low-salinity brine. Curr. Opin. Colloid Interface Sci. 2015, 20, 105−114.

Nasralla, R. A.; Nasr-El-Din, H. A. (2014) Impact of cation type and concentration in injected brine on oil recovery in sandstone reservoirs. J. Pet. Sci. Eng. 2014, 122, 384−395.

Nasralla, R.A., H. Mahani, H.A. van der Linde, F.H. Marcelis, S.K. Masalmeh, E. Sergienko, N.J. Brussee, S.G. Pieterse, S. Basu (2018) Low salinity waterflooding for a carbonate reservoir: experimental evaluation and numerical interpretation, J. Pet. Sci. Eng., 640–654. https://doi.org/10.1016/j.petrol.2018.01.028.

Nasralla, R.A., H.A. Nasr-El-Din (2012) Double-layer Expansion: Is It A Primary Mechanism of Improved Oil Recovery by Low-salinity Waterflooding? SPE Improved Oil Recovery Symposium, 14–18 April, Tulsa, Oklahoma, USA, pp. 1–17. https://doi.org/10.2118/174063-MS.

Nasralla, R.A., H.A. Nasr-El-Din (2014) Double-layer expansion: is it a primary mechanism of improved oil recovery by low-salinity waterflooding? SPE Reserv. Eval. Eng. 1–11. https://doi.org/10.2118/154334-PA.

Nasralla, R.A., M.B. Alotaibi, H.A. Nasr-El-Din (2011) Efficiency of Oil Recovery by Low Salinity Water Flooding in Sandstone Reservoirs, SPE Western North American Region Meeting, 7–11 May, Anchorage, Alaska, USA, pp. 1–16. https://doi.org/10.2118/144602-MS.

Nelson, Michael (2012) From 10 Cubic Feet to 500 Cubic Meters--Observations on 100 Years of Flotation Technology. Separation Technologies Book Edited by Courtney Young et al. Society of Mining, Metallurgy and Exploration: 539–546.

Nihill, D.N., Stewart, C.M. and Bowen, P. (1998) The McArthur River mine—the first years of operation," in: *AusIMM '98 – The Mining Cycle, Mount Isa, 19–23 April 1998* (The Australasian Institute of Mining and Metallurgy: Melbourne, 1998), 73–82.

Nutting, P.G. (1925) Chemical Problems in the Water Driving of Petroleum from Oil Sands, Ind. Eng. Chern. (Oct. 1925) 17, No. 10, 1035-36.

Nychka JA, Gentleman MM (2010) Implications of wettability in biological materials science. JOM 62:39–48.

O'Driscoll, M. I. Clarke, (2015) ** *in* Proc. SME Ann. Conf. Expo - CMA 117th Nat. West. Min. Conf., Colorado, USA (2015).

Okasha TM, Funk JJ and Al-Rashidi HN (2007) Fifty Years of Wettability Measurements in the Arab-D Carbonate Reservoir, paper SPE 105114, presented at the 15th SPE Middle East Oil & Gas Show and Conference, Bahrain, March 11–14, 2007.

Oren, P.E., Rueslåtten, H.G., Skjetne, T., Buller, A.T., 1994. Some advance in NMR characterisation of reservoir sandstones. North Sea Oil and Gas Reservoirs, vol. III. Kluwer Academic Publishers, pp. 307–316.

Ouden, L.D., R. Nasralla, H. Guo, H. Bruining, C. van Kruijsdijk (2015) Driving Mechanism of Low Salinity Flooding in Carbonate Rocks, IOR 2015 - 18th European Symposium on Improved Oil Recovery, https://doi.org/10.3997/2214- 4609.201412102.

Owens C. L., Nash G. R., Hadler K., Fitzpatrick R. S., Anderson C. G. and Wall F. (2018) Zeta potentials of the rare earth element fluorcarbonate minerals focusing on bastnäsite and parisite. *Adv Colloid Interface Sci* **256**, 152-162.

Owens, W.W. and Archer, D.L. (1971) The Effect of Rock Wettability on Oil-Water Relative Permeability Relationships, JPT (July 1971) 873-78; Trans., AIME, 251.
Padday, J. F., Pitt, A. R., Pashley, R. M. (1974) Menisci at a free liquid surface: surface tension from the maximum pull on a rod, J. Chem. Soc., Far. Trans. I, 71(10), 1919–1931 (1974)
Pagliaro, M., and Ciriminna, R. (2005). New fluorinated functional materials. Journal of Materials Chemistry, 15(47), 4981-4991. doi:10.1039/B507583C
Pak T, Butler I, Geiger S, van Dijke M, Sorbie K (2015) Droplet fragmentation: 3D imaging of a previously unidentified pore-scale process during multiphase flow in porous media. Proc Natl Acad Sci USA 112:1947–1952.
Palisch T., Chapman M. and Leasure J. (2015) Novel Proppant Surface Treatment Yields Enhanced Multiphase Flow Performance and Improved Hydraulic Fracture Clean-up. *Society of Petroleum Engineers Journal* **SPE-175537-MS**, 1-11.
Pantano, C. G. (2001). What do we know about glass surfaces? Proceedings of the 61st Conference on Glass Problems. Westerville, OH: American Ceramic Society, pp. 137–148.
Parmar J. S. (2013) Displacement of Water by Gas in Propped Fractures: Effect of Fracture Fluid Surface Tension, Viscosity, Proppant Wettability and Gravity. University of Alberta, *Department of Civil and Environmental Engineering* **M.S.**, 111.
Pease, J (2007) Increasing the energy efficiency of grinding. Presented at: Crushing and Grinding, Brisbane, September 2007. Accessed 24 May 2013.
Pirson, S.1. (1958) Oil Reservoir Engineering, McGraw-Hill Book Co. Inc., New York City.
Plumridge T. H. and Waigh R. D. (2002) Water structure theory and some implications for drug design. *J Pharm Pharmacol* **54**, 1155-1179.
Pollen, E.N., C.F. Berg (2018) Experimental Investigation of Osmosis as a Mechanism for Low-salinity EOR, Abu Dhabi International Petroleum Exhibition and Conference, 12–15 November, Abu Dhabi, UAE, pp. 1–20. https://doi.org/10.2118/192753-MS.
Pooryousefy, E., Q. Xie, Y. Chen, A.S. Ahmad Sari (2018) Drivers of low salinity effect in sandstone reservoirs, J. Mol. Liq. 250, 396–403. https://doi.org/10.1016/j.molliq.2017.11.170.
Popiel, W.J. (1978) Introduction to Colloid Science, Exposition Press, Hicksville, N.Y. (1978).
Princen, H; Zia, I; Mason, S (1967) Measurement of Interfacial Tension from the Shape of a Rotating Drop. Journal of Colloid and Interface Science. 23: 99. doi:10.1016/0021-9797(67)90090-2.
Purcell, W.R. (1950) Interpretation of Capillary Pressure Data, Trans., AIME (1950) 189, 369-71.
Purswani P., Tawfik M. S. and Karpyn Z. T. (2017) Factors and Mechanisms Governing Wettability Alteration by Chemically Tuned Waterflooding: A Review. *Energy & Fuels* **31**, 7734-7745.
Raimondi, P., Torcaso, M., and Henderson, J. (1961) The Effect of Interstitial Water on the Mixing of Hydrocarbons During a Miscible Displacement Process, Mineral Industries Experiment Station Circular No. 61, Pennsylvania State D., University Park (Oct. 23-25, 1961) 1-34.
Rayleigh, Lord (1945) The Theory of Sound, p. 371, Dover, New York.
Raza, S.H., Treiber, L.E., and Archer, D.L. (1968) Wettability of Reservoir Rocks and Its Evaluation, Producers Monthly (April 1968) 32, No.4, 2-7.
Reinholdtsen, A.J., A.R. RezaeiDoust, S. Strand, T. Austad (2011) Why Such a Small Low Salinity EOR Potential from the Snorre Formation? IOR 2011 - 16th European Symposium on Improved Oil Recovery, 2011, https://doi.org/10.3997/2214-4609.201404796.
Reisberg, J. and Doscher, T.M. (1956) Interfacial Phenomena in Crude Oil-Water Systems, Producers Monthly (Nov. 1956) 21, No. I, 43-50.
Rezaei Doust, A.; Puntervold, T.; Strand, S.; Austad, T. (2009) Smart water as wettability modifier in carbonate and sandstone: A discussion of similarities/differences in the chemical mechanisms. Energy Fuels 2009, 23, 4479−4485.
RezaeiDoust, A., T. Puntervold, S. Strand, T. Austad (2009) Smart water as wettability modifier in carbonate and sandstone: a discussion of similarities/differences in the chemical mechanisms, Energy Fuels 23, 4479-U 4485. https://doi.org/10.1021/ef900185q.

Richardson, J.G. et al. (1952) Laboratory Determination of Relative Permeability, Trans., AIME (1952) 195, 187-96.
Richardson, J.G., Perkins, F.M., and Osoba, J.S. (1955) Differences in the Behavior of Fresh and Aged East Texas Woodbine Cores, Trans., AIME (1955) 204, 86-91.'
Romanuka, J., J. Hofman, D.J. Ligthelm, B. Suijkerbuijk, F. Marcelis, S. Oedai, N. Brussee, H. van der Linde, H. Aksulu, T. Austad (2012) Low Salinity EOR in Carbonates, SPE Improved Oil Recovery Symposium, 14–18 April, Tulsa, Oklahoma, USA, https://doi.org/10.2118/153869-MS.
Rotondi, M., C. Callegaro, F. Masserano, M. Bartosek (2014) Low Salinity Water Injection: enis Experience, Abu Dhabi International Petroleum Exhibition and Conference, 10–13 November, Abu Dhabi, UAE, https://doi.org/10.2118/171794-MS.
Rulison, C. (2008). Wettability Studies for Porous Solids Including Powders and Fibrous Materials. Application Note 402. Newbury, OH: Augustine Scientific—Specialists in Surface and Interface Science.
Rust, C. F. (1957) A Laboratory Study of Wettability Effects on Basic Core Parameters, paper SPE 986G presented at the 1957 SPE Venezuelan Annual Meeting, Caracas, Nov. 6-9.
Saikia, B.D., J. Mahadevan, D.N. Rao (2018) Exploring mechanisms for wettability alteration in low-salinity waterfloods in carbonate rocks, J. Pet. Sci. Eng. 164, 595–602. https://doi.org/10.1016/j.petrol.2017.12.056.
Sakhaei, Z.; Azin, R.; Osfouri, S. (2016) Assessment of empirical/theoretical relative permeability correlations for gas-oil/condensate systems. Paper Presented at the 1st Persian Gulf Oil, Gas and Petrochemical Biennal Conference Held at the Persian Gulf University In, Bushehr, Iran, 20 April, 2016.
Salathiel, R.A. (1973) Oil Recovery by Surface Film Drainage in Mixed Wettability Rocks, JPT (Oct. 1973) 1216-24.
Salehi, M.M., P. Omidvar, F. Naeimi (2017) Salinity of injection water and its impact on oil recovery absolute permeability, residual oil saturation, interfacial tension and capillary pressure, Egypt. J. Pet. 26, 301–312. https://doi.org/10. 1016/j.ejpe.2016.05.003.
Salis A. and Ninham B. W. (2014) Models and mechanisms of Hofmeister effects in electrolyte solutions, and colloid and protein systems revisited. *Chem Soc Rev* **43**, 7358-7377.
Salter, S.J. and Mohanty, K.K. (1982) Multiphase Flow in Porous Media: 1. Macroscopic Observations and Modeling, paper SPE 11017 presented at the 1982 SPE Annual Technical Conference and Exhibition, New Orleans, Sept. 26-29.
Sanchez C, Arribart H, Madeleine M, Guille G (2005) Biomimetism and bioinspiration as tools for the design of innovative materials and systems. Nat Mater 4:277– 288.
Sandengen, K., A. Kristoffersen, K. Melhuus, L.O.J. Sang (2016) Osmosis as mechanism for low-salinity enhanced oil recovery, SPE J. https://doi.org/10.2118/179741-PA.
Sandengen, K., T.M. Tweheyo, M. Raphaug, A. Kj.lhamar, C. Crescente, V. Kippe (2011) Experimental evidence of low salinity water flooding yielding a more oil-wet behaviour, International Symposium of the Society of Core Analysts held in Austin, Texas, USA 18–21 September, 2011, http://www.jgmaas.com/SCA/2011/SCA2011-16.pdf.
Saraf, D.N., Kumar, J., Fatt, I., 1970. Determination of wettability of porous materials by the nuclear magnetic resonance technique. Indian J. Technol. 8, 125–130.
Satur J. V., Calabia B. P., Hoshino M., Morita S., Seo Y., Kon Y., Takagi T., Watanabe Y., Mutele L. and Foya S. (2016) Flotation of rare earth minerals from silicate–hematite ore using tall oil fatty acid collector. *Minerals Engineering* **89**, 52-62.
Schneider, F.N. and Owens, W.W. (1970) Sandstone and Carbonate Two- and Three-Phase Relative Permeability Characteristics, SPEJ (March 1970) 75-84; Trans., AIME, 249.
Schroth, B.K., G. Sposito (1997) Surface charge properties of kaolinite, Clays Miner. 85–91.
Seccombe, J., A. Lager, G. Jerauld, B. Jhaveri, T. Buikema, S. Bassler, J. Denis, K. Webb, A. Cockin, E. Fueg (2010) Demonstration of Low-Salinity EOR at Interwell Scale, Endicott Field, Alaska,

SPE Improved Oil Recovery Symposium, 24–28 April, Tulsa, Oklahoma, USA, https://doi.org/10.2118/129692-MS.
Seccombe, J.C., Lager, A., Webb, K.J., Jerauld, G.R., and Fueg, E. (2008) Designing a Tertiary Low Salinity EOR Waterflood for the Endicott Field, SPE 113480 presented at the SPE IOR Symposium Tulsa, OK, 19–23 April.
Seccombe, J.C., A. Lager, K.J. Webb, G. Jerauld, E. Fueg (2008) Improving wateflood recovery: Losaltm EOR field evaluation, SPE Symposium on Improved Oil Recovery, 20–23 April, Tulsa, Oklahoma, USA 1–19. https://doi.org/10.2118/113480-MS.
Shahidzadeh-Bonn, N., Tournié, A., Bichon, S., Vié, P., Rodts, S., Faure, P., Bertrand, F., Azouni, A. (2004) Effect of wetting on the dynamics of drainage in porous media, Transport in Porous Media, Volume 56, Number 2, pg 209-224, DOI:10.1023/B:TIPM.0000021876.70521.bc
Shankar, P.K. and Dullien, F.A.L. (1981) Experimental Investigation of Two-Liquid Relative Permeability and Dye Adsorption Capacity Versus Saturation Relationships in Untreated and Driftlm® Treated Sandstone Samples, Surface Phenomena in Enhanced Oil Recovery, D.O. Shah (ed.), Plenum Press, New York City, 453-77.
Sharifzadeh, S., Hassanajili, S., & Rahimpour, M. R. (2013). Wettability alteration of gas condensate reservoir rocks to gas wetness by sol–gel process using fluoroalkylsilane. Journal of Applied Polymer Science, 128(6), 4077-4085. doi:10.1002/app.38632
Sharma, H., K.K. Mohanty (2018) An experimental and modeling study to investigate brine-rock interactions during low salinity water flooding in carbonates, J. Pet. Sci. Eng. 165, 1021–1039. https://doi.org/10.1016/j.petrol.2017.11.052.
Sharma, M.M. and Wunderlich, R.W. (1985) The Alteration of Rock Properties Due to Interactions with Drilling Fluid Components," paper SPE 14302 presented at the 1985 SPE Annual Technical Conference and Exhibition, Las Vegas, Sept. 22-25.
Sheng, J. J. (2014) Critical review of low-salinity waterflooding. J. Pet. Sci. Eng. 2014, 120, 216−224.
Shi, Z.; et al. (2018) Dynamic contact angle hysteresis in liquid bridges. Colloids and Surfaces A. 555: 365–371. arXiv:1712.04703. doi:10.1016/j.colsurfa.2018.07.004
Shikhov I., Thomas D. S., Rawal A., Yao Y., Gizatullin B., Hook J. M., Stapf S. and Arns C. H. (2019) Application of low-field, $^{1}H/^{13}C$ high-field solution and solid state NMR for characterisation of oil fractions responsible for wettability change in sandstones. *Magn Reson Imaging* **56**, 77-85.
Singhal, A.K. and Dranchuk, P.M. (1975) Wettability Control of Glass Beads, Cdn. J. Chem. Eng. (Feb. 1975) 53, 3-8.
Skrettingland, K., T. Holt, M.T. Tweheyo, I. Skjevrak (2011) Snorre low-salinity-water injection-coreflooding experiments and single-well field pilot, SPE Reserv. Eval. Eng., 1–11. https://doi.org/10.2118/129877-PA.
Slobod, R.L. and Blum, B.A. (1952) Method for Determining Wettability of Reservoir Rocks, Trans., AIME (1952) 195, 1-4.
Song, J., Rezaee, S., Guo, W., Hernandez, B., Puerto, M., Vargas, F. M., Hirasaki, GJ, Biswal, SL (2020) Evaluating physicochemical properties of crude oil as indicators of low-salinity-induced wettability alteration in carbonate minerals. *Sci Rep*, *10*(1), 3762.
Song, W., A.R. Kovscek (2016) Direct visualization of pore-scale fines migration and formation damage during low-salinity waterflooding, J. Nat. Gas Sci. Eng. 34, 1276–1283. https://doi.org/10.1016/j.jngse.2016.07.055.
Soraya, B., C. Malick, C. Philipp, H.J. Bertin, G. Hamon (2009) Oil Recovery by Low- Salinity Brine Injection: Laboratory Results on Outcrop and Reservoir Cores, SPE Annual Technical Conference and Exhibition, 4–7 October, New Orleans, Louisiana, pp. 1–12. https://doi.org/10.2118/124277-MS.
Sorbie, K.S. (2010) I. Collins, Chemical mechanism of low salinity water flooding in sandstone reservoirs, SPE Improved Oil Recovery Symposium, 24–28 April, Tulsa, Oklahoma, USA https://doi.org/10.2118/129833-MS.

Stahl, C.D. and Nielsen, R.F. (1950) Residual Water and Residual Oil by Capillary Pressure Techniques, Producers Monthly (Jan. 1950) 14, No.3, 19-22.

Stern, O. (1924) Zur Theorie der Elektrolytischen Doppelschicht. *Zeitschrift für Elektrochemie*. **30**: 508.

Stocker, I. N.; Miller, K. L.; Welbourn, R. J. L.; Clarke, S. M.; Collins, I. R.; Kinane, C.; Gutfreund, P. (2014) Adsorption of Aerosol-OT at the calcite/water interface: Comparison of the sodium and calcium salts. J. Colloid Interface Sci. 2014, 418, 140−146.

Subramanyam, S. V., (1969), J. Fluid Mech. 37, 715-.

Suijkerbuijk, B., H. Kuipers, C.V. Kruijsdijk, S. Berg, J. van Winden, D. Ligthelm, H. Mahani, M.P. Almada, E. van den Pol, V.J. Niasar, J. Romanuka, E. Vermolen, I. Al-Qarshubi (2013) The Development of a Workflow to Improve Predictive Capability of Low Salinity Response, International Petroleum Technology Conference, 26– 28 March, Beijing, China, pp. 1–11. https://doi.org/10.2523/IPTC-17157- MS.

Suijkerbuijk, B., J. Hofman, D.J. Ligthelm, J. Romanuka, N. Brussee, H. van der Linde, F. Marcelis (2012) Fundamental Investigations into Wettability and Low Salinity Flooding by Parameter Isolation, SPE Improved Oil Recovery Symposium, 14–18 April, Tulsa, Oklahoma, USA, pp. 1–11. https://doi.org/10.2118/ 154204-MS.

Suleimanov, B.A., Y.A. Latifov, E.F. Veliyev, H. Frampton (2018) Comparative analysis of the EOR mechanisms by using low salinity and low hardness alkaline water, J. Pet. Sci. Eng. 162, 35–43. https://doi.org/10.1016/j.petrol.2017.12.005.

Sun T, Feng L, Gao X, Jiang L (2005) Bioinspired surfaces with special wettability. Acc Chem Res 38:644–652.

Tang, G.-Q.; Morrow, N. R. (1999) Influence of brine composition and fines migration on crude oil/brine/rock interactions and oil recovery. J. Pet. Sci. Eng. 1999, 24, 99−111.

Tang, G., N. Morrow (1997) Fundamental investigations into wettability and low salinity flooding by parameter isolation, SPE Reserv. Eng., 1–11. https://doi.org/10.2118/36680-PA.

Tang, G.Q., N.R. Morrow (1999) Influence of brine composition and fines migration on crude oil/brine/rock interactions and oil recovery, J. Pet. Sci. Eng. 24 (2-4), 1–6. https://doi.org/10.1016/S0920-4105(99)00034-0.

Tankovsky, N. and Zografov, N. (2011) Oscillations of a Hanging Liquid Drop, Driven by Interfacial Dielectric Force. Zeitschrift für Physikalische Chemie. 225 (4): 405–411. doi:10.1524/zpch.2011.0074

Tankovsky, N. and Zografov, N. (2013) Electrically Driven Resonant Oscillations of Pendant Hemispherical Liquid Droplet and Possibility to Evaluate the Surface Tension in Real Time. Zeitschrift für Physikalische Chemie. 227 (12). doi:10.1524/zpch.2013.0420.

Thomas MM, Clouse JA and Longo JM (1993) Adsorption of Organic Compounds on Carbonate Minerals – 1. Model Compounds and Their Influence on Mineral Wettability, Chemical Geology 109, no. 1–4 (October 25, 1993): 201–213.

Tiab, Djebbar, and Donaldson Erle C. (2015). Petrophysics - Theory and Practice of Measuring Reservoir Rock and Fluid Transport Properties (4th ed.).

Treiber, L.E., Archer, D.L., and Owens, W.W. (1972) A Laboratory Evaluation of the Wettability of Fifty Oil Producing Reservoirs, SPEJ (Dec. 1972) 531-40.

Trinh E. H., Marston P. L. and Robey J. L. (1988) Acoustic Measurement of the Surface Tension of Levitated Drops. *Journal of Colloid and interface science* **124**, 95-103.

Tuteja, A, Choi, W., Ma, M., Mabry, J. M., Mazzella, S. A., Rutledge, G. C., McKinley, G. H. and Cohen, R. H. (2007) Designing superoleophobic surfaces, Science 318,1618.

Udeagbara, Stephen Gekwu (2010-07-30). Effect of Temperature and Impurities on Surface Tension of Crude Oil. Universal-Publishers. ISBN 9781599423555.

Venkataramanan L, Hurlimann MD, Tarvin JA, Fellah K, Acero-Allard D, Seleznev NV (2014) Experimental study of the effects of wettability and fluid saturation on nuclear magnetic resonance and dielectric measurements in limestone. Petrophys 55:572–586.

Vicente, C.; Yao, W.; Maris, H.; Seidel, G. (2002) Surface tension of liquid 4He as measured using the vibration modes of a levitated drop. Physical Review B. 66 (21): 214504. Bibcode:2002PhRvB..66u4504V. doi:10.1103/PhysRevB.66.214504.

Vledder, P., I.E. Gonzalez, J.C.C. Fonseca, T. Wells, D.J. Ligthelm (2010) Low Salinity Water Flooding: Proof of Wettability Alteration on A Field Wide Scale, SPE Improved Oil Recovery Symposium, 24–28 April, Tulsa, Oklahoma, USA, https://doi.org/10.2118/129564-MS.

Von Engelhardt, W. and Lübben, H. (1957) Study of the Influence of Interfacial Stress and Contact Angle on the Displacement of Oil by Water in Porous Materials. I. Theoretical Principles and Performance of Tests, ErdiJI und Kohle (Nov. 1957) 10, No. 11, 747-52. English translation available from the John Crerar Library, U. of Chicago, Translation No. 62-14556.

Vonnegut, B. (1942) Rotating bubble method for the determination of surface and interfacial tensions. Rev. Sci. Instrum. 13 (6): 6–9. doi:10.1063/1.1769937.

Wan J., Kim Y. and Tokunaga T. K. (2014) Contact angle measurement ambiguity in supercritical CO_2 –water–mineral systems: Mica as an example. *International Journal of Greenhouse Gas Control* **31**, 128-137.

Wang C., Zhang K., O'Neil B., Lu W. and Quintero H. (2016) Proppant Upgrade by Wettability Alteration. *International Petroleum Technology Conference* **IPTC-18802-MS**, 1-10.

Wang, X., V. Alvarado (2010) Effects of Low-Salinity Waterflooding on Capillary Pressure Hysteresis, SPE Improved Oil Recovery Symposium, 24–28 April, Tulsa, Oklahoma, USA, https://doi.org/10.2118/179562-MS.

Warren, J.E. and Calhoun, J.C. (1955) A Study of Waterflood Efficiency in Oil-Wet Systems, JPT (Feb. 1955) 22-29: Trans., AIME, 204.

Webb, K.J., C.J.J. Black, and Al-Jeel, H. (2004) Low salinity oil recovery – log inject log. SPE, 89379.

Welge, H.J. (1952) A Simplified Method for Computing Oil Recovery by Gas or Water Drive, Trans., AIME (1952) 195,91-98.

Wenzel, R. N. (1936) Resistance of solid surfaces to wetting by water, Industrial and engineering chemistry 28, 988.

Wesolowski D. J., Sofo J. O., Bandura A. V., Zhang Z., Mamontov E., Předota M., Kumar N., Kubicki J. D., Kent P. R. C., Vlcek L., Machesky M. L., Fenter P. A., Cummings P. T., Anovitz L. M., Skelton A. A. and Rosenqvist J. (2012) Comment on Structure and dynamics of liquid water on rutile TiO (110). *Phys. Rev. B* **85**, 531.

Whyman, G.; Bormashenko, E.; Stein, T. (2008) The rigorous derivation of Young, Cassie–Baxter and Wenzel equations and the analysis of the contact angle hysteresis phenomenon. Chemical Physics Letters. 450 (4–6): 355–359.

Williams, T. (1991) The story of Lin Ma Hang lead mine, 1915-1962. Geological Society of Hong Kong Newsletter. 9: 3–27.

Wilmott, Z.M., C.J.W. Breward, S.J. Chapman (2018) Modelling low-salinity oil recovery mechanisms using an ion dissociation model, Transp. Porous Media 1–25. https://doi.org/10.1007/s11242-018-1220-1.

Winsauer, W.O., W.M. McCardell (1953) Ionic double-layer conductivity in reservoir rock, J. Pet. Technol. 1–6. https://doi.org/10.2118/953129-G.

Xie, Q., A. Saeedi, E. Pooryousefy, Y. Liu (2016) Extended DLVO-based estimates of surface force in low salinity water flooding, J. Mol. Liq. 221, 658–665. https://doi.org/10.1016/j.molliq.2016.06.004.

Xie, Q., A. Sari, W. Pu, Y.C.V. Brady, N.A. Maskari, A. Saeedi (2018) pH effect on wettability of oil/brine/carbonate system: implications for low salinity water flooding, J. Pet. Sci. Eng. 168. https://doi.org/10.1016/j.petrol.2018.05.015.

Xie, Q., F. Liu, Y. Chen, H. Yang, A. Saeedi, M.M. Hossain (2019) Effect of electrical double layer and ion exchange on low salinity EOR in a pH controlled system, J. Pet. Sci. Eng. 174, 418–424. https://doi.org/10.1016/j.petrol.2018.11.050.

Xie, Q., P.V. Brady, E. Pooryousefy, D. Zhou, Y. Liu, A. Saeedi (2017) The low salinity effect at high temperatures, Fuel 200, 419–426. https://doi.org/10.1016/ j.fuel.2017.03.088.

Xie, Q., Y. Liu, J. Wu, Q. Liu (2014) Ions tuning water flooding experiments and interpretation by thermodynamics of wettability, J. Pet. Sci. Eng. 124, 350–358. https://doi.org/10.1016/j.petrol.2014.07.015.

Yildiz, H.O., N.R. Morrow (1996) Effect of brine composition on recovery of Moutray crude oil by waterflooding, J. Pet. Sci. Eng. 14, 159–168. https://doi.org/10.1016/0920-4105(95)00041-0.

Yousef, A. A.; Al-Saleh, S.; Al-Jawfi, M. S. (2012) The Impact of the Injection Water Chemistry on Oil Recovery from Carbonate Reservoirs; Society of Petroleum Engineers, 2012.

Yousef, A., S. Ayirala (2014) A Novel Water Ionic Composition Optimization Technology for Smartwater Flooding Application in Carbonate Reservoirs, SPE Improved Oil Recovery Symposium, 12–16 April, Tulsa, Oklahoma, USA, 2014, https://doi.org/10.2118/169052-MS.

Yousef, A.A., S.H. Al-Saleh, A. Al-Kaabi, M.S. Al-Jawfi (2011) Laboratory investigation of the impact of injection-water salinity and ionic content on oil recovery from carbonate reservoirs, SPE Reserv. Eval. Eng. https://doi.org/10.2118/137634-PA.

Yu, M., A. Zeinijahromi, P. Bedrikovetsky, L. Genolet, A. Behr, P. Kowollik, F. Hussain (2019) Effects of fines migration on oil displacement by low-salinity water, J. Pet. Sci. Eng. https://doi.org/10.1016/j.petrol.2018.12.005.

Zahid, A., A.A. Shapiro, A. Skauge (2012) Experimental Studies of Low Salinity Water Flooding Carbonate: A New Promising Approach, SPE EOR Conference at Oil and Gas West Asia, 16–18 April, Muscat, Oman, pp. 1–14. https://doi.org/10. 2118/155625-MS.

Zeinijahromi, A., V. Ahmetgareev, P. Bedrikovetsky (2015) Case Study of 25 Years of Low Salinity Water Injection, SPE/IATMI Asia Pacific Oil and Gas Conference and Exhibition, 20–22 October, Nusa Dua, Bali, Indonesia, pp. 1–11. https://doi.org/10.2118/176128-MS.

Zhang C. (2018) Effect of Proppant Wettability on Two-Phase Flow Efficiency in Fractured Water-Wet Sandstone. *Petroleum Engineering* **M.S.**, 91p.

Zhang, G.Q., Huang, C.C., Hirasaki, G.J. (2000) Interpretation of wettability in sandstones with NMR analysis. Petrophysics 41, 223– 233.

Zhang, P., M.T. Tweheyo, T. Austad (2007) Wettability alteration and improved oil recovery by spontaneous imbibition of seawater into chalk: impact of the potential determining ions Ca^{2+}, Mg^{2+}, and SO_4^{2-}, J. Pet. Sci. Eng. 301, 199–208. https://doi.org/10.1016/j.colsurfa.2006.12.058.

Zhang, Y., N.R. Morrow (2006) Comparison of Secondary and Tertiary Recovery With Change in Injection Brine Composition for Crude- Oil/Sandstone Combinations, SPE/DOE Symposium on Improved Oil Recovery, 22–26 April, Tulsa, Oklahoma, USA, 2006, https://doi.org/10.2118/99757-MS.

Zhang, Y., X. Xie, N.R. Morrow (2007) Waterflood performance by injection of brine with different salinity for reservoir cores, SPE Annual Technical Conference and Exhibition, 11-14 November, Anaheim, California, U.S.A., 2007, pp. 1–12. https://doi.org/10.2118/109849-MS.

Zografov, N., and Tankovsky, N. (2013) Resonant oscillations of pendant hemispherical liquid droplet as a means to examine transient processes in the liquid-air interface. 1st Int. Workshop on Wetting and evaporation: droplets of pure and complex fluids Marseilles, France, June 17th to 20th, 2013, Abstract #145, 267-268.

Zografov, N., and Tankovsky, N. (2014) Droplet oscillations driven by an electric field. Colloids and Surfaces A: Physicochemical and Engineering Aspects. 460: 351–354. doi:10.1016/j.colsurfa.2013.12.013.

Zuidema, H.H., Waters G.W. (1941), Ind. Eng. Chem. (Anal.Ed.) **13**, 312-.

APPENDIX B

OAK RIDGE
NATIONAL LABORATORY
MANAGED BY UT-BATTELLE
FOR THE DEPARTMENT OF ENERGY

Screening of Produced Water for Rare Metals

April 2020

Prepared by
Joanna McFarlane

Date Published: April 2020

UT-BATTELLE
ORNL-27 (4-00)

CONTENTS

Page

9. LIST OF TABLES

10. ABSTRACT

Total dissolved solids (TDS) in produced water can range from less than 1000 mg/L (ppm) to over one hundred thousand ppm. Produced water associated with shale gas can be high; over 100,000 ppm is not uncommon (150,000 ppm has been cited).[1] Most of the TDS is from dissolved NaCl, and other common mineralogical constituents. However, because of the high mineral content, produced water may also be a rich source of strategic minerals. The metals of interest include iodine, bromine, lithium, cobalt, silver, gold and rare earth elements. The rare earth elements include La, Ce, Pr, Nd, Pm, Sm, Eu, Gd, Tb, Dy, Ho, Er, Tm, Yb, and Lu as well as the associated main group elements, Sc and Y. While fossil resources, such as coal and flyash have been considered as sources of rare earths alternative to mined ores,[2, 3 ,4 , 5, 6, 7] the extraction of rare earths from produced water is a new approach being considered. Although the concentrations of rare earth elements in produced water are low, the volume of water being recovered from oil and gas production and being treated before reinjection or beneficial use means that this could be a resource for these metals of strategic importance.

1. KEY DISSOLVED CONSTITUENTS IN PRODUCED WATER

11.

Produced water is analyzed to facilitate disposal and to specify treatment or separations required before disposal.[8] The discharge of produced water into the environment is covered by NPDES permits for off-shore facilities. Onshore regional discharge is regulated by the states, or through the EPA for Idaho, Massachusetts, New Hampshire, New Mexico, Oklahoma and Texas, certain territories and tribal lands. Permitting for discharge has driven development of analytical methods for produced water characterization. A thorough survey of produced water production, permitting, and treatment for beneficial use was prepared for the US Department of Energy in 2004 (Veil et al.). However, the report does not discuss water produced from oil or gas shale production because it predates the revolution of horizontal drilling and hydraulic fracturing. It does not describe extraction of strategic materials before

---

1 Gregory, K.B., Vidic, R.D, Dzomback, D.A. 2011. Water management challenges associated with the production of shale gas by hydraulic fracturing. Elements 7, 181-186.

2 Huang, Z., Fan, M., Tiand, H. 2018. Coal and coal byproducts: A large and developable unconventional resource for critical materials – Rare earth elements, J Rare Earths 36, 337-338

3 Frenzel, M., Ketris, M.P., Seifert, T., Gutzmer, J. 2016. On the current and future availability of gallium, Resources Policy 47, 38-50.

4 Lin, R., Soong, Y., Granite, E.J. 2018. Evaluation of trace elements in US coals using the USGS COALQUAL database version 3.0. Part I: Rare earth elements and yttrium (REY), Int. J Coal Geology 192, 1-13.

5 Yang, X., Werner, J., Honaker, R.Q. 2019. Leaching of rare earth elements from an Illinois basin coal source, J Rare Earths 37, 312-321.

6 Seredin, V.V., Dai, S. 2012. Coal deposits as potential alternative sources for lanthanides and yttrium, Int J Coal Geology 94, 67-93

7 Honaker, R.Q., Zhang, W., Yang, X. Rezaee, M. 2018. Conception of an integrated flowsheet for rare earth elements recovery from coal coarse refuse, Minerals Eng 122, 233-240.

8 Gogoi, T.J., Gogoi, S.B., Kallel, M., Boral, P., Barman, J. 2020. Arabian J Geosciences, 13, paper 158.

water disposal or reinjection, as these were not major considerations relative to reduction in salinity or removal of oil and grease.[9]

Standard analysis of water produced during fossil energy production includes the following determinations: total dissolved solids (TDS) and total organic carbon (TOC). Other parameters are less commonly monitored, including: oxidation and reduction potential (ORP), electrical conductivity (EC), sodium absorption ratio (SAR), stable isotopes, and major ions.[10] The most comprehensive published information on domestic produced water is available through the USGS National Produced Waters Geochemical Database.[11] The species tracked in the database include: barium, boron, bromide, hexane extractable material (HEM), methylene blue active substances (MBAS), Ra, Sr, TOC, Sulfate, TDS, and chloride. However, this database does not track many of the species of interest in this white paper, such as the rare earths. [12] The chemical constituents identified in various studies are listed in Table 1, with those of particular interest as strategic materials highlighted in yellow.

The physicochemical form of the inorganic species needs to be considered for evaluating separation processes, as some of the targeted species will be in solution or associated with insoluble particulate matter, both organic and inorganic, and suspended in the aqueous media.[13]

9 Veil, J.A., Puder, M.G., Elcock, D., Redweik, R.J.Jr. 2004. A white paper describing produced water from production of crude oil, natural gas, and coal bed methane, National Energy Technology Laboratory, Contract W-31-109-Eng-38.

10 Zhang, Z., Yan, D., Zhuang X., Yang, S., Wang, S., Wang, G., Li, G., Wang, X. 2019. Hydrogeochemistry signatures of produced water associated with coalbed methane production in the Southern Junggar Basin, NW China, Environ. Sci. Poll. Res., 26, 31956-31980.

11 Engle, M.A., Cozzarelli, I.M., Smith, B.D. USGS Investigations of Water Produced during Hydrodrocarbon Reservoir Development, US Geological Survey Fact Sheet 2014-3014, 4 p. https://dx.doi.org/10.3133/fs20143104.

12 US EPA. Study of Oil and Gas Extraction Wastewater Management Under the Clean Water Act, EPA-821-R19-001. May 2019.

13 Phan, T.T., Hakala, J.A., Bain, D.J. 2018. Influence of colloids on metal concentrations and radiogenic strontium isotopes in groundwater and oil and gas-produced waters, Applied Geochemistry 95, 85-96.

Table 1: Produced Water Analysis and Databases

Reference	Title	Elements/Source
Jubb, A.M., Geostandards and Geoanalytical Research, 2020[14]	Direct Trace Element Determination in Oil and Gas Produced Waters with Inductively Coupled Plasma Optical Emission Spectrometry: Advantages of High Salinity Tolerance	As, Al, Ba, Be, Cd, Cr, Co, Cu, Hg, Mo, Ni, Pb, Rb, Sb, U, V, Zn Eagle Ford, Marcellus, Middle Bakken/Three Forks, Wolfcamp/Cline, Utica/Point Pleasant
Nye, C.W., Proceedings of the 42nd Workshop on Geothermal reservoir Engineering, Stanford University, Stanford, CA, February 13-15, 2019, SGP-TR-212	Aqueous Rare Earth Element Patterns and Concentration in Thermal Brines Associated with Oil and Gas Production	Rare earths Wyoming River Basin and Powder River Basin
Otton, J.K. [15], GWPC, 2002	A National Produced-Water Geochemistry Database	Ba, HCO_3^-, Br^-, Ca^{2+}, Cl^-, I^-, Mg^{2+}, Na^+, Sr^{2+}, SO_4^{2-}
Phan, Applied Geochemistry 2018	Influence of colloids on metal concentrations and radiogenic strontium isotopes in groundwater and oil and gas-produced waters	B, Ca, Ga, K, Li, Mg, Na, Ga, Rb, Sr, U East Seminole Field, Emma Field, TX, Marcellus, WV
Zolfaghari, J Unconventional Oil and Gas Resources [16] Thompson, Fuel 2016[17]	Laboratory and field analysis of flowback water from gas shales Resolution of rare earth element interferences in fossil energy by-product samples using sector-field ICP-MS	Ba, Fe, sulfate, Cl, Na, K, Horn River Basin REE in the presence of large amounts of barium in flowback and produced water

14 USGS produced water database https://www.sciencebase.gov/catalog/item/5d9f2d87e4b036616293580a
15 Otton, J.K. Breit, G.N., Kharaka, Y.K., Rice, C.A. A National Produced-Water Geochemistry Database. GWPC 2002. www.gwpc.org
16 Zolfaghari, A., Dehghanpour, H., Noel, M., Bearinger, D. 2016. Laboratory and field analysis of flowback water from gas shales J Unconventional Oil and Gas Resources 14, 113-127.
17 Thompson, R.L., Bank, T., Roth, E., Granite, E. Resolution of rare earth element interferences in fossil energy by-product samples using sector-field ICP-MS, 2016. Fuel 185, 94-101.

2. CURRENT TRENDS AND BEST PRACTICES FOR SAMPLING AND ANALYTICAL TECHNIQUES

The analysis of chemical constituents follows standard methods either codified by the ASTM or by the EPA. These procedures are available on the internet and give instructions for the choice of equipment, calibration methods and recommended of standard reference materials, and citations to the primary literature where the methods have been described. As can be seen in Table 2, where methods related to produced water analysis are listed, there are multiple ways of analyzing produced water. Some of the older methods have less sensitivity than newer determinations, but are reliable and useful for constituents present at higher concentrations. For determination of the levels of strategic metals, methods for measurement of cation load are the most useful. Of these, inductively coupled plasma optical emission spectroscopy (ICP-OES) is much better for cation analysis in high salinity water than ICP-mass spectroscopy (MS), the latter having problems with clogging of the sample introduction needle with high ionic strength solutions. (Nye et al 2017) Advanced methods may be able to mitigate ion interferences in ICP-MS. (Thompson et al 2016) Ion chromatography can be used for both cation and anion analysis, but requires calibration standards and is sensitive to interferences between species.

Table 2: Standard Methods for Sampling and Analysis

Procedure	Title
ASTM D1971	Standard Practices for Digestion of Water Samples for Determination of Metals by Flame Atomic Absorption, Graphite Furnace Atomic Absorption, Plasma Emission Spectroscopy, or Plasma Mass Spectrometry
ASTM D1976	Elements in Water by Inductively-Coupled Argon Plasma Atomic Emission Spectroscopy
ASTM D3866	Test Methods for Silver in Water
ASTM D3919	Practice for Measuring Trace Elements in Water by Graphite Furnace Atomic Absorption Spectroscopy
ASTM D4190	Test Method for Elements in Water by Direct-Current Plasma Atomic Emission Spectroscopy
ASTM D4309	Practice for Sample Digestion Using Closed Vessel Microwave Heating Technique for the Determination of Toxic Metals in Water
ASTM D4691	Practice for Measuring Elements in Water by Flame Atomic Absorption Spectrophotometry

Procedure	Title
ASTM D5673	Test Method for Elements in Water by Inductively Coupled Plasma-Mass Spectrometry
EPA-600/4-79-020	Methods for Chemical Analysis of Water and Wastes, Revised March 1983
EPA-600/R-94/111	Methods for the Determination of Metals in Environmental Samples – Supplement 1
USGS Open File Report 96-225	Methods of Analysis by the US Geological Survey National Water Quality Laboratory – In-Bottle Acid Digestion of Whole Water Samples

3. PROCESSING TECHNOLOGIES FOR EXTRACTION AND SEPARATION

12.

Desalination processes have been developed for produced water streams to remove salt components so that the produced water can be reused in agriculture, irrigation, and for other beneficial uses. A 2013 review article summarizes the benefits and technologies for desalinating produced water from shale gas production.[18] The rejected stream can have a ten-fold increase in the concentrations of brine and sulfates than the input stream. (Nye et al. 2017). Besides the chlorides, sulfate minerals can lead to scaling and hydrogen sulfide production, which means that removal of sulfate minerals has received particular attention along with the reduction in TDS. The phenomenon of reservoir souring has been reviewed by Basafa and Hawbolt.[19] Rare earths have not been the target of most published studies. Rare earth elements have been tracked though, with the studies of Nye et al. and Phan et al. being specific examples. Not all of the REE behave the same way. Produced water can show an enrichment in europium relative to industrial waste waters. Cerium has a lower presence than expected, staying in the rock matrix. Depending on the source, there may be an enrichment in light rare earth elements (LREE, La, Ce, Pr, Nd, Sm) or heavy (HREE: Gd, Tb, Dy, Ho, Er, Tm, Yb, Lu). (Nye et al. 2017)

Extraction of rare metals will need to be done in the presence of chemical additives present in produced water that have introduced to facilitate hydraulic fracturing or production. These additives are included in the FracFocus database that has been developed by the Groundwater Protection Council (GWPC),[20] and shown in Figure 1. The GWPC has a mandate to protect groundwater resources and encourages the self-reporting of chemical additives by drillers and producers. Many companies take part and report at least the classes of chemicals being injected, if not proprietary information. Many of these chemicals have been chosen to increase production by manipulation of the downhole hydrochemistry, or to prevent processing issues such as scaling or corrosion. Others are chosen to change the thermophysical properties of the fluid, such as viscosity, or to reduce the microbe population downhole. All of these may affect the properties of the produced waters undergoing chemical or physical separations, potentially complicating the extraction of rare metals. There are many studies of how to mitigate the interference of these additives in desalination, for instance the removal of polyacrylaminde from water produced during polymer flooding.[21]

---

18 Shaffer, D.L., Arias Chavez, L.H., Ben-Sasson, M., Castrillon, S. R.-V., Yip, N.Y. Elimelech, M. 2013. Desalination and reuse of high-salinity shale gas produced water: Drivers, technologies, and future directions, Environmental Science & Technology, 47, 9569-9583.

19 Basafa, M., Hawbolt, K. 2019. Reservoir souring: sulfur chemistry in offshore oil and gas reservoir fluids, J Petroleum Exploration and Production Technology, 9, 1105-1118.

20 Groundwater Protection Council, GWPC. 2020. www.fracfocus.org. Chemical Disclosure Registry.

21 Wang, X., Xu, X., Dang, W., Tang, Z., Hu, C., Wei, B. 2019. Interception characteristics and pollution mechanism of the filter medium in polymer-flooding produced water filtration process, Processes 7, 927-946.

Produced water may also have a significant load of organics, primarily aliphatic or paraffinic, usually expressed as total organic carbon,[22] with concentrations up to several thousand ppm.[23] Organics in produced water that may interfere with the extraction of rare metals have been evaluated for the USGS for selected oil fields, including the Williston Basin in North Dakota.[24] Organics that were measured included non-purgeable dissolved organic carbon (NPDOC), acetate, and extractable carbons, such as polycyclic aromatic hydrocarbons (PAHs), phenolic compounds, n-gycol ethers, and cyclic ketones. These compounds, along with paraffins, can interfere with desalination or extraction processes because of the formation of oil-in-water emulsions. Thus, there are several studies that investigate how to break emulsions prior to removal of TDS and other ions, using ultrasonics coupled to ultrafiltration and membrane processing for instance.[25]

Additive	Purpose	Downhole Result
Acid	Helps dissolve minerals and initiate cracks in the rock	Reacts with minerals present in the formation to create salts, water, and carbon dioxide (neutralized)
Acid/Corrosion Inhibitor	Protects casing from corrosion	Bonds to metal surfaces (pipe) downhole. Any remaining product not bonded is broken down by micro-organisms and consumed or returned in produced water.
Biocide	Eliminates bacteria in the water that can cause corrosive by products	Reacts with micro-organisms that may be present in the treatment fluid and formation. These micro-organisms break down the product with a small amount of the product returning in produced water.
Base Carrier Fluid (water)	Create Fracture Geometry and Suspend Proppant	Some stays in formation while remainder returns with natural formation water as "produced water" (actual amounts returned vary from well to well)
Breaker	Allows a delayed break down of gels when required.	Reacts with the "crosslinker" and "gel" once in the formation making it easier for the fluid to flow to the borehole. Reaction produces ammonia and sulfate salts which are returned in produced water.
Clay and Shale Stabilization/control	Temporary or Permanent Clay Stabilizer to lock down clays in the shale structure	Reacts with clays in the formation through a sodium - potassium ion exchange. Reaction results in sodium chloride (table salt) which is returned in produced water. Also replaces binder salts like Calcium Chloride helping to keep the formation in tact as the Calcium Chloride dissolves.
Crosslinker	Maintains viscosity as temperature increases	Combines with the "breaker" in the formation to create salts that are returned in produced water
Friction Reducer	Reduces Friction effects over base water in pipe	Remains in the formation where temperature and exposure to the "breaker" allows it to be broken down and consumed by naturally occurring micro-organisms. A small amount returns with produced water.
Gel	Thickens the water in order to suspend the proppant	Combines with the "breaker" in the formation thus making it much easier for the fluid to flow to the borehole and return in produced water
Iron Control	Iron chelating agent that helps prevent precipitation of metal oxides	Reacts with minerals in the formation to create simple salts, carbon dioxide and water all of which are returned in produced water
Non-Emulsifier	Used to break or separate oil / water mixtures (emulsions)	Generally returned with produced water, but in some formations may enter the gas stream and return in the produced natural gas.
pH Adjusting Agent/Buffer	maintins the effectiveness of other additives such as crosslinkers	Reacts with acidic agents in the treatment fluid to maintain a neutral (non-acidic, non-alkaline) pH. Reaction results in mineral salts, water and carbon dioxide which is returned in produced water.
Propping Agent	Keeps Fractures Open allowing for hydrocarbon production	Stays in formation, embedded in fractures (used to "prop" fractures open)
Scale Inhibitor	Prevent Scale in Pipe and Formation	Product attaches to the formation downhole. The majority of product returns with produced water while remaining reacts with microorganisms that break down and consume the product.
Surfactant	Reduce Surface tension of the treatment fluid in the formation and helps improve fluid recovery from the well after the frac is completed	Some surfactants are made to react with the formation, some are designed to be returned with produced water, or, in some formations they may enter the gas stream and return in the produced natural gas.

Figure 1. Chemical Use in Hydraulic Fracturing, 2020, www.FracFocus.org, accessed March 5, 2020.

22 Victoria DiStefano, Joanna McFarlane; Andrew G Stack; Edmund Perfect; David F Mildner; Markus Bleuel; Steve J Chipera; Kenneth C Littrell; Michael C Cheshire; Katherine E. Manz; Lawrence M Anovitz, "Solvent-Pore Interactions in the Eagle Ford Shale Formation", Fuel 238, 298-311 (2019); V.H. DiStefano, J. McFarlane, L.M. Anovitz, A.D. Gordon, R.E. Hale, R.D. Hunt, S.A. Lewis, K.C. Littrell, A.G. Stack, S.J. Chipera, E. Perfect, "Extraction of Organic Compounds from Representative Shales and the Effect on Porosity", J Natural Gas Science and Engineering, 35, 646-660 (2016); J. McFarlane, L.M. Anovitz, V.H. DiStefano, A.G. Stack, E. Perfect, D.F.R. Mildner, M. Bleuel, S.J. Chipera, K.C. Littrell, M.C. Cheshire, K.E. Manz, "Solvent-pore interactions in Eagle Ford shale by ultra and small-angle neutron scattering", In 2019 Accomplishments and Opportunities, NIST SP 1242, NIST Center for Neutron Research, US Department of Commerce, April 1, 2020, p. 34-35.

23 Maguire-Boyle, S.J., Barron, A.R. 2014. Organic compounds in produced waters from shale gas wells. Environmental Science Processes & Impacts, 16, 2237-2248.

24 Varonka, M.S., Bates, A.L., and Orem, W.H., 2019, Organic Analysis of Oilfield Produced Water from the Williston Basin, North Dakota: U.S. Geological Survey data release, https://doi.org/10.5066/P9XMECVV, https://www.sciencebase.gov/catalog/item/5d110923e4b0941bde5503c8

25 Agi, A., Junin, R., Alqatta, A.Y.M., Gbadamosi, A., Yahya, A., Abbas, A. 2019. Ultrasonic assisted ultrafiltration process for emulsification of oil field produced water treatment, Ultrasonics – Sonochemistry 51, 214-222

Processing technologies for produced water have been studied for several decades and implemented to reduce the environmental impact of oil and gas production. (Shaffer et al. 2013, Adham et al. 2018)[26] Besides reverse osmosis, predominant technologies that have been assessed are forward osmosis, mechanical vapor compression, and membrane distillation as these should be able to process high TDS solutions. Examples of the application of these technologies are given in Table 3. Note that citations provided in Table 3 are not meant to be an exhaustive review of the literature. Metals removal methods have been applied to industrial[27] and mining[28,29,30] wastes as well as produced water. All of these methods require some pre-treatment or staged treatment approach, that may include: separation of organics, sediment removal, oxidation, flocculation, and pH adjustment. (McGinnis et al. 2012, Ahmad et al. 2020[31]) Research continues to improve the separation of the organic fraction and TDS from water. Some of the newer literature is included in the review led by Ahmadun (2009). Selective removal of rare earth elements would be done from the lower volume retentate after primary removal technologies have been applied.

Processing of minerals for rare earth recovery is multistep to achieve the separation of the lanthanides from more common ore components. Although a detailed analysis of separation methods employed by the minerals processing industry is beyond the scope of this report, there may be similarities in the composition of the feed that would benefit from application of similar methodologies. For example, Balinski et al describe a process of recovering lanthanides from Eudialyte concentrate, a sodium-rich zircon silicate.[32] Silicates are a key contaminant and the goal of Balinski's work was to prevent gel formation that impedes other processing steps. Thus, they have developed a three-step process involving sulfonation of metals with H_2SO_4, a step that also dehydrated the SiO_2, followed by thermal decomposition of non-rare-earth sulfates at 750°C. The rare earths remained in a soluble form during the roasting step and so could be removed during a subsequent leaching procedure.

Another source of information is the understanding of rare earth recovery from waste streams that are the feed for recycling of fluorescent lamp phosphors as a value-added stream to compensate for the cost of mercury removal. In general, to recover rare earths, the waste stream is acidified and then sent to specialty recovery facilities.[33] This collaboration between water purification and extraction sectors could also be done with the retentate from a membrane or distillation process derived from produced water.

---

26 Adham, S., Hussain, A., Minier-Matar, J., Janson, A., Sharma, R. 2018. Membrane applications and opportunities for water management in the oil and gas industry, Desalination 440, 2-7.

27 Xie, Y-d., Xiong, W.-L., Yu, J.-X., Tang, J.-Q., Chi, R.-A. 2018. Recovery of copper from metallurgical sludge by combined method of acid leaching and biosorption, Process Safety and Environmental Protection 116, 340-346.

28 Tabak, H.H., Scharp, R., Burckle, J., Kawahara, F.K., Govind, R. 2003. Advances in biotreatment of acid mine drainage and biorecovery of metals: 1. Metal precipitation for recovery and recycle, Biodegradation 14, 423-436.

29 Samaei, S.M., Gato-Trinidad, S., Altaee, A. 2020. Performance evaluation of reverse osmosis process in the post-treatment of mining wastewaters: Case study of Costerfield mining operations, Victoria, Australia, J Water Process Eng 34, 101116.

30 Marais, T.S., Huddy, R.J., Harrison, S.T.L., van Hille, R.P. 2020. Demonstration of simultaneous biological sulphate reduction and partial sulphide oxidation in a hybrid linear flow channel reactor. J Water Process Eng 34, 101143.

31 Ahmad, T., Guria, C., Mandal, A. 2020. Enhanced performance of salt-induced Pluronic F127 and bentonite blended polyvinyl chloride ultrafiltration membrane for the processing of oilfield produced water, J Water Process Eng 34, 101144.

32 Balinski, A., Atanasova, P., Wiche, O., Kelly, N., Reuter, M.A., Scharf, C. 2019. Selective leaching of rare earth elements (REEs) from Eudialyte concentration after sulfation and thermal decomposition of non-REE sulfates, Minerals 9, 522-533.

33 Ferron, C.J., Henry, P. 2015. A review of the recycling of rare earth metals, Canadian Metallurgical Quarterly, Can J Metallurgy and Materials Sci, 54, 383-394.

Table 3: Literature on Processing Technologies

Reference	Title	Elements or compounds targeted	Method
Li, C. , Applied Materials and Interfaces, 2013	Recycling Rare earth Elements from Industrial Wastewater with Flowerlike Nano-$Mg(OH)_2$	Rare Earths: Nd, Eu, Tb, Dy, Yb (0.04 mol/L)	Exchange into $Mg(OH)_2$ nanoparticles. Use pH to resolubilize $Mg(OH)_2$ and separate from $RE(OH)_3$ Not demonstrated at high salinity
Zhu et al.[34] Desalination, 2018	Diffusion behavior of multivalent ions at low pH through a MFI-type zeolite	Multivalent ions (Fe3+, Al3+, Ca2+, Mg2+)	Model solutions Filtration
Wang et al, J. Water Process Eng 2019[35]	A numerical study and flotation experiments of bicyclone column flotation for treating of produced water from ASP flooding	Oil and organic removal (surfactant and polymer)	Pretreatment of water from ASP flooding (handling emulsions)
Ahmadun et al., J. Hazardous Materials 2009[36]	Review of technologies for oil and gas produced water treatment	Heavy metals are mentioned, organic and inorganic components	Produced water from oil and gas production Reverse Osmosis (amongst other methods)
McGinnis et al, Desalination 2012[37]	Pilot demonstration of the NH_3/CO_2 forward osmosis desalination process on high salinity brines	TDS by method 2504C Anions (Br-,Cl-,F-, NO3-, PO43-, SO42-), cations (ammonium, calcium, magnesium, potassium, sodium)	Marcellus frac flowback and produced water Forward Osmosis

34 Zhu, B., Morris, G., Moon, I.-S., Gray, S., Duke, M. 2018, Diffusion behavior of multivalent ions at low pH through a MFI-type zeolite, Desalination 440, 88-98.
35 Wang, C., Wang, Z., Wei, X., Li, X. 2019. A numerical study and flotation experiments of bicyclone column flotation for treating of produced water from ASP flooding. J. Water Process Eng. 32, 100972.
36 Ahmadun, F.-R., Pendashtech, A., Abdullah, L.C., Biak, D.R.A., Madaeni, S.S., Abidin, Z.Z. 2009. Review of technologies for oil and gas produced water treatment, J. Hazardous Materials 170, 530-551.
37 McGinnis, R.L., Hancock, N.T., Nowosielski-Slepowron, M.S., McGurgan, G.D. 2013. Pilot demonstration of the NH_3/CO_2 forward osmosis desalination process on high salinity brines, Desalination 312, 67-74.

Reference	Title	Elements or compounds targeted	Method
Singh and Sirkar, J. Membrane Sci 2012[38]	Desalination of brine and produced water by direct contact membrane distillation at high temperatures and pressures	NaCl (1%), with cresol, naphthenic acid, phenol contaminants	Simulated hot produced water from steam assisted gravity drainage (SAGD) Membrane Distillation
Koren and Nadav, Desalination 1994[39]	Mechanical vapor compression to treat oil field produced water	Salinity and scaling compounds	Desalinate water from steam injection using Mechanical Vapor Compression (MVC)
Mazumder et al.[40] Chem Eng Technol 2019	Integrated ejector-based flare gas recovery and on-site desalination of produced water	Na^{+}, Ca^{2+}, Cl^{-}, short chain paraffins	MVC with heat coming from flared gas combustion
Wingley et al., Environmental Science and Technology[41]	Contaminants in direct contact membrane distillation (DCMD) product water	Water soluble organics and TDS	DCMD
Tabak et al., Biodegradation, 2003	Advances in biotreatment of acid mine drainage and biorecovery of metals: Metal precipitation for recovery and recycle	Fe^{2+}, Cu^{2+}, Zn^{2+}, Al^{3+}, Mn^{2+}, As^{2+}, Cd^{2+}, Co^{2+}, Pb^{2+}, Ni^{2+}	Precipitation of metals as sulfides, as pretreatment for bioreactor
Xie et al, Process Safety and Environmental Protection 2018	Recovery of copper from metallurgical sludge by combined method of acid leaching and biosorption	Cu separation from other leached metals	Metallurgical sludge Leaching with HNO_3, Separation of copper using sugarcane bagasse fixed-bed column

38 Singh, D. and Sirkar, K.K. 2012. Desalination of brine and produced water by direct contact membrane distillation, J. Membrane Sci. 389, 380-388.

39 Koren, A., Nadav, N. Mechanical vapour compression to treat oil field produced water. 1994. Desalination, 98(1-3), 41-48.

40 Mazumder, M., Chen, L., Xu, Q. 2019. Integrated ejector-based flare gas recovery and on-site desalination of produced water, Chem Eng Technol 43(2), 200-210.

41 Winglee, J.M., Bossa, N., Rosen, D., Vardner, J.T., Wiesner, M.R. 2017. Contaminants in direct contact membrane distillation (DCMD) product water, Environ. Sci. Technol. 51, 13113-13121.

Reference	Title	Elements or compounds targeted	Method
Simonsen et al[42] J Petrol Sci & Eng 2018	Potential applications of magnetic nanoparticles within separations in the petroleum industry	Removal of organics (ashphaltenes, naphthenic acids, waxes)	Functionalized magnetite nanoparticles
Abdel-Salam et al[43] Water & Environment J, 2018	Electrochemical treatment of chemical oxygen demand in produced water using flow-by porous graphite electrode	Oxidizable organic and inorganic compounds, but focus on pH and organic compounds	Natural gas produced water Electrochemical separation
Choi et al, Desalination 2018[44]	Fractional-submerged membrane distillation crystallizer (F-SMDC) for treatment of high salinity solution	Salts, NaCl, Na_2SO_4	A temperature/ concentration gradient imposed in the scrubber induces fractional crystallization

42 Simonsen, G., Strand, M., Øye, G. 2018. Potential applications of magnetic nanoparticles within separations in the petroleum industry, J Petrol Sci & Eng. 165, 488-495.
43 Abdel-Salam, O.E., Taleb, E.M.A., Afify, A.A. 2018. Electrochemical treatment of chemical oxygen demand in produced water using flow-by porous graphite electrodes, Water and Environment Journal 32, 404-411
44 Choi, Y., Naidu, G., Jeong, S., Lee, S., Vigneswaran, S. 2018. Fractional-submerged membrane distillation crystallizer (F-SMDC) for treatment of high salinity solution, Desalination 440, 59-67.

4. COMPONENTS FOR WHICH BENEFICIATION STRATEGIES DO NOT CURRENTLY EXIST

Lithium is an element that has received attention as being available from subterranean brines as well as salt flats. Lithium extraction from geothermal brines has been proposed in several studies. Geothermal brines contain lithium carbonate, as well as MgO, calcium carbonate and sodium chloride.[45] Lithium concentrations can be thousands of ppm in salty lakes, and up to hundreds of ppm in geothermal brines. These are still less than the concentration in ores or salt deposits. Seawater has 0.17 ppm of lithium. From the aqueous phase, lithium salts can be precipitated in an evaporation pond but this takes a long time depending on the feed concentration. Active electrolytic extraction can be carried out using electricity generated at a power plant, but this can be expensive. Fiber mats have been used to selectively adsorb cations, removing 46% of the lithium from a settling pond overnight, along with other mono and divalent cations.[46] Membranes, foams, and ion exchange technologies have also been investigated.[47,48,49] Advanced methods of extraction include the use of supercritical CO_2 as a solvent for crown ether extractant molecules. These latter chemicals can be made specific to lithium versus sodium or other cations.[50] Carbon dioxide can be made supercritical under fairly mild conditions, a pressure of 72.8 bar and a temperature of 31.1°C. Another technology uses selective absorbents: (i) that forms $LiCl{\cdot}Al_2(OH)_6{\cdot}nH_2O$, or Li-LDH;[51] or (ii) Octolig®, which is a polyethylenediimine used to functionalize a high-surface-area silica gel.[52]

Literature also exists on the extraction of lithium from produced water.[53] As in the case of geothermal brines, the main technologies used for separation include adsorbents, membrane-based processes and electrolysis. The adsorbent, H_2TiO_3 has been tested for lithium uptake in the presence of n-alkanes, organic contaminants present in produced water. Results indicated that pretreatment to remove the contaminants including paraffinic hydrocarbons[54] would be needed for subsequent processes to

---

45 Alkhasov, A.B., Alkhasova, D.A., Ramazanov, A.Sh. 2020. Technologies of geothermal resources development in the South of Russia, Geomechanics and Geophysics for Geo-Energy and Geo-Resources, 6, article 7.

46 Celik, A., Koc, G., Erdogan, E., Shahwan, T., Baba, A., Demire, M.M. 2017. Use of electrospun fiber mats for the remediation of hypersaline geothermal brine, Desalination and Water Treatment 62, 94-100.

47 Cetiner, Z.S., Doğan, Ö, Özdilek, G., Erdoğan, P. Ö. 2015. Toward utilizing geothermal waters for cleaner and sustainable production: potential of Li recovery from geothermal brines in Turkey, Int J Global Warming, 7(4), 439-453.

48 Zhu, G., Wang, P., Qi, P., Gao, C. 2014. Adsorption and desorption properties of Li+ on PVC-H1.6Mn1.6O4 lithium ion-sieve membrane, Chem Eng J 235, 340-348.

49 Han, Y., Kim, H., Park, J. 2012. Millimeter-sized spherical ion-sieve foams with hierarchical pore structure for recovery of lithium from seawater, Chem Eng J 210, 482-489.

50 Ruttinger, A.W., Pálsdóttir, A., Tester, J.W., Clancy, P. 2019. A quantitative metric for the design of selective supercritical CO2 extraction of lithium from geothermal brine, ChemSusChem 12(15), 3532-3540.

51 Wu, L.,Li, L., Evans, S.F., Eskander, T.A., Moyer, B.A., Hu., Z., Antonick, P.J., Harrison, S., Paranthaman, M.P., riman, R., Navrotsky, A. 2019. Lithium aluminum-layered double hydroxide chlorides (LDH): Formation enthalpies and energetics for lithium ion capture, J Am Chem Soc 102(5), 2398-2404.

52 Martin, D.F., Bisht, K.S. 2018. Efforts to remove aqueous lithium ion using Octolig® and methylated derivatives, J. Environ. Sci. & Health, Part A-Toxic/Hazardous Substances & Environ Eng, 53(10), 946-949.

53 Kumar, A., Fukada, H., Hatton, T.A., Lienhard, J.H. V. 2019. Lithium recovery from oil and gas water: A need for a growing energy industry. ACS Energy Lett. 4, 1471-1471.

54 Jang, Y., Chung, E. 2019. Lithium adsorptive properties of H2TiO3 adsorbent from shale gas produced water containing organic compounds, Chemosphere, 221, 75-80.

effectively strip lithium from the raffinate.[55] Forward osmosis-membrane distillation has been investigated for different draw solutions (NaCl, KCl, $MgCl_2$, and LiCl), with the goal of generating purified water.[56] The method was less successful for the LiCl draw solutions than for the other cations, but the concentration of lithium species, 10 M, was very different from what would be expected in produced water.

Beryllium is a light metal that is widely used in electronics and is now being considered as a component for energy production (fusion and fission nuclear reactors). Beryllium is abundant along with lithium in produced water. Concentration of both beryllium and lithium from produced water by evaporation has been considered for the Arabian Peninsula.[57]

55 Jang, Y., Chung, E. 2019. Influence of alkanes on lithium adsorption and desorption of a H2TiO3 ion sieve adsorbent in synthetic shale gas-produced water, Ind. Eng. Chem. Res. 58(48), 21897-21903.
56 Al-Furaiji, M., Benes, N., Nijmeijer, McCutcheon, J.R. 2019. Use of a forward osmosis-membrane distillation integrated process in the treatment of high-salinity oily wastewater, Ind.Eng.Chem.Res. 58, 956-962.
57 Schaller, J., Headley, T., Prigent, S., Breuer, R. 2014. Potential mining of lithium, beryllium and strontium from oilfield wastewater after enrichment in constructed wetlands and ponds, Sci Total Environ 493, 910-913.

5. SUMMARY AND CONCLUSIONS

Extraction of rare earth element from fossil resources has generated attention, particularly as a value-added activity for coal and mining activities. There have been few public efforts into researching produced and flow back water as sources of rare earth elements. However, given that the high TDS retentate from desalination of produced and flowback water may have concentrations of rare earths comparable to that from coal and flyash, it appears that this may be an area that merits further investigation. Mining of high concentration brines for rare metals should increase the valuation of desalination for beneficial reuse of produced water. However, any process or set of processes selected to extract the rare earth elements also needs to minimize the generation of a large volume waste stream. For this reason, it may be optimal to provide an acidified mixture to industries already involved in rare earth element recovery from non-traditional sources, such as recycled material.